

This item is the archived peer-reviewed author-version of:

Plasma-based dry reforming of CH<sub>4</sub> : plasma effects vs. thermal conversion

**Reference:**

Slaets Joachim, Loenders Björn, Bogaerts Annemie.- Plasma-based dry reforming of CH<sub>4</sub> : plasma effects vs. thermal conversion  
Fuel - ISSN 1873-7153 - 360(2024), 130650  
Full text (Publisher's DOI): <https://doi.org/10.1016/J.FUEL.2023.130650>  
To cite this reference: <https://hdl.handle.net/10067/2016690151162165141>

# Plasma-based dry reforming of CH<sub>4</sub>: plasma effects vs. thermal conversion

Joachim Slaets\*, Björn Loenders and Annemie Bogaerts

Research group PLASMANT, Department of Chemistry, University of Antwerp, Universiteitsplein 1,  
BE-2610 Wilrijk-Antwerp, Belgium

\*Corresponding author at: Research group PLASMANT, Department of Chemistry, University of  
Antwerp, Universiteitsplein 1, 2610 Antwerpen, Belgium. E-mail address:  
[joachim.slaets@uantwerpen.be](mailto:joachim.slaets@uantwerpen.be)

**Abstract:** In this work we evaluate the chemical kinetics of dry reforming of methane in warm plasmas (1000 – 4000 K) using modelling with a newly developed chemistry set, for a broad range of parameters (temperature, power density and CO<sub>2</sub>/CH<sub>4</sub> ratio). We compare the model against thermodynamic equilibrium concentrations, serving as validation of the thermal chemical kinetics. Our model reveals that plasma-specific reactions (i.e., electron impact collisions) accelerate the kinetics compared to thermal conversion, rather than altering the overall kinetics pathways and intermediate products, for gas temperatures below 2000 K. For higher temperatures, the kinetics are dominated by heavy species collisions and are strictly thermal, with negligible influence of the electrons and ions on the overall kinetics. When studying the effects of different gas mixtures on the kinetics, we identify important intermediate species, side reactions and side products. The use of excess CO<sub>2</sub> leads to H<sub>2</sub>O formation, at the expense of H<sub>2</sub> formation, and the CO<sub>2</sub> conversion itself is limited, only approaching full conversion near 4000 K. In contrast, full conversion of both reactants is only kinetically limited for mixtures with excess CH<sub>4</sub>, which also gives rise to the formation of C<sub>2</sub>H<sub>2</sub>, alongside syngas. Within the given parameter space, our model predicts the 30/70 ratio of CO<sub>2</sub>/CH<sub>4</sub> to be the most optimal for syngas formation with a H<sub>2</sub>/CO ratio of 2.

Keywords: plasma kinetics, computer modelling, dry reforming of methane

## 1. Introduction

In recent years there is an increasing concern regarding greenhouse gas emissions, global warming and climate change and the role of fossil fuels. There is an urgent need for alternative feedstock and production pathways for important chemicals. A possible solution can be found in carbon capture and utilization (CCU)[1], where greenhouse gasses such as CO<sub>2</sub> and CH<sub>4</sub> can be recycled for the production of chemicals instead of being emitted into the atmosphere, thus contributing to a circular economy. An interesting reaction is the so-called dry reforming of CH<sub>4</sub> (DRM) (Eq. 1) to produce syngas, a mixture of H<sub>2</sub> and CO.



Syngas can be further processed, for example into synthetic fuels through the Fischer-Tropsch process.

Plasma-based DRM is interesting as it has many advantages: it is operated with electricity and is a turnkey process, allowing it to be quickly turned on and off, or scaled, according to the amount of available renewable energy [2–4]. Plasma-based DRM has already been studied in various experimental settings. In so-called warm plasmas, such as gliding arc (GA), microwave (MW), atmospheric pressure glow discharges (APGDs) or nanosecond pulsed discharges (NPDs), where the gas temperature can reach up to 4000 K or even higher, the main reaction product is indeed syngas [5,6,15–18,7–14]. Cold plasmas, on the other hand, like dielectric barrier discharges (DBDs), also produce mainly syngas, but they also allow the formation of additional side products, such as C<sub>2</sub>- and C<sub>3</sub>-hydrocarbons and oxygenates, like methanol, ethanol or formaldehyde, especially when catalysts are integrated in the plasma zone [19–25].

While experiments are invaluable for the further development of plasma-based DRM, the obtained information is mostly limited to the effects of reactor design and operating conditions on the overall reaction performance, such as energy efficiency, reactant conversion and product yields. This only gives limited insights into the underlying chemical processes. Therefore, additional information can be obtained through kinetics modelling of the experimental setups, gaining important insights in the chemical reactions related to the performance of specific plasma types, reactor designs and the effects

of experimental parameters (e.g., flow rate, plasma power, gas mixture). However, this is also a limitation as the model only considers the specific experimental conditions, determined by e.g., flow dynamics and heat transfer, providing information relevant only for that specific reactor design and operating conditions. Although such models contribute to a better understanding of the experimental work, they use a limited range of parameters to match the corresponding experimental conditions, which hinders finding opportunities for further optimization of the chemical conversion process. For example, studies by Cleiren et al. [11] and Wanten et al. [13] consider DRM in GA and APGD plasmas, respectively, but their modelling is limited to gas temperatures between 2000 – 2700 K in the plasma. The most notable restriction is the maximum CH<sub>4</sub> fraction of only 35 %, because of experimental limitations. They also consider a thermal reaction zone with a lower temperature between 1600 – 2200 K, to obtain a better approximation of their experimental reactor. The modelling work performed by Liu et al. [26] does cover a wider range of gas mixtures, up to 50 % CH<sub>4</sub> fraction, but it still only considers a gas temperature of 2500 K in the plasma. These works show experimentally that CO, H<sub>2</sub> and H<sub>2</sub>O are the main formed products for these gas mixtures, with much smaller and trace amounts of C<sub>2</sub>H<sub>2</sub>, C<sub>2</sub>H<sub>4</sub>, C<sub>2</sub>H<sub>6</sub> and O<sub>2</sub>. Other studies consider DRM with the addition of other gasses, such as O<sub>2</sub> or N<sub>2</sub> as major components or impurities in the gas mixture [12,27,28]. There are also studies that consider a broader range of operating conditions for plasma-based DRM, but these studies are limited to low temperature DBD plasmas [29,30].

Therefore, the present study aims to gain a broader understanding of the effects of plasma parameters on the core chemical kinetics of DRM, independent of the experimental setting. We specifically focus on warm plasma conditions, such as found in GA, MW, APGDs and NPDs, because they give rise to much better energy efficiency than cold plasmas [3]. It is important to stress that such a broad study on the kinetics in this type of warm plasmas has never been conducted before; it was only performed for low temperature DBD plasmas [27,29,30]. Further, we do not limit ourselves to a specific reactor design, but we study a general plasma setting with a wider range of gas temperature, plasma power density, and most importantly, a full range of gas mixtures, ranging from 90 % CO<sub>2</sub> to 90% CH<sub>4</sub>, which has not been demonstrated before for warm plasmas. We compare the kinetics of thermal gas chemistry

with those of plasma-based conversion and illustrate differences and similarities between them. It has been shown that within plasma systems thermal chemistry can be an important contributor to the conversion process [26]. Importantly, we constructed a new chemical kinetics scheme for this broad study, which serves as an updated/revised version of the previous works from our group PLASMANT [11,12,35,13,27,29–34]. Improvements are made by careful literature review of the original sources and the use of detailed balancing to fill gaps in the chemistry. We also specifically improved the kinetics scheme by comparing the steady state concentrations from our model to thermodynamic equilibrium, which was never considered as a validation tool in previous works.

## 2. Material and methods

### 2.1. Model description

The focus of this work is to study the influence of various parameters, i.e., gas temperature, plasma power and CO<sub>2</sub>/CH<sub>4</sub> ratio, on the chemical composition in the plasma, independent of a specific reactor configuration. This makes a (zero-dimensional) chemical kinetics model ideal for this study. The simple model setup allows a wide range of parameters to be studied with reasonable calculation times. We used the ZDPlasKin code for these calculations [36].

The model solves the mass conservation equations for all plasma species included, by calculating the change in number density for each species due to chemical reactions. Eq. 2 describes the change in number density  $n$  of species  $s$  with respect to time  $t$  due to reactions  $j$ , in which  $a_{s,i}^R$  and  $a_{s,i}^L$  are the coefficients of species  $s$  on the right and left side of the reaction  $i$ , respectively, and  $R_i$  is the corresponding reaction rate. The reaction rate, given by Eq. 3, is the product of the rate coefficient  $k$  and number densities of the reactants  $n_s$ .

$$\frac{\partial n_s}{\partial t} = \sum_{i=1}^j [(a_{s,i}^R - a_{s,i}^L) R_i] \quad (\text{Eq. 2})$$

$$R = k \prod_s n_s^{a_s^L} \quad (\text{Eq. 3})$$

For the electron impact reactions, the rate coefficients are calculated using Eq. 4, where  $\varepsilon$  is the electron energy,  $\sigma_c$  the collision cross section,  $f_e$  the electron energy distribution function (EEDF) and  $v$  the electron velocity, given by Eq. 5, in which  $m_e$  is the mass of an electron. The EEDF is calculated by a Boltzmann solver, BOLSIG+ [37], which is integrated in the ZDPlasKin code. BOLSIG+ uses the two-term approximation to calculate the EEDF from the reduced electric field ( $E/N$ ), which is obtained from Eq. 6, with  $n_{tot}$  the total species number density,  $P/V$  the power density given as input to the model, and  $\sigma$  the plasma conductivity. The latter is calculated by Eq. 7, with  $\mu$  the electron mobility, also obtained from BOLSIG+,  $n_e$  the electron density and  $e$  the elementary charge.

$$k = \int_{\epsilon_{th}}^{+\infty} \sigma_c(\epsilon) f_e(\epsilon) v(\epsilon) d\epsilon \quad (\text{Eq. 4})$$

$$v(\epsilon) = \sqrt{\frac{2\epsilon}{m_e}} \quad (\text{Eq. 5})$$

$$\left(\frac{E}{N}\right) = \frac{1}{n_{tot}} \sqrt{\frac{P/V}{\sigma}} \quad (\text{Eq. 6})$$

$$\sigma = \frac{\mu}{n_{tot}} \cdot n_e \cdot e \quad (\text{Eq. 7})$$

For the other reactions, by the so-called heavy species (i.e., all species besides the electrons), the rate coefficients are given by analytical equations, e.g., modified Arrhenius equations or fall-off functions. A complete list of all reactions in the kinetics scheme, with the corresponding rate coefficients or cross sections and references, is presented in the Supporting Information (SI).

Importantly, this work serves as an updated version of the kinetic schemes for the reforming of CO<sub>2</sub> and CH<sub>4</sub> mixtures from our earlier works [11,12,35,13,27,29–34]. We updated the reaction rate coefficients using available literature, and where unavailable, we used detailed balancing to account for reverse processes.

Both plasma power and gas temperature are considered as separate input parameters, independent of each other, and they are both kept constant at fixed values throughout the simulation. This means that

the gas temperature is not calculated time-dependently using the heat balance equation, and therefore, the plasma power is not responsible for gas heating, i.e., gas temperature and plasma power are fully decoupled parameters. This has the benefit that we can evaluate their effect, independent from each other, providing more insight in the effect of individual parameters. In reality, however, the gas temperature depends on the applied plasma power and heat capacity of the gas mixture, as well as heat losses to for example the reactor walls. Hence, either external heating or cooling may be required to obtain a specific combination of plasma power and gas temperature, used as input in this study. However, this work aims to gain a better understanding of the effects of these external parameters on the chemical kinetics, without focusing on a specific experimental condition, which justifies this approach. Even more, it provides a broad picture of the overall chemistry, and thus allows to discover possible improvements in the chemical conversion process.

In total, 336 different electron impact reactions are taken into account for the calculation of the EEDF (see SI; Table S1 and S2), including 123 electron impact excitation reactions. However, the excited species formed in this way are not included in our kinetics scheme. Indeed, our model does not consider a state-to-state chemistry, but instead it assumes a vibrational-translational equilibrium, i.e., the vibrational temperature is equal to the gas temperature, and there is no overpopulation of the vibrationally excited levels. As an indication, it has been demonstrated that a vibrational-translational non-equilibrium can only be sustained for very short timescales, reaching equilibrium in less than 0.1 ms for pressures of 25 mbar [38]. With increased pressure, the higher collision frequency between species will result in even faster vibrational-translational relaxation. As our study is focused on atmospheric pressure plasmas and residence times up to 10 ms, we can reasonably assume that relaxation is sufficiently fast to result in a thermal vibrational distribution function (VDF) and a negligible influence of vibrational-translational non-equilibrium on the kinetics.

Our simulations assume a homogeneous plasma, i.e., no gradients in temperature or power density. In principle, ZDPlasKin considers a batch reactor, calculating the species number densities only as a function of time, by solving the species conservation equations (Eq. 2). However, the total number density is affected by temperature and chemical reactions, requiring a modification to account for these

changes and to maintain constant (atmospheric) pressure. Therefore, at each timestep, the number densities calculated by ZDPlasKin for all species are multiplied with a correction factor  $\beta$  (Eq. 8) to maintain the total number density corresponding to the ideal gas law at atmospheric pressure and the simulated temperature [39]. In our simulations the temperature is a constant, i.e.,  $T_g(0)$  and  $T_g(t)$  in Eq. 8 are equal. This approach can be considered a batch reactor operating at constant pressure. In a flow reactor, this correction would be equivalent to contraction or expansion of the gas volume due to chemical reactions, and correspondingly a decrease or increase of the velocity through the plasma.

$$\beta = \frac{T_g(0) \sum_i n_i(0)}{T_g(t) \sum_i n_i(t)} \quad (\text{Eq. 8})$$

## 2.2. Chemistry

The kinetics scheme considers 70 different plasma species, i.e., 40 different neutral species, 24 different positive ions, 5 different negative ions, and the electrons, which react through 1468 reactions. A list of the species included in the model is given in Table 1 and a full list of the chemical reactions with the corresponding rate coefficients and the references where the data is adopted from, is provided in the SI (Table S1).

Most rates coefficients were obtained directly from literature sources, with some exceptions. For reverse processes of reactions between neutral species for which no reliable source could be found in literature, detailed balancing was used to obtain the rate coefficients. The equilibrium constant  $K_{eq}$  is calculated using Eq. 9, with  $p$  the reference pressure (1 bar),  $\Delta v$  the change in number of species in the reaction and  $\Delta G_r$  the Gibbs free energy of the reaction, calculated using thermodynamic data from McBride et al. [40] and Burcat et al. [41].

$$K_{eq} = \left(\frac{p}{RT}\right)^{\Delta v} e^{\left(\frac{-\Delta G_r}{RT}\right)} \quad (\text{Eq. 9})$$

Furthermore, some assumptions were made in the kinetics scheme or reactions involving electrons. The associative ionization rate coefficients (reactions 549–551, 1084, 1085, 1155, 1156, 1200 in Table S1) are taken equal to the values of Park et al. for O + O (forming O<sub>2</sub><sup>+</sup> + an electron). Indeed, they could

prove important in the higher temperature range for the formation of electrons, as stated by Vialletto et al. [42]. The electron detachment reaction from OH<sup>-</sup> ions (reaction 457 in Table S1) is estimated to be equal to the detachment process of O<sup>-</sup> ions and was found to be an important reaction to balance the anions in the plasma. The electron-ion three-body recombination rate coefficients for CO<sup>+</sup> and CO<sub>2</sub><sup>+</sup> were also estimated based on the generalized formulation of Kossyi et al. [43], although these reactions turn out to have minimal impact on the overall scheme (reactions 1158-1161 in Table S1).

Table 1: Overview of species included in the chemical kinetics set, excluding the electrons

NEUTRAL SPECIES	IONS
C	C <sup>+</sup>
O, O <sub>2</sub> , O <sub>3</sub>	O <sup>+</sup> , O <sub>2</sub> <sup>+</sup> , O <sup>-</sup> , O <sub>2</sub> <sup>-</sup> , O <sub>3</sub> <sup>-</sup>
H, H <sub>2</sub>	H <sup>+</sup> , H <sub>2</sub> <sup>+</sup> , H <sub>3</sub> <sup>+</sup> , H <sup>-</sup>
CO, CO <sub>2</sub>	CO <sup>+</sup> , CO <sub>2</sub> <sup>+</sup>
CH, CH <sub>2</sub> , CH <sub>3</sub> , CH <sub>4</sub> , C <sub>2</sub> H, C <sub>2</sub> H <sub>2</sub> , C <sub>2</sub> H <sub>3</sub> , C <sub>2</sub> H <sub>4</sub> , C <sub>2</sub> H <sub>5</sub> , C <sub>2</sub> H <sub>6</sub>	CH <sup>+</sup> , CH <sub>2</sub> <sup>+</sup> , CH <sub>3</sub> <sup>+</sup> , CH <sub>4</sub> <sup>+</sup> , CH <sub>5</sub> <sup>+</sup> , C <sub>2</sub> H <sup>+</sup> , C <sub>2</sub> H <sub>2</sub> <sup>+</sup> , C <sub>2</sub> H <sub>3</sub> <sup>+</sup> , C <sub>2</sub> H <sub>4</sub> <sup>+</sup> , C <sub>2</sub> H <sub>5</sub> <sup>+</sup> , C <sub>2</sub> H <sub>6</sub> <sup>+</sup>
OH, H <sub>2</sub> O, HO <sub>2</sub> , H <sub>2</sub> O <sub>2</sub>	OH <sup>+</sup> , H <sub>2</sub> O <sup>+</sup> , H <sub>3</sub> O <sup>+</sup> , HO <sub>2</sub> <sup>+</sup> , OH <sup>-</sup>
CH <sub>2</sub> CH <sub>2</sub> OH, CH <sub>2</sub> CO, CH <sub>2</sub> OH, CH <sub>3</sub> CH <sub>2</sub> O, CH <sub>3</sub> CH <sub>2</sub> OH, CH <sub>3</sub> CHO, CH <sub>3</sub> CHOH, CH <sub>3</sub> CO, CH <sub>3</sub> COOH, HCCO, CH <sub>3</sub> O, CH <sub>3</sub> OH, CH <sub>3</sub> OO, CH <sub>3</sub> OOH, COOH, HCHO, HCO, HCOOH	HCO <sup>+</sup>

### 2.3. Overview of the simulations

In this work, we focus specifically on the kinetics in the active plasma region, without considering an afterglow or post-plasma effects. We varied the gas temperature between 1000 and 4000 K, which is in the typical range for warm plasmas [3], for five different CO<sub>2</sub>/CH<sub>4</sub> ratios (10/90, 30/70, 50/50, 70/30, 90/10). We also conducted four sets of simulations for the power density, further referred to as thermal

(0 W/cm<sup>3</sup>) and plasma (500, 1000, 1500 W/cm<sup>3</sup>) simulations. These power densities are typical for warm plasmas, as obtained from different literature sources [6,8,11–13,44–48] (see comparison in the supporting information; Table S3).

“Thermal” represents purely thermal decomposition of molecules in the gas-phase because of the high gas temperature, in which no electrons or ions are considered, but only neutral species. The comparison with the plasma simulations is performed for a residence time of 10 ms. This estimate of residence time is realistic based on the work of Van Alphen et al. [49], where a residence time distribution up to 17.5 ms was reported based on CFD simulations of their arc reactor. Additionally, Dahl et al. [50] also used a residence time of 10 ms in solar-thermal DRM operating at 2000 K. On the other hand, we also conducted the thermal simulations up to an extremely long simulation time ( $10^{10}$  s, approximately 3169 years). This is of course unrealistic in practice, but it allows the heavy species kinetics to reach a steady state. The concentrations of the neutral species can then be evaluated against thermodynamic equilibrium concentrations for the corresponding conditions, which are calculated as described by Biondo et al. [51]. This comparison provides a first validation of our heavy species kinetics. However, it is important to note that this only applies to the steady state concentrations themselves, and not the kinetic pathways to obtain them, neither the timescales in which they are obtained. The accuracy of the model for those aspects is related to the accuracy of the reaction rate coefficients used in the model. These uncertainties are typically in the order of 10 – 30 %, but can be higher than 100 %. Therefore, it is generally established that chemical kinetics models can have a large uncertainty [52–55]. Wang et al. quantified the uncertainties for their DBD model for DRM and obtained uncertainties up to 33 % for the conversion and up to 28 % for the syngas yield [55]. Therefore, the trends and relative values of the species densities predicted by the model are more important than the absolute values.

When comparing our thermal and plasma simulations and thermodynamic equilibrium calculations, we define the deviation between the species concentrations using the equation for mean absolute deviation. The large number of species with very low density reduces the value of the mean significantly, and therefore a weighted mean is employed to focus on the higher density species. This weighted mean absolute deviation (*wMAD*) is calculated by Eq. 10, with  $\Delta c_s$  the concentration difference for species *s*

between the results that are compared and  $w_s$  the weight for species  $s$ . When we compare with thermodynamic equilibrium concentrations, we use the latter as weights in the equation. When we compare thermal and plasma simulations, the weights are taken as the thermal concentrations.

$$wMAD = \frac{\sum_s (w_s \cdot |\Delta c_s|)}{\sum_s w_s} \quad (\text{Eq. 10})$$

The CO<sub>2</sub> or CH<sub>4</sub> conversion is calculated using Eq. 11, where  $s$  is CO<sub>2</sub> or CH<sub>4</sub>,  $n$  is the corresponding number density at the inlet or outlet (corresponding to the start and end of the simulations), and  $\beta$  is the correction factor defined in Eq. 8.

$$\chi_s = \left( 1 - \frac{n_s^{\text{out}}}{\beta \cdot n_s^{\text{in}}} \right) \cdot 100\% \quad (\text{Eq. 11})$$

### 3. Results and discussion

#### 3.1. Validation of the thermal chemistry

First, we quantify the deviation between the calculated species concentrations for the thermodynamic equilibrium and thermal kinetics simulations, to validate in first instance the thermal chemistry in our model, for the five different DRM mixtures, using the *wMAD* (Eq. 10), shown in Figure 1(a). The corresponding species concentrations (comparison of thermodynamic equilibrium vs. thermal kinetics simulations) for the 50/50 mixture are plotted in Figure 1(b), as a reference. The comparison at the other mixing ratios is presented in SI, figures S1(a-d).

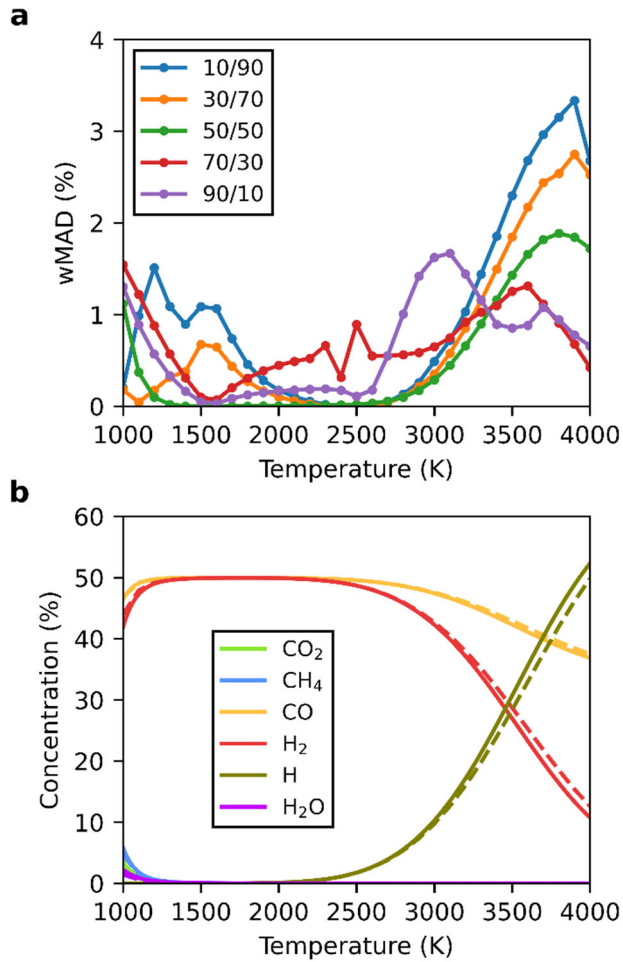


Figure 1: (a) Weighted mean absolute deviation (*wMAD*) between the calculated species concentrations of the thermal simulations (for  $t = 10^{10}$  s) and the thermodynamic equilibrium concentrations, in the temperature range of 1000 to 4000 K, for five different CO<sub>2</sub>/CH<sub>4</sub> ratios (90/10, 70/30, 50/50, 30/70, 10/90). (b) Corresponding species concentrations, calculated at thermodynamic equilibrium (solid) vs. thermal kinetics simulations (dashed) for the 50/50 mixture. The comparison at the other mixing ratios is presented in SI, figures S1(a-d). Note that at thermodynamic equilibrium (or steady state) nearly all CO<sub>2</sub> and CH<sub>4</sub> is converted into CO and H<sub>2</sub>, even at/above 1000 K, while above 2500 K, H<sub>2</sub> starts to be dissociated.

Good agreement is reached between 1700 and 2700 K, with a deviation (*wMAD*) of less than 1 %. At lower temperature, a larger deviation, up to 1.5 % for 1000 K, is obtained. At higher temperatures, the

deviation also rises, but remains below 4 %. Hence, the steady state compositions for this kinetics scheme are in good agreement with those at thermodynamic equilibrium, which serves as validation of the thermal chemistry in our model.

### **3.2. Comparison of plasma and thermal kinetics**

#### **3.2.1. Plasma species concentrations as a function of temperature**

For further characterization of the DRM chemistry, we compare different cases with and without plasma power, to compare the plasma and thermal kinetics, with timescales limited to the millisecond range. The concentrations of the main species, for both the thermal and plasma simulations, at a residence time of 10 ms and for the stoichiometric ratio of 50/50 CO<sub>2</sub>/CH<sub>4</sub>, are plotted in Figure 2. It is clear that, above 2400 K, also the plasma concentrations agree with the thermodynamic equilibrium concentrations plotted in Figure 1b. Below 2400 K, CO<sub>2</sub> and CH<sub>4</sub> are not yet dissociated within this short residence time (Figure 2a), and H<sub>2</sub>O, C<sub>2</sub>H<sub>2</sub> and C<sub>2</sub>H<sub>4</sub> are formed to some extent (Figure 2b), which will react away before thermodynamic equilibrium is established.

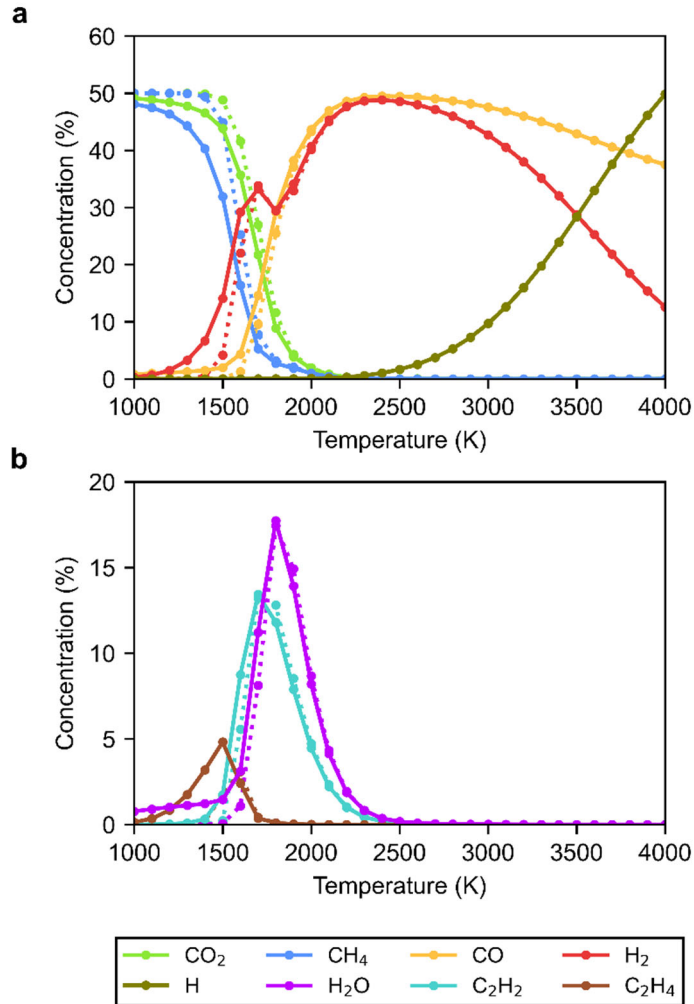


Figure 2: Calculated concentrations of the main plasma species for the temperature range of 1000 to 4000 K and a 50/50  $\text{CO}_2/\text{CH}_4$  ratio, at a residence time of 10 ms, for both thermal (dotted lines) and 1000  $\text{W}/\text{cm}^3$  plasma conditions (solid lines).

The thermal conditions show no conversion below 1400 K, and thus  $\text{CO}_2$  and  $\text{CH}_4$  are the only species present. The corresponding plasma conditions do show clear conversion already in this temperature range, being somewhat higher for  $\text{CH}_4$  than for  $\text{CO}_2$ , which is logical, based on the C-H vs C=O bond strength (i.e., 439 vs 532  $\text{kJ mol}^{-1}$ ) [56]. Both  $\text{CO}_2$  and  $\text{CH}_4$  conversion increase significantly towards 1600 K, which results in the formation of  $\text{H}_2$ ,  $\text{CO}$ ,  $\text{C}_2\text{H}_2$  and  $\text{H}_2\text{O}$  (and a limited amount of  $\text{C}_2\text{H}_4$ ), for both thermal and plasma conditions. While syngas ( $\text{CO}$  and  $\text{H}_2$ ) is the dominant product (Figure 2a), the formation of  $\text{H}_2\text{O}$  is also quite important (Figure 2b), and most significant at 1800 K, competing

with H<sub>2</sub> formation. This results in a small dip (i.e., 4.5 % and 3.9 % lower concentration) for H<sub>2</sub> at 1800 K compared to at 1700 K, for the thermal and plasma conditions, respectively. For higher temperatures, the concentrations of C<sub>2</sub>H<sub>2</sub> and H<sub>2</sub>O drop and become negligible around 2400 K. Simultaneously, the CO<sub>2</sub> and CH<sub>4</sub> conversions reach 100 % at this temperature, leading to the maximum concentrations of 49 and 50 % for H<sub>2</sub> and CO, respectively. The calculated species concentrations of the thermal and plasma conditions (dotted and full lines) fully coincide above 2000 K.

For temperatures above 2400 K, the concentration of H radicals becomes increasingly important, at the cost of H<sub>2</sub>, leading to H<sub>2</sub> and H concentrations of 13 and 50 %, respectively, at 4000 K, for both the thermal and plasma conditions. The concentration of CO also drops slightly, but this is simply due to the splitting of H<sub>2</sub>, which increases the number of species, effectively diluting CO. The other free radicals, C, O and OH, are much less significant, with calculated concentrations of 0.03 % or less. It should be noted that all radicals will recombine in the afterglow region, where the gas cools down, but this is not considered in our model.

In summary, the plasma activates the chemistry at low temperature (below 1700 - 1800 K), yielding higher conversion than the pure thermal process. As the conversion process is initiated by electron impact reactions through the creation of radicals. Even more, below 1400 K, plasma reactions already give rise to a clear conversion, whereas thermal reactions alone cannot. Above 1500 K, the differences between thermal and plasma kinetics gradually become smaller, and thus, thermal reactions start to dominate. As temperature increases, thermal reactions are accelerated, thus contribute more to the initial creation of radicals and causing conversion on even shorter timescales compared to electron impact reactions. Above 2000 K, the thermal and plasma kinetics coincide, so the chemistry becomes purely thermal. Finally, above 2400 K, the concentrations follow thermodynamic equilibrium (cf. Figure 1b), indicating that the kinetics is fast enough to reach steady state within the simulation time of 10 ms.

### 3.2.2. Deviation between plasma and thermal kinetics

We use the deviation between the simulations with and without plasma power to quantify the influence of plasma-specific reactions compared to thermal kinetics. Figure 3 presents the deviation (*wMAD*)

between the thermal and plasma concentrations for the 50/50 ratio, between 0.1 and 10 ms, for an applied power density of 1000 W/cm<sup>3</sup>. For a residence time of 0.1 ms, the difference between thermal and plasma concentrations is very small, with a *wMAD* of less than 0.4 %, but after 1 ms, the difference increases, resulting in a maximum *wMAD* of 1.8 % at a gas temperature of 1700 K. At still longer residence times of 10 ms, the maximum *wMAD* increases to 8.7 %, and shifts to a lower gas temperature of 1500 K. This larger deviation with time is logical, as a longer residence time simply allows for more reactions to occur.

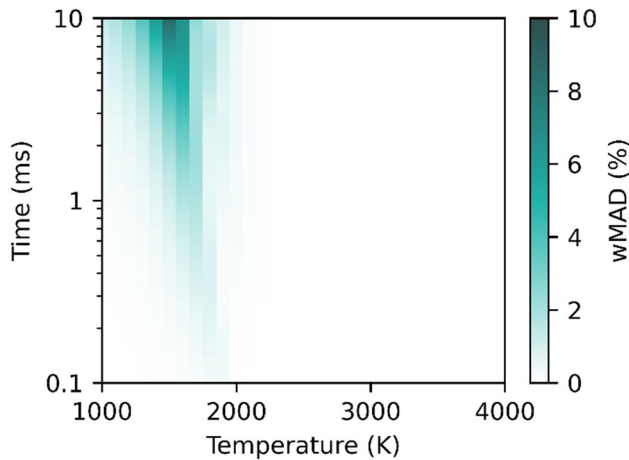


Figure 3: Weighted mean absolute deviation (*wMAD*) between the calculated species concentrations for thermal and plasma kinetics (1000 W/cm<sup>3</sup>) as a function of residence time (0.1 to 10 ms) and gas temperature (1000 to 4000 K), for a stoichiometric (50/50) CO<sub>2</sub>/CH<sub>4</sub> ratio.

The deviation obtained for low temperatures near 1000 K is due to the very small, almost negligible thermal conversion, while the plasma power activates electron impact dissociation, enabling more conversion. This is explained in more detail in section 3.2.3. Raising the temperature up to 2000 K accelerates the thermal reactions, allowing the products from electron impact dissociation to react away faster. This drives the conversion process even more forward and increases the deviation compared to pure thermal conversion, where the initial dissociation of the reactants can only occur from thermal kinetics. The deviation reaches a maximum around 1500 - 1700 K, after which the thermal kinetics increases further, taking over the conversion process. Above 2000 K, thermal chemistry fully controls

the conversion, resulting in a negligible deviation between the thermal and plasma conditions, with a *wMAD* below 0.2 %.

A similar behavior is observed for the other CO<sub>2</sub>/CH<sub>4</sub> ratios, for which the deviation also rises and shifts towards slightly lower gas temperatures with increasing residence time. In our further discussion, we only consider a residence time of 10 ms, typically giving rise to the largest deviation. The deviation between plasma and thermal kinetics depends on the gas mixture, as shown in Figure 4. For mixtures with an excess of CH<sub>4</sub> (i.e., 30/70 and 10/90 CO<sub>2</sub>/CH<sub>4</sub>), the *wMAD* reaches maxima of 11 and 13 %, respectively, at 1500 K. For mixtures with excess CO<sub>2</sub>, the maxima are obtained at slightly higher gas temperatures, i.e., at 1600 K for the 70/30 ratio (8.1 %) and at 1700 K for the 90/10 ratio (12 %). Similar to the 50/50 CO<sub>2</sub>/CH<sub>4</sub> mixture, the *wMAD* between the thermal and plasma kinetics is negligible (< 0.2 %) above 2000 K. An exception to this is the 90/10 mixture, showing a small deviation between 2000 and 3000 K, with a maximum of 0.71 % at 2500 K, which will be discussed in section 3.4.1. As expected, the difference between thermal and plasma kinetics slightly rises with the applied power density. The maximum *wMAD* for the different mixtures ranges between 4.1 and 6.4 % for 500 W/cm<sup>3</sup>, while for 1500 W/cm<sup>3</sup>, it is between 12 and 19 %, see SI (Figure S2). In the rest of our paper, we will focus only on the 1000 W/cm<sup>3</sup> case, being the intermediate power density.

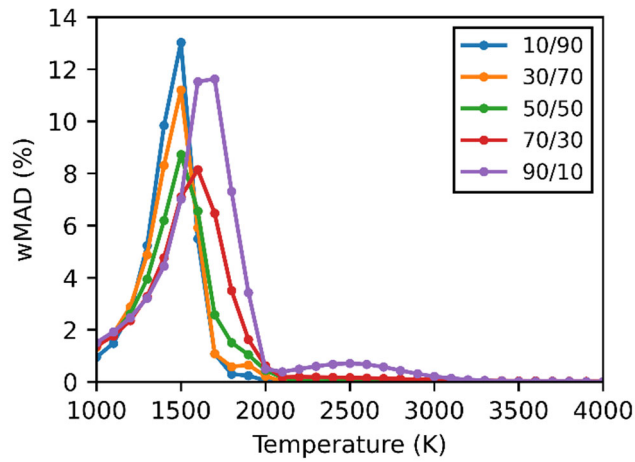


Figure 4: Weighted mean absolute deviation (*wMAD*) between the calculated species concentrations for thermal and plasma kinetics (1000 W/cm<sup>3</sup>) at a residence time of 10 ms, in the temperature range of 1000 to 4000 K, for five different CO<sub>2</sub>/CH<sub>4</sub> ratios (90/10, 70/30, 50/50, 30/70, 10/90).

From these results we can conclude again the importance of the plasma kinetics for the DRM reaction below 2000 K. Moreover, the deviation (*wMAD*) for the thermal and plasma kinetics becomes larger with longer residence times and higher power densities. On the other hand, at temperatures above 2000 K, the chemistry is almost purely thermal. These results suggest that for warm plasma conditions characterized by temperatures (largely) above 2000 K, being typical for GA, MW and APGDs, the DRM process can reasonably be described by only considering the thermal kinetics. It should be noted, however, that the energy balance is not solved in this study and electron impact collisions can still influence the plasma heating mechanisms.

### 3.2.3. Product formation as a function of time

In Figure 2 we observed only some differences in absolute values of the species concentrations between the thermal and plasma kinetics (below 2000 K), without any drastic changes in product distribution. When comparing the species concentrations at different timepoints in the simulations, we observe a clear relation with gas temperature, as the product concentrations shift towards higher gas temperatures for shorter residence times (presented in Figure S3 in the supporting information). This is logical as, for the same temperature, a shorter residence time results in less reaction, i.e., higher reactant concentrations and lower product concentrations. However, above 3000 K, thermodynamic equilibrium concentrations are already reached for a residence time of 0.1 ms. Indicating that the conversion process occurs on a much shorter time scale compared to typical residence times in warm plasma systems.

To explain this in more detail and to obtain a better picture of the kinetics responsible for the conversion process, the concentrations of the major species are plotted as a function of time in Figure 5, for a gas temperature of 1500, 2000 and 4000 K, and for both thermal and (1000 W/cm<sup>3</sup>) plasma conditions, at a 50/50 CO<sub>2</sub>/CH<sub>4</sub> ratio.

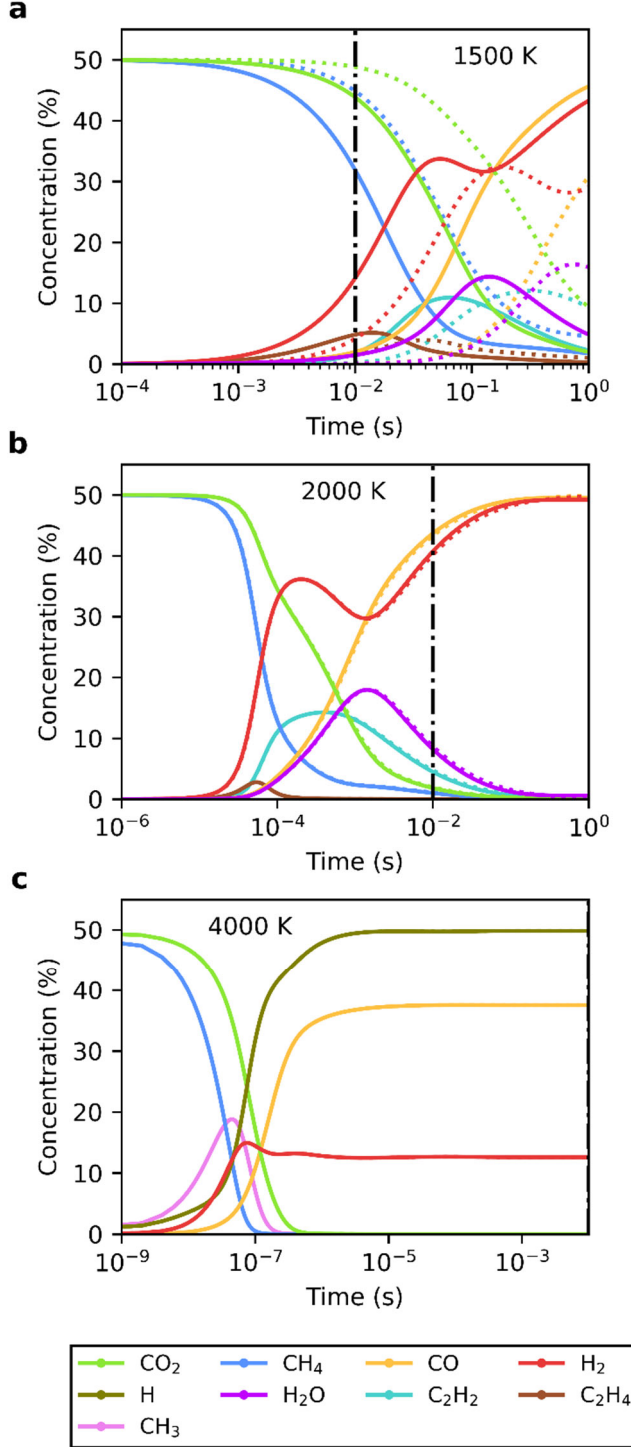


Figure 5: Concentration of the main plasma species as a function of residence time for a 50/50 mixture, at 1500 K (a), 2000 K (b) and 4000 K (c), for both thermal (dotted lines) and 1000 W/cm<sup>3</sup> plasma calculations (solid lines). For panels (a) and (b) an extended timescale is shown, with a vertical dash-dotted line marking the reference residence time of 10 ms. Panel (c) only shows up to 10 ms, because

steady state is already reached much earlier in time. Also, note that at 4000 K (panel (c)) H and CH<sub>3</sub> are major species, instead of H<sub>2</sub>O, C<sub>2</sub>H<sub>2</sub> and C<sub>2</sub>H<sub>4</sub>, which are formed less than 1%.

Figure 5a presents the time evolution at 1500 K, where the effects of the plasma kinetics were most significant, according to Figures 2 - 4. It is clear that the temporal concentration profiles (i.e., rise or drop as a function of time) are similar in both thermal and plasma kinetics, but the time-evolution occurs faster for the plasma condition. As both cases are still in the early stages of conversion at the residence time of 10 ms, we show an extended timescale to clearly indicate this shift in timescale between both conditions. Indeed, the product species reach a local maximum in concentration at a specific point in time, which is similar in absolute values, but the maximum is located earlier in time for the plasma case. For example, the maximum concentration reached for H<sub>2</sub>O is 16 % for the thermal conditions after 760 ms, while it is 14 % for the plasma condition and reached after only 142 ms. Hence, we can conclude that the plasma generally accelerates the conversion process, rather than altering the overall kinetic pathways and intermediate products. This suggests that electron impact reactions are important in the initial dissociation step, and much less in further reactions of the dissociation products.

Figure 5b illustrates the species concentrations as a function of time at 2000 K, where the plasma and thermal kinetics exhibit a negligible deviation; cf. Figure 2 - 4 (with a *wMAD* of only 0.44 %). Compared to Figure 5a (at 1500 K), the temporal concentration profiles look similar, but they are shifted to shorter timescales. Indeed, a higher temperature allows for faster reactions, so the simulations reach a further point in the reaction pathway at higher temperature. This allows the heavy species (thermal) kinetics to compete and even take over from the plasma-specific reactions, as will be further discussed in section 3.3.

Both Figures 5a and 5b indicate that the reaction pathways can be summarized as the conversion of CH<sub>4</sub> being the first step, yielding the formation of H<sub>2</sub> and C<sub>2</sub>-hydrocarbons (C<sub>2</sub>H<sub>2</sub> and C<sub>2</sub>H<sub>4</sub>). The conversion of CO<sub>2</sub> is slightly slower than for CH<sub>4</sub> and results in the formation of CO and H<sub>2</sub>O, the latter being

obtained through the reverse water gas shift reaction (Eq. 12). This explains the temporary drop in H<sub>2</sub> concentration.



Before reaching steady state, the created H<sub>2</sub>O and C<sub>2</sub> species react further into CO and H<sub>2</sub>. Hence, our calculations suggest that the conversion process can be tuned by the temperature and residence time, to more specifically target these valuable C<sub>2</sub> species. Indeed, C<sub>2</sub>H<sub>2</sub> reaches its maximum at 66 ms at 1500 K (Figure 5a) and at 0.40 ms at 2000 K (Figure 5b), while C<sub>2</sub>H<sub>4</sub> (which is even more valuable) reaches its maximum at 14 ms and 54 μs, at 1500 and 2000 K, respectively. However, these maximum concentrations are still lower than for H<sub>2</sub>, so post-plasma separation will be necessary, and even post-plasma catalysis [57], to valorize them. In general, it should be noted that further reactions in the post-plasma afterglow can also have an impact on the obtained species distribution, which is not considered in this work.

The chemical pathways clearly change upon higher temperatures, as presented in Figure 5c for 4000 K. The conversion does not proceed via H<sub>2</sub>O, C<sub>2</sub>H<sub>2</sub> or C<sub>2</sub>H<sub>4</sub>, like at 1500 and 2000 K, but instead, CH<sub>3</sub> and H radicals are formed in major concentrations, due to faster thermal CH<sub>4</sub> dissociation. The CH<sub>3</sub> radicals react further towards products (H<sub>2</sub>, CO), hence the drop in their concentration, while the H radicals build up more towards steady state, although finally they will recombine in the afterglow (not simulated here). As shown in Figures 2 - 4, at this temperature the effect of plasma is negligible, and the (thermal) kinetics is even faster, with the simulation reaching steady state well before the reference residence time of 10 ms.

It should also be noted that the time dependence in Figure 5 looks similar in shape to the temperature dependence in Figure 2. This can be explained by acceleration of the kinetics at higher temperature, resulting in the simulations reaching a further point in the reaction process. For the same reason, the formation of C<sub>2</sub>H<sub>2</sub>, C<sub>2</sub>H<sub>4</sub> and H<sub>2</sub>O shown in Figure 2b results from different points along the reaction path. The 10 ms timepoint at 1500 K (Figure 5a) is early in the reaction pathway, where the conversion just started. In contrast, the 2000 K case (Figure 5b) is already more towards the end of the pathway,

closer to reaching steady state. Hence, the maximum concentrations for C<sub>2</sub>H<sub>2</sub>, C<sub>2</sub>H<sub>4</sub> and H<sub>2</sub>O were already reached and both species are reacting away at the 10 ms timepoint, explaining why their concentrations are lower in Figure 2b at 2000 K than at 1700-1800 K.

From this analysis of the time dependence, we conclude that the plasma kinetics accelerates the conversion process, rather than changing the product distributions, but the effect is only significant for temperatures below 2000 K. Higher temperatures, on the other hand, lead to a change in reaction pathway, with radical formation being more significant due to efficient thermal dissociation. At lower temperatures, radicals are also formed, even by electron impact dissociation, but their concentrations remain below 1.5%.

### 3.3. Mechanisms of CO<sub>2</sub> and CH<sub>4</sub> conversion

The kinetic differences and similarities between the thermal and plasma conditions can also directly be explained from the (time-integrated) reaction rates. The relative contributions of the main loss reactions for CO<sub>2</sub> and CH<sub>4</sub> in a 50/50 CO<sub>2</sub>/CH<sub>4</sub> mixture are presented as a function of temperature in Figure 6. The conversion as a function of temperature is also plotted, for comparison. It is clear from Figure 6a that the CO<sub>2</sub> conversion is driven by electron impact dissociation up to 1500 K. The largest contributions are from direct electron impact dissociation (78 % at 1000 K) and dissociative attachment (21 % at 1000 K). However, the CO<sub>2</sub> conversion itself is still below 4 % in this temperature range. It only starts to rise dramatically above 1500 K, driven upon reaction with a H radical (starting from 1400 K), which is obtained from the CH<sub>4</sub> conversion. Above 1700-1800 K, the contribution of electron impact dissociation becomes negligible.

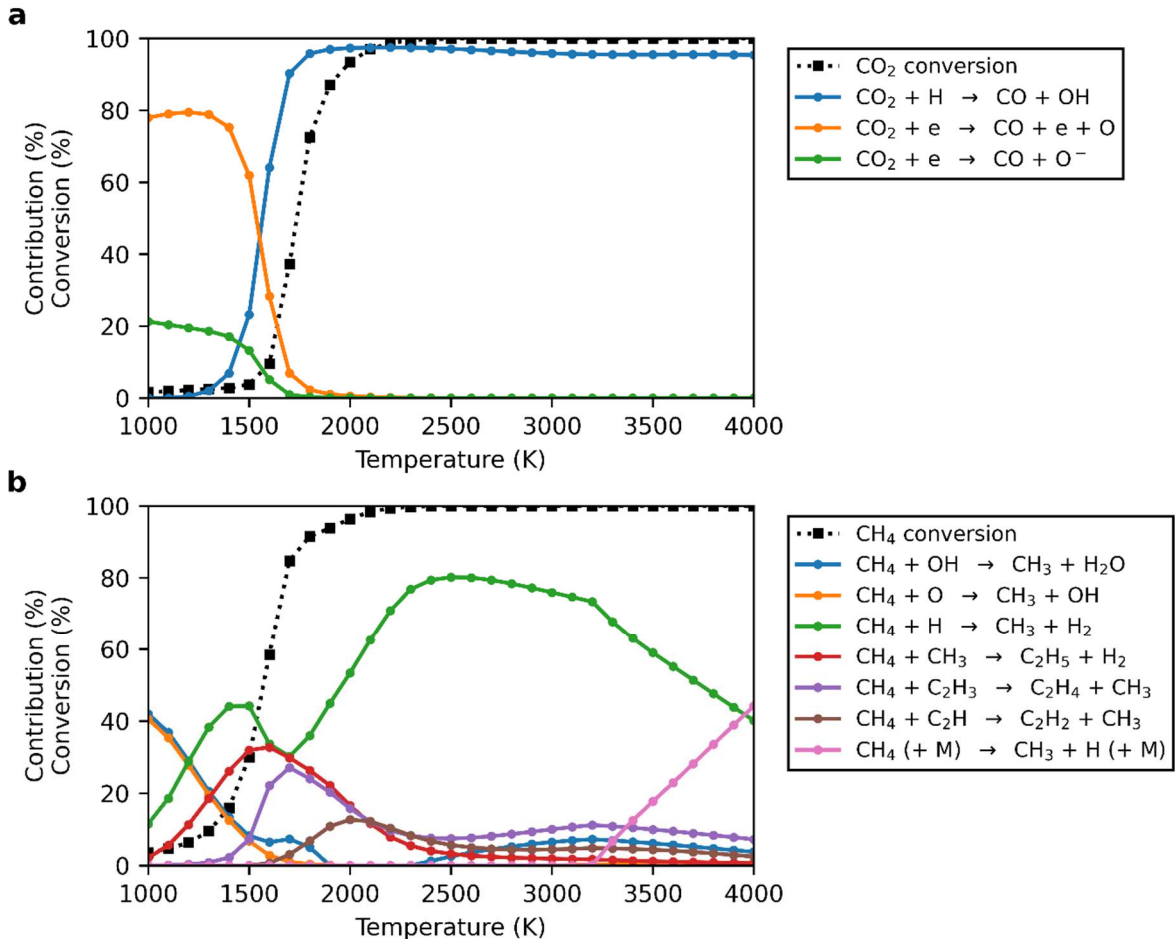


Figure 6: CO<sub>2</sub> (a) and CH<sub>4</sub> (b) conversion (dotted black lines), as well as the relative contributions of the main loss reactions (> 5 %) based on the time-integrated net reaction rates (see legends), as a function of temperature, for plasma simulations with a power density of 1000 W/cm<sup>3</sup> and for a 50/50 ratio of CO<sub>2</sub>/CH<sub>4</sub> at a residence time of 10 ms.

The CH<sub>4</sub> conversion occurs through heavy species reactions (see Figure 6b). At 1000 K the main dissociation reactions are with O and OH, contributing for 41 and 42 %, respectively, but decreasing with temperature. For temperatures below 1500 K, the O radicals originate from electron impact CO<sub>2</sub> dissociation, and OH is the product of CH<sub>4</sub> dissociation upon collision with O radicals (first reaction in the legend of Figure 6b). This means that one dissociated CO<sub>2</sub> molecule can dissociate two CH<sub>4</sub> molecules, by these two reactions. This effect, together with the lower C-H bond dissociation energy,

explains the much higher conversion of CH<sub>4</sub> compared to CO<sub>2</sub>, for temperatures below 1500 K (i.e., 30 % vs 4 % at 1500 K; cf. Figure 6).

Above 1500 K, reactions with H, CH<sub>3</sub> and C<sub>2</sub>H<sub>3</sub> take over as the main loss reactions for CH<sub>4</sub>. The reactions with CH<sub>3</sub> and C<sub>2</sub>H<sub>3</sub> have a maximum contribution of 33 % at 1600 K and 27 % at 1700 K, respectively. The highest contribution is obtained for the reaction with H radicals: it reaches a maximum of 44 % at 1500 K, then drops to 30 % at 1700 K and subsequently increases again to almost 80 % at 2500 K and above. The drop at 1700 K is due to the strong formation of H<sub>2</sub>O, effectively capturing H radicals, and thus lowering their contribution to CH<sub>4</sub> dissociation.

For temperatures above 2500 K, the CH<sub>3</sub> and C<sub>2</sub> radicals formed in the above dissociation reactions (see legend in Figure 6b) quickly convert further into CO and H<sub>2</sub>, allowing less of them to react with CH<sub>4</sub>, and thus reducing their contribution to the dissociation. On the other hand, the thermal dissociation of H<sub>2</sub> does allow H radicals to be still present and their contribution to the CH<sub>4</sub> dissociation is dominant in almost the entire temperature range, even up to 4000 K. The reaction with C<sub>2</sub>H radicals has a minor contribution to the overall CH<sub>4</sub> dissociation throughout the entire temperature range, with a maximum of 13 % at 2000 K. Above 3500 K, thermal dissociation of CH<sub>4</sub> into H and CH<sub>3</sub> upon collision with any neutral molecule (M) also becomes important, and its contribution rises with temperature to reach 44 % at 4000 K. These dissociation pathways agree with the work presented by Liu et al. [26] in which the reaction with H is the main dissociation reaction for both CO<sub>2</sub> and CH<sub>4</sub> at a gas temperature of 2500 K.

Our model indicates that direct dissociation of CH<sub>4</sub> through electron impact reactions is not important within the given parameter space. However, below 1500 K the importance of O and OH radicals links the dissociation of CH<sub>4</sub> to electron impact dissociation reactions of CO<sub>2</sub>. Therefore, the DRM reaction pathways are really a coupled process between CO<sub>2</sub> and CH<sub>4</sub>, both requiring the other species for the chemical reactions.

As the main CO<sub>2</sub> dissociation pathway for gas temperatures below 1700 K is through electron impact reactions, we also present the electron density and electron temperature, to further explain these findings (Figure 7). Firstly, this figure shows that the electron density steadily increases from around  $2 \times 10^{11}$  to

$2 \times 10^{13} \text{ cm}^{-3}$  within the studied gas temperature range. This indicates that a high electron density is not the main driver behind the electron impact dissociation of CO<sub>2</sub> below 1700 K (Figure 6). On the other hand, the electron temperature (around 17000 K) is significantly higher for these lower gas temperatures, resulting in a larger fraction of electrons with sufficient energy to dissociate CO<sub>2</sub>. This in turn leads to higher reaction rates for electron impact dissociation reactions, increasing their contributions in Figure 6. While it is logical that the electron temperature decreases upon rising electron density, the sharp decrease indicates other effects are responsible. It should also be noted that this coincides with a strong increase in conversion and the formation of CO, H<sub>2</sub>, C<sub>2</sub>H<sub>2</sub> and H<sub>2</sub>O (Figure 2). Therefore, we relate this lower electron temperature above 1700 K to these species. They have larger elastic collisional cross sections, compared to CO<sub>2</sub> and CH<sub>4</sub>, and combined with their higher concentrations, this results in more electron energy loss, i.e., a lower electron temperature.

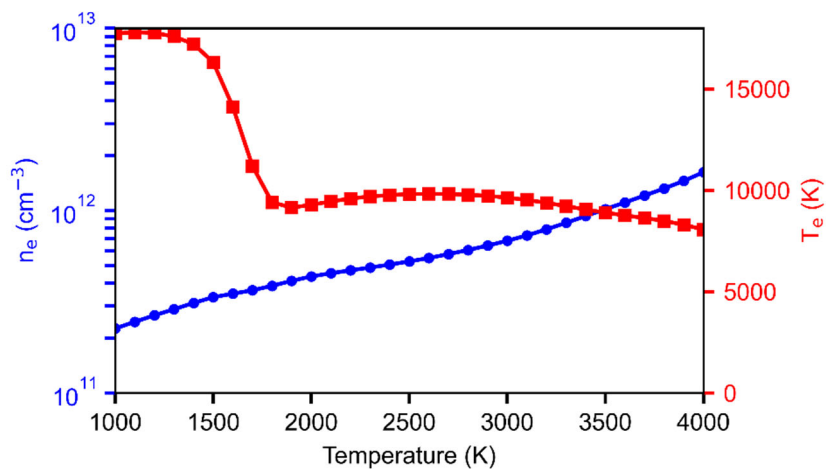


Figure 7: Calculated electron density (blue line) and electron temperature (red line) for the gas temperature range of 1000 to 4000 K and a 50/50 CO<sub>2</sub>/CH<sub>4</sub> ratio and 1000 W/cm<sup>3</sup> plasma condition, at a residence time of 10 ms.

In general, we can conclude that thermal kinetics dominates the dissociation process above 2000 K, while electron impact reactions are the main mechanism for CO<sub>2</sub> dissociation below 1500 K. Figures 4 and S2 indicate that a variation in power density within a range typical for warm plasmas does not significantly alter the temperature at which thermal kinetics starts to dominate.

Electron impact dissociation occurs through excitation to high electronically excited states, which requires more energy than direct thermal dissociation [3,58]. This explains why warm plasmas, for which the conversion is largely thermal, are more energy efficient than cold (or non-thermal) plasmas, which operate near room temperature and have a large contribution of electron impact dissociation, because thermal chemistry is negligible. In addition, cold plasmas require a higher power density to improve the conversion, due to their dependence on electron impact reactions. This is consistent with experimental findings from literature, which illustrate a much lower energy cost for DRM in warm plasmas (such as GA, MW, APGD and NPD) than in non-thermal plasmas (such as DBD) [3,4,11–14,17,59].

### 3.4. Effect of gas mixing ratio

In previous section (3.3) we only considered the stoichiometric gas mixture (50/50). In this section we extend the analysis to mixtures with excess CO<sub>2</sub> or CH<sub>4</sub>. First, we can make the same general conclusions as for the 50/50 ratio. Below 2000 K, we again observe the acceleration effect of the plasma kinetics, which becomes negligible towards 2000 K. Furthermore, thermodynamic equilibrium is also reached within the simulation timescale of 10 ms. Hence, the effects of the plasma are the same, but the product distribution is significantly altered, because of the deviation from the stoichiometric mixture. Competing side reactions cause the products to deviate from the DRM reaction as presented in Eq. 1 in the Introduction.

#### 3.4.1. Mixtures with excess CO<sub>2</sub>

For mixtures with excess CO<sub>2</sub> (i.e., 90/10 and 70/30 CO<sub>2</sub>/CH<sub>4</sub> ratio) the concentrations of the major species are plotted as a function of temperature in Figure 8. First of all, as expected, we note a significantly higher CO<sub>2</sub> concentration at 1000 K (in line with the mixing ratio), as there is no conversion yet, and a clear drop in CO<sub>2</sub> concentration upon increasing temperature. Furthermore, unlike the 50/50 ratio, where complete conversion was achieved above 2000 K, mixtures with excess CO<sub>2</sub> require higher temperatures to reach full conversion. At 2000 K, the CO<sub>2</sub> concentration is still about 10 % and even about 50 %, for the 70/30 and 90/10 CO<sub>2</sub>/CH<sub>4</sub> ratios, respectively. These values agree with

the concentrations at thermodynamic equilibrium, presented in the SI (Figure S1(a,b)). Hence, the CO<sub>2</sub> conversion for these mixtures is strongly limited by the thermodynamic equilibrium above 2000 K. Nevertheless, upon increasing temperature, the CO<sub>2</sub> concentration drops further, to 0.6 % and 2.1 % at 4000 K, for the 70/30 and 90/10 mixtures, respectively, because CO<sub>2</sub> becomes less thermodynamically favored. At these high temperatures, O and OH radicals are formed in large amounts, but they can react back to CO<sub>2</sub> in the afterglow. Hence, for mixtures containing an excess of CO<sub>2</sub> (70/30 and 90/10 CO<sub>2</sub>/CH<sub>4</sub>), the CO<sub>2</sub> conversion is strongly limited by the thermodynamic equilibrium, while a complete conversion of CH<sub>4</sub> can be achieved below 2000 K.

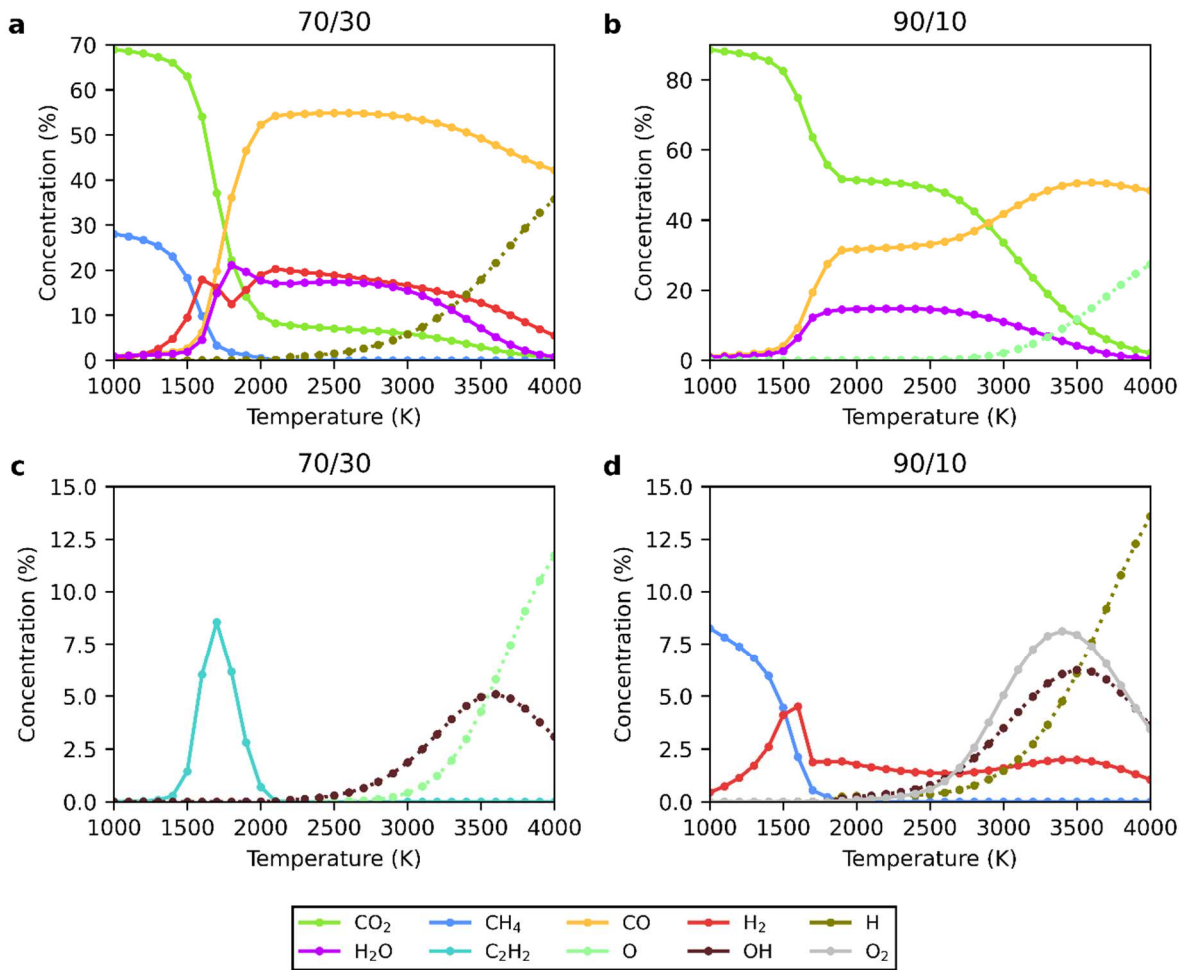
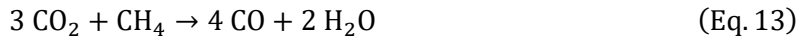


Figure 8: Calculated concentrations of the main plasma species ( $> 4\%$ ) as a function of temperature, for a 70/30 and 90/10 CO<sub>2</sub>/CH<sub>4</sub> ratio, at a residence time of 10 ms for the 1000 W/cm<sup>3</sup> plasma conditions. The species are split over 2 panels according to their concentration: the top panels (a and b) plot the largest concentration species for the 70/30 and 90/10 mixtures, respectively, while the lower

concentration species are illustrated in the bottom panels (c and d), for the 70/30 and 90/10 mixtures, respectively. The stable molecules and radicals are depicted with solid and dotted lines, respectively, for easy recognition.

It is also clear from Figure 8 that CO is the major product in case of excess CO<sub>2</sub>, with a maximum concentration of 55 % at 2600 K and 51 % at 3600 K, for the 70/30 and 90/10 CO<sub>2</sub>/CH<sub>4</sub> ratios, respectively. On the other hand, the excess of O atoms, originating from CO<sub>2</sub>, strongly reduces the formation of H<sub>2</sub>, and instead favors the formation of H<sub>2</sub>O. This is also indicated by the thermodynamic equilibrium concentrations (Figure S1). This is in contrast with the 50/50 CO<sub>2</sub>/CH<sub>4</sub> ratio, where H<sub>2</sub>O was only an intermediate species in the reaction pathway towards H<sub>2</sub> and CO (cf. Figure 5). The H<sub>2</sub> concentration reaches a maximum of 20 % at 2100 K and 4.5 % at 1600 K, for the 70/30 and 90/10 ratios, respectively. In contrast, the H<sub>2</sub>O concentration reaches similar values to H<sub>2</sub> for the 70/30 ratio (max. 21 % at 1800 K), while it is significantly higher for the 90/10 ratio (max. 15 % at 2300 K). We observe the competition of Eq. 13 as a side reaction, which is the combination of DRM (Eq. 1) and twice the reverse water gas shift reaction (Eq. 12).



Above 2500 K, H, OH and O radicals are also formed in significant amounts, due to thermal decomposition of H<sub>2</sub>, H<sub>2</sub>O and CO<sub>2</sub>. However, these radicals will react away in the post-plasma afterglow. For instance, the O radicals can recombine with CO into CO<sub>2</sub>, reducing its conversion. Indeed, this back-reaction plays an important role in the afterglow of pure CO<sub>2</sub> plasmas [39,60–62], and is thus expected to be significant in DRM as well, especially at large CO<sub>2</sub> fractions. Finally, below 2000 K, we also see the formation of C<sub>2</sub>H<sub>2</sub>, but only with a maximum concentration of 8.6 and 2.5 %, for the 70/30 and 90/10 ratios, respectively, while the C<sub>2</sub>H<sub>4</sub> concentration is even lower.

The change in gas mixture influences the dissociation mechanisms of CO<sub>2</sub> and CH<sub>4</sub> compared to the 50/50 ratio presented in Figure 6. Figure 9 depicts the relative contributions of the main loss reactions

for CO<sub>2</sub> and CH<sub>4</sub> in a 90/10 CO<sub>2</sub>/CH<sub>4</sub> mixture as a function of temperature. The same trends are observed for the 70/30 mixture, which is presented in the supporting information (Figure S4).

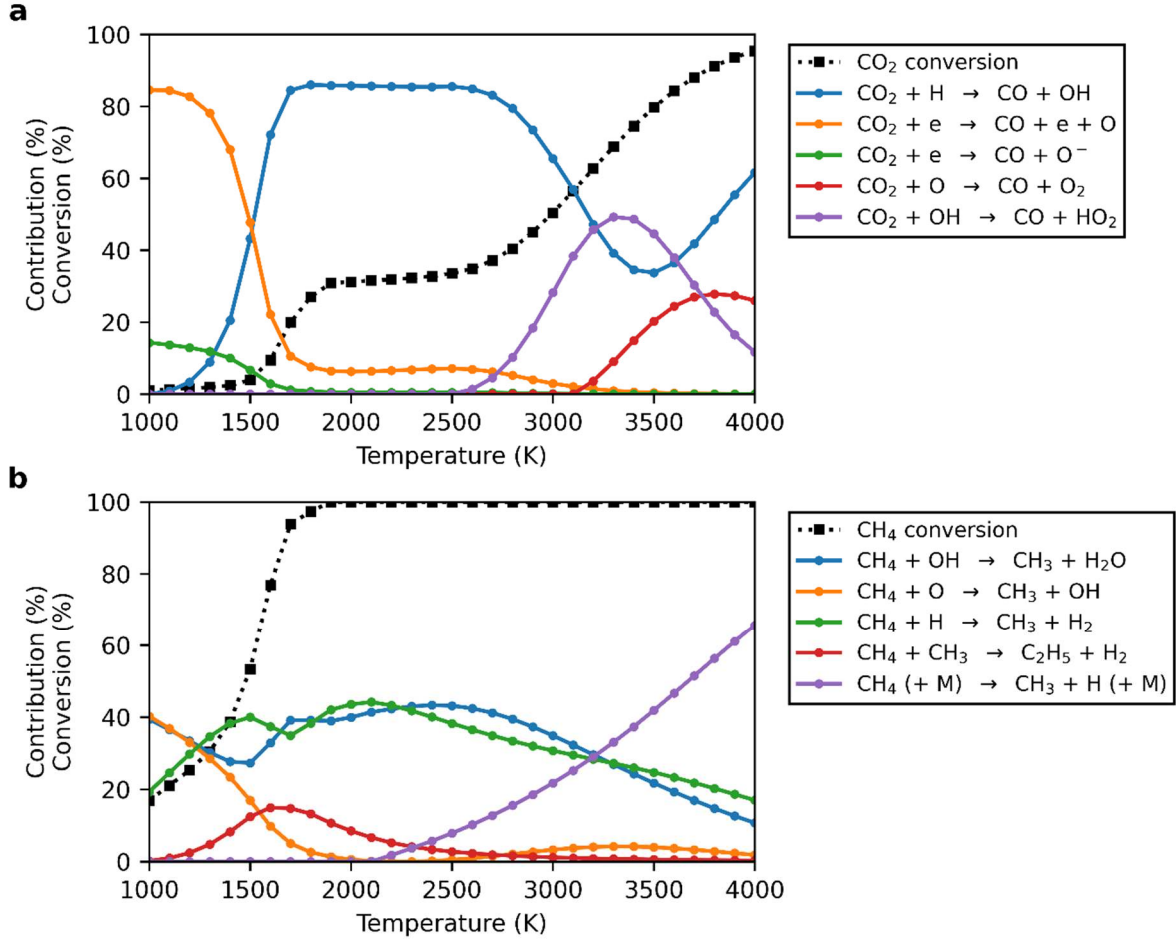


Figure 9: CO<sub>2</sub> (a) and CH<sub>4</sub> (b) conversion (dotted black lines), as well as the relative contributions of the main loss reactions (> 5 %) based on the time-integrated net reaction rates (see legends), as a function of temperature, for plasma simulations with a power density of 1000 W/cm<sup>3</sup> and for a 90/10 ratio of CO<sub>2</sub>/CH<sub>4</sub> at a residence time of 10 ms.

Electron impact dissociation is the main loss reaction for CO<sub>2</sub> below 1500 K, but still contributes for around 6.5 % between 2000 and 3000 K, in contrast to the 50/50 CO<sub>2</sub>/CH<sub>4</sub> mixture, where electron impact dissociation became negligible above 2000 K (Figure 6). Figure 4 indeed shows a slight difference between the plasma and thermal calculations in this temperature range for the 90/10 CO<sub>2</sub>/CH<sub>4</sub>

mixture (maximum *wMAD* of 0.71 % at 2500 K). This is attributed to the large amount of CO<sub>2</sub> (around 50 %) still present in the mixture, while electron impact dissociation of CO<sub>2</sub> is still notable in this temperature range. This effect is however minor and does not significantly change the overall product concentrations. Indeed, between 1500 and 3000 K, most CO<sub>2</sub> is converted upon reaction with H radicals (see Figure 9a), similar to the 50/50 ratio. Finally, for gas temperatures approaching 3000 K, the reactions with OH and O radicals become increasingly important, and the conversion further increases to nearly 100 % at 4000 K, with a negligible contribution of electron impact dissociation.

For CH<sub>4</sub> dissociation (Figure 9b), largely the same reactions and temperature dependence is observed as for the 50/50 ratio of CO<sub>2</sub>/CH<sub>4</sub> (Figure 6). However, reactions involving CH<sub>4</sub> dissociation products (H, CH<sub>3</sub>, C<sub>2</sub>H and C<sub>2</sub>H<sub>3</sub>) do contribute less, which is logical, as the excess of CO<sub>2</sub> reduces their overall concentration. The contribution of C<sub>2</sub>H and C<sub>2</sub>H<sub>3</sub> are reduced to less than 5 % over the studied temperature range (1000 – 4000 K) and therefore not shown in Figure 9b. The reaction with OH increases significantly up to 43 %, and is therefore comparable with the reaction upon collision with H radicals (which was dominant at the 50/50 ratio of CO<sub>2</sub>/CH<sub>4</sub>; Figure 6). Finally, also thermal decomposition is increasingly more important above 2200 K, with a contribution of 66 % at 4000 K.

Again, our model shows similar findings to the work of Liu et al. [26] for the same CO<sub>2</sub>/CH<sub>4</sub> ratio at 2500 K, where the reaction with H is again the largest contributor to CO<sub>2</sub> dissociation, while for CH<sub>4</sub> dissociation, H and OH have the highest contribution in our results, but we find a lower contribution of the reaction with any neutral species (M) compared to Liu et al. This is likely related to differences in the modelling approach and kinetic schemes.

### 3.4.2. Mixtures with excess CH<sub>4</sub>

Figure 10 shows the species concentrations as a function of temperature, for mixtures with excess CH<sub>4</sub> (i.e., 30/70 and 10/90 ratio). The corresponding thermodynamic equilibrium concentrations are plotted in the SI (Figure S1(c,d)). The much lower O atom concentration in the mixture limits the oxidation of CH<sub>4</sub> into CO. Consequently, the CO concentration only reaches a maximum of 30 % at 2200 K for the 30/70 ratio and 10 % at 2100 K for the 10/90 ratio. CH<sub>4</sub> is still fully converted above 2000 K, although

not to CO, but to H<sub>2</sub> and C<sub>2</sub>H<sub>2</sub>. H<sub>2</sub> is by far the most abundant product, reaching concentrations of 60 % at 2200 K and nearly 70 % at 2100 K, for the 30/70 and 10/90 ratios, respectively. C<sub>2</sub>H<sub>2</sub> is the third major product (after H<sub>2</sub> and CO) for the 30/70 ratio, with a maximum concentration of 17 % at 1700 K, and it is even the second major project after H<sub>2</sub>, reaching 22 % at 1800 K, for the 10/90 ratio. However, these values are obtained below 2000 K, where steady state is not fully reached yet at 10 ms residence time, so the concentration is expected to drop again upon longer residence time. Similarly, a maximum concentration of 11 % and 3.5 % is observed for H<sub>2</sub>O at 1800 K, for the 70/30 and 10/90 CO<sub>2</sub>/CH<sub>4</sub> mixtures, respectively. As inferred from Figure 5, H<sub>2</sub>O is formed as an intermediate species, which is present at those conditions because the conversion process is still ongoing. Finally, H atoms are the main radicals formed at high temperature, upon thermal decomposition of H<sub>2</sub>, and they become even the dominant species above 3500 K, with also small amounts (up to 7 %) of C<sub>2</sub>H.

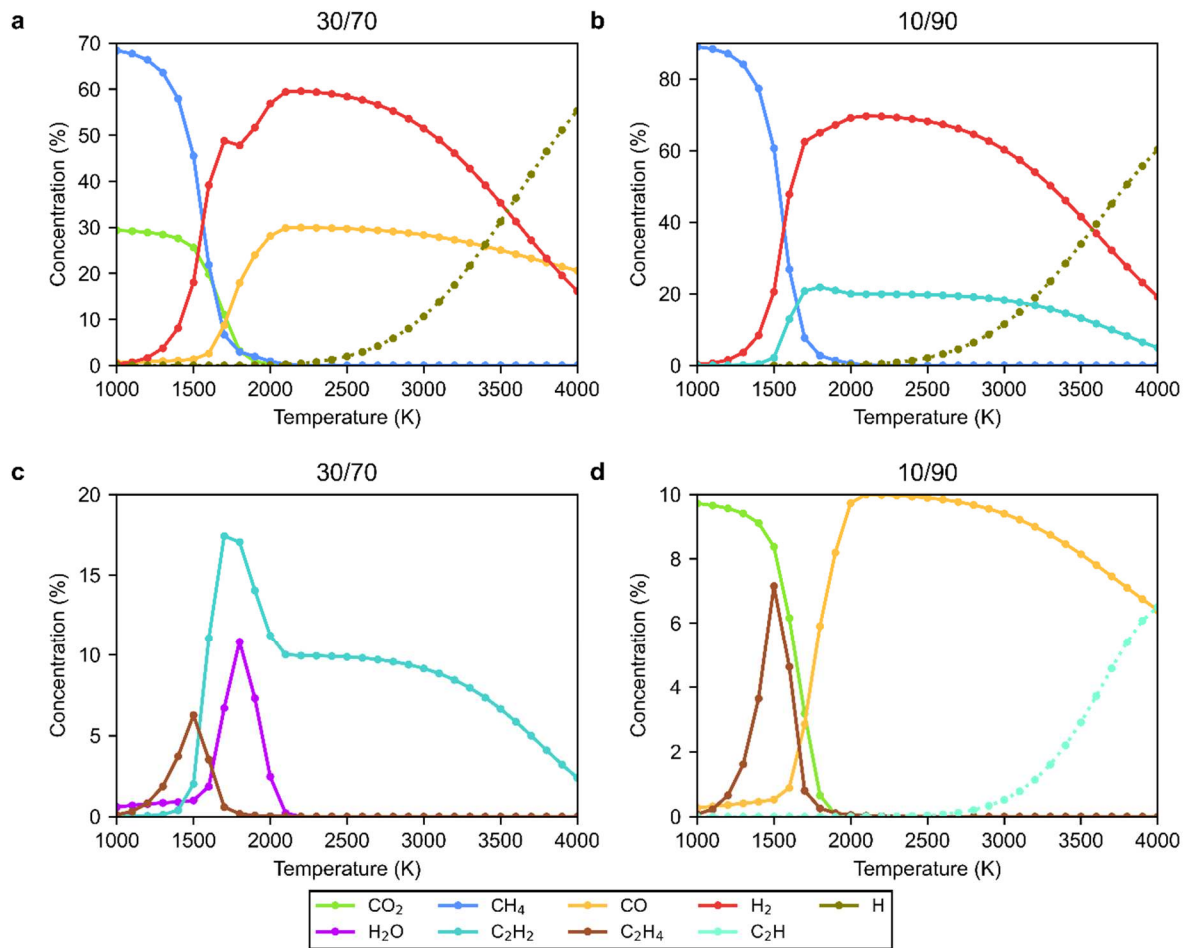


Figure 10: Calculated concentrations of the main plasma species ( $> 4\%$ ) as a function of temperature, for the 30/70 and 10/90 CO<sub>2</sub>/CH<sub>4</sub> ratio, at a residence time of 10 ms for the 1000 W/cm<sup>3</sup> plasma conditions. The species are split over 2 panels according to their concentration: the top panels (a and b) plot the large concentration species for the 30/70 and 10/90 mixtures, respectively, while the lower concentration species are illustrated in the bottom panels (c and d) for the 30/70 and 10/90 mixtures, respectively. The stable molecules and radicals are depicted with solid and dotted lines, respectively, for easy recognition.

We confirm that the lower O atom concentration, due to the limited CO<sub>2</sub> concentration in the mixture, allows Eq. 14 to be more important, producing C<sub>2</sub>H<sub>2</sub> as a final product. Furthermore, we observe several other benefits for these mixing ratios, such as full conversion of both reactants and H<sub>2</sub>/CO ratios above 1, which are preferred for the downstream processing of syngas into desired products, as discussed in depth in section 3.5. However, mixtures with excess CH<sub>4</sub> are more difficult to handle in practice, due to excessive solid carbon formation [14–18], which is not taken into account yet in our model. On the other hand, our model does show significant formation of C<sub>2</sub>H<sub>2</sub>, which might be overestimated as this is an important precursor species for the formation of solid carbon [49,63,64], which is not yet accounted for in our model.



The relative contributions of the main loss reactions for CO<sub>2</sub> and CH<sub>4</sub> in a 10/90 CO<sub>2</sub>/CH<sub>4</sub> mixture as a function of temperature are presented in Figure 11. The same trends are observed for the 30/70 mixture, which is presented in the supporting information (Figure S5).

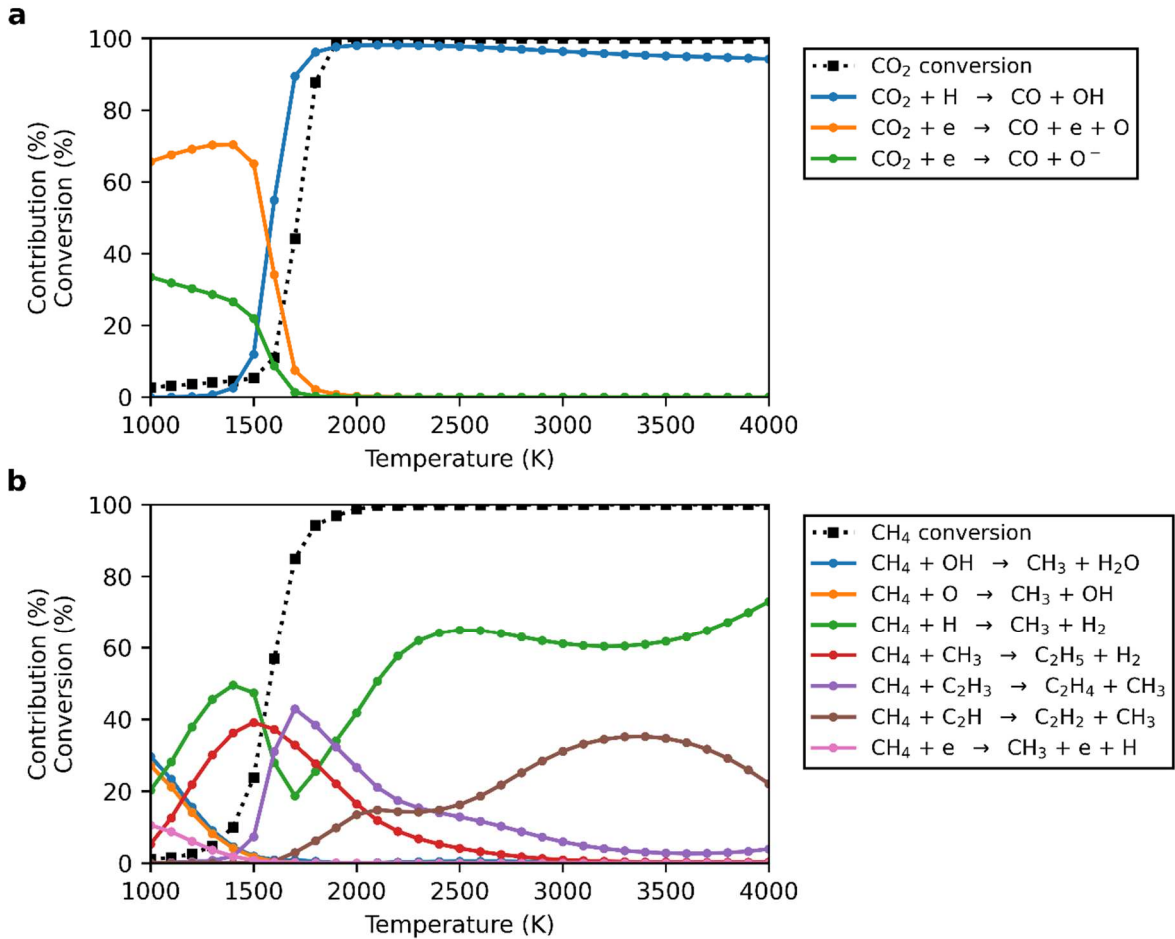


Figure 11:  $\text{CO}_2$  (a) and  $\text{CH}_4$  (b) conversion (dotted black lines), as well as the relative contributions of the main loss reactions ( $> 5\%$ ) based on the time-integrated net reaction rates (see legends), as a function of temperature, for plasma simulations with a power density of  $1000 \text{ W/cm}^3$  and for a 10/90 ratio of  $\text{CO}_2/\text{CH}_4$  at a residence time of 10 ms.

The reaction mechanism for dissociation of  $\text{CO}_2$  (Figure 11a) is very similar to that for the 50/50  $\text{CO}_2/\text{CH}_4$  mixture (Figure 6a). Below 1500 K electron impact reactions are the main dissociation mechanism, and above 1500 K the reaction with H is the most significant. However, for  $\text{CH}_4$  (Figure 11b) there are more significant changes in the dissociation reactions. Firstly, electron impact dissociation now has a non-negligible contribution in the lower temperature range ( $< 1500 \text{ K}$ ) with a maximum of 11 % at 1000 K. The higher concentrations of  $\text{CH}_4$  dissociation products further increase their contribution to the dissociation process of  $\text{CH}_4$ . Therefore, reactions with  $\text{CH}_3$  and  $\text{C}_2\text{H}_3$  become

more important, and their maximum contributions rise to 39 % at 1500 K and 43 % at 1700 K, respectively, followed by a drop towards 3000 K. The reaction with H takes over the dissociation of CH<sub>4</sub>, similar to the 50/50 ratio, however with a lower contribution, as the rate of the reaction with C<sub>2</sub>H has increased between 2000 – 4000 K. These reactions are the two most important up to 4000 K. On the other hand, the thermal dissociation of CH<sub>4</sub> remains below 5 % and is therefore not shown in Figure 11b. This is caused by the much higher concentration of CH<sub>4</sub> dissociation products in the mixture.

### 3.5. Optimization of the syngas ratio

The main product of DRM is syngas and the obtained syngas ratio (H<sub>2</sub>/CO ratio) is important to evaluate the performance of DRM, with regard to further post-processing. For the Fischer-Tropsch process and methanol synthesis from syngas, a syngas ratio around 2 is desired [65]. The CO<sub>2</sub>/CH<sub>4</sub> ratio is important for controlling the syngas ratio, as illustrated in Figure 12, which depicts the syngas ratio as a function of temperature at 10 ms for the five gas mixtures.

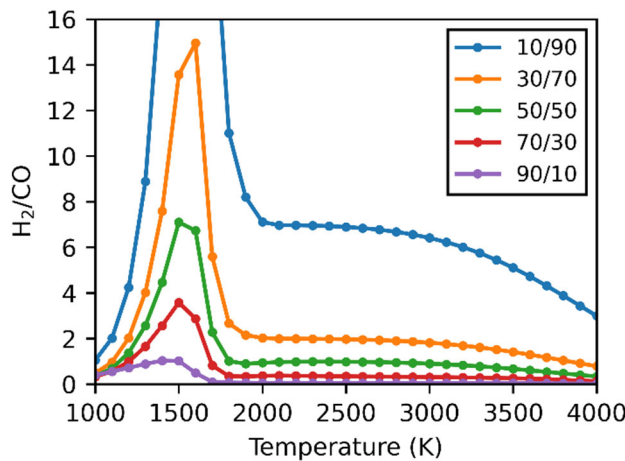


Figure 12: Syngas ratio (H<sub>2</sub>/CO) obtained at a residence time of 10 ms, as a function of temperature, for five different CO<sub>2</sub>/CH<sub>4</sub> ratios (90/10, 70/30, 50/50, 30/70, 10/90). For the 10/90 mixture, the peak in syngas ratio is 54 (outside of the y-axis scale).

Near 1000 K, all gas mixtures result in syngas ratios below 1, even though at these conditions more CH<sub>4</sub> is converted than CO<sub>2</sub>. Indeed, the syngas ratio remains low due to the formation of side products,

like  $\text{H}_2\text{O}$ ,  $\text{C}_2\text{H}_2$  and  $\text{C}_2\text{H}_4$ , which compete with  $\text{H}_2$  formation. Raising the temperature to about 1500 K strongly enhances the syngas ratio, as the  $\text{CH}_4$  conversion and  $\text{H}_2$  formation strongly increase compared to the  $\text{CO}_2$  conversion and CO production. This is attributed to the faster reaction kinetics at higher temperatures, with the  $\text{CO}_2$  conversion typically lagging behind on the  $\text{CH}_4$  conversion, and the fact that steady state is not yet reached within 10 ms at this temperature (cf. Figure 5). The difference between the  $\text{CH}_4$  and  $\text{CO}_2$  conversion reaches a maximum around 1500 K, leading to the highest syngas ratios (see Figure 12). For the most extreme cases (i.e., 10/90 and 90/10  $\text{CO}_2/\text{CH}_4$  ratios) syngas ratios of 54 and 1.0 are reached, respectively. The other  $\text{CO}_2/\text{CH}_4$  ratios provide syngas ratios (well) above 3 at this temperature, and thus, neither of the conditions seem desirable. Raising the temperature further up to 2000 K, the  $\text{CO}_2$  conversion rises further, and the  $\text{CH}_4$  approaches the steady state limit, leading to a drop in syngas ratio. At 2000 K, the syngas ratio decreases to 0.93 for the stoichiometric mixture, while we obtain lower syngas ratios for mixtures with excess  $\text{CO}_2$ , i.e., 0.36 and 0.056 for 70/30 and 90/10  $\text{CO}_2/\text{CH}_4$ , respectively. On the other hand, for mixtures with excess  $\text{CH}_4$ , the syngas ratio remains above 1, i.e., 2.0 and 7.1 for 30/70 and 10/90, respectively. These results are logical, considering the competing side reactions discussed in section 3.4, allowing for more  $\text{H}_2$  formation through Eq. 14. Finally, the syngas ratio slightly decreases upon higher temperatures, as the formation of H radicals becomes significant, resulting in less  $\text{H}_2$ . However, in practice, this will not be a problem, because after the plasma, the H radicals can recombine back into  $\text{H}_2$ , which is not simulated by our model.

Hence our model predicts that syngas ratios of 2 (and above) are achievable for all gas mixing ratios, except for 90/10  $\text{CO}_2/\text{CH}_4$ , at a temperature around 1500 K, due to kinetic effects, because the  $\text{CH}_4$  conversion initially rises faster than that of  $\text{CO}_2$ . As such, high syngas ratios can be achieved by limiting the conversion, even for mixtures with excess  $\text{CO}_2$ . However, due to the limited conversion, the corresponding syngas yield will be low. Moreover, the strong time and temperature dependences make it difficult to target these specific conditions. We believe it is better to target the temperature region above 2000 K, when steady state and maximum conversion are reached. Obviously, a syngas ratio of 2 can be obtained from the 30/70  $\text{CO}_2/\text{CH}_4$  ratio, at high conversion and thus also high syngas yield.

### 3.6. Final considerations: Limitations of our model and of DRM

Note that experimental setups are inherently more inhomogeneous than our idealized batch reactor model, due to temperature gradients, transport of species, residence time distributions, as well as the afterglow region, in which back-reactions can occur. Together these effects can introduce deviations from our model predictions, but we believe that our model is valuable to gain deeper insights in the underlying mechanism, and to search for optimized reactor conditions.

Note that our model predicts a variety of products being formed at all conditions investigated, and this is also experimentally observed, although syngas is typically the major product, in line with our calculations. Moreover, in reality the CO<sub>2</sub> and CH<sub>4</sub> conversion will be typically below 100 %, due to post-plasma recombination of the reaction products back into CO<sub>2</sub> and CH<sub>4</sub> [39,60–62,66], and because not all gas will pass through the active plasma region, and thus, being subject to conversion [6,8,11,67]. The unconverted reactants (CO<sub>2</sub> and CH<sub>4</sub>), as well as the side products (like C<sub>2</sub>H<sub>2</sub> and H<sub>2</sub>O) next to syngas require an extra separation step before further processing. Unfortunately, this cannot be avoided when considering only a binary mixture of CO<sub>2</sub> and CH<sub>4</sub>, because there exists no mixing ratio that allows complete conversion, in combination with the optimal syngas ratio of 2, and no side products. Therefore, it might be interesting to explore other mixtures, such as CO<sub>2</sub>/CH<sub>4</sub>/H<sub>2</sub>O (so-called bi-reforming of methane). Indeed, theoretically, this mixture, in a ratio of 1/3/2, can stoichiometrically produce pure syngas with a ratio of 2 at full conversion without side products [68,69]. This may be interesting to investigate in future work.

#### 4. Conclusion

We studied the chemical kinetics of plasma-based DRM by means of batch reactor simulations, in a temperature range between 1000 and 4000 K relevant for warm plasma conditions and a wide range of CO<sub>2</sub>/CH<sub>4</sub> ratios, and we compared with pure thermal conversion, as well as thermodynamic equilibrium calculations. This computational study provides a broad view of the influence of plasma parameters on conversion and product distribution, and insights into possible improvements to the process. Importantly, we provided an update of the chemical kinetics scheme compared to earlier models by our group PLASMANT, consisting of 70 different species and 1468 different chemical reactions. We were

able to verify and validate the thermal chemistry in our model at steady state, by reproducing thermodynamic equilibrium concentrations.

Furthermore, we used the model to compare plasma-based DRM to purely thermal gas-phase DRM, thereby isolating the influence of electron and ion reactions and thus revealing the contribution of the plasma-specific chemistry. Our simulations show that plasma can significantly improve the conversion below 2000 K, compared to the pure thermal chemistry. This is attributed to electron impact dissociation of CO<sub>2</sub>, which creates O atoms, that give rise to CH<sub>4</sub> conversion. This electron impact reaction can occur at low gas temperatures, allowing the first step in the conversion process to proceed. On the other hand, the purely thermal conversion, without electrons, must rely on molecular collisions to dissociate CO<sub>2</sub> and CH<sub>4</sub> which in this temperature range (below 2000 K) are much slower and cannot obtain significant dissociation. Note that this acceleration does not significantly alter the product distribution, but only the timescale at which they are formed, as the further reactions to product species are through radical reactions, which are the same in both the plasma and thermal process. Consequently, the residence time is an important parameter to target certain products, because for this temperature range (below 2000 K) steady state is not yet reached for residence times in the ms-range.

When increasing the temperature above 2000 K, thermal reactions start to dominate the kinetics in the plasma, even when varying the power density between 500 and 1500 W/cm<sup>3</sup> (i.e., the typical range characteristic for warm plasmas). Hence the kinetics of warm plasmas, which typically operate above 2000 K, can be described by thermal chemistry. The importance of thermal conversion at these high temperatures explains why warm plasmas are typically more energy-efficient than non-thermal (cold) plasmas, where the conversion occurs by electron impact dissociation, requiring more energy than strictly needed for bond breaking.

Furthermore, we studied the effect of the CO<sub>2</sub>/CH<sub>4</sub> ratio on the conversion, product distribution and syngas ratio. Mixtures containing excess CO<sub>2</sub> lead to the formation of H<sub>2</sub>O, at the expense of H<sub>2</sub> production. Moreover, at temperature where steady state is reached, the CO<sub>2</sub> conversion is limited by thermodynamic equilibrium. As a result, full conversion can only be achieved at extremely high temperatures above 4000 K, through dissociation into radicals. Yet, such large concentrations of

radicals can recombine back into CO<sub>2</sub> in the afterglow, which will lower the final conversion. From this we conclude that mixtures with excess CO<sub>2</sub> have several disadvantages; mainly the limited conversion combined with the low H<sub>2</sub>, and high H<sub>2</sub>O production are unfavorable for further processing. On the other hand, for gas mixtures with an excess of CH<sub>4</sub>, full conversion can be achieved, as this is thermodynamically favored at temperatures for which steady state is reached (above approximately 2100 K). Due to the increased H content in the mixture, a high concentration of H<sub>2</sub> can be obtained, while C<sub>2</sub>H<sub>2</sub> becomes a major carbon product, competing with CO.

Finally, our model predicts that high syngas ratios can be achieved in the temperature range between 1000 and 2000 K, by carefully exploring the kinetics (i.e., selecting the right residence time and temperature), due to the faster destruction of CH<sub>4</sub> compared to CO<sub>2</sub> at these conditions. However, this also limits the conversion and consequently the syngas yield. At higher temperatures, where steady state is reached, high syngas ratios can be obtained by using gas mixtures with an excess of CH<sub>4</sub>. We found a mixture of 30/70 CO<sub>2</sub>/CH<sub>4</sub> to be optimal for obtaining a syngas ratio of 2, which is important for further processing using the Fischer-Tropsch process and methanol synthesis.

Altogether, we believe our model predictions are useful to gain deeper insights in the underlying chemical kinetics of DRM, for a broad range of conditions, independent of actual reactor designs. This knowledge can be further employed in designing and optimizing experimental reactors to improve the DRM process.

## Acknowledgments

This research was supported by the European Research Council (ERC) under the European Union's Horizon 2020 research and innovation programme (Grant Agreement No. 810182 – SCOPE ERC Synergy project), the Catalisti-ICON project BluePlasma (Project No. HBC.2022.0445), the FWO-SBO project PlasMaCatDESIGN (FWO Grant ID S001619N), the Independent Research Fund Denmark (Project No. 0217-00231B) and through long-term structural funding (Methusalem). The computational resources and services used in this work were provided by the HPC core facility CalcUA of the

Universiteit Antwerpen, and VSC (Flemish Supercomputer Center), funded by the Research Foundation - Flanders (FWO) and the Flemish Government. We also thank Bart Wanten, Roel Michiels, Pepijn Heirman, Claudia Verheyen, dr. Senne Van Alphen, dr. Elise Vervloessem, dr. Kevin van 't Veer, dr. Joshua Boothroyd, dr. Omar Biondo and dr. Eduardo Morais for their expertise and feedback regarding the kinetics scheme.

## References

- [1] Cuéllar-Franca RM, Azapagic A. Carbon capture, storage and utilisation technologies: A critical analysis and comparison of their life cycle environmental impacts. *J CO<sub>2</sub> Util* 2015;9:82–102. <https://doi.org/10.1016/j.jcou.2014.12.001>.
- [2] Bogaerts A, Neyts EC. Plasma Technology: An Emerging Technology for Energy Storage. *ACS Energy Lett* 2018;3:1013–27. <https://doi.org/10.1021/acsenergylett.8b00184>.
- [3] Snoeckx R, Bogaerts A. Plasma technology – a novel solution for CO<sub>2</sub> conversion? *Chem Soc Rev* 2017;46:5805–63. <https://doi.org/10.1039/C6CS00066E>.
- [4] Vadikkeettil Y, Subramaniam Y, Murugan R, Ananthapadmanabhan PV, Mostaghimi J, Pershin L, et al. Plasma assisted decomposition and reforming of greenhouse gases: A review of current status and emerging trends. *Renew Sustain Energy Rev* 2022;161:112343. <https://doi.org/10.1016/j.rser.2022.112343>.
- [5] Scapinello M, Martini LM, Dilecce G, Tosi P. Conversion of CH<sub>4</sub>/CO<sub>2</sub> by a nanosecond repetitively pulsed discharge. *J Phys D Appl Phys* 2016;49:075602. <https://doi.org/10.1088/0022-3727/49/7/075602>.
- [6] Ramakers M, Trenchev G, Heijkers S, Wang W, Bogaerts A. Gliding Arc Plasmatron: Providing an Alternative Method for Carbon Dioxide Conversion. *ChemSusChem* 2017;10:2642–52. <https://doi.org/10.1002/cssc.201700589>.
- [7] Zhang H, Wang W, Li X, Han L, Yan M, Zhong Y, et al. Plasma activation of methane for hydrogen production in a N<sub>2</sub> rotating gliding arc warm plasma: A chemical kinetics study. *Chem Eng J* 2018;345:67–78. <https://doi.org/10.1016/j.cej.2018.03.123>.
- [8] Trenchev G, Nikiforov A, Wang W, Kolev S, Bogaerts A. Atmospheric pressure glow discharge for CO<sub>2</sub> conversion: Model-based exploration of the optimum reactor configuration. *Chem Eng J* 2019;362:830–41. <https://doi.org/10.1016/j.cej.2019.01.091>.
- [9] Martin-del-Campo J, Coulombe S, Kopyscinski J. Influence of Operating Parameters on

Plasma-Assisted Dry Reforming of Methane in a Rotating Gliding Arc Reactor. *Plasma Chem Plasma Process* 2020;40:857–81. <https://doi.org/10.1007/s11090-020-10074-2>.

- [10] Devid E, Zhang D, Wang D, Ronda-Lloret M, Huang Q, Rothenberg G, et al. Dry Reforming of Methane under Mild Conditions Using Radio Frequency Plasma. *Energy Technol* 2020;8:1900886. <https://doi.org/10.1002/ente.201900886>.
- [11] Cleiren E, Heijkers S, Ramakers M, Bogaerts A. Dry Reforming of Methane in a Gliding Arc Plasmatron: Towards a Better Understanding of the Plasma Chemistry. *ChemSusChem* 2017;10:4025–36. <https://doi.org/10.1002/cssc.201701274>.
- [12] Slaets J, Aghaei M, Ceulemans S, Van Alphen S, Bogaerts A. CO 2 and CH 4 conversion in “real” gas mixtures in a gliding arc plasmatron: how do N 2 and O 2 affect the performance? *Green Chem* 2020;22:1366–77. <https://doi.org/10.1039/C9GC03743H>.
- [13] Wanten B, Maerivoet S, Vantomme C, Slaets J, Trenchev G, Bogaerts A. Dry reforming of methane in an atmospheric pressure glow discharge: Confining the plasma to expand the performance. *J CO2 Util* 2022;56:101869. <https://doi.org/10.1016/j.jcou.2021.101869>.
- [14] Kelly S, Mercer E, De Meyer R, Ciocarlan R-G, Bals S, Bogaerts A. Microwave plasma-based dry reforming of methane: Reaction performance and carbon formation. *J CO2 Util* 2023;75:102564. <https://doi.org/10.1016/j.jcou.2023.102564>.
- [15] Lu N, Sun D, Xia Y, Shang K, Wang B, Jiang N, et al. Dry reforming of CH<sub>4</sub>CO<sub>2</sub> in AC rotating gliding arc discharge: Effect of electrode structure and gas parameters. *Int J Hydrogen Energy* 2018;43:13098–109. <https://doi.org/10.1016/j.ijhydene.2018.05.053>.
- [16] Raja RB, Sarathi R, Vinu R. Selective Production of Hydrogen and Solid Carbon via Methane Pyrolysis Using a Swirl-Induced Point–Plane Non-thermal Plasma Reactor. *Energy & Fuels* 2022;36:826–36. <https://doi.org/10.1021/acs.energyfuels.1c03383>.
- [17] Kwon H, Kim T, Song S. Dry reforming of methane in a rotating gliding arc plasma: Improving efficiency and syngas cost by quenching product gas. *J CO2 Util* 2023;70:102448.

<https://doi.org/10.1016/j.jcou.2023.102448>.

- [18] Raja RB, Halageri AC, Sankar R, Sarathi R, Vinu R. Dry Reforming of Methane Using a Swirl-Induced Plasma Discharge Reactor. *Energies* 2023;16:1823.  
<https://doi.org/10.3390/en16041823>.
- [19] Khoja AH, Tahir M, Amin NAS. Dry reforming of methane using different dielectric materials and DBD plasma reactor configurations. *Energy Convers Manag* 2017;144:262–74.  
<https://doi.org/10.1016/j.enconman.2017.04.057>.
- [20] Tu X, Whitehead JC. Plasma-catalytic dry reforming of methane in an atmospheric dielectric barrier discharge: Understanding the synergistic effect at low temperature. *Appl Catal B Environ* 2012;125:439–48. <https://doi.org/10.1016/j.apcatb.2012.06.006>.
- [21] Uytdenhouwen Y, Hereijgers J, Breugelmans T, Cool P, Bogaerts A. How gas flow design can influence the performance of a DBD plasma reactor for dry reforming of methane. *Chem Eng J* 2021;405:126618. <https://doi.org/10.1016/j.cej.2020.126618>.
- [22] Uytdenhouwen Y, Bal KM, Neyts EC, Meynen V, Cool P, Bogaerts A. On the kinetics and equilibria of plasma-based dry reforming of methane. *Chem Eng J* 2021;405:126630.  
<https://doi.org/10.1016/j.cej.2020.126630>.
- [23] Michielsen I, Uytdenhouwen Y, Bogaerts A, Meynen V. Altering Conversion and Product Selectivity of Dry Reforming of Methane in a Dielectric Barrier Discharge by Changing the Dielectric Packing Material. *Catalysts* 2019;9:51. <https://doi.org/10.3390/catal9010051>.
- [24] Wang A, Harrhy JH, Meng S, He P, Liu L, Song H. Nonthermal plasma-catalytic conversion of biogas to liquid chemicals with low coke formation. *Energy Convers Manag* 2019;191:93–101. <https://doi.org/10.1016/j.enconman.2019.04.026>.
- [25] Li D, Rohani V, Fabry F, Parakkulam Ramaswamy A, Sennour M, Fulcheri L. Direct conversion of CO<sub>2</sub> and CH<sub>4</sub> into liquid chemicals by plasma-catalysis. *Appl Catal B Environ* 2020;261:118228. <https://doi.org/10.1016/j.apcatb.2019.118228>.

- [26] Liu J, Xue Z, Zhang Z, Sun B, Zhu A. Mechanism study on gliding arc (GA) plasma reforming: Unraveling the decisive role of CH<sub>4</sub> /CO<sub>2</sub> ratio in the dry reforming reaction. *Plasma Process Polym* 2023;20. <https://doi.org/10.1002/ppap.202200175>.
- [27] Wang W, Snoeckx R, Zhang X, Cha MS, Bogaerts A. Modeling Plasma-based CO<sub>2</sub> and CH<sub>4</sub> Conversion in Mixtures with N<sub>2</sub>, O<sub>2</sub>, and H<sub>2</sub>O: The Bigger Plasma Chemistry Picture. *J Phys Chem C* 2018;122:8704–23. <https://doi.org/10.1021/acs.jpcc.7b10619>.
- [28] Van Alphen S, Slaets J, Ceulemans S, Aghaei M, Snyders R, Bogaerts A. Effect of N<sub>2</sub> on CO<sub>2</sub>-CH<sub>4</sub> conversion in a gliding arc plasmatron: Can this major component in industrial emissions improve the energy efficiency? *J CO<sub>2</sub> Util* 2021;54:101767. <https://doi.org/10.1016/j.jcou.2021.101767>.
- [29] Snoeckx R, Aerts R, Tu X, Bogaerts A. Plasma-Based Dry Reforming: A Computational Study Ranging from the Nanoseconds to Seconds Time Scale. *J Phys Chem C* 2013;117:4957–70. <https://doi.org/10.1021/jp311912b>.
- [30] De Bie C, van Dijk J, Bogaerts A. The Dominant Pathways for the Conversion of Methane into Oxygenates and Syngas in an Atmospheric Pressure Dielectric Barrier Discharge. *J Phys Chem C* 2015;119:22331–50. <https://doi.org/10.1021/acs.jpcc.5b06515>.
- [31] Snoeckx R, Setareh M, Aerts R, Simon P, Maghari A, Bogaerts A. Influence of N<sub>2</sub> concentration in a CH<sub>4</sub>/N<sub>2</sub> dielectric barrier discharge used for CH<sub>4</sub> conversion into H<sub>2</sub>. *Int J Hydrogen Energy* 2013;38:16098–120. <https://doi.org/10.1016/j.ijhydene.2013.09.136>.
- [32] Snoeckx R, Ozkan A, Reniers F, Bogaerts A. The Quest for Value-Added Products from Carbon Dioxide and Water in a Dielectric Barrier Discharge: A Chemical Kinetics Study. *ChemSusChem* 2017;10:409–24. <https://doi.org/10.1002/cssc.201601234>.
- [33] Snoeckx R, Heijkers S, Van Wesenbeeck K, Lenaerts S, Bogaerts A. CO<sub>2</sub> conversion in a dielectric barrier discharge plasma: N<sub>2</sub> in the mix as a helping hand or problematic impurity? *Energy Environ Sci* 2016;9:999–1011. <https://doi.org/10.1039/C5EE03304G>.

- [34] De Bie C, Verheyde B, Martens T, van Dijk J, Paulussen S, Bogaerts A. Fluid Modeling of the Conversion of Methane into Higher Hydrocarbons in an Atmospheric Pressure Dielectric Barrier Discharge. *Plasma Process Polym* 2011;8:1033–58.  
<https://doi.org/10.1002/ppap.201100027>.
- [35] Aerts R, Snoeckx R, Bogaerts A. In-Situ Chemical Trapping of Oxygen in the Splitting of Carbon Dioxide by Plasma. *Plasma Process Polym* 2014;11:985–92.  
<https://doi.org/10.1002/ppap.201400091>.
- [36] Pancheshnyi S, Eismann B, Hagelaar GJM, Pitchford LC. Computer code ZDPlasKin, <http://www.zdplaskin.laplace.univ-tlse.fr> (University of Toulouse, LAPLACE, CNRS-UPSINP, Toulouse, France, 2008). <Http://WwwZdplaskinLaplaceUniv-TlseFr> 2008.
- [37] Hagelaar GJM, Pitchford LC. Solving the Boltzmann equation to obtain electron transport coefficients and rate coefficients for fluid models. *Plasma Sources Sci Technol* 2005;14:722–33. <https://doi.org/10.1088/0963-0252/14/4/011>.
- [38] van de Steeg AW, Butterworth T, van den Bekerom DCM, Silva AF, van de Sanden MCM, van Rooij GJ. Plasma activation of N<sub>2</sub>, CH<sub>4</sub> and CO<sub>2</sub>: an assessment of the vibrational non-equilibrium time window. *Plasma Sources Sci Technol* 2020;29:115001.  
<https://doi.org/10.1088/1361-6595/abbae4>.
- [39] Vermeiren V, Bogaerts A. Plasma-Based CO<sub>2</sub> Conversion: To Quench or Not to Quench? *J Phys Chem C* 2020;124:18401–15. <https://doi.org/10.1021/acs.jpcc.0c04257>.
- [40] McBride BJ, Zehe MJ, Gordon S. NASA Glenn coefficients for calculating thermodynamic properties of individual species: National Aeronautics and Space Administration. John H Glenn Res Cent Lewis F 2002:295.
- [41] Burcat A, Ruscic B, Chemistry. Third millennium ideal gas and condensed phase thermochemical database for combustion (with update from active thermochemical tables). Argonne, IL: 2005. <https://doi.org/10.2172/925269>.

- [42] Vialletto L, van de Steeg AW, Viegas P, Longo S, van Rooij GJ, van de Sanden MCM, et al. Charged particle kinetics and gas heating in CO<sub>2</sub> microwave plasma contraction: comparisons of simulations and experiments. *Plasma Sources Sci Technol* 2022;31:055005. <https://doi.org/10.1088/1361-6595/ac56c5>.
- [43] Kossyi IA, Kostinsky AY, Matveyev AA, Silakov VP. Kinetic scheme of the non-equilibrium discharge in nitrogen-oxygen mixtures. *Plasma Sources Sci Technol* 1992;1:207–20. <https://doi.org/10.1088/0963-0252/1/3/011>.
- [44] Dinh DK, Trenchev G, Lee DH, Bogaerts A. Arc plasma reactor modification for enhancing performance of dry reforming of methane. *J CO<sub>2</sub> Util* 2020;42:101352. <https://doi.org/10.1016/j.jcou.2020.101352>.
- [45] Green KM, Borras MC, Woskov PP, Flores GJ, Hadidi K, Thomas P. Electronic excitation temperature profiles in an air microwave plasma torch. *IEEE Trans Plasma Sci* 2001;29:399–406. <https://doi.org/10.1109/27.922753>.
- [46] Heijkers S, Aghaei M, Bogaerts A. Plasma-Based CH<sub>4</sub> Conversion into Higher Hydrocarbons and H<sub>2</sub>: Modeling to Reveal the Reaction Mechanisms of Different Plasma Sources. *J Phys Chem C* 2020;124:7016–30. <https://doi.org/10.1021/acs.jpcc.0c00082>.
- [47] Liu J-L, Park H-W, Chung W-J, Ahn W-S, Park D-W. Simulated biogas oxidative reforming in AC-pulsed gliding arc discharge. *Chem Eng J* 2016;285:243–51. <https://doi.org/10.1016/j.cej.2015.09.100>.
- [48] Moon SY, Choe W. Parametric study of atmospheric pressure microwave-induced Ar/O<sub>2</sub> plasmas and the ambient air effect on the plasma. *Phys Plasmas* 2006;13. <https://doi.org/10.1063/1.2357722>.
- [49] Van Alphen S, Jardali F, Creel J, Trenchev G, Snyders R, Bogaerts A. Sustainable gas conversion by gliding arc plasmas: a new modelling approach for reactor design improvement. *Sustain Energy Fuels* 2021;5:1786–800. <https://doi.org/10.1039/D0SE01782E>.

- [50] Dahl JK, Weimer AW, Lewandowski A, Bingham C, Bruetsch F, Steinfeld A. Dry Reforming of Methane Using a Solar-Thermal Aerosol Flow Reactor. *Ind Eng Chem Res* 2004;43:5489–95. <https://doi.org/10.1021/ie030307h>.
- [51] Biondo O, Hughes A, van de Steeg A, Maerivoet S, Loenders B, van Rooij G, et al. Power concentration determined by thermodynamic properties in complex gas mixtures: the case of plasma-based dry reforming of methane. *Plasma Sources Sci Technol* 2023;32:045001. <https://doi.org/10.1088/1361-6595/acc6ec>.
- [52] Turner MM. Uncertainty and error in complex plasma chemistry models. *Plasma Sources Sci Technol* 2015;24:035027. <https://doi.org/10.1088/0963-0252/24/3/035027>.
- [53] Turner MM. Uncertainty and sensitivity analysis in complex plasma chemistry models. *Plasma Sources Sci Technol* 2016;25:015003. <https://doi.org/10.1088/0963-0252/25/1/015003>.
- [54] Berthelot A, Bogaerts A. Modeling of CO<sub>2</sub> plasma: effect of uncertainties in the plasma chemistry. *Plasma Sources Sci Technol* 2017;26:115002. <https://doi.org/10.1088/1361-6595/aa8ffb>.
- [55] Wang W, Berthelot A, Zhang Q, Bogaerts A. Modelling of plasma-based dry reforming: how do uncertainties in the input data affect the calculation results? *J Phys D Appl Phys* 2018;51:204003. <https://doi.org/10.1088/1361-6463/aab97a>.
- [56] Haynes WM, Lide DR, Bruno TJ, editors. CRC Handbook of Chemistry and Physics. CRC Press; 2016. <https://doi.org/10.1201/9781315380476>.
- [57] Delikontantis E, Scapinello M, Stefanidis GD. Low energy cost conversion of methane to ethylene in a hybrid plasma-catalytic reactor system. *Fuel Process Technol* 2018;176:33–42. <https://doi.org/10.1016/j.fuproc.2018.03.011>.
- [58] Fridman A. Plasma Chemistry. Cambridge University Press; 2008. <https://doi.org/10.1017/CBO9780511546075>.
- [59] Abiev RS, Sladkovskiy DA, Semikin K V., Murzin DY, Rebrov E V. Non-Thermal Plasma for

Process and Energy Intensification in Dry Reforming of Methane. *Catalysts* 2020;10:1358.

<https://doi.org/10.3390/catal10111358>.

- [60] Li J, Zhang X, Shen J, Ran T, Chen P, Yin Y. Dissociation of CO<sub>2</sub> by thermal plasma with contracting nozzle quenching. *J CO<sub>2</sub> Util* 2017;21:72–6.  
<https://doi.org/10.1016/j.jcou.2017.04.003>.
- [61] Mercer ER, Van Alphen S, van Deursen CFAM, Righart TWH, Bongers WA, Snyders R, et al. Post-plasma quenching to improve conversion and energy efficiency in a CO<sub>2</sub> microwave plasma. *Fuel* 2023;334:126734. <https://doi.org/10.1016/j.fuel.2022.126734>.
- [62] Van Alphen S, Hecimovic A, Kiefer CK, Fantz U, Snyders R, Bogaerts A. Modelling post-plasma quenching nozzles for improving the performance of CO<sub>2</sub> microwave plasmas. *Chem Eng J* 2023;462:142217. <https://doi.org/10.1016/j.cej.2023.142217>.
- [63] De Bleecker K, Bogaerts A, Goedheer W. Aromatic ring generation as a dust precursor in acetylene discharges. *Appl Phys Lett* 2006;88. <https://doi.org/10.1063/1.2193796>.
- [64] De Bleecker K, Bogaerts A, Goedheer W. Detailed modeling of hydrocarbon nanoparticle nucleation in acetylene discharges. *Phys Rev E* 2006;73:026405.  
<https://doi.org/10.1103/PhysRevE.73.026405>.
- [65] Spath PL, Dayton DC. Preliminary Screening -- Technical and Economic Assessment of Synthesis Gas to Fuels and Chemicals with Emphasis on the Potential for Biomass-Derived Syngas. Golden, CO (United States): 2003. <https://doi.org/10.2172/15006100>.
- [66] YANG T, SHEN J, RAN T, LI J, CHEN P, YIN Y. Understanding CO<sub>2</sub> decomposition by thermal plasma with supersonic expansion quench. *Plasma Sci Technol* 2018;20:65502.  
<https://doi.org/10.1088/2058-6272/aaa969>.
- [67] Heijkers S, Bogaerts A. CO<sub>2</sub> Conversion in a Gliding Arc Plasmatron: Elucidating the Chemistry through Kinetic Modeling. *J Phys Chem C* 2017;121:22644–55.  
<https://doi.org/10.1021/acs.jpcc.7b06524>.

- [68] Kumar N, Shojaee M, Spivey J. Catalytic bi-reforming of methane: from greenhouse gases to syngas. *Curr Opin Chem Eng* 2015;9:8–15. <https://doi.org/10.1016/j.coche.2015.07.003>.
- [69] Mohanty US, Ali M, Azhar MR, Al-Yaseri A, Keshavarz A, Iglauer S. Current advances in syngas ( $\text{CO} + \text{H}_2$ ) production through bi-reforming of methane using various catalysts: A review. *Int J Hydrogen Energy* 2021;46:32809–45.  
<https://doi.org/10.1016/j.ijhydene.2021.07.097>.

# Supporting Information

## Plasma-based dry reforming of CH<sub>4</sub>: plasma effects vs. thermal conversion

Joachim Slaets<sup>1</sup>, Björn Loenders<sup>1</sup>, and Annemie Bogaerts<sup>1</sup>

<sup>1</sup>Research group PLASMANT, Department of Chemistry, University of Antwerp,  
Universiteitsplein 1, BE-2610 Wilrijk-Antwerp, Belgium

### List of Figures

S1	Calculated species concentrations of the thermal kinetics simulations (for t = 10 <sup>10</sup> s) (dashed) and corresponding thermodynamic equilibrium concentrations (solid), in the temperature range of 1000 to 4000 K, for four different CO <sub>2</sub> /CH <sub>4</sub> ratios (70/30 (a), 90/10 (b), 30/70 (c), 10/90 (d)).	2
S2	Weighted mean absolute deviation (wMAD) between the calculated species concentrations at thermal and plasma conditions at 500 W cm <sup>-3</sup> (a) and 1500 W cm <sup>-3</sup> (b), at a residence time of 10 ms, in the temperature range of 1000 to 4000 K, for five different CO <sub>2</sub> /CH <sub>4</sub> ratios (90/10, 70/30, 50/50, 30/70, 10/90).	3
S3	Calculated concentrations of the main plasma species for the temperature range of 1000 to 4000 K and a 50/50 CO <sub>2</sub> /CH <sub>4</sub> ratio and 1000 W cm <sup>-3</sup> plasma condition, at a residence time of 10 ms (solid lines), 1 ms (dashed lines) and 0.1 ms (dotted lines).	4
S4	CO <sub>2</sub> (a) and CH <sub>4</sub> (b) conversion (dotted black lines), as well as the relative contributions of the main loss reactions (>5 %) based on the time-integrated net reaction rates (see legends), as a function of temperature, for plasma simulations with a power density of 1000 W cm <sup>-3</sup> and for a 70/30 ratio of CO <sub>2</sub> /CH <sub>4</sub> at a residence time of 10 ms.	5
S5	CO <sub>2</sub> (a) and CH <sub>4</sub> (b) conversion (dotted black lines), as well as the relative contributions of the main loss reactions (>5 %) based on the time-integrated net reaction rates (see legends), as a function of temperature, for plasma simulations with a power density of 1000 W cm <sup>-3</sup> and for a 30/70 ratio of CO <sub>2</sub> /CH <sub>4</sub> at a residence time of 10 ms.	6

### List of Tables

S1	Reactions reference list with the rate coefficients (third column) expressed in cm <sup>3</sup> s <sup>-1</sup> for two-body reactions, and in cm <sup>6</sup> s <sup>-1</sup> for three-body reactions. In the rate equations, N <sub>A</sub> is Avogadro's constant, k <sub>B</sub> is the Boltzmann constant, R is the ideal gas constant, T <sub>g</sub> is the gas temperature in K and n <sub>M</sub> is the total number density of neutral species in cm <sup>-3</sup> .	7
S2	Cross sections reference list	48
S3	Overview of estimated power density from various literature sources. The plasma volume is not specifically measured in these sources and therefore, we could only make a rough estimate of the power density. Despite some outliers above 1500 W cm <sup>-3</sup> , our chosen power density values (500, 1000 and 1500 W cm <sup>-3</sup> ) provide good coverage of this literature data.	54

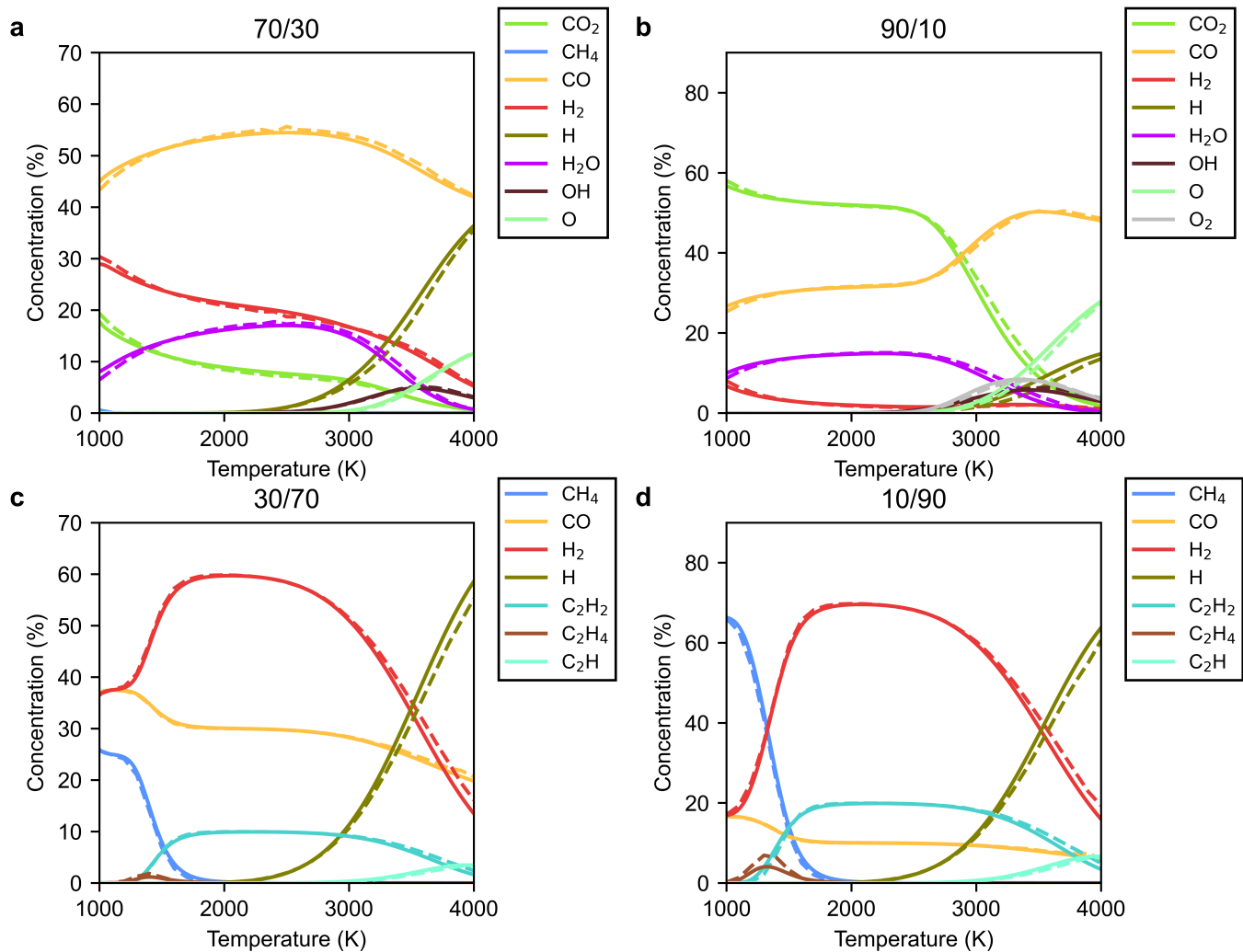


Figure S1: Calculated species concentrations of the thermal kinetics simulations (for  $t = 10^{10}$  s) (dashed) and corresponding thermodynamic equilibrium concentrations (solid), in the temperature range of 1000 to 4000 K, for four different CO<sub>2</sub>/CH<sub>4</sub> ratios (70/30 (a), 90/10 (b), 30/70 (c), 10/90 (d)).

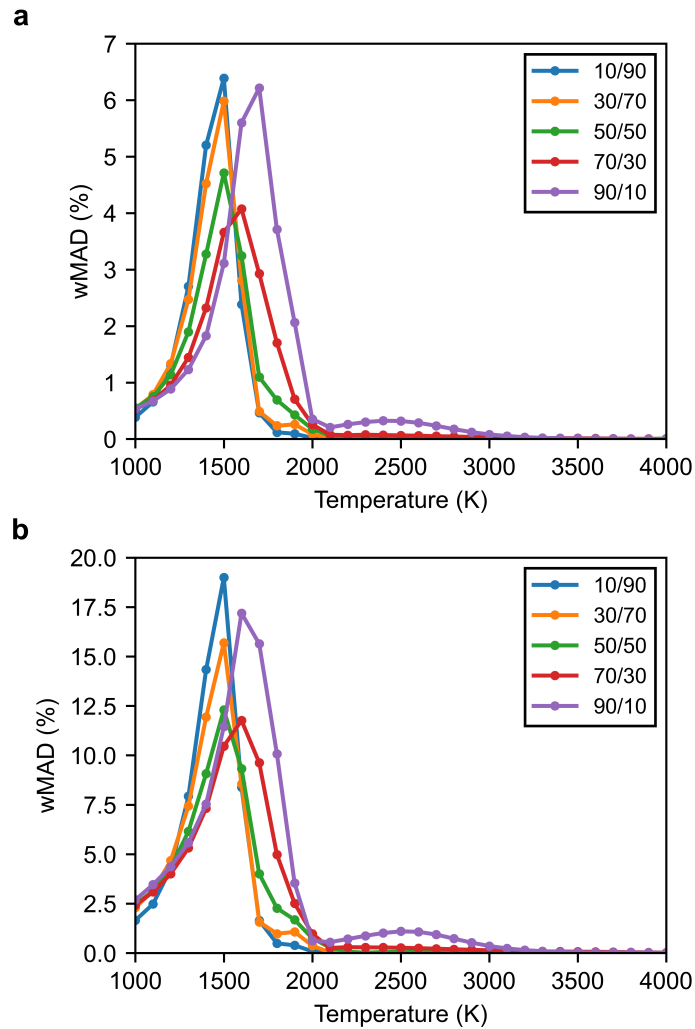


Figure S2: Weighted mean absolute deviation (wMAD) between the calculated species concentrations at thermal and plasma conditions at  $500 \text{ W cm}^{-3}$  (a) and  $1500 \text{ W cm}^{-3}$  (b), at a residence time of 10 ms, in the temperature range of 1000 to 4000 K, for five different  $\text{CO}_2/\text{CH}_4$  ratios (90/10, 70/30, 50/50, 30/70, 10/90).

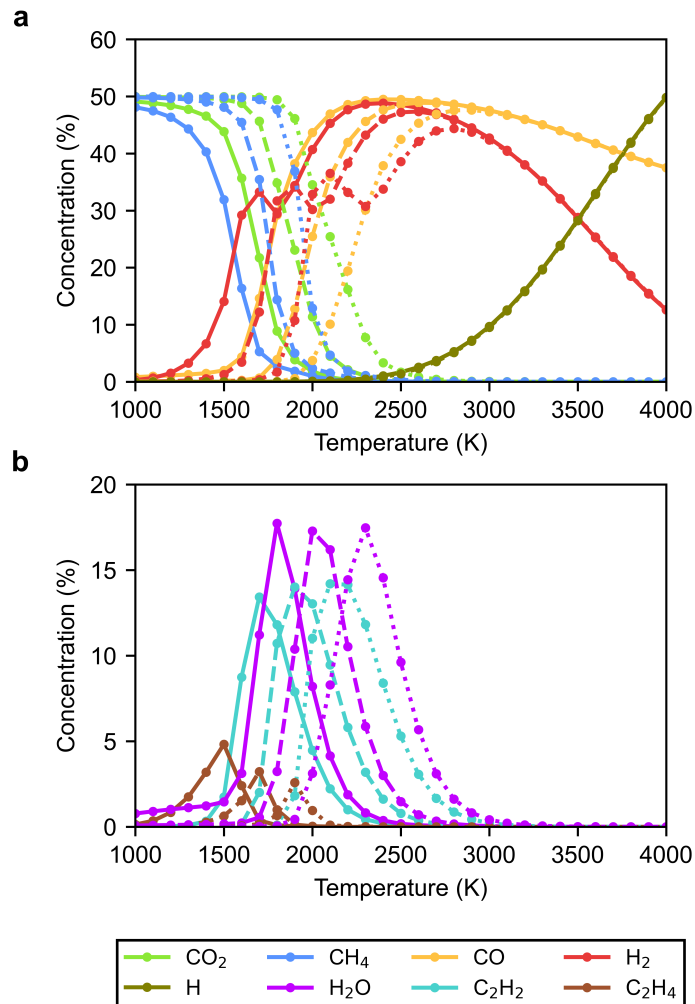


Figure S3: Calculated concentrations of the main plasma species for the temperature range of 1000 to 4000 K and a 50/50  $\text{CO}_2/\text{CH}_4$  ratio and  $1000 \text{ W cm}^{-3}$  plasma condition, at a residence time of 10 ms (solid lines), 1 ms (dashed lines) and 0.1 ms (dotted lines).

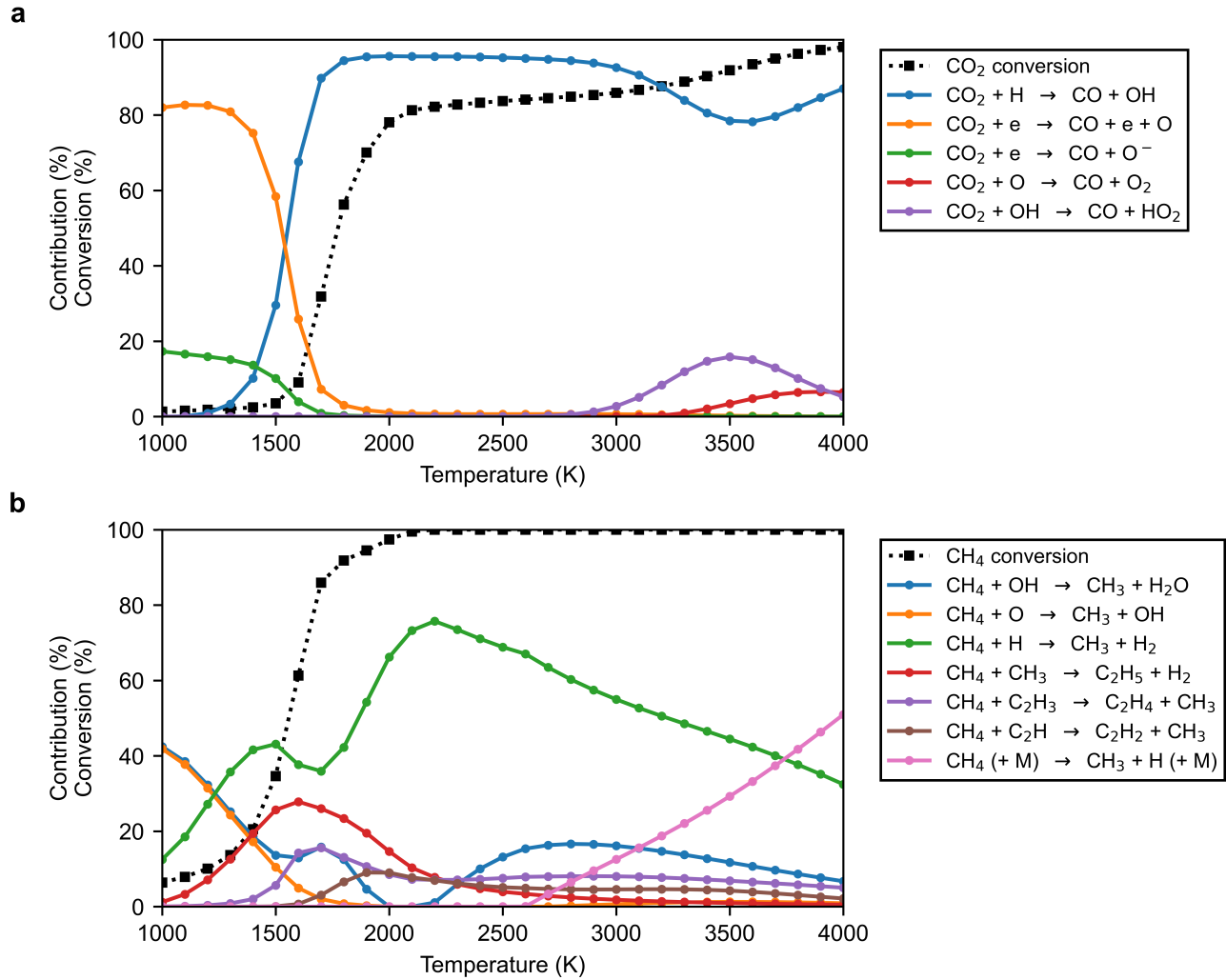


Figure S4:  $\text{CO}_2$  (a) and  $\text{CH}_4$  (b) conversion (dotted black lines), as well as the relative contributions of the main loss reactions (>5 %) based on the time-integrated net reaction rates (see legends), as a function of temperature, for plasma simulations with a power density of  $1000 \text{ W cm}^{-3}$  and for a 70/30 ratio of  $\text{CO}_2/\text{CH}_4$  at a residence time of 10 ms.

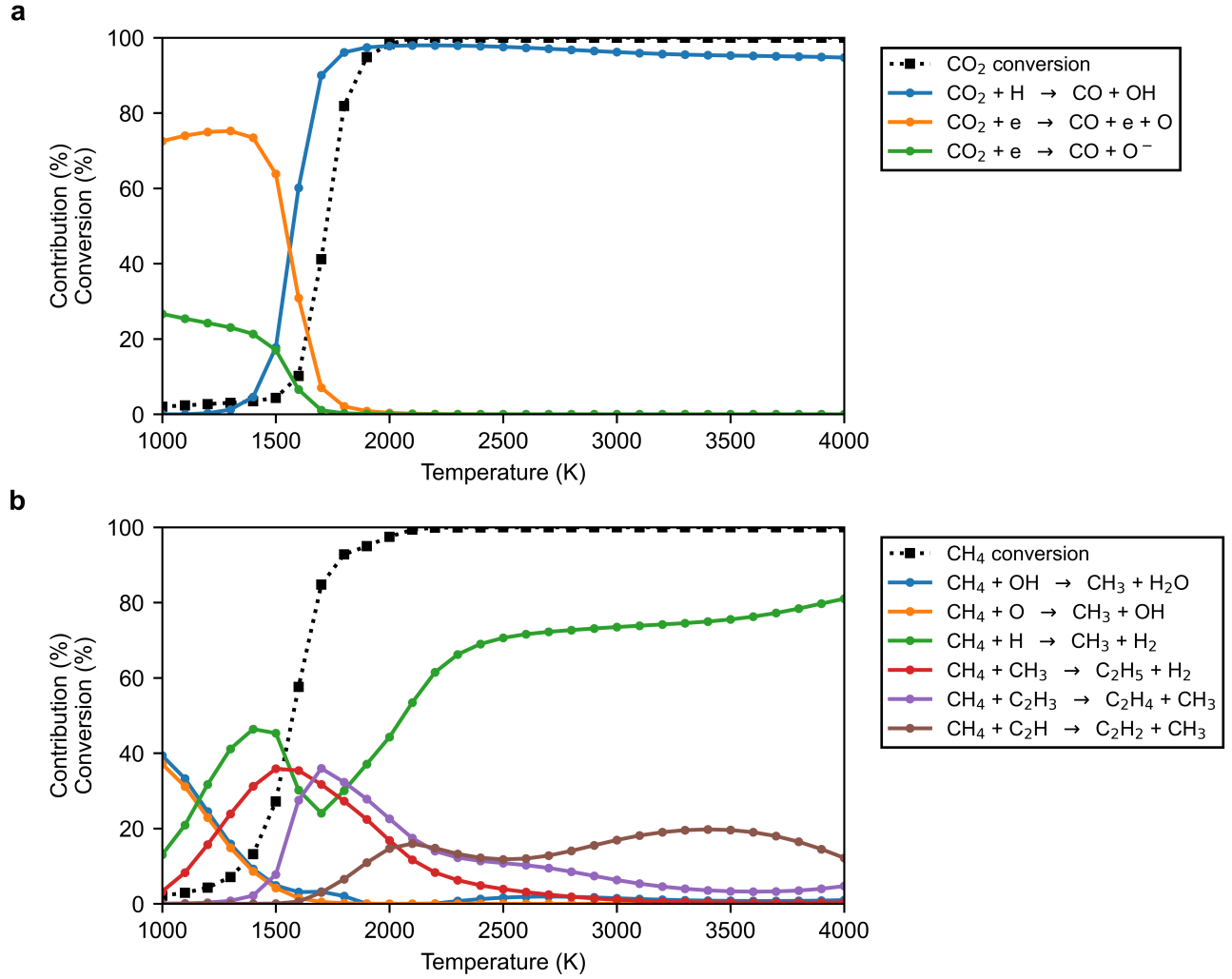


Figure S5: CO<sub>2</sub> (a) and CH<sub>4</sub> (b) conversion (dotted black lines), as well as the relative contributions of the main loss reactions (>5 %) based on the time-integrated net reaction rates (see legends), as a function of temperature, for plasma simulations with a power density of 1000 W cm<sup>-3</sup> and for a 30/70 ratio of CO<sub>2</sub>/CH<sub>4</sub> at a residence time of 10 ms.

Table S1: Reactions reference list with the rate coefficients (third column) expressed in  $\text{cm}^3 \text{ s}^{-1}$  for two-body reactions, and in  $\text{cm}^6 \text{ s}^{-1}$  for three-body reactions. In the rate equations,  $N_A$  is Avogadro's constant,  $k_B$  is the Boltzmann constant,  $R$  is the ideal gas constant,  $T_g$  is the gas temperature in  $K$  and  $n_M$  is the total number density of neutral species in  $\text{cm}^{-3}$ .

#	Reaction	Rate equation	Ref.
1	$C + H^- \rightarrow CH + e$	$1 \times 10^{-9}$	[1]
2	$C + H_3^+ \rightarrow CH^+ + H_2$	$2 \times 10^{-9}$	[1]
3	$C + H_2^+ \rightarrow CH^+ + H$	$2.4 \times 10^{-9}$	[1]
4	$C^+ + H^- \rightarrow C + H$	$7.51 \times 10^{-8} \cdot \left( \frac{T_g}{3 \times 10^2} \right)^{-0.5}$	[2, 3]
5	$CH_4 + H \rightarrow CH_3 + H_2$	$6.4 \times 10^{-18} \cdot T_g^{2.11} \cdot \exp\left(\frac{-3.9 \times 10^3}{T_g}\right)$	[4]
6	$CH_3 + H_2 \rightarrow CH_4 + H$	$6.62 \times 10^{-20} \cdot T_g^{2.24} \cdot \exp\left(\frac{-3.22 \times 10^3}{T_g}\right)$	[4]
7	$CH_3 + H \rightarrow CH_2 + H_2$	$2.1 \times 10^{-8} \cdot T_g^{-0.56} \cdot \exp\left(\frac{-8.0 \times 10^3}{T_g}\right)$	[5]
8	$CH_3 + H \rightarrow CH_4$	$k_0 = 1.7 \times 10^{-24} \cdot T_g^{-1.8}$ $k_\infty = 3.5 \times 10^{-10}$ $F_c = 0.63 \cdot \exp\left(\frac{-T_g}{3.3150 \times 10^3}\right)$ $+ 0.37 \cdot \exp\left(\frac{-T_g}{6.10 \times 10^1}\right)$	[5] <sup>a</sup>
9	$CH_2 + H_2 \rightarrow CH_3 + H$	$7.32 \times 10^{-19} \cdot T_g^{2.3} \cdot \exp\left(\frac{-3.6990 \times 10^3}{T_g}\right)$	[6]
10	$CH_2 + H \rightarrow CH + H_2$	$2 \times 10^{-10}$	[5]
11	$CH + H_2 \rightarrow CH_2 + H$	$2.9 \times 10^{-10} \cdot \exp\left(\frac{-1.670 \times 10^3}{T_g}\right)$	[5]
12	$CH + H_2 \rightarrow CH_3$	$k_0 = 4.7 \times 10^{-26} \cdot T_g^{-1.6}$ $k_\infty = 8.5 \times 10^{-11} \cdot T_g^{0.15}$ $F_c = 0.48$ $+ 0.25 \cdot \exp\left(\frac{-T_g}{3.0 \times 10^2}\right)$	[5] <sup>a</sup>
13	$CH + H \rightarrow C + H_2$	$2 \times 10^{-10}$	[5]
14	$CH_4 + H^+ \rightarrow CH_4^+ + H$	$1.5 \times 10^{-9}$	[1]
15	$CH_4 + H^+ \rightarrow CH_3^+ + H_2$	$2.3 \times 10^{-9}$	[1]
16	$CH_3 + H^+ \rightarrow CH_3^+ + H$	$3.4 \times 10^{-9}$	[1]
17	$CH_2 + H^+ \rightarrow CH_2^+ + H$	$1.4 \times 10^{-9}$	[1]
18	$CH_2 + H^+ \rightarrow CH^+ + H_2$	$1.4 \times 10^{-9}$	[1]
19	$CH + H^+ \rightarrow CH^+ + H$	$1.9 \times 10^{-9}$	[1]
20	$CH_4 + H_2^+ \rightarrow CH_5^+ + H$	$1.14 \times 10^{-10}$	[7]
21	$CH_4 + H_2^+ \rightarrow CH_4^+ + H_2$	$1.406 \times 10^{-9}$	[7]
22	$CH_4 + H_2^+ \rightarrow CH_3^+ + H + H_2$	$2.28 \times 10^{-9}$	[7]
23	$CH_2 + H_2^+ \rightarrow CH_3^+ + H$	$1 \times 10^{-9}$	[1]
24	$CH_2 + H_2^+ \rightarrow CH_2^+ + H_2$	$1 \times 10^{-9}$	[1]
25	$CH + H_2^+ \rightarrow CH_2^+ + H$	$7.1 \times 10^{-10}$	[1]
26	$CH + H_2^+ \rightarrow CH^+ + H_2$	$7.1 \times 10^{-10}$	[1]
27	$CH_4 + H_3^+ \rightarrow CH_5^+ + H_2$	$2.4 \times 10^{-9}$	[1]
28	$CH_3 + H_3^+ \rightarrow CH_4^+ + H_2$	$2.1 \times 10^{-9}$	[1]
29	$CH_2 + H_3^+ \rightarrow CH_3^+ + H_2$	$1.7 \times 10^{-9}$	[1]
30	$CH + H_3^+ \rightarrow CH_2^+ + H_2$	$1.2 \times 10^{-9}$	[1]
31	$CH_3 + H^- \rightarrow CH_4 + e$	$1 \times 10^{-9}$	[1]
32	$CH_2 + H^- \rightarrow CH_3 + e$	$1 \times 10^{-9}$	[1]

#	Reaction	Rate equation	Ref.
33	$CH + H^- \rightarrow CH_2 + e$	$1 \times 10^{-10}$	[1]
34	$CH_5^+ + H \rightarrow CH_4^+ + H_2$	$1.5 \times 10^{-10}$	[8]
35	$CH_4^+ + H_2 \rightarrow CH_5^+ + H$	$3.3 \times 10^{-11}$	[9]
36	$CH_4^+ + H \rightarrow CH_3^+ + H_2$	$2 \times 10^{-10}$	[1]
37	$CH_2^+ + H_2 \rightarrow CH_3^+ + H$	$1.6 \times 10^{-9}$	[9]
38	$CH^+ + H_2 \rightarrow CH_2^+ + H$	$1.2 \times 10^{-9}$	[8]
39	$CH_3^+ + H^- \rightarrow CH_3 + H$	$7.51 \times 10^{-8} \cdot \left(\frac{T_g}{3 \times 10^2}\right)^{-0.5}$	[2, 3]
40	$C + CH_4 \rightarrow C_2H_4$	$5 \times 10^{-15}$	[10]
41	$C + CH_3 \rightarrow C_2H_2 + H$	$8.3 \times 10^{-11}$	[11]
42	$C + CH_2 \rightarrow C_2H + H$	$8.3 \times 10^{-11}$	[11]
43	$CH_4 + C^+ \rightarrow C_2H_3^+ + H$	$1 \times 10^{-9}$	[12]
44	$CH_4 + C^+ \rightarrow C_2H_2^+ + H_2$	$3.89 \times 10^{-10}$	[12]
45	$CH_3 + C^+ \rightarrow C_2H_2^+ + H$	$1.3 \times 10^{-9}$	[1]
46	$CH_3 + C^+ \rightarrow C_2H^+ + H_2$	$1 \times 10^{-9}$	[13]
47	$CH_2 + C^+ \rightarrow C + CH_2^+$	$5.2 \times 10^{-10}$	[1]
48	$CH_2 + C^+ \rightarrow C_2H^+ + H$	$5.2 \times 10^{-10}$	[1]
49	$CH + C^+ \rightarrow C + CH^+$	$3.8 \times 10^{-10}$	[1]
50	$C + CH_5^+ \rightarrow CH_4 + CH^+$	$1.2 \times 10^{-9}$	[1]
51	$C + CH_3^+ \rightarrow C_2H^+ + H_2$	$1.2 \times 10^{-9}$	[1]
52	$C + CH_2^+ \rightarrow C_2H^+ + H$	$1.2 \times 10^{-9}$	[1]
53	$CH_3 + CH_4 \rightarrow C_2H_6 + H$	$\frac{8 \times 10^{13}}{N_A} \cdot \exp\left(\frac{-1.6736 \times 10^5}{R \cdot T_g}\right)$	[14]
54	$CH_3 + CH_4 \rightarrow C_2H_5 + H_2$	$\frac{1 \times 10^{13}}{N_A} \cdot \exp\left(\frac{-9.6232 \times 10^4}{R \cdot T_g}\right)$	[14]
55	$CH_2 + CH_4 \rightarrow CH_3 + CH_3$	$7.14 \times 10^{-12} \cdot \exp\left(\frac{-4.199 \times 10^4}{R \cdot T_g}\right)$	[15]
56	$CH + CH_4 \rightarrow C_2H_4 + H$	$2.2 \times 10^{-8} \cdot T_g^{-0.94} \cdot \exp\left(\frac{-2.9 \times 10^1}{T_g}\right)$	[5]
57	$CH_3 + CH_3 \rightarrow C_2H_6$	$k_0 = 3.5 \times 10^{-7} \cdot T_g^{-7} \cdot \exp\left(\frac{-1.39 \times 10^3}{T_g}\right)$ $k_\infty = 6 \times 10^{-11}$ $F_c = 0.38 \cdot \exp\left(\frac{-T_g}{7.3 \times 10^1}\right)$ $+ 0.62 \cdot \exp\left(\frac{-T_g}{1.18 \times 10^3}\right)$	[5] <sup>a</sup>
58	$CH_3 + CH_3 \rightarrow C_2H_5 + H$	$9 \times 10^{-11} \cdot \exp\left(\frac{-8.08 \times 10^3}{T_g}\right)$	[5]
59	$CH_3 + CH_3 \rightarrow CH_2 + CH_4$	$5.6 \times 10^{-17} \cdot T_g^{1.34} \cdot \exp\left(\frac{-6.791 \times 10^4}{R \cdot T_g}\right)$	[16]
60	$CH_2 + CH_3 \rightarrow C_2H_4 + H$	$1.2 \times 10^{-10}$	[5]
61	$CH_2 + CH_2 \rightarrow C_2H_2 + H_2$	$\frac{10^{1.52 \times 10^1}}{N_A} \cdot \exp\left(\frac{-5 \times 10^4}{R \cdot T_g}\right)$	[17]
62	$CH + CH \rightarrow C_2H_2$	$\frac{1.2 \times 10^{14}}{N_A}$	[18]
63	$CH_2 + CH_5^+ \rightarrow CH_3^+ + CH_4$	$9.6 \times 10^{-10}$	[1]
64	$CH + CH_5^+ \rightarrow CH_2^+ + CH_4$	$6.9 \times 10^{-10}$	[1]
65	$CH_4 + CH_4^+ \rightarrow CH_3 + CH_5^+$	$1.5 \times 10^{-9}$	[9]
66	$CH_3^+ + CH_4 \rightarrow CH_3 + CH_4^+$	$1.36 \times 10^{-10}$	[19]
67	$CH_3^+ + CH_4 \rightarrow C_2H_5^+ + H_2$	$1.2 \times 10^{-9}$	[20]
68	$CH_2 + CH_3^+ \rightarrow C_2H_3^+ + H_2$	$9.9 \times 10^{-10}$	[1]
69	$CH + CH_3^+ \rightarrow C_2H_2^+ + H_2$	$7.1 \times 10^{-10}$	[1]

#	Reaction	Rate equation	Ref.
70	$CH_2^+ + CH_4 \rightarrow CH_3 + CH_3^+$	$1.38 \times 10^{-10}$	[21]
71	$CH_2^+ + CH_4 \rightarrow C_2H_5^+ + H$	$3.6 \times 10^{-10}$	[9]
72	$CH_2^+ + CH_4 \rightarrow C_2H_4^+ + H_2$	$8.4 \times 10^{-10}$	[9]
73	$CH_2^+ + CH_4 \rightarrow C_2H_3^+ + H + H_2$	$2.31 \times 10^{-10}$	[21]
74	$CH_2^+ + CH_4 \rightarrow C_2H_2^+ + H_2 + H_2$	$3.97 \times 10^{-10}$	[21]
75	$CH_4 + CH^+ \rightarrow C_2H_4^+ + H$	$6.5 \times 10^{-11}$	[9]
76	$CH_4 + CH^+ \rightarrow C_2H_3^+ + H_2$	$1.09 \times 10^{-9}$	[9]
77	$CH_4 + CH^+ \rightarrow C_2H_2^+ + H + H_2$	$1.43 \times 10^{-10}$	[9]
78	$CH_2 + CH^+ \rightarrow C_2H^+ + H_2$	$1 \times 10^{-9}$	[1]
79	$CH_4 + e \rightarrow CH_4^+ + e + e$	$f(\sigma)$	[22, 23]
80	$CH_3 + e \rightarrow CH_3^+ + e + e$	$f(\sigma)$	[22, 23]
81	$CH_2 + e \rightarrow CH_2^+ + e + e$	$f(\sigma)$	[22, 23]
82	$CH + e \rightarrow CH^+ + e + e$	$f(\sigma)$	[22, 23]
83	$CH_4 + e \rightarrow CH_3^+ + e + e + H$	$f(\sigma)$	[22, 23]
84	$CH_4 + e \rightarrow CH_2^+ + e + e + H_2$	$f(\sigma)$	[22, 23]
85	$CH_4 + e \rightarrow CH_2^+ + e + e + H + H$	$f(\sigma)$	[22, 23]
86	$CH_4 + e \rightarrow CH^+ + e + e + H + H_2$	$f(\sigma)$	[22, 23]
87	$CH_3 + e \rightarrow CH_2^+ + e + e + H$	$f(\sigma)$	[22, 23]
88	$CH_3 + e \rightarrow CH^+ + e + e + H_2$	$f(\sigma)$	[22, 23]
89	$CH_3 + e \rightarrow CH^+ + e + e + H + H$	$f(\sigma)$	[22, 23]
90	$CH_3 + e \rightarrow C^+ + e + e + H + H_2$	$f(\sigma)$	[22, 23]
91	$CH_3 + e \rightarrow CH_2 + e + e + H^+$	$f(\sigma)$	[22, 23]
92	$CH_2 + e \rightarrow CH^+ + e + e + H$	$f(\sigma)$	[22, 23]
93	$CH_2 + e \rightarrow C^+ + e + e + H_2$	$f(\sigma)$	[22, 23]
94	$CH_2 + e \rightarrow C^+ + e + e + H + H$	$f(\sigma)$	[22, 23]
95	$CH_2 + e \rightarrow CH + e + e + H^+$	$f(\sigma)$	[22, 23]
96	$CH_2 + e \rightarrow C + e + e + H_2^+$	$f(\sigma)$	[22, 23]
97	$CH + e \rightarrow C^+ + e + e + H$	$f(\sigma)$	[22, 23]
98	$CH + e \rightarrow C + e + e + H^+$	$f(\sigma)$	[22, 23]
99	$CH_4 + e \rightarrow CH_3 + e + H$	$f(\sigma)$	[22, 23]
100	$CH_4 + e \rightarrow CH + e + H + H_2$	$f(\sigma)$	[22, 23]
101	$CH_4 + e \rightarrow C + e + H + H + H_2$	$f(\sigma)$	[22, 23]
102	$CH_4 + e \rightarrow C + e + H_2 + H_2$	$f(\sigma)$	[22, 23]
103	$CH_4 + e \rightarrow CH_2 + e + H_2$	$f(\sigma)$	[22, 23]
104	$CH_4 + e \rightarrow CH_2 + e + H + H$	$f(\sigma)$	[22, 23]
105	$CH_3 + e \rightarrow CH + e + H_2$	$f(\sigma)$	[22, 23]
106	$CH_3 + e \rightarrow C + e + H + H_2$	$f(\sigma)$	[22, 23]
107	$CH_3 + e \rightarrow CH + e + H + H$	$f(\sigma)$	[22, 23]
108	$CH_3 + e \rightarrow CH_2 + e + H$	$f(\sigma)$	[22, 23]
109	$CH_2 + e \rightarrow C + e + H_2$	$f(\sigma)$	[22, 23]

#	Reaction	Rate equation	Ref.
110	$CH_2 + e \rightarrow CH + e + H$	$f(\sigma)$	[22, 23]
111	$CH_2 + e \rightarrow C + e + H + H$	$f(\sigma)$	[22, 23]
112	$CH + e \rightarrow C + e + H$	$f(\sigma)$	[22, 23]
113	$CH_4^+ + e \rightarrow CH_3^+ + e + e + H^+$	$f(\sigma)$	[22, 23]
114	$CH_4^+ + e \rightarrow CH_3^+ + e + H$	$f(\sigma)$	[22, 23]
115	$CH_4^+ + e \rightarrow CH_2^+ + e + H_2$	$f(\sigma)$	[22, 23]
116	$CH_4^+ + e \rightarrow CH_2^+ + e + H + H$	$f(\sigma)$	[22, 23]
117	$CH_4^+ + e \rightarrow CH^+ + e + H + H_2$	$f(\sigma)$	[22, 23]
118	$CH_4^+ + e \rightarrow CH^+ + e + H + H + H$	$f(\sigma)$	[22, 23]
119	$CH_4^+ + e \rightarrow C^+ + e + H_2 + H_2$	$f(\sigma)$	[22, 23]
120	$CH_4^+ + e \rightarrow C^+ + e + H + H + H_2$	$f(\sigma)$	[22, 23]
121	$CH_4^+ + e \rightarrow C^+ + e + H + H + H + H$	$f(\sigma)$	[22, 23]
122	$CH_4^+ + e \rightarrow CH + e + H_3^+$	$f(\sigma)$	[22, 23]
123	$CH_4^+ + e \rightarrow C + e + H_2 + H_2^+$	$f(\sigma)$	[22, 23]
124	$CH_4^+ + e \rightarrow CH + e + H + H_2^+$	$f(\sigma)$	[22, 23]
125	$CH_4^+ + e \rightarrow CH_2 + e + H_2^+$	$f(\sigma)$	[22, 23]
126	$CH_4^+ + e \rightarrow C + e + H + H + H_2^+$	$f(\sigma)$	[22, 23]
127	$CH_4^+ + e \rightarrow CH_2 + e + H + H^+$	$f(\sigma)$	[22, 23]
128	$CH_4^+ + e \rightarrow CH_3 + e + H^+$	$f(\sigma)$	[22, 23]
129	$CH_4^+ + e \rightarrow CH + e + H_2 + H^+$	$f(\sigma)$	[22, 23]
130	$CH_3^+ + e \rightarrow CH_2^+ + e + H$	$f(\sigma)$	[22, 23]
131	$CH_3^+ + e \rightarrow CH^+ + e + H_2$	$f(\sigma)$	[22, 23]
132	$CH_3^+ + e \rightarrow CH^+ + e + H + H$	$f(\sigma)$	[22, 23]
133	$CH_3^+ + e \rightarrow C^+ + e + H + H_2$	$f(\sigma)$	[22, 23]
134	$CH_3^+ + e \rightarrow C^+ + e + H + H + H$	$f(\sigma)$	[22, 23]
135	$CH_3^+ + e \rightarrow C + e + H + H_2^+$	$f(\sigma)$	[22, 23]
136	$CH_3^+ + e \rightarrow CH + e + H_2^+$	$f(\sigma)$	[22, 23]
137	$CH_3^+ + e \rightarrow C + e + H_2 + H^+$	$f(\sigma)$	[22, 23]
138	$CH_3^+ + e \rightarrow CH_2 + e + H^+$	$f(\sigma)$	[22, 23]
139	$CH_3^+ + e \rightarrow CH + e + H + H^+$	$f(\sigma)$	[22, 23]
140	$CH_2^+ + e \rightarrow CH^+ + e + H$	$f(\sigma)$	[22, 23]
141	$CH_2^+ + e \rightarrow C^+ + e + H_2$	$f(\sigma)$	[22, 23]
142	$CH_2^+ + e \rightarrow C^+ + e + H + H$	$f(\sigma)$	[22, 23]
143	$CH_2^+ + e \rightarrow C + e + H_2^+$	$f(\sigma)$	[22, 23]
144	$CH_2^+ + e \rightarrow CH + e + H^+$	$f(\sigma)$	[22, 23]
145	$CH_2^+ + e \rightarrow C + e + H + H^+$	$f(\sigma)$	[22, 23]
146	$CH^+ + e \rightarrow C + e + H^+$	$f(\sigma)$	[22, 23]
147	$CH^+ + e \rightarrow C^+ + e + H$	$f(\sigma)$	[22, 23]
148	$CH_4^+ + e \rightarrow CH_3 + H$	$f(\sigma)$	[22, 23]
149	$CH_4^+ + e \rightarrow CH + H + H_2$	$f(\sigma)$	[22, 23]

#	Reaction	Rate equation	Ref.
150	$CH_4^+ + e \rightarrow C + H_2 + H_2$	$f(\sigma)$	[22, 23]
151	$CH_4^+ + e \rightarrow CH_2 + H_2$	$f(\sigma)$	[22, 23]
152	$CH_4^+ + e \rightarrow CH_2 + H + H$	$f(\sigma)$	[22, 23]
153	$CH_3^+ + e \rightarrow CH + H_2$	$f(\sigma)$	[22, 23]
154	$CH_3^+ + e \rightarrow C + H + H_2$	$f(\sigma)$	[22, 23]
155	$CH_3^+ + e \rightarrow CH + H + H$	$f(\sigma)$	[22, 23]
156	$CH_3^+ + e \rightarrow CH_2 + H$	$f(\sigma)$	[22, 23]
157	$CH_2^+ + e \rightarrow C + H_2$	$f(\sigma)$	[22, 23]
158	$CH_2^+ + e \rightarrow CH + H$	$f(\sigma)$	[22, 23]
159	$CH_2^+ + e \rightarrow C + H + H$	$f(\sigma)$	[22, 23]
160	$CH^+ + e \rightarrow C + H$	$f(\sigma)$	[22, 23]
161	$CH_4 + e \rightarrow CH_3 + H^-$	$f(\sigma)$	[24]
162	$CH_4 \rightarrow CH_3 + H$	$k_0 = 7.5 \times 10^{-7} \cdot \exp\left(\frac{-4.570 \times 10^4}{T_g}\right)$ $k_\infty = 2.4 \times 10^{16} \cdot \exp\left(\frac{-5.280 \times 10^4}{T_g}\right)$ $F_c = \exp\left(\frac{-T_g}{1.350 \times 10^3}\right)$ $+ \exp\left(\frac{-7.8340 \times 10^3}{T_g}\right)$	[5] <sup>a</sup>
163	$CH_3 \rightarrow CH + H_2$	$1.1 \times 10^{-8} \cdot \exp\left(\frac{-4.280 \times 10^4}{T_g}\right) \cdot n_M$	[5]
164	$CH_3 \rightarrow CH_2 + H$	$1.7 \times 10^{-8} \cdot \exp\left(\frac{-4.560 \times 10^4}{T_g}\right) \cdot n_M$	[5]
165	$CH_2 \rightarrow CH + H$	$1.56 \times 10^{-8} \cdot \exp\left(\frac{-4.488 \times 10^4}{T_g}\right) \cdot n_M$	[5]
166	$CH_2 \rightarrow C + H_2$	$5 \times 10^{-10} \cdot \exp\left(\frac{-3.26 \times 10^4}{T_g}\right) \cdot n_M$	[5]
167	$CH \rightarrow C + H$	$\frac{1.9 \times 10^{14}}{N_A} \cdot \exp\left(\frac{-3.37 \times 10^4}{T_g}\right) \cdot n_M$	[11]
168	$C_2H_6 + H \rightarrow C_2H_5 + H_2$	$1.63 \times 10^{-10} \cdot \exp\left(\frac{-4.640 \times 10^3}{T_g}\right)$	[5]
169	$C_2H_5 + H_2 \rightarrow C_2H_6 + H$	$5.1 \times 10^{-24} \cdot T_g^{3.6} \cdot \exp\left(\frac{-4.253 \times 10^3}{T_g}\right)$	[5]
170	$C_2H_5 + H \rightarrow CH_3 + CH_3$	$7 \times 10^{-11}$	[5]
171	$C_2H_5 + H \rightarrow C_2H_6$	$\frac{6 \times 10^{-11}}{1 + 10^{-1.915 + 2.69 \times 10^{-3} \cdot T_g - 2.35 \times 10^{-7} \cdot T_g^2}}$	[25]
172	$C_2H_5 + H \rightarrow C_2H_4 + H_2$	$3 \times 10^{-12}$	[25]
173	$C_2H_4 + H_2 \rightarrow C_2H_5 + H$	$1.7 \times 10^{-11} \cdot \exp\left(\frac{-3.43 \times 10^4}{T_g}\right)$	[25]
174	$C_2H_4 + H \rightarrow C_2H_3 + H_2$	$3.9 \times 10^{-22} \cdot T_g^{3.62} \cdot \exp\left(\frac{-5.67 \times 10^3}{T_g}\right)$	[5]
175	$C_2H_4 + H \rightarrow C_2H_5$	$k_0 = 1.3 \times 10^{-29} \cdot \exp\left(\frac{-3.8 \times 10^2}{T_g}\right)$ $k_\infty = 6.6 \times 10^{-15} \cdot T_g^{1.28} \cdot \exp\left(\frac{-6.5 \times 10^2}{T_g}\right)$ $F_c = 0.24 \cdot \exp\left(\frac{-T_g}{4 \times 10^1}\right)$ $+ 0.76 \cdot \exp\left(\frac{-T_g}{1.025 \times 10^3}\right)$	[5] <sup>a</sup>
176	$C_2H_3 + H_2 \rightarrow C_2H_4 + H$	$1.57 \times 10^{-20} \cdot T_g^{2.56} \cdot \exp\left(\frac{-2.529 \times 10^3}{T_g}\right)$	[26]
177	$C_2H_3 + H \rightarrow C_2H_2 + H_2$	$7 \times 10^{-11}$	[5]
178	$C_2H_3 + H \rightarrow C_2H_4$	$k_0 = 3.5 \times 10^{-27}$ $k_\infty = 1.6 \times 10^{-10}$ $F_c = 0.5$	[5] <sup>a</sup>
179	$C_2H_2 + H_2 \rightarrow C_2H_3 + H$	$4 \times 10^{-12} \cdot \exp\left(\frac{-3.27 \times 10^4}{T_g}\right)$	[25]
180	$C_2H_2 + H_2 \rightarrow C_2H_4$	$5 \times 10^{-13} \cdot \exp\left(\frac{-1.96 \times 10^4}{T_g}\right)$	[25]

#	Reaction	Rate equation	Ref.
181	$C_2H_2 + H \rightarrow C_2H_3$	$k_0 = 1 \times 10^{-20} \cdot T_g^{-3.38} \cdot \exp\left(\frac{-4.26 \times 10^2}{T_g}\right)$ $k_\infty = 9.2 \times 10^{-16} \cdot T_g^{1.64} \cdot \exp\left(\frac{-1.055 \times 10^3}{T_g}\right)$ $F_c = 7.37 \times 10^{-4} \cdot T_g^{0.8}$	[5] <sup>a</sup>
182	$C_2H_2 + H \rightarrow C_2H + H_2$	$1.67 \times 10^{-14} \cdot T_g^{1.64} \cdot \exp\left(\frac{-1.525 \times 10^4}{T_g}\right)$	[5]
183	$C_2H + H_2 \rightarrow C_2H_2 + H$	$3.5 \times 10^{-18} \cdot T_g^{2.32} \cdot \exp\left(\frac{-4.44 \times 10^2}{T_g}\right)$	[5]
184	$C_2H + H \rightarrow C_2H_2$	$3 \times 10^{-10}$	[25]
185	$C_2H_6^+ + H \rightarrow C_2H_5^+ + H_2$	$1 \times 10^{-10}$	[27]
186	$C_2H_5^+ + H \rightarrow C_2H_4^+ + H_2$	$1 \times 10^{-11}$	[8]
187	$C_2H_4^+ + H \rightarrow C_2H_3^+ + H_2$	$3 \times 10^{-10}$	[8]
188	$C_2H_3^+ + H \rightarrow C_2H_2^+ + H_2$	$6.8 \times 10^{-11}$	[8]
189	$C_2H_2^+ + H_2 \rightarrow C_2H_3^+ + H$	$1 \times 10^{-11}$	[8]
190	$C_2H^+ + H_2 \rightarrow C_2H_2^+ + H$	$1.1 \times 10^{-9}$	[8]
191	$C_2H_6 + H^+ \rightarrow C_2H_5^+ + H_2$	$1.287 \times 10^{-9}$	[28]
192	$C_2H_6 + H^+ \rightarrow C_2H_4^+ + H + H_2$	$1.287 \times 10^{-9}$	[28]
193	$C_2H_6 + H^+ \rightarrow C_2H_3^+ + H_2 + H_2$	$1.287 \times 10^{-9}$	[28]
194	$C_2H_4 + H^+ \rightarrow C_2H_4^+ + H$	$9.8 \times 10^{-10}$	[29]
195	$C_2H_4 + H^+ \rightarrow C_2H_3^+ + H_2$	$2.94 \times 10^{-9}$	[29]
196	$C_2H_4 + H^+ \rightarrow C_2H_2^+ + H + H_2$	$9.8 \times 10^{-10}$	[29]
197	$C_2H_3 + H^+ \rightarrow C_2H_3^+ + H$	$2 \times 10^{-9}$	[13]
198	$C_2H_3 + H^+ \rightarrow C_2H_2^+ + H_2$	$2 \times 10^{-9}$	[13]
199	$C_2H_2 + H^+ \rightarrow C_2H_2^+ + H$	$5.4 \times 10^{-10}$	[29]
200	$C_2H + H^+ \rightarrow C_2H^+ + H$	$1.5 \times 10^{-9}$	[1]
201	$C_2H_6 + H_2^+ \rightarrow C_2H_6^+ + H_2$	$2.94 \times 10^{-10}$	[7]
202	$C_2H_6 + H_2^+ \rightarrow C_2H_5^+ + H + H_2$	$1.372 \times 10^{-9}$	[7]
203	$C_2H_6 + H_2^+ \rightarrow C_2H_4^+ + H_2 + H_2$	$2.352 \times 10^{-9}$	[7]
204	$C_2H_6 + H_2^+ \rightarrow C_2H_3^+ + H + H_2 + H_2$	$6.86 \times 10^{-10}$	[7]
205	$C_2H_6 + H_2^+ \rightarrow C_2H_2^+ + H_2 + H_2 + H_2$	$1.96 \times 10^{-10}$	[7]
206	$C_2H_4 + H_2^+ \rightarrow C_2H_4^+ + H_2$	$2.205 \times 10^{-9}$	[7]
207	$C_2H_4 + H_2^+ \rightarrow C_2H_3^+ + H + H_2$	$1.813 \times 10^{-9}$	[7]
208	$C_2H_4 + H_2^+ \rightarrow C_2H_2^+ + H_2 + H_2$	$8.82 \times 10^{-10}$	[7]
209	$C_2H_2 + H_2^+ \rightarrow C_2H_3^+ + H$	$4.77 \times 10^{-10}$	[7]
210	$C_2H_2 + H_2^+ \rightarrow C_2H_2^+ + H_2$	$4.823 \times 10^{-9}$	[7]
211	$C_2H + H_2^+ \rightarrow C_2H_2^+ + H$	$1 \times 10^{-9}$	[1]
212	$C_2H + H_2^+ \rightarrow C_2H^+ + H_2$	$1 \times 10^{-9}$	[1]
213	$C_2H_6 + H_3^+ \rightarrow C_2H_5^+ + H_2 + H_2$	$3.4 \times 10^{-9}$	[30, 31]
214	$C_2H_4 + H_3^+ \rightarrow C_2H_5^+ + H_2$	$1.44 \times 10^{-9}$	[30, 31]
215	$C_2H_4 + H_3^+ \rightarrow C_2H_3^+ + H_2 + H_2$	$2.16 \times 10^{-9}$	[30, 31]
216	$C_2H_2 + H_3^+ \rightarrow C_2H_3^+ + H_2$	$3.5 \times 10^{-9}$	[30, 31]
217	$C_2H + H_3^+ \rightarrow C_2H_2^+ + H_2$	$1.7 \times 10^{-9}$	[1]
218	$C_2H + H^- \rightarrow C_2H_2 + e$	$1 \times 10^{-9}$	[1]

#	Reaction	Rate equation	Ref.
219	$C_2H_2^+ + H^- \rightarrow C_2H_2 + H$	$7.51 \times 10^{-8} \cdot \left(\frac{T_g}{3 \times 10^2}\right)^{-0.5}$	[2, 3]
220	$C_2H_3^+ + H^- \rightarrow C_2H_3 + H$	$7.51 \times 10^{-8} \cdot \left(\frac{T_g}{3 \times 10^2}\right)^{-0.5}$	[2, 3]
221	$C + C_2H_4 \rightarrow C_2H_2 + CH_2$	$1.239 \times 10^{-11}$	[32, 33]
222	$C_2H_6 + CH_3 \rightarrow C_2H_5 + CH_4$	$9.3 \times 10^{-14} \cdot \exp\left(\frac{-4.740 \times 10^3}{T_g}\right) + 1.4 \times 10^{-9} \cdot \exp\left(\frac{-1.120 \times 10^4}{T_g}\right)$	[5]
223	$C_2H_6 + CH_2 \rightarrow C_2H_5 + CH_3$	$\frac{6.5 \times 10^{12}}{N_A} \cdot \exp\left(\frac{-3.31 \times 10^4}{R \cdot T_g}\right)$	[15]
224	$C_2H_6 + CH \rightarrow C_2H_4 + CH_3$	$1.3 \times 10^{-10}$	[34]
225	$C_2H_5 + CH_4 \rightarrow C_2H_6 + CH_3$	$1.43 \times 10^{-25} \cdot T_g^{4.14} \cdot \exp\left(\frac{-6.322 \times 10^3}{T_g}\right)$	[25]
226	$C_2H_5 + CH_3 \rightarrow C_2H_4 + CH_4$	$1.5 \times 10^{-12}$	[5]
227	$C_2H_5 + CH_3 \rightarrow C_2H_6 + CH_2$	$3 \times 10^{-44} \cdot T_g^{9.0956}$	[35]
228	$C_2H_5 + CH_2 \rightarrow C_2H_4 + CH_3$	$3 \times 10^{-11}$	[25]
229	$C_2H_4 + CH_3 \rightarrow C_2H_3 + CH_4$	$1 \times 10^{-16} \cdot T_g^{1.56} \cdot \exp\left(\frac{-8.37 \times 10^3}{T_g}\right)$	[5]
230	$C_2H_3 + CH_4 \rightarrow C_2H_4 + CH_3$	$2.4 \times 10^{-24} \cdot T_g^{4.02} \cdot \exp\left(\frac{-2.754 \times 10^3}{T_g}\right)$	[25]
231	$C_2H_3 + CH_3 \rightarrow C_2H_2 + CH_4$	$1.5 \times 10^{-11} \cdot \exp\left(\frac{3.850 \times 10^2}{T_g}\right)$	[36]
232	$C_2H_3 + CH_2 \rightarrow C_2H_2 + CH_3$	$3 \times 10^{-11}$	[25]
233	$C_2H_2 + CH_3 \rightarrow C_2H + CH_4$	$3 \times 10^{-13} \cdot \exp\left(\frac{-8.7 \times 10^3}{T_g}\right)$	[25]
234	$C_2H + CH_4 \rightarrow C_2H_2 + CH_3$	$3.6 \times 10^{-14} \cdot T_g^{0.94} \cdot \exp\left(\frac{-3.28 \times 10^2}{T_g}\right)$	[5]
235	$C_2H + CH_2 \rightarrow C_2H_2 + CH$	$3 \times 10^{-11}$	[25]
236	$C_2H_6 + CH_5^+ \rightarrow C_2H_5^+ + CH_4 + H_2$	$2.25 \times 10^{-10}$	[28]
237	$C_2H_4 + CH_5^+ \rightarrow C_2H_5^+ + CH_4$	$1.5 \times 10^{-8}$	[37]
238	$C_2H_2 + CH_5^+ \rightarrow C_2H_3^+ + CH_4$	$1.56 \times 10^{-9}$	[38]
239	$C_2H + CH_5^+ \rightarrow C_2H_2^+ + CH_4$	$9 \times 10^{-10}$	[1]
240	$C_2H_6 + CH_4^+ \rightarrow C_2H_4^+ + CH_4 + H_2$	$1.91 \times 10^{-9}$	[39]
241	$C_2H_4 + CH_4^+ \rightarrow C_2H_4^+ + CH_4$	$1.38 \times 10^{-9}$	[39]
242	$C_2H_4 + CH_4^+ \rightarrow C_2H_5^+ + CH_3$	$4.232 \times 10^{-10}$	[39]
243	$C_2H_2 + CH_4^+ \rightarrow C_2H_2^+ + CH_4$	$1.134 \times 10^{-9}$	[39]
244	$C_2H_2 + CH_4^+ \rightarrow C_2H_3^+ + CH_3$	$1.2348 \times 10^{-9}$	[39]
245	$C_2H_6 + CH_3^+ \rightarrow C_2H_5^+ + CH_4$	$1.479 \times 10^{-9}$	[39]
246	$C_2H_4 + CH_3^+ \rightarrow C_2H_3^+ + CH_4$	$3.496 \times 10^{-10}$	[39]
247	$C_2H_2^+ + CH_4 \rightarrow C_2H_3^+ + CH_3$	$4.1 \times 10^{-9}$	[21]
248	$C_2H^+ + CH_4 \rightarrow C_2H_2^+ + CH_3$	$3.74 \times 10^{-10}$	[9]
249	$C_2H_3 + C_2H_6 \rightarrow C_2H_4 + C_2H_5$	$1 \times 10^{-21} \cdot T_g^{3.3} \cdot \exp\left(\frac{-5.285 \times 10^3}{T_g}\right)$	[25]
250	$C_2H + C_2H_6 \rightarrow C_2H_2 + C_2H_5$	$6.75 \times 10^{-12} \cdot T_g^{0.28} \cdot \exp\left(\frac{6.2 \times 10^1}{T_g}\right)$	[5]
251	$C_2H_5 + C_2H_5 \rightarrow C_2H_4 + C_2H_6$	$2.3 \times 10^{-12}$	[5]
252	$C_2H_4 + C_2H_5 \rightarrow C_2H_3 + C_2H_6$	$8.1 \times 10^{-31} \cdot T_g^{5.82} \cdot \exp\left(\frac{-6 \times 10^3}{T_g}\right)$	[5]
253	$C_2H_3 + C_2H_5 \rightarrow C_2H_2 + C_2H_6$	$2.3985 \times 10^{-11}$	[40, 41]
254	$C_2H_3 + C_2H_5 \rightarrow C_2H_4 + C_2H_4$	$4.42 \times 10^{-11}$	[40, 41]
255	$C_2H_2 + C_2H_5 \rightarrow C_2H + C_2H_6$	$4.5 \times 10^{-13} \cdot \exp\left(\frac{-1.18 \times 10^4}{T_g}\right)$	[25]
256	$C_2H + C_2H_5 \rightarrow C_2H_2 + C_2H_4$	$3 \times 10^{-12}$	[25]

#	Reaction	Rate equation	Ref.
257	$C_2H_4 + C_2H_4 \rightarrow C_2H_3 + C_2H_5$	$8 \times 10^{-10} \cdot \exp\left(\frac{-3.6 \times 10^4}{T_g}\right)$	[25]
258	$C_2H_2 + C_2H_4 \rightarrow C_2H_3 + C_2H_3$	$4 \times 10^{-11} \cdot \exp\left(\frac{-3.44 \times 10^4}{T_g}\right)$	[25]
259	$C_2H + C_2H_4 \rightarrow C_2H_2 + C_2H_3$	$3.35 \times 10^{-18} \cdot T_g^{2.24}$	[42]
260	$C_2H_3 + C_2H_3 \rightarrow C_2H_2 + C_2H_4$	$1.6 \times 10^{-12}$	[25]
261	$C_2H + C_2H_3 \rightarrow C_2H_2 + C_2H_2$	$1.6 \times 10^{-12}$	[25]
262	$C_2H_2 + C_2H_2 \rightarrow C_2H + C_2H_3$	$1.6 \times 10^{-11} \cdot \exp\left(\frac{-4.25 \times 10^4}{T_g}\right)$	[25]
263	$C_2H_4 + C_2H_6^+ \rightarrow C_2H_4^+ + C_2H_6$	$1.15 \times 10^{-9}$	[39]
264	$C_2H_2 + C_2H_6^+ \rightarrow C_2H_3 + C_2H_5^+$	$2.223 \times 10^{-10}$	[39]
265	$C_2H_3^+ + C_2H_6 \rightarrow C_2H_4 + C_2H_5^+$	$2.914 \times 10^{-10}$	[39]
266	$C_2H_3^+ + C_2H_4 \rightarrow C_2H_2 + C_2H_5^+$	$9.3 \times 10^{-10}$	[39]
267	$C_2H_2^+ + C_2H_6 \rightarrow C_2H_3 + C_2H_5^+$	$1.314 \times 10^{-10}$	[39]
268	$C_2H_2^+ + C_2H_6 \rightarrow C_2H_4 + C_2H_4^+$	$2.628 \times 10^{-10}$	[39]
269	$C_2H_2^+ + C_2H_4 \rightarrow C_2H_2 + C_2H_4^+$	$4.012 \times 10^{-10}$	[39]
270	$C_2H + e \rightarrow C_2H^+ + e + e$	$f(\sigma)$	[23, 43]
271	$C_2H_2 + e \rightarrow C_2H_2^+ + e + e$	$f(\sigma)$	[23, 43]
272	$C_2H_3 + e \rightarrow C_2H_3^+ + e + e$	$f(\sigma)$	[23, 43]
273	$C_2H_4 + e \rightarrow C_2H_4^+ + e + e$	$f(\sigma)$	[23, 43]
274	$C_2H_5 + e \rightarrow C_2H_5^+ + e + e$	$f(\sigma)$	[23, 43]
275	$C_2H_6 + e \rightarrow C_2H_6^+ + e + e$	$f(\sigma)$	[23, 43]
276	$C_2H + e \rightarrow C + CH^+ + e + e$	$f(\sigma)$	[23, 43]
277	$C_2H + e \rightarrow CH + C^+ + e + e$	$f(\sigma)$	[23, 43]
278	$C_2H_2 + e \rightarrow C_2H^+ + e + e + H$	$f(\sigma)$	[23, 43]
279	$C_2H_2 + e \rightarrow C_2H + e + e + H^+$	$f(\sigma)$	[23, 43]
280	$C_2H_3 + e \rightarrow C_2H_2^+ + e + e + H$	$f(\sigma)$	[23, 43]
281	$C_2H_3 + e \rightarrow C_2H^+ + e + e + H_2$	$f(\sigma)$	[23, 43]
282	$C_2H_3 + e \rightarrow C_2H^+ + e + e + H + H$	$f(\sigma)$	[23, 43]
283	$C_2H_3 + e \rightarrow CH + CH_2^+ + e + e$	$f(\sigma)$	[23, 43]
284	$C_2H_3 + e \rightarrow CH_2 + CH^+ + e + e$	$f(\sigma)$	[23, 43]
285	$C_2H_3 + e \rightarrow CH_3 + C^+ + e + e$	$f(\sigma)$	[23, 43]
286	$C_2H_3 + e \rightarrow C_2H_2 + e + e + H^+$	$f(\sigma)$	[23, 43]
287	$C_2H_4 + e \rightarrow C_2H_3^+ + e + e + H$	$f(\sigma)$	[23, 43]
288	$C_2H_4 + e \rightarrow C_2H_2^+ + e + e + H_2$	$f(\sigma)$	[23, 43]
289	$C_2H_4 + e \rightarrow C_2H_2^+ + e + e + H + H$	$f(\sigma)$	[23, 43]
290	$C_2H_4 + e \rightarrow C_2H^+ + e + e + H + H + H$	$f(\sigma)$	[23, 43]
291	$C_2H_4 + e \rightarrow CH + CH_3^+ + e + e$	$f(\sigma)$	[23, 43]
292	$C_2H_4 + e \rightarrow CH_2 + CH_2^+ + e + e$	$f(\sigma)$	[23, 43]
293	$C_2H_4 + e \rightarrow CH_3 + CH^+ + e + e$	$f(\sigma)$	[23, 43]
294	$C_2H_4 + e \rightarrow CH_4 + C^+ + e + e$	$f(\sigma)$	[23, 43]
295	$C_2H_5 + e \rightarrow C_2H_4^+ + e + e + H$	$f(\sigma)$	[23, 43]
296	$C_2H_5 + e \rightarrow C_2H_3^+ + e + e + H_2$	$f(\sigma)$	[23, 43]

#	Reaction	Rate equation	Ref.
297	$C_2H_5 + e \rightarrow C_2H_3^+ + e + e + H + H$	$f(\sigma)$	[23, 43]
298	$C_2H_5 + e \rightarrow C_2H_2^+ + e + e + H + H_2$	$f(\sigma)$	[23, 43]
299	$C_2H_5 + e \rightarrow C_2H^+ + e + e + H_2 + H_2$	$f(\sigma)$	[23, 43]
300	$C_2H_5 + e \rightarrow CH_2 + CH_3^+ + e + e$	$f(\sigma)$	[23, 43]
301	$C_2H_5 + e \rightarrow CH_2^+ + CH_3 + e + e$	$f(\sigma)$	[23, 43]
302	$C_2H_5 + e \rightarrow CH_4 + CH^+ + e + e$	$f(\sigma)$	[23, 43]
303	$C_2H_5 + e \rightarrow CH_4 + C^+ + e + e + H$	$f(\sigma)$	[23, 43]
304	$C_2H_5 + e \rightarrow CH_3 + C^+ + e + e + H_2$	$f(\sigma)$	[23, 43]
305	$C_2H_6 + e \rightarrow C_2H_5^+ + e + e + H$	$f(\sigma)$	[23, 43]
306	$C_2H_6 + e \rightarrow C_2H_4^+ + e + e + H_2$	$f(\sigma)$	[23, 43]
307	$C_2H_6 + e \rightarrow C_2H_3^+ + e + e + H + H_2$	$f(\sigma)$	[23, 43]
308	$C_2H_6 + e \rightarrow C_2H_2^+ + e + e + H_2 + H_2$	$f(\sigma)$	[23, 43]
309	$C_2H_6 + e \rightarrow C_2H_2^+ + e + e + H + H + H_2$	$f(\sigma)$	[23, 43]
310	$C_2H_6 + e \rightarrow CH_3 + CH_3^+ + e + e$	$f(\sigma)$	[23, 43]
311	$C_2H_6 + e \rightarrow C_2H_4 + e + e + H_2^+$	$f(\sigma)$	[23, 43]
312	$C_2H_6 + e \rightarrow C_2H_2 + e + H_2 + H_2$	$f(\sigma)$	[23, 43]
313	$C_2H_6 + e \rightarrow C_2H_5 + e + H$	$f(\sigma)$	[23, 43]
314	$C_2H_6 + e \rightarrow CH_2 + CH_4 + e$	$f(\sigma)$	[23, 43]
315	$C_2H_6 + e \rightarrow C_2H_4 + e + H_2$	$f(\sigma)$	[23, 43]
316	$C_2H_6 + e \rightarrow C_2H_3 + e + H + H_2$	$f(\sigma)$	[23, 43]
317	$C_2H_6 + e \rightarrow CH_3 + CH_3 + e$	$f(\sigma)$	[23, 43]
318	$C_2H_5 + e \rightarrow CH_2 + CH_3 + e$	$f(\sigma)$	[23, 43]
319	$C_2H_5 + e \rightarrow C_2H_3 + e + H_2$	$f(\sigma)$	[23, 43]
320	$C_2H_5 + e \rightarrow C_2H_4 + e + H$	$f(\sigma)$	[23, 43]
321	$C_2H_5 + e \rightarrow C_2H + e + H_2 + H_2$	$f(\sigma)$	[23, 43]
322	$C_2H_5 + e \rightarrow C_2H_2 + e + H + H_2$	$f(\sigma)$	[23, 43]
323	$C_2H_5 + e \rightarrow CH + CH_4 + e$	$f(\sigma)$	[23, 43]
324	$C_2H_5 + e \rightarrow C_2H_3 + e + H + H$	$f(\sigma)$	[23, 43]
325	$C_2H_4 + e \rightarrow C + CH_4 + e$	$f(\sigma)$	[23, 43]
326	$C_2H_4 + e \rightarrow C_2H_2 + e + H + H$	$f(\sigma)$	[23, 43]
327	$C_2H_4 + e \rightarrow C_2H_2 + e + H_2$	$f(\sigma)$	[23, 43]
328	$C_2H_4 + e \rightarrow C_2H + e + H + H_2$	$f(\sigma)$	[23, 43]
329	$C_2H_4 + e \rightarrow CH + CH_3 + e$	$f(\sigma)$	[23, 43]
330	$C_2H_4 + e \rightarrow CH_2 + CH_2 + e$	$f(\sigma)$	[23, 43]
331	$C_2H_4 + e \rightarrow C_2H_3 + e + H$	$f(\sigma)$	[23, 43]
332	$C_2H_3 + e \rightarrow C_2H + e + H_2$	$f(\sigma)$	[23, 43]
333	$C_2H_3 + e \rightarrow CH + CH_2 + e$	$f(\sigma)$	[23, 43]
334	$C_2H_3 + e \rightarrow C_2H_2 + e + H$	$f(\sigma)$	[23, 43]
335	$C_2H_3 + e \rightarrow C + CH_3 + e$	$f(\sigma)$	[23, 43]
336	$C_2H_3 + e \rightarrow C_2H + e + H + H$	$f(\sigma)$	[23, 43]

#	Reaction	Rate equation	Ref.
337	$C_2H_2 + e \rightarrow C + CH_2 + e$	$f(\sigma)$	[23, 43]
338	$C_2H_2 + e \rightarrow C_2H + e + H$	$f(\sigma)$	[23, 43]
339	$C_2H_2 + e \rightarrow CH + CH + e$	$f(\sigma)$	[23, 43]
340	$C_2H + e \rightarrow C + CH + e$	$f(\sigma)$	[23, 43]
341	$C_2H^+ + e \rightarrow C + CH^+ + e$	$f(\sigma)$	[23, 43]
342	$C_2H^+ + e \rightarrow CH + C^+ + e$	$f(\sigma)$	[23, 43]
343	$C_2H_2^+ + e \rightarrow C_2H^+ + e + H$	$f(\sigma)$	[23, 43]
344	$C_2H_2^+ + e \rightarrow C_2H + e + H^+$	$f(\sigma)$	[23, 43]
345	$C_2H_2^+ + e \rightarrow CH_2 + C^+ + e$	$f(\sigma)$	[23, 43]
346	$C_2H_2^+ + e \rightarrow CH + CH^+ + e$	$f(\sigma)$	[23, 43]
347	$C_2H_2^+ + e \rightarrow C + CH_2^+ + e$	$f(\sigma)$	[23, 43]
348	$C_2H_3^+ + e \rightarrow CH_2 + CH^+ + e$	$f(\sigma)$	[23, 43]
349	$C_2H_3^+ + e \rightarrow C_2H_2 + e + H^+$	$f(\sigma)$	[23, 43]
350	$C_2H_3^+ + e \rightarrow C_2H + e + H_2^+$	$f(\sigma)$	[23, 43]
351	$C_2H_3^+ + e \rightarrow C_2H^+ + e + H_2$	$f(\sigma)$	[23, 43]
352	$C_2H_3^+ + e \rightarrow C + CH_3^+ + e$	$f(\sigma)$	[23, 43]
353	$C_2H_3^+ + e \rightarrow C_2H_2^+ + e + H$	$f(\sigma)$	[23, 43]
354	$C_2H_3^+ + e \rightarrow CH + CH_2^+ + e$	$f(\sigma)$	[23, 43]
355	$C_2H_3^+ + e \rightarrow CH_3 + C^+ + e$	$f(\sigma)$	[23, 43]
356	$C_2H_4^+ + e \rightarrow CH + CH_3^+ + e$	$f(\sigma)$	[23, 43]
357	$C_2H_4^+ + e \rightarrow CH_2 + CH_2^+ + e$	$f(\sigma)$	[23, 43]
358	$C_2H_4^+ + e \rightarrow CH_3 + CH^+ + e$	$f(\sigma)$	[23, 43]
359	$C_2H_4^+ + e \rightarrow CH_4 + C^+ + e$	$f(\sigma)$	[23, 43]
360	$C_2H_4^+ + e \rightarrow C_2H_2 + e + H_2^+$	$f(\sigma)$	[23, 43]
361	$C_2H_4^+ + e \rightarrow C_2H_2^+ + e + H_2$	$f(\sigma)$	[23, 43]
362	$C_2H_4^+ + e \rightarrow C_2H_3^+ + e + H$	$f(\sigma)$	[23, 43]
363	$C_2H_5^+ + e \rightarrow C_2H_3^+ + e + H + H$	$f(\sigma)$	[23, 43]
364	$C_2H_5^+ + e \rightarrow CH_2^+ + CH_3 + e$	$f(\sigma)$	[23, 43]
365	$C_2H_5^+ + e \rightarrow C_2H_3^+ + e + H_2$	$f(\sigma)$	[23, 43]
366	$C_2H_5^+ + e \rightarrow C_2H_4^+ + e + H$	$f(\sigma)$	[23, 43]
367	$C_2H_5^+ + e \rightarrow CH_2 + CH_3^+ + e$	$f(\sigma)$	[23, 43]
368	$C_2H_6^+ + e \rightarrow CH_3 + CH_3^+ + e$	$f(\sigma)$	[23, 43]
369	$C_2H_6^+ + e \rightarrow C_2H_4^+ + e + H_2$	$f(\sigma)$	[23, 43]
370	$C_2H_6^+ + e \rightarrow C_2H_5^+ + e + H$	$f(\sigma)$	[23, 43]
371	$C_2H_6^+ + e \rightarrow C_2H_5 + H$	$f(\sigma)$	[23, 43]
372	$C_2H_6^+ + e \rightarrow CH_2 + CH_2 + H_2$	$f(\sigma)$	[23, 43]
373	$C_2H_6^+ + e \rightarrow C_2H_4 + H + H$	$f(\sigma)$	[23, 43]
374	$C_2H_6^+ + e \rightarrow CH_2 + CH_3 + H$	$f(\sigma)$	[23, 43]
375	$C_2H_6^+ + e \rightarrow CH_2 + CH_4$	$f(\sigma)$	[23, 43]
376	$C_2H_6^+ + e \rightarrow C_2H_4 + H_2$	$f(\sigma)$	[23, 43]

#	Reaction	Rate equation	Ref.
377	$C_2H_6^+ + e \rightarrow C_2H_3 + H + H_2$	$f(\sigma)$	[23, 43]
378	$C_2H_6^+ + e \rightarrow CH_3 + CH_3$	$f(\sigma)$	[23, 43]
379	$C_2H_5^+ + e \rightarrow C_2H_2 + H + H + H$	$f(\sigma)$	[23, 43]
380	$C_2H_5^+ + e \rightarrow C_2H_3 + H_2$	$f(\sigma)$	[23, 43]
381	$C_2H_5^+ + e \rightarrow CH_2 + CH_3$	$f(\sigma)$	[23, 43]
382	$C_2H_5^+ + e \rightarrow C_2H_4 + H$	$f(\sigma)$	[23, 43]
383	$C_2H_5^+ + e \rightarrow C_2H_2 + H + H_2$	$f(\sigma)$	[23, 43]
384	$C_2H_5^+ + e \rightarrow CH + CH_4$	$f(\sigma)$	[23, 43]
385	$C_2H_5^+ + e \rightarrow C_2H_3 + H + H$	$f(\sigma)$	[23, 43]
386	$C_2H_4^+ + e \rightarrow CH + CH_3$	$f(\sigma)$	[23, 43]
387	$C_2H_4^+ + e \rightarrow C_2H_2 + H + H$	$f(\sigma)$	[23, 43]
388	$C_2H_4^+ + e \rightarrow C + CH_4$	$f(\sigma)$	[23, 43]
389	$C_2H_4^+ + e \rightarrow C_2H_2 + H_2$	$f(\sigma)$	[23, 43]
390	$C_2H_4^+ + e \rightarrow C_2H + H + H_2$	$f(\sigma)$	[23, 43]
391	$C_2H_4^+ + e \rightarrow CH_2 + CH_2$	$f(\sigma)$	[23, 43]
392	$C_2H_4^+ + e \rightarrow C_2H_3 + H$	$f(\sigma)$	[23, 43]
393	$C_2H_3^+ + e \rightarrow C_2H + H_2$	$f(\sigma)$	[23, 43]
394	$C_2H_3^+ + e \rightarrow C + CH_3$	$f(\sigma)$	[23, 43]
395	$C_2H_3^+ + e \rightarrow CH + CH_2$	$f(\sigma)$	[23, 43]
396	$C_2H_3^+ + e \rightarrow C_2H_2 + H$	$f(\sigma)$	[23, 43]
397	$C_2H_3^+ + e \rightarrow C_2H + H + H$	$f(\sigma)$	[23, 43]
398	$C_2H_2^+ + e \rightarrow C_2H + H$	$f(\sigma)$	[23, 43]
399	$C_2H_2^+ + e \rightarrow CH + CH$	$f(\sigma)$	[23, 43]
400	$C_2H_2^+ + e \rightarrow C + CH_2$	$f(\sigma)$	[23, 43]
401	$C_2H^+ + e \rightarrow C + CH$	$f(\sigma)$	[23, 43]
402	$C_2H^+ + e \rightarrow C + C + H$	$f(\sigma)$	[23, 43]
403	$C_2H_6 \rightarrow CH_3 + CH_3$	$k_0 = 2.6 \times 10^{25} \cdot T_g^{-8.37} \cdot \exp\left(\frac{-4.729 \times 10^4}{T_g}\right)$ $k_\infty = 4.5 \times 10^{21} \cdot T_g^{-1.37} \cdot \exp\left(\frac{-4.59 \times 10^4}{T_g}\right)$ $F_c = 0.38 \cdot \exp\left(\frac{-T_g}{7.3 \times 10^1}\right)$ $+ 0.62 \cdot \exp\left(\frac{-T_g}{1.18 \times 10^3}\right)$	[5] <sup>a</sup>
404	$C_2H_6 \rightarrow C_2H_5 + H$	$k_0 = \frac{10^{4.2839 \times 10^1}}{n_M} \cdot T_g^{-6.431} \cdot \exp\left(\frac{-5.3938 \times 10^4}{T_g}\right)$ $k_\infty = 10^{2.0947 \times 10^1} \cdot T_g^{-1.228} \cdot \exp\left(\frac{-5.1439 \times 10^4}{T_g}\right)$ $F_c = 4.761 \times 10^1 \cdot \exp\left(\frac{-1.6182 \times 10^4}{T_g}\right)$ $+ \exp\left(\frac{-T_g}{3.371 \times 10^3}\right)$	[44] <sup>a</sup>
405	$C_2H_5 \rightarrow C_2H_4 + H$	$k_0 = 1.7 \times 10^{-6} \cdot \exp\left(\frac{-1.68 \times 10^4}{T_g}\right)$ $k_\infty = 8.2 \times 10^{13} \cdot \exp\left(\frac{-2.007 \times 10^4}{T_g}\right)$ $F_c = 0.25 \cdot \exp\left(\frac{-T_g}{9.7 \times 10^1}\right)$ $+ 0.75 \cdot \exp\left(\frac{-T_g}{1.379 \times 10^3}\right)$	[5] <sup>a</sup>
406	$C_2H_4 \rightarrow C_2H_3 + H$	$10^{1.63 \times 10^1} \cdot \exp\left(\frac{-4.6 \times 10^5}{R \cdot T_g}\right)$	[45]
407	$C_2H_4 \rightarrow C_2H_2 + H_2$	$10^{1.29 \times 10^1} \cdot T_g^{0.44} \cdot \exp\left(\frac{-4.467 \times 10^4}{T_g}\right)$	[25]

#	Reaction	Rate equation	Ref.
408	$C_2H_3 \rightarrow C_2H_2 + H$	$k_0 = 4.3 \times 10^3 \cdot T_g^{-3.4} \cdot \exp\left(\frac{-1.802 \times 10^4}{T_g}\right)$ $k_\infty = 3.9 \times 10^8 \cdot T_g^{1.62} \cdot \exp\left(\frac{-1.865 \times 10^4}{T_g}\right)$ $F_c = 7.37 \times 10^{-4} \cdot T_g^{0.8}$	[5] <sup>a</sup>
409	$C_2H_2 \rightarrow C_2H + H$	$10^{1.542 \times 10^1} \cdot \exp\left(\frac{-6.2445 \times 10^4}{T_g}\right)$	[25]
410	$e + H_2O \rightarrow e + e + H_2O^+$	$f(\sigma)$	[46, 47]
411	$e + H_2O \rightarrow H_2 + O^-$	$f(\sigma)$	[46, 48]
412	$e + H_2O \rightarrow H^- + OH$	$f(\sigma)$	[46, 48]
413	$e + H_2O \rightarrow e + H + OH$	$f(\sigma)$	[48]
414	$e + H_2O \rightarrow e + e + H^+ + OH$	$f(\sigma)$	[46, 47]
415	$e + H_2O \rightarrow e + e + H + OH^+$	$f(\sigma)$	[46, 47]
416	$e + H_2O \rightarrow e + e + H_2 + O^+$	$f(\sigma)$	[46, 47]
417	$e + H_2O \rightarrow e + e + H_2^+ + O$	$f(\sigma)$	[46, 47]
418	$e + H_2O \rightarrow H + OH^-$	$f(\sigma)$	[46, 47]
419	$e + H_2O_2 \rightarrow H_2O + O^-$	$f(\sigma)$	[49]
420	$e + H_2O_2 \rightarrow OH + OH^-$	$f(\sigma)$	[49]
421	$e + OH^- \rightarrow e + e + OH$	$f(\sigma)$	[46]
422	$e + OH \rightarrow e + H + O$	$2.55 \times 10^{-4} \cdot T_e^{-0.76} \cdot \exp\left(\frac{-8.01074 \times 10^4}{T_e}\right)$	[50]
423	$e + OH \rightarrow e + e + OH^+$	$1.16 \times 10^{-17} \cdot T_e^{1.78} \cdot \exp\left(\frac{-1.602671 \times 10^5}{T_e}\right)$	[50]
424	$M + e + OH \rightarrow M + OH^-$	$3 \times 10^{-31}$	[51]
425	$e + OH^+ \rightarrow H + O$	$3.19 \times 10^4 \cdot T_e^{-2.04} \cdot \exp\left(\frac{-1.754618 \times 10^5}{T_e}\right)$	[50]
426	$e + H_2O^+ \rightarrow H_2 + O$	$3.9 \times 10^{-8} \cdot \left(\frac{T_e}{3.0 \times 10^2}\right)^{-0.5}$	[3]
427	$e + H_2O^+ \rightarrow H + H + O$	$3.05 \times 10^{-7} \cdot \left(\frac{T_e}{3.0 \times 10^2}\right)^{-0.5}$	[3]
428	$e + H_2O^+ \rightarrow H + OH$	$8.6 \times 10^{-8} \cdot \left(\frac{T_e}{3.0 \times 10^2}\right)^{-0.5}$	[3]
429	$e + H_3O^+ \rightarrow H + H + OH$	$3.05 \times 10^{-7} \cdot \left(\frac{T_e}{3.0 \times 10^2}\right)^{-0.5}$	[3]
430	$e + H_3O^+ \rightarrow H + H_2O$	$7.09 \times 10^{-8} \cdot \left(\frac{T_e}{3.0 \times 10^2}\right)^{-0.5}$	[3]
431	$e + H_3O^+ \rightarrow H + H_2 + O$	$5.6 \times 10^{-9} \cdot \left(\frac{T_e}{3.0 \times 10^2}\right)^{-0.5}$	[3]
432	$e + H_3O^+ \rightarrow H_2 + OH$	$5.37 \times 10^{-8} \cdot \left(\frac{T_e}{3.0 \times 10^2}\right)^{-0.5}$	[3]
433	$O_2^- + OH \rightarrow O_2 + OH^-$	$1 \times 10^{-10}$	[51]
434	$OH + O^+ \rightarrow O + OH^+$	$3.6 \times 10^{-10}$	[1]
435	$OH + O^+ \rightarrow H + O_2^+$	$3.6 \times 10^{-10}$	[1]
436	$H_2^+ + OH \rightarrow H_2 + OH^+$	$7.6 \times 10^{-10}$	[1]
437	$H_2^+ + OH \rightarrow H + H_2O^+$	$7.6 \times 10^{-10}$	[1]
438	$H^+ + OH \rightarrow H + OH^+$	$2.1 \times 10^{-9}$	[1]
439	$O + OH \rightarrow H + O_2$	$4.33 \times 10^{-11} \cdot \left(\frac{T_g}{3.0 \times 10^2}\right)^{-0.5} \cdot \exp\left(\frac{-3.0 \times 10^1}{T_g}\right)$	[25]
440	$H + OH \rightarrow H_2 + O$	$4.1 \times 10^{-12} \cdot \frac{T_g}{3.0 \times 10^2} \cdot \exp\left(\frac{-3.50 \times 10^3}{T_g}\right)^{1.4}$	[52]
441	$OH + OH \rightarrow H_2O + O$	$1.02 \times 10^{-12} \cdot \left(\frac{T_g}{3.0 \times 10^2}\right)^{1.4} \cdot \exp\left(\frac{2.0 \times 10^2}{T_g}\right)$	[25]
442	$OH + OH \rightarrow H + HO_2$	$2 \times 10^{-11} \cdot \exp\left(\frac{-2.020 \times 10^4}{T_g}\right)$	[52]
443	$OH + OH \rightarrow H_2 + O_2$	$1.82 \times 10^{-13} \cdot T_g^{0.51} \cdot \exp\left(\frac{-2.54 \times 10^4}{T_g}\right)$	[53]
444	$M + OH \rightarrow M + H + O$	$4.7 \times 10^{-8} \cdot \left(\frac{T_g}{3.0 \times 10^2}\right)^{-1.0} \cdot \exp\left(\frac{-5.0830 \times 10^4}{T_g}\right)$	[52]

#	Reaction	Rate equation	Ref.
445	$H_2 + OH \rightarrow H + H_2O$	$3.6 \times 10^{-16} \cdot T_g^{1.52} \cdot \exp\left(\frac{-1.74 \times 10^3}{T_g}\right)$	[5]
446	$O_2 + OH \rightarrow H + O_3$	$2.7 \times 10^{-13} \cdot \left(\frac{T_g}{3.0 \times 10^2}\right)^{1.44} \cdot \exp\left(\frac{-3.860 \times 10^4}{T_g}\right)$	[52]
447	$O_2 + OH \rightarrow HO_2 + O$	$2.2 \times 10^{-11} \cdot \exp\left(\frac{-2.820 \times 10^4}{T_g}\right)$	[52]
448	$O_3 + OH \rightarrow HO_2 + O_2$	$1.69 \times 10^{-12} \cdot \exp\left(\frac{-9.410 \times 10^2}{T_g}\right)$	[54]
449	$H_2O + OH \rightarrow H + H_2O_2$	$4 \times 10^{-10} \cdot \exp\left(\frac{-4.050 \times 10^4}{T_g}\right)$	[52]
450	$HO_2 + OH \rightarrow H_2O + O_2$	$8.05 \times 10^{-11} \cdot \left(\frac{T_g}{3.0 \times 10^2}\right)^{-1.0}$	[25]
451	$HO_2 + OH \rightarrow H_2O_2 + O$	$1.5 \times 10^{-12} \cdot \left(\frac{T_g}{3.0 \times 10^2}\right)^{0.5} \cdot \exp\left(\frac{-1.060 \times 10^4}{T_g}\right)$	[52]
452	$H_2O_2 + OH \rightarrow H_2O + HO_2$	$2.9 \times 10^{-12} \cdot \exp\left(\frac{-1.60 \times 10^2}{T_g}\right)$	[25]
453	$O + OH^+ \rightarrow H + O_2^+$	$7.1 \times 10^{-10}$	[1]
454	$O_2 + OH^+ \rightarrow O_2^+ + OH$	$3.8 \times 10^{-10}$	[27]
455	$H_2O + OH^+ \rightarrow H_2O^+ + OH$	$1.5895 \times 10^{-9}$	[27]
456	$H_2O + OH^+ \rightarrow H_3O^+ + O$	$1.3005 \times 10^{-9}$	[27]
457	$M + OH^- \rightarrow M + e + OH$	$2 \times 10^{-10} \cdot \left(\frac{T_g}{3 \times 10^2}\right)^{0.5}$	c
458	$H + OH^- \rightarrow e + H_2O$	$1.8 \times 10^{-9}$	[55]
459	$O + OH^- \rightarrow e + HO_2$	$2 \times 10^{-10}$	[56]
460	$O_2 + OH^- \rightarrow O_2^- + OH$	$8.7 \times 10^{-10} \cdot \exp\left(\frac{-1.663 \times 10^4}{T_g}\right)$	[51]
461	$O_3 + OH^- \rightarrow O_3^- + OH$	$9 \times 10^{-10}$	[56]
462	$O_3 + OH^- \rightarrow HO_2 + O_2^-$	$1.08 \times 10^{-11}$	[57]
463	$OH^- + OH^+ \rightarrow H + H + O + O$	$1 \times 10^{-7}$	[57]
464	$M + OH^- + OH^+ \rightarrow M + OH + OH$	$2 \times 10^{-25} \cdot \left(\frac{T_g}{3.0 \times 10^2}\right)^{-2.5}$	[57]
465	$OH^- + OH^+ \rightarrow H + O + OH$	$1 \times 10^{-7}$	[57]
466	$OH^- + O^+ \rightarrow H + O + O$	$1 \times 10^{-7}$	[57]
467	$OH^- + O^+ \rightarrow O + OH$	$2 \times 10^{-7} \cdot \left(\frac{T_g}{3.0 \times 10^2}\right)^{-0.5}$	[57]
468	$M + OH^- + O^+ \rightarrow M + HO_2$	$2 \times 10^{-25} \cdot \left(\frac{T_g}{3.0 \times 10^2}\right)^{-2.5}$	[57]
469	$O_2^+ + OH^- \rightarrow H + O + O_2$	$1 \times 10^{-7}$	[57]
470	$O_2^+ + OH^- \rightarrow O_2 + OH$	$2 \times 10^{-7}$	[57]
471	$O_2^+ + OH^- \rightarrow O + O + OH$	$1 \times 10^{-7}$	[57]
472	$M + O_2^+ + OH^- \rightarrow M + O_2 + OH$	$2 \times 10^{-25} \cdot \left(\frac{T_g}{3.0 \times 10^2}\right)^{-2.5}$	[57]
473	$M + H_2O^+ + OH^- \rightarrow M + H_2O + OH$	$2 \times 10^{-25} \cdot \left(\frac{T_g}{3.0 \times 10^2}\right)^{-2.5}$	[57]
474	$H^+ + OH^- \rightarrow H + OH$	$7.51 \times 10^{-8} \cdot \left(\frac{T_g}{3 \times 10^2}\right)^{-0.5}$	[2, 3]
475	$H_3^+ + OH^- \rightarrow H + H_2 + OH$	$7.51 \times 10^{-8} \cdot \left(\frac{T_g}{3 \times 10^2}\right)^{-0.5}$	[2, 3]
476	$H_3O^+ + OH^- \rightarrow H + H_2O + OH$	$7.51 \times 10^{-8} \cdot \left(\frac{T_g}{3 \times 10^2}\right)^{-0.5}$	[2, 3]
477	$H + HO_2 \rightarrow H_2 + O_2$	$1.1 \times 10^{-10} \cdot \exp\left(\frac{-1.070 \times 10^3}{T_g}\right)$	[25]
478	$H + HO_2 \rightarrow OH + OH$	$2.8 \times 10^{-10} \cdot \exp\left(\frac{-4.40 \times 10^2}{T_g}\right)$	[25]
479	$H + HO_2 \rightarrow H_2O + O$	$5 \times 10^{-11} \cdot \exp\left(\frac{-8.660 \times 10^2}{T_g}\right)$	[58]
480	$H_2O + HO_2 \rightarrow H_2O_2 + OH$	$3 \times 10^{-11} \cdot \exp\left(\frac{-1.510 \times 10^4}{T_g}\right)$	[52]
481	$H_2 + HO_2 \rightarrow H_2O + OH$	$1.1 \times 10^{-12} \cdot \exp\left(\frac{-9.40 \times 10^3}{T_g}\right)$	[52]
482	$H_2 + HO_2 \rightarrow H + H_2O_2$	$1 \times 10^{-12} \cdot \exp\left(\frac{-9.30 \times 10^3}{T_g}\right)$	[52]

#	Reaction	Rate equation	Ref.
483	$HO_2 + HO_2 \rightarrow H_2O_2 + O_2$	$2.2 \times 10^{-13} \cdot \exp\left(\frac{6.0 \times 10^2}{T_g}\right)$	[59]
484	$HO_2 + O \rightarrow O_2 + OH$	$2.9 \times 10^{-11} \cdot \exp\left(\frac{2.0 \times 10^2}{T_g}\right)$	[25]
485	$HO_2 + O_2 \rightarrow O_3 + OH$	$1.5 \times 10^{-15}$	[52]
486	$H + H_2O_2 \rightarrow H_2 + HO_2$	$8 \times 10^{-11} \cdot \exp\left(\frac{-4.0 \times 10^3}{T_g}\right)$	[25]
487	$H + H_2O_2 \rightarrow H_2O + OH$	$4 \times 10^{-11} \cdot \exp\left(\frac{-2.0 \times 10^3}{T_g}\right)$	[25]
488	$H_2O_2 + O \rightarrow HO_2 + OH$	$1.44 \times 10^{-12} \cdot \left(\frac{T_g}{3.0 \times 10^2}\right)^{2.0} \cdot \exp\left(\frac{-2.0 \times 10^3}{T_g}\right)$	[25]
489	$H_2O_2 \rightarrow OH + OH$	$k_0 = 3.8 \times 10^{-8} \cdot \exp\left(\frac{-2.196 \times 10^4}{T_g}\right)$ $k_\infty = 3 \times 10^{14} \cdot \exp\left(\frac{-2.44 \times 10^4}{T_g}\right)$ $F_c = 0.5$	[5] <sup>a</sup>
490	$H_2O_2 + O_2 \rightarrow HO_2 + HO_2$	$5 \times 10^{-11} \cdot \exp\left(\frac{-2.160 \times 10^4}{T_g}\right)$	[52]
491	$H_2O + O^- \rightarrow OH + OH^-$	$3 \times 10^{-13}$	[56]
492	$H_2O + O^- \rightarrow e + H_2O_2$	$3 \times 10^{-13}$	[56]
493	$H_2O + H^- \rightarrow H_2 + OH^-$	$3.7 \times 10^{-9}$	[56]
494	$H_2O + O^+ \rightarrow H_2O^+ + O$	$2.2 \times 10^{-9}$	[29]
495	$H_2O + H_2O^+ \rightarrow H_3O^+ + OH$	$1.67 \times 10^{-9}$	[56, 60]
496	$H_2O + H^+ \rightarrow H + H_2O^+$	$6.9 \times 10^{-9}$	[29]
497	$H_2O + O \rightarrow OH + OH$	$7.6 \times 10^{-15} \cdot T_g^{1.3} \cdot \exp\left(\frac{-8.6 \times 10^3}{T_g}\right)$	[25]
498	$M + H_2O \rightarrow M + H + OH$	$5.9 \times 10^{-7} \cdot \left(\frac{T_g}{3.0 \times 10^2}\right)^{-2.2} \cdot \exp\left(\frac{-5.90 \times 10^4}{T_g}\right)$	[52]
499	$H + H_2O \rightarrow H_2 + OH$	$7.5 \times 10^{-16} \cdot T_g^{1.6} \cdot \exp\left(\frac{-9.03 \times 10^3}{T_g}\right)$	[5]
500	$H_2O + OH \rightarrow H_2 + HO_2$	$1.4 \times 10^{-13} \cdot \exp\left(\frac{-3.610 \times 10^4}{T_g}\right)$	[52]
501	$H_2O + O \rightarrow H + HO_2$	$2.8 \times 10^{-12} \cdot \left(\frac{T_g}{3.0 \times 10^2}\right)^{0.37} \cdot \exp\left(\frac{-2.87430 \times 10^4}{T_g}\right)$	[52]
502	$H_2O + O_2 \rightarrow H_2O_2 + O$	$9.8 \times 10^{-8} \cdot \left(\frac{T_g}{3.0 \times 10^2}\right)^{0.5} \cdot \exp\left(\frac{-4.480 \times 10^4}{T_g}\right)$	[52]
503	$H_2O + O_2 \rightarrow HO_2 + OH$	$4.3 \times 10^{-12} \cdot \left(\frac{T_g}{3.0 \times 10^2}\right)^{0.5} \cdot \exp\left(\frac{-3.660 \times 10^4}{T_g}\right)$	[52]
504	$H_2 + H_2O^+ \rightarrow H + H_3O^+$	$6.4 \times 10^{-10}$	[61]
505	$H_2O^+ + O_2 \rightarrow H_2O + O_2^+$	$2 \times 10^{-10}$	[56]
506	$H_2O^+ + O^- \rightarrow H_2O + O$	$2 \times 10^{-7} \cdot \left(\frac{T_g}{3.0 \times 10^2}\right)^{-0.5}$	[57]
507	$H_2O^+ + O_2^- \rightarrow H_2O + O_2$	$2 \times 10^{-7} \cdot \left(\frac{T_g}{3.0 \times 10^2}\right)^{-0.5}$	[57]
508	$H_2O^+ + O_3^- \rightarrow H_2O + O_3$	$2 \times 10^{-7} \cdot \left(\frac{T_g}{3.0 \times 10^2}\right)^{-0.5}$	[57]
509	$M + H_2O^+ + O^- \rightarrow M + H_2O + O$	$2 \times 10^{-25} \cdot \left(\frac{T_g}{3.0 \times 10^2}\right)^{-2.5}$	[57]
510	$M + H_2O^+ + O^- \rightarrow M + H_2O_2$	$2 \times 10^{-25} \cdot \left(\frac{T_g}{3.0 \times 10^2}\right)^{-2.5}$	[57]
511	$M + H_2O^+ + O_3^- \rightarrow M + H_2O + O_3$	$2 \times 10^{-25} \cdot \left(\frac{T_g}{3.0 \times 10^2}\right)^{-2.5}$	[57]
512	$H + H_3O^+ \rightarrow H_2 + H_2O^+$	$6.1 \times 10^{-10} \cdot \exp\left(\frac{-2.05 \times 10^4}{T_g}\right)$	[62]
513	$H_3O^+ + O^- \rightarrow H + H_2O + O$	$7.51 \times 10^{-8} \cdot \left(\frac{T_g}{3 \times 10^2}\right)^{-0.5}$	[2, 3]
514	$H_3O^+ + O_2^- \rightarrow H + H_2O + O_2$	$7.51 \times 10^{-8} \cdot \left(\frac{T_g}{3 \times 10^2}\right)^{-0.5}$	[2, 3]
515	$H_3O^+ + O_2^- \rightarrow H + H_2O + O + O$	$1 \times 10^{-7}$	[57]
516	$H + O^- \rightarrow e + OH$	$5 \times 10^{-10}$	[1]
517	$H + O_2^- \rightarrow e + HO_2$	$7 \times 10^{-10}$	[56]
518	$H + O_2^- \rightarrow H^- + O_2$	$7 \times 10^{-10}$	[56]

#	Reaction	Rate equation	Ref.
519	$H + O^+ \rightarrow H^+ + O$	$7 \times 10^{-10}$	[1]
520	$M + H + O \rightarrow M + OH$	$4.33 \times 10^{-32} \cdot \left(\frac{T_g}{3 \times 10^2}\right)^{-1}$	[25]
521	$H + O_2 \rightarrow O + OH$	$1.62 \times 10^{-10} \cdot \exp\left(\frac{-7.4740 \times 10^3}{T_g}\right)$	[58]
522	$M + H + O_2 \rightarrow M + HO_2$	$3.33 \times 10^{-31} \cdot \left(\frac{T_g}{3.0 \times 10^2}\right)^{-1}$	[5]
523	$H + O_3 \rightarrow HO_2 + O$	$7.76 \times 10^{-13}$	[63]
524	$H + O_3 \rightarrow O_2 + OH$	$2.36 \times 10^{-11}$	[63]
525	$H^- + O_2 \rightarrow e + HO_2$	$1.2 \times 10^{-9}$	[56]
526	$H^- + O \rightarrow e + OH$	$1 \times 10^{-9}$	[1]
527	$H^- + OH \rightarrow e + H_2O$	$1 \times 10^{-10}$	[1]
528	$M + H^- + O_2^+ \rightarrow M + HO_2$	$2 \times 10^{-25} \cdot \left(\frac{T_g}{3.0 \times 10^2}\right)^{-2.5}$	[57]
529	$H^- + O^+ \rightarrow H + O$	$7.51 \times 10^{-8} \cdot \left(\frac{T_g}{3 \times 10^2}\right)^{-0.5}$	[2, 3]
530	$H_3O^+ + H^- \rightarrow H + H + H_2O$	$7.51 \times 10^{-8} \cdot \left(\frac{T_g}{3 \times 10^2}\right)^{-0.5}$	[2, 3]
531	$H^+ + O \rightarrow H + O^+$	$6.86 \times 10^{-10} \cdot \left(\frac{T_g}{3.0 \times 10^2}\right)^{0.26} \cdot \exp\left(\frac{2.243 \times 10^2}{T_g}\right)$	[3]
532	$H^+ + O_2 \rightarrow H + O_2^+$	$2 \times 10^{-9}$	[29]
533	$H^+ + O^- \rightarrow H + O$	$7.51 \times 10^{-8} \cdot \left(\frac{T_g}{3 \times 10^2}\right)^{-0.5}$	[2, 3]
534	$H^+ + O_2^- \rightarrow H + O_2$	$7.51 \times 10^{-8} \cdot \left(\frac{T_g}{3 \times 10^2}\right)^{-0.5}$	[2, 3]
535	$H_2 + O^- \rightarrow H + OH^-$	$3.1 \times 10^{-11}$	[56]
536	$H_2 + O^- \rightarrow e + H_2O$	$5.98 \times 10^{-10}$	[56]
537	$H_2 + O_2^- \rightarrow OH + OH^-$	$5 \times 10^{-13}$	[56, 57]
538	$H_2 + O_2^- \rightarrow HO_2 + H^-$	$5 \times 10^{-13}$	[56, 57]
539	$H_2 + O^+ \rightarrow H + OH^+$	$1.7 \times 10^{-9}$	[56]
540	$H_2 + O_3 \rightarrow HO_2 + OH$	$1 \times 10^{-13} \cdot \exp\left(\frac{-1.0 \times 10^4}{T_g}\right)$	[52]
541	$H_2 + O_2 \rightarrow H + HO_2$	$3.2 \times 10^{-11} \cdot \exp\left(\frac{-2.410 \times 10^4}{T_g}\right)$	[52]
542	$H_2 + O \rightarrow H + OH$	$9 \times 10^{-12} \cdot \frac{T_g}{3.0 \times 10^2} \cdot \exp\left(\frac{-4.480 \times 10^3}{T_g}\right)$	[52]
543	$H_2^+ + O_2 \rightarrow H_2 + O_2^+$	$7.8 \times 10^{-10}$	[7]
544	$H_2^+ + O_2 \rightarrow H + HO_2^+$	$1.9 \times 10^{-9}$	[64]
545	$H_3^+ + O \rightarrow H + H_2O^+$	$8.87 \times 10^{-10} \cdot \left(\frac{T_g}{3.0 \times 10^2}\right)^{-0.32}$	[65]
546	$H_3^+ + O \rightarrow H_2 + OH^+$	$5.26 \times 10^{-11} \cdot \left(\frac{T_g}{3.0 \times 10^2}\right)^{-0.32}$	[65]
547	$H_3^+ + O^- \rightarrow H + H_2 + O$	$7.51 \times 10^{-8} \cdot \left(\frac{T_g}{3 \times 10^2}\right)^{-0.5}$	[2, 3]
548	$H_3^+ + O_2^- \rightarrow H + H_2 + O_2$	$7.51 \times 10^{-8} \cdot \left(\frac{T_g}{3 \times 10^2}\right)^{-0.5}$	[2, 3]
549	$H + O \rightarrow e + OH^+$	$\frac{1.12 \times 10^{13}}{N_A} \cdot \exp\left(\frac{-8.06 \times 10^4}{T_g}\right)$	d
550	$H + OH \rightarrow e + H_2O^+$	$\frac{1.12 \times 10^{13}}{N_A} \cdot \exp\left(\frac{-8.06 \times 10^4}{T_g}\right)$	d
551	$H_2 + O \rightarrow e + H_2O^+$	$\frac{1.12 \times 10^{13}}{N_A} \cdot \exp\left(\frac{-8.06 \times 10^4}{T_g}\right)$	d
552	$C + OH \rightarrow CO + H$	$\frac{5 \times 10^{13}}{N_A}$	[66]
553	$C + OH^+ \rightarrow CH^+ + O$	$1.2 \times 10^{-9}$	[1]
554	$C + H_2O^+ \rightarrow CH^+ + OH$	$1.1 \times 10^{-9}$	[1]
555	$C + H_3O^+ \rightarrow H_2 + HCO^+$	$1 \times 10^{-11}$	[1]
556	$C + HO_2^+ \rightarrow CH^+ + O_2$	$1 \times 10^{-9}$	[1]

#	Reaction	Rate equation	Ref.
557	$C + OH^- \rightarrow e + HCO$	$5 \times 10^{-10}$	[1]
558	$C^+ + OH \rightarrow CO^+ + H$	$7.7 \times 10^{-10}$	[1]
559	$C^+ + H_2O \rightarrow H + HCO^+$	$2.7 \times 10^{-9}$	[67]
560	$C^+ + OH^- \rightarrow C + OH$	$7.51 \times 10^{-8} \cdot \left(\frac{T_g}{3 \times 10^2}\right)^{-0.5}$	[2, 3]
561	$CO_2 + H \rightarrow CO + OH$	$4.7 \times 10^{-10} \cdot \exp\left(\frac{-1.3915 \times 10^4}{T_g}\right)$	[5]
562	$CO + H \rightarrow HCO$	$2 \times 10^{-35} \cdot T_g^{0.2} \cdot n_M$	[5]
563	$CO_2 + H^+ \rightarrow HCO^+ + O$	$3.5 \times 10^{-9}$	[29]
564	$CO + H_2^+ \rightarrow CO^+ + H_2$	$6.44 \times 10^{-10}$	[7]
565	$CO + H_2^+ \rightarrow H + HCO^+$	$2.16 \times 10^{-9}$	[7]
566	$CO + H_3^+ \rightarrow H_2 + HCO^+$	$1.36 \times 10^{-9} \cdot \left(\frac{T_g}{3 \times 10^2}\right)^{-0.142} \cdot \exp\left(\frac{3.41}{T_g}\right)$	[68]
567	$CO + H^- \rightarrow e + HCO$	$2 \times 10^{-11}$	[69]
568	$CO_2^+ + H \rightarrow HCO^+ + O$	$2.9 \times 10^{-10}$	[70]
569	$CO^+ + H \rightarrow CO + H^+$	$7.5 \times 10^{-10}$	[71]
570	$CO^+ + H_2 \rightarrow H + HCO^+$	$1.5 \times 10^{-9}$	[72]
571	$CO + OH \rightarrow CO_2 + H$	$\frac{3.3 \times 10^6}{N_A} \cdot T_g^{1.55} \cdot \exp\left(\frac{4.02 \times 10^2}{T_g}\right)$	[73]
572	$CO + HO_2 \rightarrow CO_2 + OH$	$\frac{5.8 \times 10^{13}}{N_A} \cdot \exp\left(\frac{-2.293 \times 10^4 \cdot 4.184}{R \cdot T_g}\right)$	[74]
573	$CO + H_2O_2 \rightarrow COOH + OH$	$\frac{3.6 \times 10^4}{N_A} \cdot T_g^{2.5} \cdot \exp\left(\frac{-1.4425 \times 10^4}{T_g}\right)$	[75]
574	$CO_2 + OH^+ \rightarrow HCO^+ + O_2$	$5.4 \times 10^{-10}$	[1]
575	$CO + OH^+ \rightarrow HCO^+ + O$	$1.05 \times 10^{-9}$	[76]
576	$CO + H_2O^+ \rightarrow HCO^+ + OH$	$5 \times 10^{-10}$	[76]
577	$CO + HO_2^+ \rightarrow HCO^+ + O_2$	$8.4 \times 10^{-10}$	[1]
578	$CO_2^+ + H_2O \rightarrow CO_2 + H_2O^+$	$2.044 \times 10^{-9}$	[77]
579	$CO^+ + OH \rightarrow CO + OH^+$	$3.1 \times 10^{-10}$	[1]
580	$CO^+ + OH \rightarrow HCO^+ + O$	$3.1 \times 10^{-10}$	[1]
581	$CO^+ + H_2O \rightarrow CO + H_2O^+$	$1.7 \times 10^{-9}$	[78]
582	$CO^+ + H_2O \rightarrow HCO^+ + OH$	$9 \times 10^{-10}$	[78]
583	$CH_4 + O \rightarrow CH_3 + OH$	$7.3 \times 10^{-19} \cdot T_g^{2.5} \cdot \exp\left(\frac{-3.31 \times 10^3}{T_g}\right)$	[5]
584	$CH_4 + O_2 \rightarrow CH_3 + HO_2$	$8.1 \times 10^{-19} \cdot T_g^{2.5} \cdot \exp\left(\frac{-2.637 \times 10^4}{T_g}\right)$	[5]
585	$CH_4 + O_2 \rightarrow CH_3OO + H$	$\frac{4.3 \times 10^{13}}{N_A} \cdot \left(\frac{T_g}{1 \times 10^3}\right)^{1.96} \cdot \exp\left(\frac{-8.73 \times 10^4 \cdot 4.184 \times 10^3}{R \cdot T_g}\right)$	[79]
586	$CH_3 + O \rightarrow H + HCHO$	$1.12 \times 10^{-10}$	[5]
587	$CH_3 + O_2 \rightarrow HCHO + OH$	$3.7 \times 10^{-12} \cdot \exp\left(\frac{-1.114 \times 10^4}{T_g}\right)$	[5]
588	$CH_3 + O_2 \rightarrow CH_3O + O$	$3.5 \times 10^{-11} \cdot \exp\left(\frac{-1.634 \times 10^4}{T_g}\right)$	[5]
589	$CH_3 + O_2 \rightarrow CH_3OO$	$1.3 \times 10^{-15} \cdot T_g^{1.2}$	[5]
590	$CH_2 + O \rightarrow CO + H_2$	$0.4 \cdot 3.4 \times 10^{-10} \cdot \exp\left(\frac{-2.7 \times 10^2}{T_g}\right)$	[5]
591	$CH_2 + O_2 \rightarrow HCHO + O$	$\frac{4 \times 10^{10}}{N_A}$	[80]
592	$CH_2 + O_2 \rightarrow CO + H_2O$	$4.2 \times 10^{-13}$	[25]
593	$CH + O \rightarrow CO + H$	$6.6 \times 10^{-11}$	[5]
594	$CH + O \rightarrow e + HCO^+$	$4.2 \times 10^{-13} \cdot \exp\left(\frac{-8.5 \times 10^2}{T_g}\right)$	[5]
595	$CH + O_2 \rightarrow CO_2 + H$	$4.2 \times 10^{-11}$	[5]

#	Reaction	Rate equation	Ref.
596	$CH + O_2 \rightarrow CO + OH$	$2.8 \times 10^{-11}$	[5]
597	$CH + O_2 \rightarrow HCO + O$	$2.8 \times 10^{-11}$	[5]
598	$CH_4 + O^+ \rightarrow CH_3^+ + OH$	$1.1 \times 10^{-10}$	[27]
599	$CH_4 + O^+ \rightarrow CH_4^+ + O$	$8.9 \times 10^{-10}$	[27]
600	$CH_4 + O^- \rightarrow CH_3 + OH^-$	$1 \times 10^{-10}$	[1]
601	$CH_2 + O^+ \rightarrow CH_2^+ + O$	$9.7 \times 10^{-10}$	[1]
602	$CH_2 + O_2^+ \rightarrow CH_2^+ + O_2$	$4.3 \times 10^{-10}$	[1]
603	$CH_2 + O^- \rightarrow e + HCHO$	$5 \times 10^{-10}$	[1]
604	$CH + O^+ \rightarrow CH^+ + O$	$3.5 \times 10^{-10}$	[1]
605	$CH + O^+ \rightarrow CO^+ + H$	$3.5 \times 10^{-10}$	[1]
606	$CH + O_2^+ \rightarrow CH^+ + O_2$	$3.1 \times 10^{-10}$	[1]
607	$CH + O_2^+ \rightarrow HCO^+ + O$	$3.1 \times 10^{-10}$	[1]
608	$CH + O^- \rightarrow e + HCO$	$5 \times 10^{-10}$	[1]
609	$CH_5^+ + O \rightarrow CH_2 + H_3O^+$	$2.156 \times 10^{-10}$	[81]
610	$CH_4^+ + O_2 \rightarrow CH_4 + O_2^+$	$3.9 \times 10^{-10}$	[27]
611	$CH_3^+ + O \rightarrow H_2 + HCO^+$	$3.08 \times 10^{-10}$	[82]
612	$CH_3^+ + O \rightarrow CO + H_3^+$	$8.8 \times 10^{-11}$	[82]
613	$CH_3^+ + O_2 \rightarrow H_2O + HCO^+$	$4.3 \times 10^{-11}$	[27]
614	$CH_3^+ + O^- \rightarrow CH_3 + O$	$7.51 \times 10^{-8} \cdot \left(\frac{T_g}{3 \times 10^2}\right)^{-0.5}$	[2, 3]
615	$CH_3^+ + O_2^- \rightarrow CH_3 + O_2$	$7.51 \times 10^{-8} \cdot \left(\frac{T_g}{3 \times 10^2}\right)^{-0.5}$	[2, 3]
616	$CH_2^+ + O \rightarrow H + HCO^+$	$7.5 \times 10^{-10}$	[1]
617	$CH_2^+ + O_2 \rightarrow HCO^+ + OH$	$4.55 \times 10^{-10}$	[27]
618	$CH^+ + O \rightarrow CO^+ + H$	$1.75 \times 10^{-10}$	[81]
619	$CH^+ + O \rightarrow CO + H^+$	$1.75 \times 10^{-10}$	[81]
620	$CH^+ + O_2 \rightarrow HCO + O^+$	$9.7 \times 10^{-10}$	[27]
621	$CH^+ + O_2 \rightarrow CO_2^+ + H$	$4.8 \times 10^{-10}$	[1]
622	$CH_3 + CO \rightarrow CH_3CO$	$k_0 = 1.6 \times 10^{-37} \cdot T_g^{1.05} \cdot \exp\left(\frac{-1.3 \times 10^3}{T_g}\right)$ $k_\infty = 3.1 \times 10^{-16} \cdot T_g^{1.05} \cdot \exp\left(\frac{-2.85 \times 10^3}{T_g}\right)$ $F_c = 0.5$	[5] <sup>a</sup>
623	$CH_2 + CO_2 \rightarrow CO + HCHO$	$3.9 \times 10^{-14}$	[25]
624	$CH_2 + CO \rightarrow CH_2CO$	$1 \times 10^{-15}$	[25]
625	$CH + CO_2 \rightarrow CO + HCO$	$0.5 \cdot 1.06 \times 10^{-16} \cdot T_g^{1.51} \cdot \exp\left(\frac{3.6 \times 10^2}{T_g}\right)$	[5]
626	$CH + CO \rightarrow HCCO$	$k_0 = 6.3 \times 10^{-24} \cdot T_g^{-2.5}$ $k_\infty = 1.7 \times 10^{-9} \cdot T_g^{-0.4}$ $F_c = 0.6$	[5] <sup>a</sup>
627	$CH_4 + CO_2^+ \rightarrow CH_4^+ + CO_2$	$5.5 \times 10^{-10}$	[83]
628	$CH_4 + CO^+ \rightarrow CH_4^+ + CO$	$8.978 \times 10^{-10}$	[27]
629	$CH_4 + CO^+ \rightarrow CH_3 + HCO^+$	$3.752 \times 10^{-10}$	[27]
630	$CH_2 + CO^+ \rightarrow CH_2^+ + CO$	$4.3 \times 10^{-10}$	[1]
631	$CH_2 + CO^+ \rightarrow CH + HCO^+$	$4.3 \times 10^{-10}$	[1]
632	$CH + CO^+ \rightarrow CH^+ + CO$	$3.2 \times 10^{-10}$	[1]

#	Reaction	Rate equation	Ref.
633	$CH + CO^+ \rightarrow C + HCO^+$	$3.2 \times 10^{-10}$	[1]
634	$CH_5^+ + CO \rightarrow CH_4 + HCO^+$	$9.9 \times 10^{-10}$	[27]
635	$CH_4^+ + CO \rightarrow CH_3 + HCO^+$	$1.0368 \times 10^{-9}$	[27]
636	$CH^+ + CO_2 \rightarrow CO + HCO^+$	$1.6 \times 10^{-9}$	[27]
637	$CH^+ + CO \rightarrow C + HCO^+$	$7 \times 10^{-12}$	[27]
638	$CH_4 + OH \rightarrow CH_3 + H_2O$	$1.66 \times 10^{-18} \cdot T_g^{2.182} \cdot \exp\left(\frac{-1.231 \times 10^3}{T_g}\right)$	[84]
639	$CH_4 + HO_2 \rightarrow CH_3 + H_2O_2$	$7.8 \times 10^{-20} \cdot T_g^{2.5} \cdot \exp\left(\frac{-1.057 \times 10^4}{T_g}\right)$	[5]
640	$CH_3 + OH \rightarrow CH_3OH$	$k_0 = 1.06 \times 10^{-10} \cdot T_g^{-6.21} \cdot \exp\left(\frac{-6.71 \times 10^2}{T_g}\right)$ $k_\infty = 7.2 \times 10^{-9} \cdot T_g^{-0.79}$ $F_c = 0.75 \cdot \exp\left(\frac{-T_g}{2.1 \times 10^2}\right)$ $+ 0.25 \cdot \exp\left(\frac{-T_g}{1.434 \times 10^3}\right)$	[5] <sup>a</sup>
641	$CH_3 + OH \rightarrow CH_2 + H_2O$	$\frac{k}{n_M}$ $k_0 = 1.8 \times 10^{-8} \cdot T_g^{-0.91} \cdot \exp\left(\frac{-2.75 \times 10^2}{T_g}\right)$ $k_\infty = 6.4 \times 10^{-8} \cdot T_g^{5.8} \cdot \exp\left(\frac{4.85 \times 10^2}{T_g}\right)$ $F_c = 0.664 \cdot \exp\left(\frac{-T_g}{3.569 \times 10^3}\right)$ $+ 0.336 \cdot \exp\left(\frac{-T_g}{1.08 \times 10^2}\right)$ $+ \exp\left(\frac{-3.24 \times 10^3}{T_g}\right)$	[5] <sup>a</sup>
642	$CH_3 + OH \rightarrow CH_2OH + H$	$1.2 \times 10^{-12} \cdot \exp\left(\frac{-2.76 \times 10^3}{T_g}\right)$	[5]
643	$CH_3 + OH \rightarrow CH_3O + H$	$2 \times 10^{-14} \cdot \exp\left(\frac{-6.99 \times 10^3}{T_g}\right)$	[5]
644	$CH_3 + OH \rightarrow H_2 + HCHO$	$5.3 \times 10^{-15} \cdot \exp\left(\frac{-2.53 \times 10^3}{T_g}\right)$	[5]
645	$CH_3 + OH \rightarrow CH_4 + O$	$1.16 \times 10^{-19} \cdot T_g^{2.2} \cdot \exp\left(\frac{-2.24 \times 10^3}{T_g}\right)$	[85]
646	$CH_3 + H_2O \rightarrow CH_4 + OH$	$8 \times 10^{-22} \cdot T_g^{2.9} \cdot \exp\left(\frac{-7.48 \times 10^3}{T_g}\right)$	[86]
647	$CH_3 + HO_2 \rightarrow CH_3O + OH$	$3 \times 10^{-11}$	[5]
648	$CH_3 + HO_2 \rightarrow CH_4 + O_2$	$6 \times 10^{-12}$	[25]
649	$CH_3 + H_2O_2 \rightarrow CH_4 + HO_2$	$2 \times 10^{-14} \cdot \exp\left(\frac{3.0 \times 10^2}{T_g}\right)$	[25]
650	$CH_2 + OH \rightarrow H + HCHO$	$5 \times 10^{-11}$	[25]
651	$CH_2 + H_2O \rightarrow CH_3 + OH$	$1 \times 10^{-16}$	[25]
652	$CH_2 + HO_2 \rightarrow HCHO + OH$	$3 \times 10^{-11}$	[25]
653	$CH_2 + H_2O_2 \rightarrow CH_3 + HO_2$	$1 \times 10^{-14}$	[25]
654	$CH + OH \rightarrow C + H_2O$	$\frac{4 \times 10^7}{N_A} \cdot T_g^2 \cdot \exp\left(\frac{-3 \times 10^3 \cdot 4.184}{R \cdot T_g}\right)$	[74]
655	$CH + OH \rightarrow H + HCO$	$\frac{3 \times 10^{13}}{N_A}$	[74]
656	$CH + H_2O \rightarrow H + HCHO$	$\frac{8.5 \times 10^8}{N_A} \cdot T_g^{1.144} \cdot \exp\left(\frac{2.051 \times 10^3 \cdot 4.184}{R \cdot T_g}\right)$	[66]
657	$CH_4 + OH^+ \rightarrow CH_5^+ + O$	$1.885 \times 10^{-10}$	[27]
658	$CH_4 + OH^+ \rightarrow CH_2 + H_3O^+$	$1.2615 \times 10^{-9}$	[27]
659	$CH_4 + H_2O^+ \rightarrow CH_3 + H_3O^+$	$1.12 \times 10^{-9}$	[27]
660	$CH_4 + HO_2^+ \rightarrow CH_3^+ + H_2 + O_2$	$8 \times 10^{-11}$	[27]
661	$CH_4 + HO_2^+ \rightarrow CH_5^+ + O_2$	$9.2 \times 10^{-10}$	[27]
662	$CH_3 + OH^- \rightarrow CH_3OH + e$	$1 \times 10^{-9}$	[1]
663	$CH_2 + OH^+ \rightarrow CH_2^+ + OH$	$4.8 \times 10^{-10}$	[1]
664	$CH_2 + OH^+ \rightarrow CH_3^+ + O$	$4.8 \times 10^{-10}$	[1]

#	Reaction	Rate equation	Ref.
665	$CH_2 + H_2O^+ \rightarrow CH_2^+ + H_2O$	$4.7 \times 10^{-10}$	[1]
666	$CH_2 + H_2O^+ \rightarrow CH_3^+ + OH$	$4.7 \times 10^{-10}$	[1]
667	$CH_2 + H_3O^+ \rightarrow CH_3^+ + H_2O$	$9.4 \times 10^{-10}$	[1]
668	$CH_2 + HO_2^+ \rightarrow CH_3^+ + O_2$	$8.5 \times 10^{-10}$	[1]
669	$CH + OH^+ \rightarrow CH^+ + OH$	$3.5 \times 10^{-10}$	[1]
670	$CH + OH^+ \rightarrow CH_2^+ + O$	$3.5 \times 10^{-10}$	[1]
671	$CH + H_2O^+ \rightarrow CH^+ + H_2O$	$3.4 \times 10^{-10}$	[1]
672	$CH + H_2O^+ \rightarrow CH_2^+ + OH$	$3.4 \times 10^{-10}$	[1]
673	$CH + H_3O^+ \rightarrow CH_2^+ + H_2O$	$6.8 \times 10^{-10}$	[1]
674	$CH + HO_2^+ \rightarrow CH_2^+ + O_2$	$6.2 \times 10^{-10}$	[1]
675	$CH + OH^- \rightarrow e + HCHO$	$5 \times 10^{-10}$	[1]
676	$CH_5^+ + OH \rightarrow CH_4 + H_2O^+$	$7 \times 10^{-10}$	[1]
677	$CH_5^+ + H_2O \rightarrow CH_4 + H_3O^+$	$3.7 \times 10^{-9}$	[27]
678	$CH_4^+ + H_2O \rightarrow CH_3 + H_3O^+$	$2.5 \times 10^{-9}$	[27]
679	$CH_3^+ + OH^- \rightarrow CH_3 + OH$	$7.51 \times 10^{-8} \cdot \left(\frac{T_g}{3 \times 10^2}\right)^{-0.5}$	[2, 3]
680	$CH^+ + OH \rightarrow CO^+ + H_2$	$7.5 \times 10^{-10}$	[1]
681	$CH^+ + H_2O \rightarrow C + H_3O^+$	$1.45 \times 10^{-9}$	[27]
682	$C^+ + HCO \rightarrow C + HCO^+$	$4.8 \times 10^{-10}$	[1]
683	$C^+ + HCO \rightarrow CH^+ + CO$	$4.8 \times 10^{-10}$	[1]
684	$C^+ + HCHO \rightarrow CH_2^+ + CO$	$2.112 \times 10^{-9}$	[87]
685	$C^+ + HCHO \rightarrow CH + HCO^+$	$9.24 \times 10^{-10}$	[87]
686	$CH_3OH + C^+ \rightarrow CH_3 + HCO^+$	$3.28 \times 10^{-10}$	[87]
687	$CH_3OH + C^+ \rightarrow CH_3^+ + HCO$	$1.189 \times 10^{-9}$	[87]
688	$C + HCO^+ \rightarrow CH^+ + CO$	$1.1 \times 10^{-9}$	[1]
689	$CO + COOH \rightarrow CO_2 + HCO$	$1 \times 10^{-14}$	[88]
690	$CH_3O + CO \rightarrow CH_3 + CO_2$	$2.6 \times 10^{-11} \cdot \exp\left(\frac{-5.94 \times 10^3}{T_g}\right)$	[25]
691	$CH_3O + CO \rightarrow HCHO + HCO$	$5.23 \times 10^{-15}$	[89]
692	$CH_3OO + CO \rightarrow CH_3O + CO_2$	$7 \times 10^{-18}$	[90]
693	$CO^+ + HCO \rightarrow CO + HCO^+$	$7.4 \times 10^{-10}$	[1]
694	$CO^+ + HCHO \rightarrow HCO + HCO^+$	$1.65 \times 10^{-9}$	[91]
695	$H + HCO \rightarrow CO + H_2$	$1.5 \times 10^{-10}$	[5]
696	$H + HCO \rightarrow CH_2 + O$	$\frac{3.98107171 \times 10^{13}}{N_A} \cdot \exp\left(\frac{-4.29 \times 10^5}{R \cdot T_g}\right)$	[92]
697	$H + HCHO \rightarrow H_2 + HCO$	$3.34 \times 10^{-23} \cdot T_g^{-3.81} \cdot \exp\left(\frac{-2.02 \times 10^2}{T_g}\right)$	[5]
698	$H + HCHO \rightarrow CH_3O$	$\frac{2.4 \times 10^{13}}{N_A} \cdot \exp\left(\frac{-4.11 \times 10^3 \cdot 4.184}{T_g}\right)$	[93]
699	$CH_3O + H \rightarrow H_2 + HCHO$	$3.3 \times 10^{-11}$	[25]
700	$CH_3O + H \rightarrow CH_3OH$	$3.4 \times 10^{-10} \cdot \left(\frac{T_g}{3 \times 10^2}\right)^{0.33}$	[94]
701	$CH_3O + H_2 \rightarrow CH_3OH + H$	$1.7 \times 10^{-15} \cdot \left(\frac{T_g}{3 \times 10^2}\right)^4 \cdot \exp\left(\frac{-2.47 \times 10^3}{T_g}\right)$	[95]
702	$CH_2OH + H \rightarrow H_2 + HCHO$	$1 \times 10^{-11}$	[96]
703	$CH_2OH + H \rightarrow CH_3 + OH$	$1.6 \times 10^{-10}$	[96]

#	Reaction	Rate equation	Ref.
704	$CH_2OH + H_2 \rightarrow CH_3OH + H$	$1.12 \times 10^{-18} \cdot T_g^2 \cdot \exp\left(\frac{-6.722 \times 10^3}{T_g}\right)$	[96]
705	$CH_3OH + H \rightarrow CH_2OH + H_2$	$5.7 \times 10^{-15} \cdot T_g^{1.24} \cdot \exp\left(\frac{-2.26 \times 10^3}{T_g}\right)$	[5]
706	$CH_3OH + H \rightarrow CH_3 + H_2O$	$\frac{2 \times 10^{12}}{N_A} \cdot \exp\left(\frac{-5.3 \cdot 4.184 \times 10^3}{R \cdot T_g}\right)$	[97]
707	$CH_3OO + H \rightarrow CH_4 + O_2$	$\frac{4.02 \times 10^{13}}{N_A} \cdot \left(\frac{T_g}{1 \times 10^3}\right)^{1.02} \cdot \exp\left(\frac{-1.66 \times 10^1 \cdot 4.184 \times 10^3}{R \cdot T_g}\right)$	[79]
708	$CH_3OO + H \rightarrow CH_3O + OH$	$1.6 \times 10^{-10}$	[25]
709	$CH_3OO + H_2 \rightarrow CH_3OOH + H$	$5 \times 10^{-11} \cdot \exp\left(\frac{-1.31 \times 10^4}{T_g}\right)$	[25]
710	$HCO + H^+ \rightarrow H + HCO^+$	$9.4 \times 10^{-10}$	[1]
711	$HCO + H^+ \rightarrow CO^+ + H_2$	$9.4 \times 10^{-10}$	[1]
712	$HCO + H^+ \rightarrow CO + H_2^+$	$9.4 \times 10^{-10}$	[1]
713	$H_2^+ + HCO \rightarrow H_2 + HCO^+$	$1 \times 10^{-9}$	[1]
714	$H_2^+ + HCO \rightarrow CO + H_3^+$	$1 \times 10^{-9}$	[1]
715	$HCO + H^- \rightarrow e + HCHO$	$1 \times 10^{-9}$	[1]
716	$HCHO + H^+ \rightarrow CO^+ + H + H_2$	$1.064 \times 10^{-9}$	[98]
717	$HCHO + H^+ \rightarrow H_2 + HCO^+$	$3.572 \times 10^{-9}$	[98]
718	$H_2^+ + HCHO \rightarrow H + H_2 + HCO^+$	$1.4 \times 10^{-9}$	[1]
719	$H_3^+ + HCOOH \rightarrow CO + H_2 + H_3O^+$	$1.83 \times 10^{-9}$	[99]
720	$H_3^+ + HCOOH \rightarrow H_2 + H_2O + HCO^+$	$4.27 \times 10^{-9}$	[99]
721	$CH_3OH + H^+ \rightarrow CH_3^+ + H_2O$	$7.4 \times 10^{-10}$	[29]
722	$CH_3OH + H^+ \rightarrow H_2 + H_2 + HCO^+$	$1.11 \times 10^{-9}$	[29]
723	$CH_3OH + H_3^+ \rightarrow CH_3^+ + H_2 + H_2O$	$3.71 \times 10^{-9}$	[100]
724	$CH_3OH + H_3^+ \rightarrow H_2 + H_2 + H_2 + HCO^+$	$1.26 \times 10^{-9}$	[100]
725	$HCO^+ + H^- \rightarrow CO + H + H$	$3.76 \times 10^{-8} \cdot \left(\frac{T_g}{3 \times 10^2}\right)^{-0.5}$	[2, 3]
726	$HCO^+ + H^- \rightarrow H + HCO$	$3.76 \times 10^{-8} \cdot \left(\frac{T_g}{3 \times 10^2}\right)^{-0.5}$	[2, 3]
727	$HCO^+ + H^- \rightarrow CO + H_2$	$2.3 \times 10^{-7} \cdot \left(\frac{T_g}{3 \times 10^2}\right)^{-0.5}$	[1]
728	$HCO + OH \rightarrow CO + H_2O$	$1.8 \times 10^{-10}$	[5]
729	$H_2O + HCO \rightarrow HCHO + OH$	$3.9 \times 10^{-16} \cdot T_g^{1.35} \cdot \exp\left(\frac{-1.3146 \times 10^4}{T_g}\right)$	[25]
730	$H_2O_2 + HCO \rightarrow HCHO + HO_2$	$1.7 \times 10^{-13} \cdot \exp\left(\frac{-3.486 \times 10^3}{T_g}\right)$	[25]
731	$HCHO + OH \rightarrow H_2O + HCO$	$2.31 \times 10^{-11} \cdot \exp\left(\frac{-3.04 \times 10^2}{T_g}\right)$	[5]
732	$HCHO + OH \rightarrow H + HCOOH$	$2 \times 10^{-13}$	[101]
733	$HCHO + HO_2 \rightarrow H_2O_2 + HCO$	$6.8 \times 10^{-20} \cdot T_g^{2.5} \cdot \exp\left(\frac{-5.14 \times 10^3}{T_g}\right)$	[5]
734	$HCHO + HO_2 \rightarrow CH_2OH + O_2$	$\frac{3.38844156 \times 10^{12}}{N_A} \cdot \exp\left(\frac{-8 \times 10^4}{R \cdot T_g}\right)$	[92]
735	$HCOOH + OH \rightarrow COOH + H_2O$	$\frac{5.93 \times 10^8 \cdot 1 \times 10^3}{N_A} \cdot \exp\left(\frac{-1.036 \times 10^3}{T_g}\right)$	[102]
736	$CH_3O + OH \rightarrow H_2O + HCHO$	$3 \times 10^{-11}$	[25]
737	$CH_3O + HO_2 \rightarrow H_2O_2 + HCHO$	$5 \times 10^{-13}$	[25]
738	$CH_3O + HO_2 \rightarrow CH_3OH + O_2$	$4.7 \times 10^{-11}$	[103]
739	$CH_2OH + OH \rightarrow H_2O + HCHO$	$4 \times 10^{-11}$	[96]
740	$CH_2OH + H_2O \rightarrow CH_3OH + OH$	$\frac{1.54881662 \times 10^{14}}{N_A} \cdot \exp\left(\frac{-1.1 \times 10^5}{R \cdot T_g}\right)$	[92]
741	$CH_2OH + HO_2 \rightarrow H_2O_2 + HCHO$	$\frac{1.3 \times 10^6 \cdot 1 \times 10^3}{N_A} \cdot \left(\frac{T_g}{2.98 \times 10^2}\right)^{5.31} \cdot \exp\left(\frac{-6.01 \times 10^4}{R \cdot T_g}\right)$	[104]

#	Reaction	Rate equation	Ref.
742	$CH_2OH + HO_2 \rightarrow CH_3OH + O_2$	$\frac{5.7 \times 10^4 \cdot 1 \times 10^3}{N_A} \cdot \left( \frac{T_g}{2.98 \times 10^2} \right)^{3.2} \cdot \exp \left( \frac{-6.8 \times 10^3}{R \cdot T_g} \right)$	[104]
743	$CH_2OH + HO_2 \rightarrow H_2O + HCOOH$	$\frac{3.6 \times 10^9 \cdot 1 \times 10^3}{N_A} \cdot T_g^{0.12} \cdot \exp \left( \frac{-1.9 \times 10^3}{R \cdot T_g} \right)$	[104]
744	$CH_2OH + H_2O_2 \rightarrow CH_3OH + HO_2$	$5 \times 10^{-15} \cdot \exp \left( \frac{-1.3 \times 10^3}{T_g} \right)$	[96]
745	$CH_3OH + HO_2 \rightarrow CH_2OH + H_2O_2$	$5.41 \times 10^{-11} \cdot \exp \left( \frac{-9.2 \times 10^3}{T_g} \right)$	[105]
746	$CH_3OH + HO_2 \rightarrow CH_3O + H_2O_2$	$2.02 \times 10^{-12} \cdot \exp \left( \frac{-1.01 \times 10^4}{T_g} \right)$	[105]
747	$CH_3OOH + OH \rightarrow CH_3OO + H_2O$	$1.8 \times 10^{-12} \cdot \exp \left( \frac{2.2 \times 10^2}{T_g} \right)$	[5]
748	$CH_3OO + OH \rightarrow CH_3OH + O_2$	$1 \times 10^{-10}$	[25]
749	$CH_3OO + HO_2 \rightarrow CH_3OOH + O_2$	$0.9 \cdot 4.2 \times 10^{-13} \cdot \exp \left( \frac{7.5 \times 10^2}{T_g} \right)$	[5]
750	$CH_3OO + H_2O_2 \rightarrow CH_3OOH + HO_2$	$4 \times 10^{-12} \cdot \exp \left( \frac{-5 \times 10^3}{T_g} \right)$	[25]
751	$HCO + OH^+ \rightarrow HCO^+ + OH$	$2.8 \times 10^{-10}$	[1]
752	$HCO + OH^+ \rightarrow CO + H_2O^+$	$2.8 \times 10^{-10}$	[1]
753	$H_2O^+ + HCO \rightarrow H_2O + HCO^+$	$2.8 \times 10^{-10}$	[1]
754	$H_2O^+ + HCO \rightarrow CO + H_3O^+$	$2.8 \times 10^{-10}$	[1]
755	$HCO^+ + OH \rightarrow CO + H_2O^+$	$6.2 \times 10^{-10}$	[1]
756	$H_2O + HCO^+ \rightarrow CO + H_3O^+$	$2.5 \times 10^{-9}$	[91]
757	$HCO^+ + OH^- \rightarrow CO + H + OH$	$3.76 \times 10^{-8} \cdot \left( \frac{T_g}{3 \times 10^2} \right)^{-0.5}$	[2, 3]
758	$HCO^+ + OH^- \rightarrow HCO + OH$	$3.76 \times 10^{-8} \cdot \left( \frac{T_g}{3 \times 10^2} \right)^{-0.5}$	[2, 3]
759	$HCO + O \rightarrow CO + OH$	$5 \times 10^{-11}$	[25]
760	$HCO + O \rightarrow CO_2 + H$	$5 \times 10^{-11}$	[25]
761	$HCO + O_2 \rightarrow CO + HO_2$	$4.5 \times 10^{-14} \cdot T_g^{0.68} \cdot \exp \left( \frac{2.36 \times 10^2}{T_g} \right)$	[5]
762	$HCHO + O \rightarrow HCO + OH$	$6.9 \times 10^{-13} \cdot T_g^{0.57} \cdot \exp \left( \frac{-1.39 \times 10^3}{T_g} \right)$	[5]
763	$HCHO + O_2 \rightarrow HCO + HO_2$	$4.05 \times 10^{-19} \cdot T_g^{2.5} \cdot \exp \left( \frac{-1.835 \times 10^4}{T_g} \right)$	[5]
764	$CH_3O + O \rightarrow CH_3 + O_2$	$1.875 \times 10^{-11}$	[5]
765	$CH_3O + O \rightarrow HCHO + OH$	$6.25 \times 10^{-12}$	[5]
766	$CH_3O + O_2 \rightarrow HCHO + HO_2$	$3.6 \times 10^{-14} \cdot \exp \left( \frac{-8.8 \times 10^2}{T_g} \right)$	[5]
767	$CH_2OH + O_2 \rightarrow HCHO + HO_2$	$4.8 \times 10^{-8} \cdot T_g^{-1.5} + 1.2 \times 10^{-10} \cdot \exp \left( \frac{-1.88 \times 10^3}{T_g} \right)$	[5]
768	$CH_3OH + O \rightarrow CH_2OH + OH$	$4.1 \times 10^{-11} \cdot \exp \left( \frac{-2.67 \times 10^3}{T_g} \right)$	[5]
769	$CH_3OH + O_2 \rightarrow CH_2OH + HO_2$	$3.4 \times 10^{-11} \cdot \exp \left( \frac{-2.26 \times 10^4}{T_g} \right)$	[96]
770	$CH_3OO + O \rightarrow CH_3O + O_2$	$6 \times 10^{-11}$	[25]
771	$HCO + O^+ \rightarrow HCO^+ + O$	$4.3 \times 10^{-10}$	[1]
772	$HCO + O^+ \rightarrow CO + OH^+$	$4.3 \times 10^{-10}$	[1]
773	$HCO + O_2^+ \rightarrow HCO^+ + O_2$	$3.6 \times 10^{-10}$	[1]
774	$HCO + O_2^+ \rightarrow CO + HO_2^+$	$3.6 \times 10^{-10}$	[1]
775	$HCHO + O^+ \rightarrow CO + H_2O^+$	$4 \times 10^{-10}$	[1]
776	$HCO^+ + O^- \rightarrow CO + H + O$	$3.76 \times 10^{-8} \cdot \left( \frac{T_g}{3 \times 10^2} \right)^{-0.5}$	[2, 3]
777	$HCO^+ + O^- \rightarrow HCO + O$	$3.76 \times 10^{-8} \cdot \left( \frac{T_g}{3 \times 10^2} \right)^{-0.5}$	[2, 3]
778	$HCO^+ + O_2^- \rightarrow CO + H + O_2$	$3.76 \times 10^{-8} \cdot \left( \frac{T_g}{3 \times 10^2} \right)^{-0.5}$	[2, 3]
779	$HCO^+ + O_2^- \rightarrow HCO + O_2$	$3.76 \times 10^{-8} \cdot \left( \frac{T_g}{3 \times 10^2} \right)^{-0.5}$	[2, 3]

#	Reaction	Rate equation	Ref.
780	$CH_4 + HCO \rightarrow CH_3 + HCHO$	$1.21 \times 10^{-20} \cdot T_g^{2.85} \cdot \exp\left(\frac{-1.133 \times 10^4}{T_g}\right)$	[25]
781	$CH_3 + HCO \rightarrow CH_4 + CO$	$2 \times 10^{-10}$	[25]
782	$CH_3 + HCO \rightarrow CH_3CHO$	$3 \times 10^{-11}$	[25]
783	$CH_2 + HCO \rightarrow CH_3 + CO$	$3 \times 10^{-11}$	[25]
784	$CH_3 + COOH \rightarrow CH_2CO + H_2O$	$(1.52 + 1.95 \times 10^{-4} \cdot T_g) \cdot 3.24 \times 10^{-11} \cdot T_g^{0.1024}$	[106]
785	$CH_3 + COOH \rightarrow CH_4 + CO_2$	$3.24 \times 10^{-11} \cdot T_g^{0.1024}$	[106]
786	$CH_3 + HCHO \rightarrow CH_3CH_2O$	$\frac{3 \times 10^{11}}{N_A} \cdot \exp\left(\frac{-6.336 \times 10^3 \cdot 4.186}{R \cdot T_g}\right)$	[93]
787	$CH_3 + HCHO \rightarrow CH_4 + HCO$	$5.3 \times 10^{-23} \cdot T_g^{3.36} \cdot \exp\left(\frac{-2.17 \times 10^3}{T_g}\right)$	[5]
788	$CH_2 + HCHO \rightarrow CH_3 + HCO$	$1 \times 10^{-14}$	[25]
789	$CH + HCHO \rightarrow CH_2CO + H$	$7.62 \times 10^{-10} \cdot T_g^{-0.32} \cdot \exp\left(\frac{3.86 \times 10^2}{T_g}\right)$	[107]
790	$CH_3O + CH_4 \rightarrow CH_3 + CH_3OH$	$2.6 \times 10^{-13} \cdot \exp\left(\frac{-4.45 \times 10^3}{T_g}\right)$	[25]
791	$CH_3 + CH_3O \rightarrow CH_4 + HCHO$	$4 \times 10^{-11}$	[25]
792	$CH_2 + CH_3O \rightarrow CH_3 + HCHO$	$3 \times 10^{-11}$	[25]
793	$CH_2OH + CH_4 \rightarrow CH_3 + CH_3OH$	$3.6 \times 10^{-23} \cdot T_g^{3.1} \cdot \exp\left(\frac{-8.166 \times 10^3}{T_g}\right)$	[96]
794	$CH_2OH + CH_3 \rightarrow CH_3CH_2OH$	$2 \times 10^{-11}$	[96]
795	$CH_2OH + CH_3 \rightarrow CH_4 + HCHO$	$4 \times 10^{-12}$	[96]
796	$CH_2 + CH_2OH \rightarrow C_2H_4 + OH$	$4 \times 10^{-11}$	[96]
797	$CH_2 + CH_2OH \rightarrow CH_3 + HCHO$	$2 \times 10^{-12}$	[96]
798	$CH_3 + CH_3OH \rightarrow CH_2OH + CH_4$	$0.33 \cdot 5 \times 10^{-23} \cdot T_g^{3.45} \cdot \exp\left(\frac{-4.02 \times 10^3}{T_g}\right)$	[5]
799	$CH_3 + CH_3OH \rightarrow CH_3O + CH_4$	$0.67 \cdot 5 \times 10^{-23} \cdot T_g^{3.45} \cdot \exp\left(\frac{-4.02 \times 10^3}{T_g}\right)$	[5]
800	$CH_2 + CH_3OH \rightarrow CH_2OH + CH_3$	$5.3 \times 10^{-23} \cdot T_g^{3.2} \cdot \exp\left(\frac{-3.609 \times 10^3}{T_g}\right)$	[96]
801	$CH_2 + CH_3OH \rightarrow CH_3 + CH_3O$	$2.4 \times 10^{-23} \cdot T_g^{3.1} \cdot \exp\left(\frac{-3.49 \times 10^3}{T_g}\right)$	[96]
802	$CH_3OO + CH_4 \rightarrow CH_3 + CH_3OOH$	$3 \times 10^{-13} \cdot \exp\left(\frac{-9.3 \times 10^3}{T_g}\right)$	[25]
803	$CH_3 + CH_3OO \rightarrow CH_3O + CH_3O$	$4 \times 10^{-11}$	[25]
804	$CH_2 + CH_3OO \rightarrow CH_3O + HCHO$	$3 \times 10^{-11}$	[25]
805	$CH_2 + CH_3OO \rightarrow C_2H_5 + O_2$	$3 \times 10^{-11}$	[25]
806	$CH_3^+ + HCO \rightarrow CH_3 + HCO^+$	$4.4 \times 10^{-10}$	[1]
807	$CH_3^+ + HCO \rightarrow CH_4^+ + CO$	$4.4 \times 10^{-10}$	[1]
808	$CH_2^+ + HCO \rightarrow CH_3^+ + CO$	$4.5 \times 10^{-10}$	[1]
809	$CH^+ + HCO \rightarrow CH + HCO^+$	$4.6 \times 10^{-10}$	[1]
810	$CH^+ + HCO \rightarrow CH_2^+ + CO$	$4.6 \times 10^{-10}$	[1]
811	$CH_3^+ + HCHO \rightarrow CH_4 + HCO^+$	$1.6 \times 10^{-9}$	[20]
812	$CH_2 + HCO^+ \rightarrow CH_3^+ + CO$	$8.6 \times 10^{-10}$	[1]
813	$CH + HCO^+ \rightarrow CH_2^+ + CO$	$6.3 \times 10^{-10}$	[1]
814	$HCO + HCO \rightarrow CO + HCHO$	$4.265 \times 10^{-11}$	[5]
815	$CH_3O + HCO \rightarrow CH_3OH + CO$	$1.5 \times 10^{-10}$	[25]
816	$CH_2OH + HCO \rightarrow CH_3OH + CO$	$2 \times 10^{-10}$	[96]
817	$CH_2OH + HCO \rightarrow HCHO + HCHO$	$3 \times 10^{-10}$	[96]
818	$CH_3OH + HCO \rightarrow CH_2OH + HCHO$	$1.6 \times 10^{-20} \cdot T_g^{2.9} \cdot \exp\left(\frac{-6.596 \times 10^3}{T_g}\right)$	[96]

#	Reaction	Rate equation	Ref.
819	$CH_3OH + HCO \rightarrow CH_3O + HCHO$	$1.6 \times 10^{-22} \cdot T_g^{2.9} \cdot \exp\left(\frac{-6.596 \times 10^3}{T_g}\right)$	[96]
820	$CH_3O + HCHO \rightarrow CH_3OH + HCO$	$1.7 \times 10^{-13} \cdot \exp\left(\frac{-1.5 \times 10^3}{T_g}\right)$	[25]
821	$CH_2OH + HCHO \rightarrow CH_3OH + HCO$	$9.1 \times 10^{-21} \cdot T_g^{2.8} \cdot \exp\left(\frac{-2.95 \times 10^3}{T_g}\right)$	[96]
822	$CH_3O + CH_3O \rightarrow CH_3OH + HCHO$	$1 \times 10^{-10}$	[25]
823	$CH_2OH + CH_3O \rightarrow CH_3OH + HCHO$	$4 \times 10^{-11}$	[96]
824	$CH_3O + CH_3OH \rightarrow CH_2OH + CH_3OH$	$5 \times 10^{-13} \cdot \exp\left(\frac{-2.05 \times 10^3}{T_g}\right)$	[96]
825	$CH_2OH + CH_2OH \rightarrow CH_3OH + HCHO$	$8 \times 10^{-12}$	[96]
826	$CH_2OH + CH_3OH \rightarrow CH_3O + CH_3OH$	$1.3 \times 10^{-14} \cdot \exp\left(\frac{-6.07 \times 10^3}{T_g}\right)$	[96]
827	$CH_3O + CH_3OO \rightarrow CH_3OOH + HCHO$	$5 \times 10^{-13}$	[25]
828	$CH_3OH + CH_3OO \rightarrow CH_2OH + CH_3OOH$	$3.421 \times 10^{-33} \cdot T_g^{6.2} \cdot \exp\left(\frac{-2.9826 \times 10^4}{R \cdot T_g}\right)$	[108]
829	$CH_3OH + CH_3OO \rightarrow CH_3O + CH_3OOH$	$1.318 \times 10^{-27} \cdot T_g^{4.71} \cdot \exp\left(\frac{-5.6739 \times 10^4}{R \cdot T_g}\right)$	[108]
830	$CH_2OH + CH_3OO \rightarrow CH_3OOH + HCHO$	$1.047 \times 10^{-24} \cdot T_g^{2.69} \cdot \exp\left(\frac{1.4344 \times 10^4}{R \cdot T_g}\right)$	[108]
831	$CH_2OH + CH_3OO \rightarrow CH_3OH + HCOOH$	$3.89 \times 10^{-24} \cdot T_g^{2.74} \cdot \exp\left(\frac{1.4922 \times 10^4}{R \cdot T_g}\right)$	[108]
832	$CH_3OO + HCHO \rightarrow CH_3OOH + HCO$	$3.3 \times 10^{-12} \cdot \exp\left(\frac{-5.87 \times 10^3}{T_g}\right)$	[25]
833	$C_2H_6 + OH \rightarrow C_2H_5 + H_2O$	$1.52 \times 10^{-17} \cdot T_g^2 \cdot \exp\left(\frac{-5 \times 10^2}{T_g}\right)$	[5]
834	$C_2H_6 + HO_2 \rightarrow C_2H_5 + H_2O_2$	$1.83 \times 10^{-19} \cdot T_g^{2.5} \cdot \exp\left(\frac{-8.48 \times 10^3}{T_g}\right)$	[5]
835	$C_2H_5 + OH \rightarrow C_2H_6 + O$	$1.7 \times 10^{-40} \cdot T_g^{8.8} \cdot \exp\left(\frac{-2.5 \times 10^2}{T_g}\right)$	[85]
836	$C_2H_5 + OH \rightarrow C_2H_4 + H_2O$	$4 \times 10^{-11}$	[25]
837	$C_2H_5 + H_2O \rightarrow C_2H_6 + OH$	$5.6 \times 10^{-18} \cdot T_g^{1.44} \cdot \exp\left(\frac{-1.015 \times 10^4}{T_g}\right)$	[25]
838	$C_2H_5 + HO_2 \rightarrow C_2H_6 + O_2$	$5 \times 10^{-13}$	[25]
839	$C_2H_5 + HO_2 \rightarrow C_2H_4 + H_2O_2$	$5 \times 10^{-13}$	[25]
840	$C_2H_5 + H_2O_2 \rightarrow C_2H_6 + HO_2$	$1.45 \times 10^{-14} \cdot \exp\left(\frac{-4.9 \times 10^2}{T_g}\right)$	[25]
841	$C_2H_4 + OH \rightarrow CH_3 + HCHO$	$\frac{1}{3} \cdot 3.4 \times 10^{-11} \cdot \exp\left(\frac{-2.99 \times 10^3}{T_g}\right)$	[5]
842	$C_2H_4 + OH \rightarrow CH_3CHO + H$	$\frac{1}{3} \cdot 3.4 \times 10^{-11} \cdot \exp\left(\frac{-2.99 \times 10^3}{T_g}\right)$	[5]
843	$C_2H_4 + HO_2 \rightarrow C_2H_5 + O_2$	$1 \times 10^{-13} \cdot T_g^{0.07} \cdot \exp\left(\frac{-6.58 \times 10^3}{T_g}\right)$	[5]
844	$C_2H_3 + OH \rightarrow CH_3 + HCO$	$1.09 \times 10^{-5} \cdot T_g^{-1.85} \cdot \exp\left(\frac{-5.01 \times 10^2}{T_g}\right)$	[109]
845	$C_2H_3 + OH \rightarrow CH_3CO + H$	$9.42 \times 10^{-9} \cdot T_g^{-1.014} \cdot \exp\left(\frac{-1.95 \times 10^2}{T_g}\right)$	[109]
846	$C_2H_3 + OH \rightarrow C_2H_2 + H_2O$	$3.96 \times 10^{-13} \cdot T_g^{0.081} \cdot \exp\left(\frac{1.91 \times 10^2}{T_g}\right)$	[109]
847	$C_2H_3 + OH \rightarrow CH_2CO + H_2$	$1.26 \times 10^{-8} \cdot T_g^{-1.517} \cdot \exp\left(\frac{-3.63 \times 10^2}{T_g}\right)$	[109]
848	$C_2H_3 + OH \rightarrow CH_4 + CO$	$1.32 \times 10^{-8} \cdot T_g^{-1.328} \cdot \exp\left(\frac{-2.98 \times 10^2}{T_g}\right)$	[109]
849	$C_2H_3 + H_2O \rightarrow C_2H_4 + OH$	$8 \times 10^{-22} \cdot T_g^{2.9} \cdot \exp\left(\frac{-7.48 \times 10^3}{T_g}\right)$	[25]
850	$C_2H_3 + H_2O_2 \rightarrow C_2H_4 + HO_2$	$2 \times 10^{-14} \cdot \exp\left(\frac{3 \times 10^2}{T_g}\right)$	[25]
851	$C_2H_2 + OH \rightarrow CH_2CO + H$	$0.5 \cdot 1.3 \times 10^{-10} \cdot \exp\left(\frac{-6.8 \times 10^3}{T_g}\right)$	[5]
852	$C_2H_2 + OH \rightarrow C_2H + H_2O$	$0.5 \cdot 1.3 \times 10^{-10} \cdot \exp\left(\frac{-6.8 \times 10^3}{T_g}\right)$	[5]
853	$C_2H_2 + HO_2 \rightarrow C_2H_3 + O_2$	$5.18 \times 10^{-18} \cdot T_g^{1.61} \cdot \exp\left(\frac{-7.1309 \times 10^3}{T_g}\right)$	[110]
854	$C_2H + OH \rightarrow C_2H_2 + O$	$3 \times 10^{-11}$	[25]
855	$C_2H + OH \rightarrow CH_2 + CO$	$3 \times 10^{-11}$	[25]
856	$C_2H + H_2O \rightarrow C_2H_2 + OH$	$2.2 \times 10^{-21} \cdot T_g^{3.05} \cdot \exp\left(\frac{-3.76 \times 10^2}{T_g}\right)$	[111]

#	Reaction	Rate equation	Ref.
857	$C_2H + HO_2 \rightarrow C_2H_2 + O_2$	$3 \times 10^{-11}$	[25]
858	$C_2H + HO_2 \rightarrow HCCO + OH$	$3 \times 10^{-11}$	[25]
859	$C_2H_6 + OH^+ \rightarrow C_2H_4^+ + H_2 + OH$	$1.04 \times 10^{-9}$	[28]
860	$C_2H_6 + OH^+ \rightarrow C_2H_5^+ + H_2 + O$	$3.2 \times 10^{-10}$	[28]
861	$C_2H_6 + OH^+ \rightarrow C_2H_4 + H_3O^+$	$1.6 \times 10^{-10}$	[28]
862	$C_2H_6 + OH^+ \rightarrow C_2H_6^+ + OH$	$4.8 \times 10^{-11}$	[28]
863	$C_2H_6 + H_2O^+ \rightarrow C_2H_5 + H_3O^+$	$1.328 \times 10^{-9}$	[28]
864	$C_2H_6 + H_2O^+ \rightarrow C_2H_4^+ + H_2 + H_2O$	$1.92 \times 10^{-10}$	[28]
865	$C_2H_6 + H_2O^+ \rightarrow C_2H_6^+ + H_2O$	$6.4 \times 10^{-11}$	[28]
866	$C_2H_6 + H_2O^+ \rightarrow C_2H_5^+ + H + H_2O$	$1.6 \times 10^{-11}$	[28]
867	$C_2H_4 + H_2O^+ \rightarrow C_2H_4^+ + H_2O$	$1.5 \times 10^{-9}$	[61]
868	$C_2H_2 + H_2O^+ \rightarrow C_2H_2^+ + H_2O$	$1.9 \times 10^{-9}$	[61]
869	$C_2H + OH^+ \rightarrow C_2H^+ + OH$	$4.5 \times 10^{-10}$	[1]
870	$C_2H + OH^+ \rightarrow C_2H_2^+ + O$	$4.5 \times 10^{-10}$	[1]
871	$C_2H + H_2O^+ \rightarrow C_2H^+ + H_2O$	$4.4 \times 10^{-10}$	[1]
872	$C_2H + H_2O^+ \rightarrow C_2H_2^+ + OH$	$4.4 \times 10^{-10}$	[1]
873	$C_2H + HO_2^+ \rightarrow C_2H_2^+ + O_2$	$7.6 \times 10^{-10}$	[1]
874	$C_2H_6^+ + H_2O \rightarrow C_2H_5 + H_3O^+$	$2.95 \times 10^{-9}$	[87]
875	$C_2H_5^+ + H_2O \rightarrow C_2H_4 + H_3O^+$	$1.4 \times 10^{-9}$	[112]
876	$C_2H_3^+ + H_2O \rightarrow C_2H_2 + H_3O^+$	$8.5 \times 10^{-10}$	[1]
877	$C_2H_3^+ + OH^- \rightarrow C_2H_3 + OH$	$7.51 \times 10^{-8} \cdot \left(\frac{T_g}{3 \times 10^2}\right)^{-0.5}$	[2, 3]
878	$C_2H_2^+ + H_2O \rightarrow C_2H + H_3O^+$	$2.2 \times 10^{-10}$	[1]
879	$C_2H_2^+ + OH^- \rightarrow C_2H_2 + OH$	$7.51 \times 10^{-8} \cdot \left(\frac{T_g}{3 \times 10^2}\right)^{-0.5}$	[2, 3]
880	$C_2H_4^+ + OH^- \rightarrow C_2H_3 + H + OH$	$7.51 \times 10^{-8} \cdot \left(\frac{T_g}{3 \times 10^2}\right)^{-0.5}$	[2, 3]
881	$C_2H_6 + O \rightarrow C_2H_5 + OH$	$3 \times 10^{-19} \cdot T_g^{2.8} \cdot \exp\left(\frac{-2.92 \times 10^3}{T_g}\right)$	[5]
882	$C_2H_6 + O_2 \rightarrow C_2H_5 + HO_2$	$1.21 \times 10^{-18} \cdot T_g^{2.5} \cdot \exp\left(\frac{-2.474 \times 10^4}{T_g}\right)$	[5]
883	$C_2H_5 + O \rightarrow CH_3CHO + H$	$8.8 \times 10^{-11}$	[5]
884	$C_2H_5 + O \rightarrow CH_3 + HCHO$	$6.6 \times 10^{-11}$	[5]
885	$C_2H_5 + O \rightarrow C_2H_4 + OH$	$4.4 \times 10^{-11}$	[5]
886	$C_2H_5 + O_2 \rightarrow C_2H_4 + HO_2$	$1 \times 10^{-13}$	[5]
887	$C_2H_4 + O \rightarrow CH_3 + HCO$	$0.6 \cdot 2.25 \times 10^{-17} \cdot T_g^{1.88} \cdot \exp\left(\frac{-9.2 \times 10^1}{T_g}\right)$	[5]
888	$C_2H_4 + O \rightarrow CH_2CO + H_2$	$0.05 \cdot 2.25 \times 10^{-17} \cdot T_g^{1.88} \cdot \exp\left(\frac{-9.2 \times 10^1}{T_g}\right)$	[5]
889	$C_2H_4 + O_2 \rightarrow C_2H_3 + HO_2$	$7 \times 10^{-11} \cdot \exp\left(\frac{-2.9 \times 10^4}{T_g}\right)$	[25]
890	$C_2H_3 + O \rightarrow C_2H_2 + OH$	$1.6666667 \times 10^{-11}$	[5]
891	$C_2H_3 + O \rightarrow CH_3 + CO$	$1.6666667 \times 10^{-11}$	[5]
892	$C_2H_3 + O \rightarrow CH_2 + HCO$	$1.6666667 \times 10^{-11}$	[5]
893	$C_2H_3 + O_2 \rightarrow C_2H_2 + HO_2$	$\frac{6.6 \times 10^{21}}{N_A} \cdot T_g^{-3.3} \cdot \exp\left(\frac{-5.41 \times 10^3 \cdot 4.184}{R \cdot T_g}\right)$	[113]
894	$C_2H_3 + O_2 \rightarrow HCHO + HCO$	$\frac{4 \times 10^{21}}{N_A} \cdot T_g^{-3} \cdot \exp\left(\frac{-2.4 \times 10^3 \cdot 4.184}{R \cdot T_g}\right)$	[113]
895	$C_2H_2 + O \rightarrow CH_2 + CO$	$0.2 \cdot 1.95 \times 10^{-15} \cdot T_g^{1.4} \cdot \exp\left(\frac{-1.11 \times 10^3}{T_g}\right)$	[5]

#	Reaction	Rate equation	Ref.
896	$C_2H_2 + O \rightarrow H + HCCO$	$0.8 \cdot 1.95 \times 10^{-15} \cdot T_g^{1.4} \cdot \exp\left(\frac{-1.11 \times 10^3}{T_g}\right)$	[5]
897	$C_2H_2 + O_2 \rightarrow HCO + HCO$	$\frac{6.1 \times 10^{12}}{N_A} \cdot \exp\left(\frac{-5.325 \times 10^4 \cdot 4.184}{R \cdot T_g}\right)$	[114]
898	$C_2H + O \rightarrow CH + CO$	$9.9 \times 10^{-11}$	[5]
899	$C_2H + O_2 \rightarrow CO + HCO$	$0.45 \cdot 2.7 \times 10^{-10} \cdot T_g^{-0.35}$	[5]
900	$C_2H + O_2 \rightarrow CH + CO_2$	$0.1 \cdot 2.7 \times 10^{-10} \cdot T_g^{-0.35}$	[5]
901	$C_2H_6 + O^+ \rightarrow C_2H_4^+ + H_2O$	$1.33 \times 10^{-9}$	[28]
902	$C_2H_6 + O^+ \rightarrow C_2H_5^+ + OH$	$5.7 \times 10^{-10}$	[28]
903	$C_2H_4 + O^+ \rightarrow C_2H_4^+ + O$	$7 \times 10^{-11}$	[29]
904	$C_2H_4 + O^+ \rightarrow C_2H_2^+ + H_2O$	$1.12 \times 10^{-9}$	[29]
905	$C_2H_4 + O^+ \rightarrow C_2H_3^+ + OH$	$2.1 \times 10^{-10}$	[29]
906	$C_2H_4 + O_2^+ \rightarrow C_2H_4^+ + O_2$	$6.8 \times 10^{-10}$	[115]
907	$C_2H_2 + O^+ \rightarrow C_2H_2^+ + O$	$3.9 \times 10^{-11}$	[29]
908	$C_2H_2 + O_2^+ \rightarrow C_2H_2^+ + O_2$	$1.105 \times 10^{-9}$	[116]
909	$C_2H_2 + O_2^+ \rightarrow CO + H + HCO^+$	$6.5 \times 10^{-11}$	[116]
910	$C_2H + O^+ \rightarrow C_2H^+ + O$	$4.6 \times 10^{-10}$	[1]
911	$C_2H + O^+ \rightarrow CH + CO^+$	$4.6 \times 10^{-10}$	[1]
912	$C_2H_4^+ + O \rightarrow CH_3^+ + HCO$	$1.08 \times 10^{-10}$	[117]
913	$C_2H_4^+ + O \rightarrow CH_3 + HCO^+$	$8.4 \times 10^{-11}$	[117]
914	$C_2H_4^+ + O^- \rightarrow C_2H_3 + H + O$	$7.51 \times 10^{-8} \cdot \left(\frac{T_g}{3 \times 10^2}\right)^{-0.5}$	[2, 3]
915	$C_2H_3^+ + O \rightarrow CH_3^+ + CO$	$5 \times 10^{-12}$	[117]
916	$C_2H_3^+ + O^- \rightarrow C_2H_3 + O$	$7.51 \times 10^{-8} \cdot \left(\frac{T_g}{3 \times 10^2}\right)^{-0.5}$	[2, 3]
917	$C_2H_3^+ + O^- \rightarrow C_2H + H_2 + O$	$7.51 \times 10^{-8} \cdot \left(\frac{T_g}{3 \times 10^2}\right)^{-0.5}$	[2, 3]
918	$C_2H_3^+ + O_2^- \rightarrow C_2H_3 + O_2$	$7.51 \times 10^{-8} \cdot \left(\frac{T_g}{3 \times 10^2}\right)^{-0.5}$	[2, 3]
919	$C_2H_2^+ + O \rightarrow CH + HCO^+$	$8.5 \times 10^{-11}$	[81]
920	$C_2H_2^+ + O^- \rightarrow C_2H_2 + O$	$7.51 \times 10^{-8} \cdot \left(\frac{T_g}{3 \times 10^2}\right)^{-0.5}$	[2, 3]
921	$C_2H_2^+ + O_2^- \rightarrow C_2H_2 + O_2$	$7.51 \times 10^{-8} \cdot \left(\frac{T_g}{3 \times 10^2}\right)^{-0.5}$	[2, 3]
922	$C_2H^+ + O \rightarrow C + HCO^+$	$1 \times 10^{-11}$	[1]
923	$C_2H_4 + CO \rightarrow C_2H_3 + HCO$	$2.5 \times 10^{-10} \cdot \exp\left(\frac{-4.56 \times 10^4}{T_g}\right)$	[25]
924	$C_2H_2 + CO \rightarrow C_2H + HCO$	$8 \times 10^{-10} \cdot \exp\left(\frac{-5.37 \times 10^4}{T_g}\right)$	[25]
925	$C_2H_4 + CO_2^+ \rightarrow C_2H_4^+ + CO_2$	$8.775 \times 10^{-10}$	[61]
926	$C_2H_2 + CO_2^+ \rightarrow C_2H_2^+ + CO_2$	$7.3 \times 10^{-10}$	[61]
927	$C_2H + CO^+ \rightarrow C_2H^+ + CO$	$3.9 \times 10^{-10}$	[1]
928	$C_2H_6 + HCO \rightarrow C_2H_5 + HCHO$	$7.8 \times 10^{-20} \cdot T_g^{2.72} \cdot \exp\left(\frac{-9.176 \times 10^3}{T_g}\right)$	[25]
929	$C_2H_6 + CH_3O \rightarrow C_2H_5 + CH_3OH$	$4 \times 10^{-13} \cdot \exp\left(\frac{-3.57 \times 10^3}{T_g}\right)$	[25]
930	$C_2H_6 + CH_2OH \rightarrow C_2H_5 + CH_3OH$	$3.3 \times 10^{-22} \cdot T_g^{2.95} \cdot \exp\left(\frac{-7.033 \times 10^3}{T_g}\right)$	[96]
931	$C_2H_6 + CH_3OO \rightarrow C_2H_5 + CH_3OOH$	$4.9 \times 10^{-13} \cdot \exp\left(\frac{-7.52 \times 10^3}{T_g}\right)$	[25]
932	$C_2H_5 + HCO \rightarrow C_2H_6 + CO$	$2 \times 10^{-10}$	[25]
933	$C_2H_5 + HCHO \rightarrow C_2H_6 + HCO$	$9.2 \times 10^{-21} \cdot T_g^{2.81} \cdot \exp\left(\frac{-2.95 \times 10^3}{T_g}\right)$	[25]
934	$C_2H_5 + CH_3O \rightarrow C_2H_6 + HCHO$	$4 \times 10^{-11}$	[25]

#	Reaction	Rate equation	Ref.
935	$C_2H_5 + CH_2OH \rightarrow C_2H_4 + CH_3OH$	$4 \times 10^{-12}$	[96]
936	$C_2H_5 + CH_2OH \rightarrow C_2H_6 + HCHO$	$4 \times 10^{-12}$	[96]
937	$C_2H_5 + CH_3OH \rightarrow C_2H_6 + CH_2OH$	$5.3 \times 10^{-23} \cdot T_g^{3.2} \cdot \exp\left(\frac{-4.61 \times 10^3}{T_g}\right)$	[96]
938	$C_2H_5 + CH_3OH \rightarrow C_2H_6 + CH_3O$	$2.4 \times 10^{-23} \cdot T_g^{3.1} \cdot \exp\left(\frac{-4.5 \times 10^3}{T_g}\right)$	[96]
939	$C_2H_5 + CH_3OO \rightarrow CH_3CH_2O + CH_3O$	$4 \times 10^{-11}$	[25]
940	$C_2H_4 + COOH \rightarrow C_2H_5 + CO_2$	$1 \times 10^{-14}$	[88]
941	$C_2H_4 + CH_2OH \rightarrow C_2H_5 + HCHO$	$\frac{8 \times 10^{-14} \cdot \exp\left(\frac{-3.5 \times 10^3}{T_g}\right) \cdot \exp\left(\frac{-2 \times 10^3}{T_g}\right)}{1.0 + \exp\left(\frac{-2 \times 10^3}{T_g}\right)}$	[96]
942	$C_2H_3 + HCO \rightarrow C_2H_4 + CO$	$1.5 \times 10^{-10}$	[25]
943	$C_2H_3 + HCHO \rightarrow C_2H_4 + HCO$	$9 \times 10^{-21} \cdot T_g^{2.81} \cdot \exp\left(\frac{-2.95 \times 10^3}{T_g}\right)$	[25]
944	$C_2H_3 + CH_3O \rightarrow C_2H_4 + HCHO$	$4 \times 10^{-11}$	[25]
945	$C_2H_3 + CH_2OH \rightarrow C_2H_4 + HCHO$	$5 \times 10^{-11}$	[96]
946	$C_2H_3 + CH_3OH \rightarrow C_2H_4 + CH_2OH$	$5.3 \times 10^{-23} \cdot T_g^{3.2} \cdot \exp\left(\frac{-3.609 \times 10^3}{T_g}\right)$	[96]
947	$C_2H_3 + CH_3OH \rightarrow C_2H_4 + CH_3O$	$2.4 \times 10^{-23} \cdot T_g^{3.1} \cdot \exp\left(\frac{-3.49 \times 10^3}{T_g}\right)$	[96]
948	$C_2H_2 + COOH \rightarrow C_2H_3 + CO_2$	$3 \times 10^{-14}$	[88]
949	$C_2H_2 + CH_2OH \rightarrow C_2H_3 + HCHO$	$1.2 \times 10^{-12} \cdot \exp\left(\frac{-4.531 \times 10^3}{T_g}\right)$	[96]
950	$C_2H + HCO \rightarrow C_2H_2 + CO$	$1 \times 10^{-10}$	[25]
951	$C_2H + CH_3O \rightarrow C_2H_2 + HCHO$	$4 \times 10^{-11}$	[25]
952	$C_2H + CH_2OH \rightarrow C_2H_2 + HCHO$	$6 \times 10^{-11}$	[96]
953	$C_2H + CH_3OH \rightarrow C_2H_2 + CH_2OH$	$1 \times 10^{-11}$	[96]
954	$C_2H + CH_3OH \rightarrow C_2H_2 + CH_3O$	$2 \times 10^{-12}$	[96]
955	$C_2H + CH_3OO \rightarrow CH_3O + HCCO$	$4 \times 10^{-11}$	[25]
956	$C_2H_4 + HCO^+ \rightarrow C_2H_5^+ + CO$	$1.4 \times 10^{-9}$	[13]
957	$C_2H_3 + HCO^+ \rightarrow C_2H_4^+ + CO$	$1.4 \times 10^{-9}$	[13]
958	$C_2H_2 + HCO^+ \rightarrow C_2H_3^+ + CO$	$1.4 \times 10^{-9}$	[38]
959	$C_2H + HCO^+ \rightarrow C_2H_2^+ + CO$	$7.8 \times 10^{-10}$	[1]
960	$C_2H_2^+ + HCO \rightarrow C_2H_2 + HCO^+$	$5 \times 10^{-10}$	[1]
961	$C_2H_2^+ + HCO \rightarrow C_2H_3^+ + CO$	$3.7 \times 10^{-10}$	[1]
962	$C_2H_2^+ + HCHO \rightarrow C_2H_3 + HCO^+$	$5.375 \times 10^{-10}$	[87]
963	$C_2H_2^+ + HCHO \rightarrow C_2H_4^+ + CO$	$2.795 \times 10^{-10}$	[87]
964	$C_2H^+ + HCO \rightarrow C_2H_2^+ + CO$	$7.6 \times 10^{-10}$	[1]
965	$H + HCCO \rightarrow CH_2 + CO$	$9.92 \times 10^{-13} \cdot T_g^{0.76} \cdot \exp\left(\frac{4.38 \times 10^2}{T_g}\right)$	[118]
966	$CH_2CO + H \rightarrow CH_3 + CO$	$\frac{1.11 \times 10^7}{N_A} \cdot T_g^2 \cdot \exp\left(\frac{-2 \times 10^3 \cdot 4.184}{R \cdot T_g}\right)$	[119]
967	$CH_2CO + H \rightarrow H_2 + HCCO$	$\frac{1.8 \times 10^{14}}{N_A} \cdot \exp\left(\frac{-8.6 \times 10^3 \cdot 4.184}{R \cdot T_g}\right)$	[119]
968	$CH_2CO + H \rightarrow CH_3CO$	$\frac{1.63 \times 10^9}{N_A} \cdot T_g^{1.3766} \cdot \exp\left(\frac{-1.664 \times 10^3 \cdot 4.184}{R \cdot T_g}\right)$	[120]
969	$CH_3CO + H \rightarrow CH_3 + HCO$	$\frac{0.65 \cdot 2 \times 10^{13}}{N_A}$	[121, 122]
970	$CH_3CO + H \rightarrow CH_2CO + H_2$	$\frac{0.35 \cdot 2 \times 10^{13}}{N_A}$	[121, 122]
971	$CH_3CO + H \rightarrow CH_3CHO$	$6.02 \times 10^{-11} \cdot T_g^{0.16}$	[109]
972	$CH_3CO + H_2 \rightarrow CH_3CHO + H$	$6.8 \times 10^{-18} \cdot T_g^{1.82} \cdot \exp\left(\frac{-8.862 \times 10^3}{T_g}\right)$	[25]

#	Reaction	Rate equation	Ref.
973	$CH_3CHO + H \rightarrow CH_3CO + H_2$	$2.18 \times 10^{-19} \cdot T_g^{2.58} \cdot \exp\left(\frac{-6.14 \times 10^2}{T_g}\right)$	[123]
974	$CH_3CHO + H \rightarrow CH_3CH_2O$	$7.66 \times 10^{-17} \cdot T_g^{1.71} \cdot \exp\left(\frac{-3.57 \times 10^3}{T_g}\right)$	[123]
975	$CH_3CHO + H \rightarrow CH_3CHOH$	$2.89 \times 10^{-18} \cdot T_g^{2.2} \cdot \exp\left(\frac{-3.78 \times 10^3}{T_g}\right)$	[123]
976	$CH_3CH_2O + H \rightarrow CH_2OH + CH_3$	$2.26 \times 10^{-12} \cdot T_g^{0.701} \cdot \exp\left(\frac{-1.74 \times 10^2}{T_g}\right)$	[124]
977	$CH_3CH_2O + H \rightarrow CH_3CH_2OH$	$5.11 \times 10^{-13} \cdot T_g^{0.894} \cdot \exp\left(\frac{-6.5}{T_g}\right)$	[124]
978	$CH_3CH_2O + H \rightarrow C_2H_5 + OH$	$9.04 \times 10^{-16} \cdot T_g^{1.27} \cdot \exp\left(\frac{-1.57 \times 10^2}{T_g}\right)$	[124]
979	$CH_3CH_2O + H \rightarrow CH_3CHOH + H$	$1.33 \times 10^{-22} \cdot T_g^{3.1} \cdot \exp\left(\frac{-1.42 \times 10^2}{T_g}\right)$	[124]
980	$CH_3CH_2O + H \rightarrow C_2H_4 + H_2O$	$9.95 \times 10^{-10} \cdot T_g^{-0.813} \cdot \exp\left(\frac{-3.59 \times 10^2}{T_g}\right)$	[124]
981	$CH_3CH_2O + H \rightarrow CH_3CHO + H_2$	$1.25 \times 10^{-20} \cdot T_g^{1.78} \cdot \exp\left(\frac{-4.07 \times 10^1}{T_g}\right) + 1.24 \times 10^{-14} \cdot T_g^{1.15} \cdot \exp\left(\frac{-3.39 \times 10^2}{T_g}\right)$	[124]
982	$CH_3CH_2O + H \rightarrow CH_4 + HCHO$	$1.32 \times 10^{-21} \cdot T_g^{2.21} \cdot \exp\left(\frac{9.05 \times 10^1}{T_g}\right)$	[124]
983	$CH_3CHOH + H \rightarrow CH_3CH_2OH$	$5.99 \times 10^{-11} \cdot T_g^{0.06} \cdot \exp\left(\frac{-2.2 \times 10^2}{T_g}\right)$	[124]
984	$CH_3CHOH + H \rightarrow CH_2OH + CH_3$	$1.44 \times 10^{-7} \cdot T_g^{-0.891} \cdot \exp\left(\frac{-1.461 \times 10^3}{T_g}\right)$	[124]
985	$CH_3CHOH + H \rightarrow C_2H_5 + OH$	$4.02 \times 10^{-9} \cdot T_g^{-0.83} \cdot \exp\left(\frac{-2.414 \times 10^3}{T_g}\right)$	[124]
986	$CH_3CHOH + H \rightarrow CH_3CH_2O + H$	$4.95 \times 10^{-23} \cdot T_g^{2.94} \cdot \exp\left(\frac{-4.266 \times 10^3}{T_g}\right)$	[124]
987	$CH_3CHOH + H \rightarrow C_2H_4 + H_2O$	$7.81 \times 10^{-3} \cdot T_g^{-3.02} \cdot \exp\left(\frac{-1.432 \times 10^3}{T_g}\right)$	[124]
988	$CH_3CHOH + H \rightarrow CH_3CHO + H_2$	$7.42 \times 10^{-21} \cdot T_g^{1.62} \cdot \exp\left(\frac{5.4}{T_g}\right) + 2.26 \times 10^{-15} \cdot T_g^{1.29} \cdot \exp\left(\frac{-1.421 \times 10^3}{T_g}\right)$	[124]
989	$CH_3CHOH + H \rightarrow CH_4 + HCHO$	$5.56 \times 10^{-22} \cdot T_g^{2.1} \cdot \exp\left(\frac{-1.07 \times 10^2}{T_g}\right)$	[124]
990	$CH_3CH_2OH + H \rightarrow C_2H_5 + H_2O$	$\frac{5.9 \times 10^{11}}{N_A} \cdot \exp\left(\frac{-3.45 \times 10^3 \cdot 4.184}{R \cdot T_g}\right)$	[125]
991	$CH_3CH_2OH + H \rightarrow CH_3CHOH + H_2$	$1.46 \times 10^{-19} \cdot T_g^{2.68} \cdot \exp\left(\frac{-1.467 \times 10^3}{T_g}\right)$	[126]
992	$CH_3CH_2OH + H \rightarrow CH_2CH_2OH + H_2$	$8.82 \times 10^{-20} \cdot T_g^{2.81} \cdot \exp\left(\frac{-3.772 \times 10^3}{T_g}\right)$	[126]
993	$CH_3CH_2OH + H \rightarrow CH_3CH_2O + H_2$	$1.57 \times 10^{-21} \cdot T_g^{3.14} \cdot \exp\left(\frac{-4.379 \times 10^3}{T_g}\right)$	[126]
994	$CH_3CHO + H_3^+ \rightarrow C_2H_3^+ + H_2 + H_2O$	$8.97 \times 10^{-10}$	[100]
995	$CH_3CHO + H_3^+ \rightarrow C_2H_5^+ + H_2O$	$7.59 \times 10^{-10}$	[100]
996	$CH_3CHO + H_3^+ \rightarrow CH_3OH + CH_3^+$	$1.449 \times 10^{-9}$	[100]
997	$CH_3CHO + H_3^+ \rightarrow CH_5^+ + CO + H_2$	$8.28 \times 10^{-10}$	[100]
998	$CH_3CHO + H_3^+ \rightarrow C_2H_4 + H_3O^+$	$1.035 \times 10^{-9}$	[100]
999	$CH_3CH_2OH + H_3^+ \rightarrow CH_3^+ + CH_4 + H_2O$	$1.5 \times 10^{-9}$	[100]
1000	$CH_3CH_2OH + H_3^+ \rightarrow C_2H_3^+ + H_2 + H_2 + H_2O$	$4 \times 10^{-10}$	[100]
1001	$CH_3CH_2OH + H_3^+ \rightarrow CH_4 + H_2 + H_2 + HCO^+$	$1.1 \times 10^{-9}$	[100]
1002	$CH_3CH_2OH + H_3^+ \rightarrow C_2H_5^+ + H_2 + H_2O$	$1.1 \times 10^{-9}$	[100]
1003	$HCCO + OH \rightarrow CH_2CO + O$	$2.1 \times 10^{-18} \cdot T_g^{1.99} \cdot \exp\left(\frac{-1.128 \times 10^4 \cdot 4.184}{R \cdot T_g}\right)$	[127]
1004	$CH_2CO + OH \rightarrow CH_2OH + CO$	$0.6 \cdot 2.8 \times 10^{-12} \cdot \exp\left(\frac{5.1 \times 10^2}{T_g}\right)$	[5]
1005	$CH_2CO + OH \rightarrow H_2O + HCCO$	$0.01 \cdot 2.8 \times 10^{-12} \cdot \exp\left(\frac{5.1 \times 10^2}{T_g}\right)$	[5]
1006	$CH_2CO + OH \rightarrow HCHO + HCO$	$0.02 \cdot 2.8 \times 10^{-12} \cdot \exp\left(\frac{5.1 \times 10^2}{T_g}\right)$	[5]
1007	$CH_2CO + OH \rightarrow CH_3 + CO_2$	$0.37 \cdot 2.8 \times 10^{-12} \cdot \exp\left(\frac{5.1 \times 10^2}{T_g}\right)$	[5]
1008	$CH_3CO + OH \rightarrow CH_2CO + H_2O$	$2 \times 10^{-11}$	[25]

#	Reaction	Rate equation	Ref.
1009	$CH_3CO + H_2O_2 \rightarrow CH_3CHO + HO_2$	$3 \times 10^{-13} \cdot \exp\left(\frac{-4.14 \times 10^3}{T_g}\right)$	[25]
1010	$CH_3CHO + OH \rightarrow CH_3CO + H_2O$	$0.93 \cdot 4.8 \times 10^{-16} \cdot T_g^{1.35} \cdot \exp\left(\frac{7.92 \times 10^2}{T_g}\right)$	[5]
1011	$CH_3CHO + OH \rightarrow CH_3 + HCOOH$	$0.03 \cdot 4.8 \times 10^{-16} \cdot T_g^{1.35} \cdot \exp\left(\frac{7.92 \times 10^2}{T_g}\right)$	[5, 128]
1012	$CH_3CHO + OH \rightarrow CH_3COOH + H$	$0.02 \cdot 4.8 \times 10^{-16} \cdot T_g^{1.35} \cdot \exp\left(\frac{7.92 \times 10^2}{T_g}\right)$	[5, 128]
1013	$CH_3CHO + HO_2 \rightarrow CH_3CO + H_2O_2$	$6.8 \times 10^{-20} \cdot T_g^{2.5} \cdot \exp\left(\frac{-5.135 \times 10^3}{T_g}\right)$	[5]
1014	$CH_3CH_2OH + OH \rightarrow CH_2CH_2OH + H_2O$	$\frac{1.74 \times 10^{11}}{N_A} \cdot T_g^{0.27} \cdot \exp\left(\frac{-6 \times 10^2 \cdot 4.184}{R \cdot T_g}\right)$	[129]
1015	$CH_3CH_2OH + OH \rightarrow CH_3CHOH + H_2O$	$\frac{4.64 \times 10^{11}}{N_A} \cdot T_g^{0.15}$	[129]
1016	$CH_3CH_2OH + OH \rightarrow CH_3CH_2O + H_2O$	$\frac{7.46 \times 10^{11}}{N_A} \cdot T_g^{0.3} \cdot \exp\left(\frac{-1.634 \times 10^3 \cdot 4.184}{R \cdot T_g}\right)$	[129]
1017	$CH_3CH_2OH + HO_2 \rightarrow CH_3CHOH + H_2O_2$	$\frac{5.544 \times 10^{18}}{N_A} \cdot T_g^{-1.808} \cdot \exp\left(\frac{-8.29197 \times 10^3}{T_g}\right)$	[130]
1018	$HCCO + O \rightarrow CH + CO_2$	$4.9 \times 10^{-11} \cdot \exp\left(\frac{-5.6 \times 10^2}{T_g}\right)$	[5]
1019	$CH_2CO + O \rightarrow HCCO + OH$	$3.11 \times 10^{-10} \cdot \exp\left(\frac{-1.669 \times 10^4 \cdot 4.184}{R \cdot T_g}\right)$	[127]
1020	$CH_2CO + O \rightarrow CO + HCHO$	$0.2 \cdot 3 \times 10^{-12} \cdot \exp\left(\frac{-6.8 \times 10^2}{T_g}\right)$	[5]
1021	$CH_2CO + O \rightarrow HCO + HCO$	$0.1 \cdot 3 \times 10^{-12} \cdot \exp\left(\frac{-6.8 \times 10^2}{T_g}\right)$	[5]
1022	$CH_2CO + O \rightarrow CH_2 + CO_2$	$0.6 \cdot 3 \times 10^{-12} \cdot \exp\left(\frac{-6.8 \times 10^2}{T_g}\right)$	[5]
1023	$CH_3CO + O \rightarrow CH_2CO + OH$	$8.75 \times 10^{-11}$	[5]
1024	$CH_3CO + O \rightarrow CH_3 + CO_2$	$2.625 \times 10^{-10}$	[5]
1025	$CH_3CHO + O \rightarrow CH_3CO + OH$	$\frac{5 \times 10^{12}}{N_A} \cdot \exp\left(\frac{-7.5 \times 10^3}{R \cdot T_g}\right)$	[122]
1026	$CH_3CHO + O_2 \rightarrow CH_3CO + HO_2$	$2 \times 10^{-19} \cdot T_g^{2.5} \cdot \exp\left(\frac{-1.89 \times 10^4}{T_g}\right)$	[5]
1027	$CH_3CH_2O + O_2 \rightarrow CH_3CHO + HO_2$	$3.8 \times 10^{-14} \cdot \exp\left(\frac{-4.4 \times 10^2}{T_g}\right)$	[5]
1028	$CH_3CHOH + O \rightarrow CH_3 + HCOOH$	$3.9 \times 10^{-10} \cdot \left(\frac{T_g}{3 \times 10^2}\right)^{0.18} \cdot \exp\left(\frac{-0.49}{T_g}\right)$	[131]
1029	$CH_3CHOH + O \rightarrow CH_3CHO + OH$	$4.8 \times 10^{-11} \cdot \left(\frac{T_g}{3 \times 10^2}\right)^{0.19} \cdot \exp\left(\frac{-0.39}{T_g}\right)$	[131]
1030	$CH_3CHOH + O \rightarrow CH_3COOH + H$	$2.2 \times 10^{-10} \cdot \left(\frac{T_g}{3 \times 10^2}\right)^{0.16} \cdot \exp\left(\frac{-0.59}{T_g}\right)$	[131]
1031	$CH_3CHOH + O_2 \rightarrow CH_3CHO + HO_2$	$\frac{5.28 \times 10^{17}}{N_A} \cdot T_g^{-1.638} \cdot \exp\left(\frac{-0.839 \cdot 4.184 \times 10^3}{R \cdot T_g}\right)$	[132]
1032	$CH_2CH_2OH + O \rightarrow CH_2OH + HCHO$	$4.6 \times 10^{-10} \cdot \left(\frac{T_g}{3 \times 10^2}\right)^{0.17} \cdot \exp\left(\frac{-0.51}{T_g}\right)$	[131]
1033	$CH_3CH_2OH + O \rightarrow CH_3CHOH + OH$	$0.99 \cdot 1 \times 10^{-18} \cdot T_g^{2.5} \cdot \exp\left(\frac{-9.3 \times 10^2}{T_g}\right)$	[5]
1034	$CH_3CH_2OH + O \rightarrow CH_2CH_2OH + OH$	$0.005 \cdot 1 \times 10^{-18} \cdot T_g^{2.5} \cdot \exp\left(\frac{-9.3 \times 10^2}{T_g}\right)$	[5]
1035	$CH_3CH_2OH + O \rightarrow CH_3CH_2O + OH$	$0.005 \cdot 1 \times 10^{-18} \cdot T_g^{2.5} \cdot \exp\left(\frac{-9.3 \times 10^2}{T_g}\right)$	[5]
1036	$CH_3CH_2OH + O_2 \rightarrow CH_3CHOH + HO_2$	$4 \times 10^{-19} \cdot T_g^{2.5} \cdot \exp\left(\frac{-2.217 \times 10^4}{T_g}\right)$	[5]
1037	$CH_3CH_2OH + O_2 \rightarrow CH_2CH_2OH + HO_2$	$6 \times 10^{-19} \cdot T_g^{2.5} \cdot \exp\left(\frac{-2.403 \times 10^4}{T_g}\right)$	[5]
1038	$CH_3CH_2OH + O_2 \rightarrow CH_3CH_2O + HO_2$	$2 \times 10^{-19} \cdot T_g^{2.5} \cdot \exp\left(\frac{-2.653 \times 10^4}{T_g}\right)$	[5]
1039	$CH_2CO + CH_3 \rightarrow C_2H_5 + CO$	$\frac{1.24 \times 10^5}{N_A} \cdot T_g^{2.29} \cdot \exp\left(\frac{-1.0642 \times 10^4 \cdot 4.184}{R \cdot T_g}\right)$	[133]
1040	$CH_2CO + CH_3 \rightarrow CH_4 + HCCO$	$\frac{1.55 \times 10^2}{N_A} \cdot T_g^{3.38} \cdot \exp\left(\frac{-1.0512 \times 10^4 \cdot 4.184}{R \cdot T_g}\right)$	[133]
1041	$CH_2 + CH_2CO \rightarrow C_2H_4 + CO$	$\frac{1 \times 10^{12}}{N_A}$	[134]
1042	$CH_2 + CH_2CO \rightarrow CH_3 + HCCO$	$\frac{3.6 \times 10^{13}}{N_A} \cdot \exp\left(\frac{-1.1 \times 10^4 \cdot 4.184}{R \cdot T_g}\right)$	[119]
1043	$CH_3CO + CH_4 \rightarrow CH_3 + CH_3CHO$	$3.6 \times 10^{-21} \cdot T_g^{2.88} \cdot \exp\left(\frac{-1.08 \times 10^4}{T_g}\right)$	[25]
1044	$CH_3 + CH_3CO \rightarrow CH_2CO + CH_4$	$\frac{6.1 \times 10^9 \cdot 1 \times 10^3}{N_A}$	[135]
1045	$CH_2 + CH_3CO \rightarrow CH_2CO + CH_3$	$3 \times 10^{-11}$	[25]
1046	$CH_3 + CH_3CHO \rightarrow CH_3CO + CH_4$	$0.993 \cdot 5.8 \times 10^{-32} \cdot T_g^{6.21} \cdot \exp\left(\frac{-8.2 \times 10^2}{T_g}\right)$	[5]

#	Reaction	Rate equation	Ref.
1047	$CH_3 + CH_3CH_2OH \rightarrow CH_3CHOH + CH_4$	$\frac{2.476 \times 10^1}{N_A} \cdot T_g^{3.368} \cdot \exp\left(\frac{-3.95579 \times 10^3}{T_g}\right)$	[130]
1048	$CH_3 + CH_3CH_2OH \rightarrow CH_2CH_2OH + CH_4$	$\frac{1.861 \times 10^2}{N_A} \cdot T_g^{3.45} \cdot \exp\left(\frac{-5.54285 \times 10^3}{T_g}\right)$	[130]
1049	$CH_3 + CH_3CH_2OH \rightarrow CH_3CH_2O + CH_4$	$\frac{0.09533}{N_A} \cdot T_g^{4.159} \cdot \exp\left(\frac{-4.119 \times 10^3}{T_g}\right)$	[130]
1050	$C_2H_6 + CH_3CO \rightarrow C_2H_5 + CH_3CHO$	$3 \times 10^{-20} \cdot T_g^{2.75} \cdot \exp\left(\frac{-8.82 \times 10^3}{T_g}\right)$	[25]
1051	$C_2H_5 + CH_3CHO \rightarrow C_2H_6 + CH_3CO$	$\frac{1.25892541 \times 10^{12}}{N_A} \cdot \exp\left(\frac{-8.5 \cdot 4.184 \times 10^3}{R \cdot T_g}\right)$	[136]
1052	$CH_3CO + HCO \rightarrow CH_3CHO + CO$	$1.5 \times 10^{-11}$	[25]
1053	$CH_3CO + HCHO \rightarrow CH_3CHO + HCO$	$3 \times 10^{-13} \cdot \exp\left(\frac{-6.5 \times 10^3}{T_g}\right)$	[25]
1054	$CH_3CO + CH_3O \rightarrow CH_2CO + CH_3OH$	$1 \times 10^{-11}$	[25]
1055	$CH_3CO + CH_3O \rightarrow CH_3CHO + HCHO$	$1 \times 10^{-11}$	[25]
1056	$CH_3CO + CH_3OH \rightarrow CH_2OH + CH_3CHO$	$8.06 \times 10^{-21} \cdot T_g^{2.99} \cdot \exp\left(\frac{-6.21 \times 10^3}{T_g}\right)$	[96]
1057	$CH_3CHO + CH_3O \rightarrow CH_3CO + CH_3OH$	$\frac{1.69 \times 10^5}{N_A} \cdot T_g^{2.04} \cdot \exp\left(\frac{-2.353 \times 10^3 \cdot 4.184}{R \cdot T_g}\right) + \frac{9.62 \times 10^3}{N_A} \cdot T_g^{2.5} \cdot \exp\left(\frac{-1.59 \times 10^2 \cdot 4.184}{R \cdot T_g}\right)$	[137]
1058	$CH_3CHO + CH_3OO \rightarrow CH_3CO + CH_3OOH$	$\frac{0.322}{N_A} \cdot T_g^{3.94} \cdot \exp\left(\frac{-9.503 \times 10^3 \cdot 4.184}{R \cdot T_g}\right) + \frac{4.99 \times 10^{-6}}{N_A} \cdot T_g^{4.98} \cdot \exp\left(\frac{-5.2682 \times 10^3 \cdot 4.184}{R \cdot T_g}\right)$	[137]
1059	$CH_3CO + CH_3CO \rightarrow CH_2CO + CH_3CHO$	$\frac{9 \times 10^9 \cdot 1 \times 10^3}{N_A}$	[135]
1060	$COOH \rightarrow CO + OH$	$k_0 = \frac{10^{2.5137 \times 10^1}}{N_A} \cdot T_g^{-2.396} \cdot \exp\left(\frac{-1.8862 \times 10^4}{T_g}\right)$ $k_\infty = 10^{1.4074 \times 10^1} \cdot T_g^{0.132} \cdot \exp\left(\frac{-1.8349 \times 10^4}{T_g}\right)$ $F_c = 0.729 \cdot \exp\left(\frac{-5.13 \times 10^2}{T_g}\right) + \exp\left(\frac{-T_g}{5.4 \times 10^2}\right)$	[138] <sup>a</sup>
1061	$COOH \rightarrow CO_2 + H$	$k_0 = \frac{10^{2.6775 \times 10^1}}{N_A} \cdot T_g^{-3.148} \cdot \exp\left(\frac{-1.8629 \times 10^4}{T_g}\right)$ $k_\infty = 10^{1.1915 \times 10^1} \cdot T_g^{0.413} \cdot \exp\left(\frac{-1.7783 \times 10^4}{T_g}\right)$ $F_c = 1.049 \cdot \exp\left(\frac{-2.407 \times 10^3}{T_g}\right) + \exp\left(\frac{-T_g}{8.23 \times 10^2}\right)$	[138] <sup>a</sup>
1062	$HCHO \rightarrow H + HCO$	$8.09 \times 10^{-9} \cdot \exp\left(\frac{-3.805 \times 10^4}{T_g}\right) \cdot n_M$	[5]
1063	$CH_2OH \rightarrow H + HCHO$	$k_0 = \frac{6.01 \times 10^{33}}{N_A} \cdot T_g^{-5.39} \cdot \exp\left(\frac{-3.62 \times 10^4 \cdot 4.184}{R \cdot T_g}\right)$ $k_\infty = 2.8 \times 10^{14} \cdot T_g^{-0.73} \cdot \exp\left(\frac{-3.282 \times 10^4 \cdot 4.184}{R \cdot T_g}\right)$ $F_c = (1 - 0.96) \cdot \exp\left(\frac{-T_g}{6.76 \times 10^1}\right) + 0.96 \cdot \exp\left(\frac{-T_g}{1.855 \times 10^3}\right) + \exp\left(\frac{-7.543 \times 10^3}{T_g}\right)$	[139] <sup>a</sup>
1064	$CH_3OH \rightarrow CH_3 + OH$	$0.8 \cdot k$ $k_0 = 1.1 \times 10^{-7} \cdot \exp\left(\frac{-3.308 \times 10^4}{T_g}\right)$ $k_\infty = 2.5 \times 10^{19} \cdot T_g^{-0.94} \cdot \exp\left(\frac{-4.703 \times 10^4}{T_g}\right)$ $F_c = 0.18 \cdot \exp\left(\frac{-T_g}{2 \times 10^2}\right) + 0.82 \cdot \exp\left(\frac{-T_g}{1.438 \times 10^3}\right)$	[5, 140] <sup>a</sup>
1065	$CH_3OH \rightarrow CH_2 + H_2O$	$0.15 \cdot k$ $k_0 = 1.1 \times 10^{-7} \cdot \exp\left(\frac{-3.308 \times 10^4}{T_g}\right)$ $k_\infty = 2.5 \times 10^{19} \cdot T_g^{-0.94} \cdot \exp\left(\frac{-4.703 \times 10^4}{T_g}\right)$ $F_c = 0.18 \cdot \exp\left(\frac{-T_g}{2 \times 10^2}\right) + 0.82 \cdot \exp\left(\frac{-T_g}{1.438 \times 10^3}\right)$	[5, 140] <sup>a</sup>

#	Reaction	Rate equation	Ref.
1066	$CH_3OH \rightarrow CH_2OH + H$	$0.05 \cdot k$ $k_0 = 1.1 \times 10^{-7} \cdot \exp\left(\frac{-3.308 \times 10^4}{T_g}\right)$ $k_\infty = 2.5 \times 10^{19} \cdot T_g^{-0.94} \cdot \exp\left(\frac{-4.703 \times 10^4}{T_g}\right)$ $F_c = 0.18 \cdot \exp\left(\frac{-T_g}{2 \times 10^2}\right)$ $+ 0.82 \cdot \exp\left(\frac{-T_g}{1.438 \times 10^3}\right)$	[5, 140] <sup>a</sup>
1067	$CH_3OOH \rightarrow CH_3O + OH$	$6 \times 10^{14} \cdot \exp\left(\frac{-2.13 \times 10^4}{T_g}\right)$	[5]
1068	$HCCO \rightarrow CH + CO$	$\frac{6 \times 10^{15}}{N_A} \cdot \exp\left(\frac{-2.96 \times 10^4}{T_g}\right) \cdot n_M$	[141]
1069	$CH_2CO \rightarrow CH_2 + CO$	$\frac{2.3 \times 10^{15}}{N_A} \cdot \exp\left(\frac{-2.899 \times 10^4}{T_g}\right) \cdot n_M$	[134]
1070	$CH_3CO \rightarrow CH_3 + CO$	$k_0 = 1 \times 10^{-8} \cdot \exp\left(\frac{-7.08 \times 10^3}{T_g}\right)$ $k_\infty = 2 \times 10^{13} \cdot \exp\left(\frac{-8.63 \times 10^3}{T_g}\right)$ $F_c = 0.5$	[5] <sup>a</sup>
1071	$CH_3CO \rightarrow CH_2CO + H$	$1.36 \times 10^8 \cdot T_g^{1.9433} \cdot \exp\left(\frac{-4.6005 \times 10^4 \cdot 4.184}{R \cdot T_g}\right)$	[120]
1072	$CH_3CHO \rightarrow CH_3CO + H$	$5 \times 10^{14} \cdot \exp\left(\frac{-8.79 \times 10^4 \cdot 4.184}{R \cdot T_g}\right)$	[142]
1073	$CH_3CHO \rightarrow CH_3 + HCO$	$2.1 \times 10^{16} \cdot \exp\left(\frac{-4.1135 \times 10^4}{T_g}\right)$	[5]
1074	$CH_3COOH \rightarrow CH_3 + COOH$	$10^{5.7 \times 10^1} \cdot T_g^{-1.204 \times 10^1} \cdot \exp\left(\frac{-1.1313 \times 10^5 \cdot 4.182}{R \cdot T_g}\right)$	[143]
1075	$CH_3CH_2O \rightarrow CH_3CHO + H$	$\frac{5.43 \times 10^{15}}{N_A} \cdot T_g^{-0.69} \cdot \exp\left(\frac{-2.223 \times 10^4 \cdot 4.184}{R \cdot T_g}\right)$	[93]
1076	$CH_3CH_2O \rightarrow CH_3 + HCHO$	$k_0 = \frac{4.7 \times 10^{25}}{N_A} \cdot T_g^{-3} \cdot \exp\left(\frac{-8.32 \times 10^3}{T_g}\right)$ $k_\infty = 6.31 \times 10^{10} \cdot T_g^{0.93} \cdot \exp\left(\frac{-8.605 \times 10^3}{T_g}\right)$ $F_c = (1 - 0.426) \cdot \exp\left(\frac{-T_g}{0.3}\right)$ $+ 0.426 \cdot \exp\left(\frac{-T_g}{2.278 \times 10^3}\right)$ $+ \exp\left(\frac{-1 \times 10^5}{T_g}\right)$	[144] <sup>a</sup>
1077	$CH_3CHOH \rightarrow CH_3CHO + H$	$k_0 = \frac{1.77 \times 10^{16}}{N_A} \cdot \exp\left(\frac{-1.0458 \times 10^4}{T_g}\right)$ $k_\infty = 6.17 \times 10^9 \cdot T_g^{1.31} \cdot \exp\left(\frac{-1.6998 \times 10^4}{T_g}\right)$ $F_c = (1 - 0.187) \cdot \exp\left(\frac{-T_g}{6.52 \times 10^1}\right)$ $+ 0.187 \cdot \exp\left(\frac{-T_g}{2.568 \times 10^3}\right)$ $+ \exp\left(\frac{-4.1226 \times 10^4}{T_g}\right)$	[144] <sup>a</sup>
1078	$CH_3CHOH \rightarrow CH_3 + HCHO$	$k_0 = \frac{5.86 \times 10^{15}}{N_A} \cdot \exp\left(\frac{-1.0735 \times 10^4}{T_g}\right)$ $k_\infty = 2.22 \times 10^9 \cdot T_g^{1.18} \cdot \exp\left(\frac{-1.7103 \times 10^4}{T_g}\right)$ $F_c = (1 - 0.124) \cdot \exp\left(\frac{-T_g}{1}\right)$ $+ 0.124 \cdot \exp\left(\frac{-T_g}{1.729 \times 10^3}\right)$ $+ \exp\left(\frac{-5 \times 10^4}{T_g}\right)$	[144] <sup>a</sup>
1079	$CH_2CH_2OH \rightarrow C_2H_4 + OH$	$3.52 \times 10^{-34} \cdot T_g^{1.184 \times 10^1} \cdot \exp\left(\frac{9.429 \times 10^3}{T_g}\right)$	[145]
1080	$CH_3CH_2OH \rightarrow CH_2OH + CH_3$	$k_0 = \frac{2.88 \times 10^{85}}{N_A} \cdot T_g^{-1.89 \times 10^1} \cdot \exp\left(\frac{-5.5317 \times 10^4}{T_g}\right)$ $k_\infty = 5.94 \times 10^{23} \cdot T_g^{-1.68} \cdot \exp\left(\frac{-4.588 \times 10^4}{T_g}\right)$ $F_c = 0.5 \cdot \exp\left(\frac{-T_g}{2 \times 10^2}\right)$ $+ 0.5 \cdot \exp\left(\frac{-T_g}{8.9 \times 10^2}\right)$ $+ \exp\left(\frac{-4.6 \times 10^3}{T_g}\right)$	[129] <sup>a</sup>
1081	$e + HCO^+ \rightarrow CO + H$	$0.88 \cdot 2.4 \times 10^{-7} \cdot \left(\frac{T_e}{3 \times 10^2}\right)^{-0.69}$	[146, 147]
1082	$e + HCO^+ \rightarrow C + OH$	$0.06 \cdot 2.4 \times 10^{-7} \cdot \left(\frac{T_e}{3 \times 10^2}\right)^{-0.69}$	[146, 147]
1083	$e + HCO^+ \rightarrow CH + O$	$0.06 \cdot 2.4 \times 10^{-7} \cdot \left(\frac{T_e}{3 \times 10^2}\right)^{-0.69}$	[146, 147]

#	Reaction	Rate equation	Ref.
1084	$C + OH \rightarrow e + HCO^+$	$\frac{1.12 \times 10^{13}}{N_A} \cdot \exp\left(\frac{-8.06 \times 10^4}{T_g}\right)$	d
1085	$CO + H \rightarrow e + HCO^+$	$\frac{1.12 \times 10^{13}}{N_A} \cdot \exp\left(\frac{-8.06 \times 10^4}{T_g}\right)$	d
1086	$e + O \rightarrow e + e + O^+$	$f(\sigma)$	[24]
1087	$e + O^- \rightarrow e + e + O$	$f(\sigma)$	[148]
1088	$e + O_2 \rightarrow e + e + O_2^+$	$f(\sigma)$	[24]
1089	$e + O_2 \rightarrow e + e + O + O^+$	$f(\sigma)$	[149]
1090	$e + O_2 \rightarrow e + O + O$	$f(\sigma)$	[24]
1091	$e + O_2 \rightarrow e + O + O$	$f(\sigma)$	[24]
1092	$e + O_2 \rightarrow O + O^-$	$f(\sigma)$	[24]
1093	$e + O_3 \rightarrow O + O_2^-$	$f(\sigma)$	[148]
1094	$e + O_3 \rightarrow O_2 + O^-$	$f(\sigma)$	[148]
1095	$M + e + O \rightarrow M + O^-$	$1 \times 10^{-31}$	[52, 150]
1096	$M + e + O_2 \rightarrow M + O_2^-$	$1 \times 10^{-31}$	[52, 150]
1097	$M + e + O_3 \rightarrow M + O_3^-$	$1 \times 10^{-31}$	[52, 150]
1098	$e + e + O^+ \rightarrow e + O$	$7 \times 10^{-20} \cdot \left(\frac{3.0 \times 10^2}{T_e}\right)^{4.5}$	[52]
1099	$M + e + O^+ \rightarrow M + O$	$6 \times 10^{-27} \cdot \left(\frac{3.0 \times 10^2}{T_e}\right)^{1.5}$	[52, 150]
1100	$e + e + O_2^+ \rightarrow e + O_2$	$1 \times 10^{-19} \cdot \left(\frac{3.0 \times 10^2}{T_e}\right)^{4.5}$	[150]
1101	$M + e + O_2^+ \rightarrow M + O_2$	$6 \times 10^{-27} \cdot \left(\frac{3.0 \times 10^2}{T_e}\right)^{1.5}$	[52, 150]
1102	$e + O_2^+ \rightarrow O + O$	$2.7 \times 10^{-7} \cdot \left(\frac{3.0 \times 10^2}{T_e}\right)^{0.7}$	[52]
1103	$M + O + O \rightarrow M + O_2$	$5.2 \times 10^{-35} \cdot \exp\left(\frac{9 \times 10^2}{T_g}\right)$	[25]
1104	$O + O \rightarrow e + O_2^+$	$\frac{1.12 \times 10^{13}}{N_A} \cdot \exp\left(\frac{-8.06 \times 10^4}{T_g}\right)$	[151]
1105	$O + O^- \rightarrow e + O_2$	$2.3 \times 10^{-10}$	[152]
1106	$M + O + O^+ \rightarrow M + O_2^+$	$1 \times 10^{-29}$	[52, 150]
1107	$O + O_2^- \rightarrow O_2 + O^-$	$3.3 \times 10^{-10}$	[52, 150]
1108	$O + O_2^- \rightarrow e + O_3$	$1.5 \times 10^{-10}$	[52, 150]
1109	$O + O_3^- \rightarrow e + O_2 + O_2$	$1 \times 10^{-13}$	[153]
1110	$O + O_3^- \rightarrow O_2 + O_2^-$	$2.5 \times 10^{-10}$	[154]
1111	$O + O_3 \rightarrow O_2 + O_2$	$8 \times 10^{-12} \cdot \exp\left(\frac{-2.060 \times 10^3}{T_g}\right)$	[54]
1112	$M + O + O_2 \rightarrow M + O_3$	$5.4 \times 10^{-34} \cdot \left(\frac{3 \times 10^2}{T_g}\right)^{1.9}$	[52]
1113	$O_2 + O^+ \rightarrow O + O_2^+$	$2 \times 10^{-11} \cdot \left(\frac{T_g}{3.0 \times 10^2}\right)^{-0.5}$	[52]
1114	$O_3 + O^+ \rightarrow O_2 + O_2^+$	$1 \times 10^{-10}$	[52, 150]
1115	$O^- + O^+ \rightarrow O + O$	$2 \times 10^{-7} \cdot \left(\frac{3.0 \times 10^2}{T_g}\right)^{0.5}$	[150]
1116	$O_2^- + O^+ \rightarrow O + O_2$	$2 \times 10^{-7} \cdot \left(\frac{3.0 \times 10^2}{T_g}\right)^{0.5}$	[150]
1117	$O_3^- + O^+ \rightarrow O + O_3$	$2 \times 10^{-7} \cdot \left(\frac{3.0 \times 10^2}{T_g}\right)^{0.5}$	[150]
1118	$M + O_2^- + O^+ \rightarrow M + O + O_2$	$2 \times 10^{-25} \cdot \left(\frac{3.0 \times 10^2}{T_g}\right)^{2.5}$	[150]
1119	$M + O^- + O^+ \rightarrow M + O + O$	$2 \times 10^{-25} \cdot \left(\frac{3.0 \times 10^2}{T_g}\right)^{2.5}$	[150]
1120	$M + O_2^- + O^+ \rightarrow M + O_3$	$2 \times 10^{-25} \cdot \left(\frac{3.0 \times 10^2}{T_g}\right)^{2.5}$	[150]
1121	$M + O^- + O^+ \rightarrow M + O_2$	$2 \times 10^{-25} \cdot \left(\frac{3.0 \times 10^2}{T_g}\right)^{2.5}$	[150]

#	Reaction	Rate equation	Ref.
1122	$M + O_3^- + O^+ \rightarrow M + O + O_3$	$2 \times 10^{-25} \cdot \left(\frac{3.0 \times 10^2}{T_g}\right)^{2.5}$	[155]
1123	$O_2^+ + O^- \rightarrow O + O + O$	$1 \times 10^{-7}$	[150]
1124	$O_2^+ + O^- \rightarrow O + O_2$	$2 \times 10^{-7} \cdot \left(\frac{3.0 \times 10^2}{T_g}\right)^{0.5}$	[150]
1125	$O_2 + O^- \rightarrow e + O_3$	$5 \times 10^{-15}$	[52, 150]
1126	$M + O_2 + O^- \rightarrow M + O_3^-$	$1.1 \times 10^{-30} \cdot \left(\frac{T_g}{3.0 \times 10^2}\right)^{-1}$	[52, 150, 156]
1127	$O_3 + O^- \rightarrow e + O_2 + O_2$	$3 \times 10^{-10}$	[52, 157]
1128	$O_3 + O^- \rightarrow O + O_3^-$	$8 \times 10^{-10}$	[52]
1129	$M + O^- \rightarrow M + e + O$	$6.9 \times 10^{-10} \cdot \left(\frac{T_g}{3 \times 10^2}\right)^{0.5}$	[158]
1130	$M + O_2^+ + O^- \rightarrow M + O + O_2$	$2 \times 10^{-25} \cdot \left(\frac{3.0 \times 10^2}{T_g}\right)^{2.5}$	[150]
1131	$M + O_2^+ + O^- \rightarrow M + O_3$	$2 \times 10^{-25} \cdot \left(\frac{3.0 \times 10^2}{T_g}\right)^{2.5}$	[150]
1132	$O_2 + O_2 \rightarrow O + O_3$	$2 \times 10^{-11} \cdot \exp\left(\frac{-4.980 \times 10^4}{T_g}\right)$	[52]
1133	$M + O_2 \rightarrow M + O + O$	$3 \times 10^{-6} \cdot T_g^{-1} \cdot \exp\left(\frac{-5.938 \times 10^4}{T_g}\right)$	[25]
1134	$M + O_2^+ + O_3^- \rightarrow M + O_2 + O_3$	$2 \times 10^{-25} \cdot \left(\frac{3.0 \times 10^2}{T_g}\right)^{2.5}$	[155]
1135	$O_2^+ + O_3^- \rightarrow O + O + O_3$	$1 \times 10^{-7}$	[150]
1136	$O_2^+ + O_3^- \rightarrow O_2 + O_3$	$2 \times 10^{-7} \cdot \left(\frac{3.0 \times 10^2}{T_g}\right)^{0.5}$	[150]
1137	$M + O_2^- + O_2^+ \rightarrow M + O_2 + O_2$	$2 \times 10^{-25} \cdot \left(\frac{3.0 \times 10^2}{T_g}\right)^{2.5}$	[150]
1138	$O_2^- + O_2^+ \rightarrow O + O + O_2$	$1 \times 10^{-7}$	[150]
1139	$O_2^- + O_2^+ \rightarrow O_2 + O_2$	$2 \times 10^{-7} \cdot \left(\frac{3.0 \times 10^2}{T_g}\right)^{0.5}$	[150, 159]
1140	$M + O_2^- \rightarrow M + e + O_2$	$2 \times 10^{-10} \cdot \left(\frac{T_g}{3 \times 10^2}\right)^{0.5}$	[158]
1141	$O_2^- + O_3 \rightarrow O_2 + O_3^-$	$3.5 \times 10^{-10}$	[52]
1142	$O_3 + O_3^- \rightarrow e + O_2 + O_2 + O_2$	$3 \times 10^{-10}$	[154]
1143	$M + O_3 \rightarrow M + O + O_2$	$6.6 \times 10^{-10} \cdot \exp\left(\frac{-1.160 \times 10^4}{T_g}\right)$	[52]
1144	$O_2 + O_3^- \rightarrow e + O_2 + O_3$	$2.3 \times 10^{-11}$	[160]
1145	$CO_2 + e \rightarrow CO_2^+ + e + e$	$f(\sigma)$	[24]
1146	$CO_2 + e \rightarrow CO + e + O$	$f(\sigma)$	[161]
1147	$CO_2 + e \rightarrow CO + e + O$	$f(\sigma)$	[161]
1148	$CO_2 + e \rightarrow CO + O^-$	$f(\sigma)$	[162]
1149	$CO + e \rightarrow CO^+ + e + e$	$f(\sigma)$	[24]
1150	$CO + e \rightarrow C + O^-$	$f(\sigma)$	[24]
1151	$CO + e \rightarrow C + e + O$	$f(\sigma)$	[24]
1152	$CO^+ + e \rightarrow C + O$	$6.8 \times 10^{-7} \cdot \left(\frac{T_e}{3 \times 10^2}\right)^{-0.4}$	[160]
1153	$CO_2^+ + e \rightarrow CO + O$	$0.5 \cdot 3.4 \times 10^{-6} \cdot \left(\frac{T_e}{3 \times 10^2}\right)^{-0.4}$	[160]
1154	$CO_2^+ + e \rightarrow C + O_2$	$0.5 \cdot 3.4 \times 10^{-6} \cdot \left(\frac{T_e}{3 \times 10^2}\right)^{-0.4}$	[160]
1155	$CO + O \rightarrow CO_2^+ + e$	$\frac{1.12 \times 10^{13}}{N_A} \cdot \exp\left(\frac{-8.06 \times 10^4}{T_g}\right)$	d
1156	$C + O_2 \rightarrow CO_2^+ + e$	$\frac{1.12 \times 10^{13}}{N_A} \cdot \exp\left(\frac{-8.06 \times 10^4}{T_g}\right)$	d
1157	$C + O \rightarrow CO^+ + e$	$\frac{5.28 \times 10^{12}}{N_A} \cdot \exp\left(\frac{-3.2 \times 10^4}{T_g}\right)$	[151, 163]
1158	$CO^+ + e + e \rightarrow CO + e$	$1 \times 10^{-19} \cdot \left(\frac{3 \times 10^2}{T_e}\right)^{4.5}$	e
1159	$M + CO^+ + e \rightarrow M + CO$	$6 \times 10^{-27} \cdot \left(\frac{3 \times 10^2}{T_e}\right)^{1.5}$	f

#	Reaction	Rate equation	Ref.
1160	$CO_2^+ + e + e \rightarrow CO_2 + e$	$1 \times 10^{-19} \cdot \left(\frac{3 \times 10^2}{T_e}\right)^{4.5}$	e
1161	$M + CO_2^+ + e \rightarrow M + CO_2$	$6 \times 10^{-27} \cdot \left(\frac{3 \times 10^2}{T_e}\right)^{1.5}$	f
1162	$M + C + O \rightarrow M + CO$	$9.1 \times 10^{-22} \cdot T_g^{-3.08} \cdot \exp\left(\frac{-2.114 \times 10^3}{T_g}\right)$	[160]
1163	$C + O_2 \rightarrow CO + O$	$\frac{1.2 \times 10^{14}}{N_A} \cdot \exp\left(\frac{-2.01 \times 10^3}{T_g}\right)$	[164]
1164	$M + C + O^+ \rightarrow M + CO^+$	$1 \times 10^{-19} \cdot T_g^{-3.08} \cdot \exp\left(\frac{-2.114 \times 10^3}{T_g}\right)$	[165]
1165	$C + O_2^+ \rightarrow CO^+ + O$	$5.2 \times 10^{-11}$	[1]
1166	$C + O_2^+ \rightarrow C^+ + O_2$	$5.2 \times 10^{-11}$	[1]
1167	$C + O^- \rightarrow CO + e$	$5 \times 10^{-10}$	[1]
1168	$M + C^+ + O \rightarrow M + CO^+$	$1 \times 10^{-19} \cdot T_g^{-3.08} \cdot \exp\left(\frac{-2.114 \times 10^3}{T_g}\right)$	[165]
1169	$C^+ + O_2 \rightarrow CO + O^+$	$6.138 \times 10^{-10}$	[56]
1170	$C^+ + O_2 \rightarrow CO^+ + O$	$3.762 \times 10^{-10}$	[56]
1171	$CO_2 + O \rightarrow CO + O_2$	$\frac{1.7 \times 10^{13}}{N_A} \cdot \exp\left(\frac{-2.65 \times 10^4}{T_g}\right)$	[160]
1172	$CO_2 + O^+ \rightarrow CO_2^+ + O$	$4.5 \times 10^{-10}$	[56]
1173	$CO_2 + O^+ \rightarrow CO + O_2^+$	$4.5 \times 10^{-10}$	[56]
1174	$M + CO + O \rightarrow M + CO_2$	$8.3 \times 10^{-34} \cdot \exp\left(\frac{-1.51 \times 10^3}{T_g}\right)$	[25]
1175	$CO + O_2 \rightarrow CO_2 + O$	$4.2 \times 10^{-12} \cdot \exp\left(\frac{-2.4 \times 10^4}{T_g}\right)$	[25]
1176	$CO + O_3 \rightarrow CO_2 + O_2$	$4 \times 10^{-25}$	[166]
1177	$CO + O^+ \rightarrow CO^+ + O$	$2 \times 10^{-11} \cdot \left(\frac{T_g}{5 \times 10^3}\right)^{0.5} \cdot \exp\left(\frac{-4.58 \times 10^3}{T_g}\right)$	[165]
1178	$CO + O^- \rightarrow CO_2 + e$	$6 \times 10^{-10} \cdot \left(\frac{T_g}{3 \times 10^2}\right)^{-0.39}$	[167]
1179	$CO_2^+ + O \rightarrow CO_2 + O^+$	$9.62 \times 10^{-11}$	[56]
1180	$CO_2^+ + O \rightarrow CO + O_2^+$	$1.638 \times 10^{-10}$	[56]
1181	$CO_2^+ + O_2 \rightarrow CO_2 + O_2^+$	$5.3 \times 10^{-11}$	[83]
1182	$CO^+ + O \rightarrow CO + O^+$	$1.4 \times 10^{-10}$	[168]
1183	$CO^+ + O_2 \rightarrow CO + O_2^+$	$1.2 \times 10^{-10}$	[91]
1184	$C + CO_2 \rightarrow CO + CO$	$1 \times 10^{-15}$	[169]
1185	$CO_2 + C^+ \rightarrow CO + CO^+$	$1.1 \times 10^{-9}$	[170]
1186	$C + CO^+ \rightarrow CO + C^+$	$1.1 \times 10^{-10}$	[1]
1187	$M + CO_2 \rightarrow M + CO + O$	$\frac{3.65 \times 10^{14}}{N_A} \cdot \exp\left(\frac{-5.2525 \times 10^4}{T_g}\right)$	[171]
1188	$CO_2 + CO^+ \rightarrow CO + CO_2^+$	$1 \times 10^{-9}$	[91]
1189	$M + CO \rightarrow M + C + O$	$1.46 \times 10^6 \cdot T_g^{-3.52} \cdot \exp\left(\frac{-1.287 \times 10^5}{T_g}\right)$	[160]
1190	$e + H \rightarrow e + e + H^+$	$f(\sigma)$	[24]
1191	$e + H_2 \rightarrow e + e + H_2^+$	$f(\sigma)$	[24]
1192	$e + H_2 \rightarrow e + H + H$	$f(\sigma)$	[149]
1193	$e + H_2 \rightarrow e + e + H + H^+$	$f(\sigma)$	[149]
1194	$e + H_2 \rightarrow H + H^-$	$f(\sigma)$	[149]
1195	$e + H_2^+ \rightarrow H + H$	$7.51 \times 10^{-09} - 1.12 \times 10^{-09} \cdot \frac{T_e}{1.16045052e4}^{2.0}$ $+ 1.03 \times 10^{-10} \cdot \left(\frac{T_e}{1.16045052e4}\right)^{2.0}$ $- 4.15 \times 10^{-12} \cdot \left(\frac{T_e}{1.16045052e4}\right)^{3.0}$ $+ 5.86 \times 10^{-14} \cdot \left(\frac{T_e}{1.16045052e4}\right)^{4.0}$	[172]

#	Reaction	Rate equation	Ref.
1196	$e + H_3^+ \rightarrow H + H + H$	$5 \times 10^{-01} \cdot (8.39 \times 10^{-09} + 3.02 \times 10^{-09} \cdot \frac{T_e}{1.16045052e4}) \\ + 5 \times 10^{-01} \cdot (-3.8 \times 10^{-10} \cdot (\frac{T_e}{1.16045052e4})^{2.0}) \\ + 5 \times 10^{-01} \cdot (1.31 \times 10^{-11} \cdot (\frac{T_e}{1.16045052e4})^{3.0}) \\ + 5 \times 10^{-01} \cdot (2.42 \times 10^{-13} \cdot (\frac{T_e}{1.16045052e4})^{4.0}) \\ + 5 \times 10^{-01} \cdot (-2.3 \times 10^{-14} \cdot (\frac{T_e}{1.16045052e4})^{5.0}) \\ + 5 \times 10^{-01} \cdot (3.55 \times 10^{-16} \cdot (\frac{T_e}{1.16045052e4})^{6.0})$	[172]
1197	$e + H_3^+ \rightarrow H + H_2$	$5 \times 10^{-01} \cdot (8.39 \times 10^{-09} + 3.02 \times 10^{-09} \cdot \frac{T_e}{1.16045052e4}) \\ + 5 \times 10^{-01} \cdot (-3.8 \times 10^{-10} \cdot (\frac{T_e}{1.16045052e4})^{2.0}) \\ + 5 \times 10^{-01} \cdot (1.31 \times 10^{-11} \cdot (\frac{T_e}{1.16045052e4})^{3.0}) \\ + 5 \times 10^{-01} \cdot (2.42 \times 10^{-13} \cdot (\frac{T_e}{1.16045052e4})^{4.0}) \\ + 5 \times 10^{-01} \cdot (-2.3 \times 10^{-14} \cdot (\frac{T_e}{1.16045052e4})^{5.0}) \\ + 5 \times 10^{-01} \cdot (3.55 \times 10^{-16} \cdot (\frac{T_e}{1.16045052e4})^{6.0})$	[172]
1198	$H + H_2^+ \rightarrow H_2 + H^+$	$6.4 \times 10^{-10}$	[27]
1199	$M + H + H \rightarrow M + H_2$	$\frac{1.5 \times 10^{-29}}{N_A} \cdot T_g^{-1.3}$	[25]
1200	$H + H \rightarrow e + H_2^+$	$\frac{1.12 \times 10^{13}}{N_A} \cdot \exp\left(\frac{-8.06 \times 10^4}{T_g}\right)$	d
1201	$M + H^- \rightarrow M + e + H$	$8 \times 10^{-12} \cdot \left(\frac{T_g}{3 \times 10^2}\right)^{0.5}$	[173]
1202	$H_2^+ + H^- \rightarrow H + H + H$	$2 \times 10^{-7} \cdot \frac{3.0 \times 10^2}{T_g}$	[174]
1203	$H_3^+ + H^- \rightarrow H + H + H_2$	$2 \times 10^{-7} \cdot \frac{3.0 \times 10^2}{T_g}$	[174]
1204	$H^- + H^+ \rightarrow H + H$	$7.51 \times 10^{-8} \cdot \left(\frac{T_g}{3 \times 10^2}\right)^{-0.5}$	[2, 3]
1205	$H_2 + H_2^+ \rightarrow H + H_3^+$	$2 \times 10^{-9}$	[27]
1206	$M + H_2 \rightarrow M + H + H$	$\frac{7.6 \times 10^{-5}}{N_A} \cdot T_g^{-1.4} \cdot \exp\left(\frac{-5.253 \times 10^4}{T_g}\right)$	[25]
1207	$C + e \rightarrow C^+ + e + e$	$f(\sigma)$	[148]
1208	$C + H_2 \rightarrow CH + H$	$k_{rev} \cdot K_{eq}$	b
1209	$C_2H_4 \rightarrow C + CH_4$	$k_{rev} \cdot K_{eq}$	b
1210	$C_2H_2 + H \rightarrow C + CH_3$	$k_{rev} \cdot K_{eq}$	b
1211	$C_2H + H \rightarrow C + CH_2$	$k_{rev} \cdot K_{eq}$	b
1212	$C_2H_6 + H \rightarrow CH_3 + CH_4$	$k_{rev} \cdot K_{eq}$	b
1213	$C_2H_5 + H_2 \rightarrow CH_3 + CH_4$	$k_{rev} \cdot K_{eq}$	b
1214	$C_2H_4 + H \rightarrow CH + CH_4$	$k_{rev} \cdot K_{eq}$	b
1215	$C_2H_4 + H \rightarrow CH_2 + CH_3$	$k_{rev} \cdot K_{eq}$	b
1216	$C_2H_2 + H_2 \rightarrow CH_2 + CH_2$	$k_{rev} \cdot K_{eq}$	b
1217	$C_2H_2 \rightarrow CH + CH$	$k_{rev} \cdot K_{eq}$	b
1218	$CH_2 + H \rightarrow CH_3$	$k_{rev} \cdot K_{eq}$	b
1219	$CH + H \rightarrow CH_2$	$k_{rev} \cdot K_{eq}$	b
1220	$C + H_2 \rightarrow CH_2$	$k_{rev} \cdot K_{eq}$	b
1221	$C + H \rightarrow CH$	$k_{rev} \cdot K_{eq}$	b
1222	$C_2H_2 + CH_2 \rightarrow C + C_2H_4$	$k_{rev} \cdot K_{eq}$	b
1223	$C_2H_4 + CH_3 \rightarrow C_2H_6 + CH$	$k_{rev} \cdot K_{eq}$	b
1224	$C_2H_4 + CH_4 \rightarrow C_2H_5 + CH_3$	$k_{rev} \cdot K_{eq}$	b
1225	$C_2H_4 + CH_3 \rightarrow C_2H_5 + CH_2$	$k_{rev} \cdot K_{eq}$	b

#	Reaction	Rate equation	Ref.
1226	$C_2H_2 + CH_4 \rightarrow C_2H_3 + CH_3$	$k_{rev} \cdot K_{eq}$	b
1227	$C_2H_2 + CH_3 \rightarrow C_2H_3 + CH_2$	$k_{rev} \cdot K_{eq}$	b
1228	$C_2H_2 + CH \rightarrow C_2H + CH_2$	$k_{rev} \cdot K_{eq}$	b
1229	$C_2H_4 + C_2H_6 \rightarrow C_2H_5 + C_2H_5$	$k_{rev} \cdot K_{eq}$	b
1230	$C_2H_2 + C_2H_6 \rightarrow C_2H_3 + C_2H_5$	$k_{rev} \cdot K_{eq}$	b
1231	$C_2H_2 + C_2H_4 \rightarrow C_2H + C_2H_5$	$k_{rev} \cdot K_{eq}$	b
1232	$C_2H_2 + C_2H_3 \rightarrow C_2H + C_2H_4$	$k_{rev} \cdot K_{eq}$	b
1233	$H_2 + O_2 \rightarrow OH + OH$	$k_{rev} \cdot K_{eq}$	b
1234	$OH + OH \rightarrow H_2O_2$	$k_{rev} \cdot K_{eq}$	b
1235	$M + H + OH \rightarrow M + H_2O$	$k_{rev} \cdot K_{eq}$	b
1236	$H_2O_2 + O \rightarrow H_2O + O_2$	$k_{rev} \cdot K_{eq}$	b
1237	$M + HO_2 \rightarrow M + H + O_2$	$k_{rev} \cdot K_{eq}$	b
1238	$HO_2 + O \rightarrow H + O_3$	$k_{rev} \cdot K_{eq}$	b
1239	$HO_2 + OH \rightarrow H_2 + O_3$	$k_{rev} \cdot K_{eq}$	b
1240	$CO + H \rightarrow C + OH$	$k_{rev} \cdot K_{eq}$	b
1241	$HCO \rightarrow CO + H$	$k_{rev} \cdot K_{eq}$	b
1242	$CO_2 + OH \rightarrow CO + HO_2$	$k_{rev} \cdot K_{eq}$	b
1243	$COOH + OH \rightarrow CO + H_2O_2$	$k_{rev} \cdot K_{eq}$	b
1244	$H + HCHO \rightarrow CH_3 + O$	$k_{rev} \cdot K_{eq}$	b
1245	$HCHO + OH \rightarrow CH_3 + O_2$	$k_{rev} \cdot K_{eq}$	b
1246	$CH_3OO \rightarrow CH_3 + O_2$	$k_{rev} \cdot K_{eq}$	b
1247	$CO + H_2 \rightarrow CH_2 + O$	$k_{rev} \cdot K_{eq}$	b
1248	$HCHO + O \rightarrow CH_2 + O_2$	$k_{rev} \cdot K_{eq}$	b
1249	$CO + H_2O \rightarrow CH_2 + O_2$	$k_{rev} \cdot K_{eq}$	b
1250	$CO + H \rightarrow CH + O$	$k_{rev} \cdot K_{eq}$	b
1251	$CO_2 + H \rightarrow CH + O_2$	$k_{rev} \cdot K_{eq}$	b
1252	$CO + OH \rightarrow CH + O_2$	$k_{rev} \cdot K_{eq}$	b
1253	$HCO + O \rightarrow CH + O_2$	$k_{rev} \cdot K_{eq}$	b
1254	$CO + HCHO \rightarrow CH_2 + CO_2$	$k_{rev} \cdot K_{eq}$	b
1255	$CO + HCO \rightarrow CH + CO_2$	$k_{rev} \cdot K_{eq}$	b
1256	$CH_3O + H \rightarrow CH_3 + OH$	$k_{rev} \cdot K_{eq}$	b
1257	$H_2 + HCHO \rightarrow CH_3 + OH$	$k_{rev} \cdot K_{eq}$	b
1258	$CH_3O + OH \rightarrow CH_3 + HO_2$	$k_{rev} \cdot K_{eq}$	b
1259	$H + HCHO \rightarrow CH_2 + OH$	$k_{rev} \cdot K_{eq}$	b
1260	$HCHO + OH \rightarrow CH_2 + HO_2$	$k_{rev} \cdot K_{eq}$	b
1261	$CH_3 + HO_2 \rightarrow CH_2 + H_2O_2$	$k_{rev} \cdot K_{eq}$	b
1262	$C + H_2O \rightarrow CH + OH$	$k_{rev} \cdot K_{eq}$	b
1263	$H + HCO \rightarrow CH + OH$	$k_{rev} \cdot K_{eq}$	b
1264	$H + HCHO \rightarrow CH + H_2O$	$k_{rev} \cdot K_{eq}$	b
1265	$CO_2 + HCO \rightarrow CO + COOH$	$k_{rev} \cdot K_{eq}$	b

#	Reaction	Rate equation	Ref.
1266	$CH_3 + CO_2 \rightarrow CH_3O + CO$	$k_{rev} \cdot K_{eq}$	b
1267	$HCHO + HCO \rightarrow CH_3O + CO$	$k_{rev} \cdot K_{eq}$	b
1268	$CH_3O + CO_2 \rightarrow CH_3OO + CO$	$k_{rev} \cdot K_{eq}$	b
1269	$CO + H_2 \rightarrow H + HCO$	$k_{rev} \cdot K_{eq}$	b
1270	$CH_2 + O \rightarrow H + HCO$	$k_{rev} \cdot K_{eq}$	b
1271	$H_2 + HCO \rightarrow H + HCHO$	$k_{rev} \cdot K_{eq}$	b
1272	$CH_3O \rightarrow H + HCHO$	$k_{rev} \cdot K_{eq}$	b
1273	$H_2 + HCHO \rightarrow CH_3O + H$	$k_{rev} \cdot K_{eq}$	b
1274	$CH_3OH \rightarrow CH_3O + H$	$k_{rev} \cdot K_{eq}$	b
1275	$CH_3OH + H \rightarrow CH_3O + H_2$	$k_{rev} \cdot K_{eq}$	b
1276	$H_2 + HCHO \rightarrow CH_2OH + H$	$k_{rev} \cdot K_{eq}$	b
1277	$CH_3 + H_2O \rightarrow CH_3OH + H$	$k_{rev} \cdot K_{eq}$	b
1278	$CH_3O + OH \rightarrow CH_3OO + H$	$k_{rev} \cdot K_{eq}$	b
1279	$CH_3OOH + H \rightarrow CH_3OO + H_2$	$k_{rev} \cdot K_{eq}$	b
1280	$CO + H_2O \rightarrow HCO + OH$	$k_{rev} \cdot K_{eq}$	b
1281	$H + HCOOH \rightarrow HCHO + OH$	$k_{rev} \cdot K_{eq}$	b
1282	$COOH + H_2O \rightarrow HCOOH + OH$	$k_{rev} \cdot K_{eq}$	b
1283	$H_2O + HCHO \rightarrow CH_3O + OH$	$k_{rev} \cdot K_{eq}$	b
1284	$H_2O_2 + HCHO \rightarrow CH_3O + HO_2$	$k_{rev} \cdot K_{eq}$	b
1285	$CH_3OH + O_2 \rightarrow CH_3O + HO_2$	$k_{rev} \cdot K_{eq}$	b
1286	$H_2O + HCHO \rightarrow CH_2OH + OH$	$k_{rev} \cdot K_{eq}$	b
1287	$CH_3OH + OH \rightarrow CH_2OH + H_2O$	$k_{rev} \cdot K_{eq}$	b
1288	$H_2O_2 + HCHO \rightarrow CH_2OH + HO_2$	$k_{rev} \cdot K_{eq}$	b
1289	$H_2O + HCOOH \rightarrow CH_2OH + HO_2$	$k_{rev} \cdot K_{eq}$	b
1290	$CH_3O + H_2O_2 \rightarrow CH_3OH + HO_2$	$k_{rev} \cdot K_{eq}$	b
1291	$CH_3OO + H_2O \rightarrow CH_3OOH + OH$	$k_{rev} \cdot K_{eq}$	b
1292	$CH_3OH + O_2 \rightarrow CH_3OO + OH$	$k_{rev} \cdot K_{eq}$	b
1293	$CH_3OOH + O_2 \rightarrow CH_3OO + HO_2$	$k_{rev} \cdot K_{eq}$	b
1294	$CH_3OOH + HO_2 \rightarrow CH_3OO + H_2O_2$	$k_{rev} \cdot K_{eq}$	b
1295	$CO + OH \rightarrow HCO + O$	$k_{rev} \cdot K_{eq}$	b
1296	$CO_2 + H \rightarrow HCO + O$	$k_{rev} \cdot K_{eq}$	b
1297	$CO + HO_2 \rightarrow HCO + O_2$	$k_{rev} \cdot K_{eq}$	b
1298	$HCO + OH \rightarrow HCHO + O$	$k_{rev} \cdot K_{eq}$	b
1299	$HCO + HO_2 \rightarrow HCHO + O_2$	$k_{rev} \cdot K_{eq}$	b
1300	$HCHO + OH \rightarrow CH_3O + O$	$k_{rev} \cdot K_{eq}$	b
1301	$HCHO + HO_2 \rightarrow CH_3O + O_2$	$k_{rev} \cdot K_{eq}$	b
1302	$CH_2OH + OH \rightarrow CH_3OH + O$	$k_{rev} \cdot K_{eq}$	b
1303	$CH_3O + O_2 \rightarrow CH_3OO + O$	$k_{rev} \cdot K_{eq}$	b
1304	$CH_4 + CO \rightarrow CH_3 + HCO$	$k_{rev} \cdot K_{eq}$	b
1305	$CH_3 + CO \rightarrow CH_2 + HCO$	$k_{rev} \cdot K_{eq}$	b

#	Reaction	Rate equation	Ref.
1306	$CH_2CO + H_2O \rightarrow CH_3 + COOH$	$k_{rev} \cdot K_{eq}$	b
1307	$CH_4 + CO_2 \rightarrow CH_3 + COOH$	$k_{rev} \cdot K_{eq}$	b
1308	$CH_3 + HCO \rightarrow CH_2 + HCHO$	$k_{rev} \cdot K_{eq}$	b
1309	$CH_2CO + H \rightarrow CH + HCHO$	$k_{rev} \cdot K_{eq}$	b
1310	$CH_4 + HCHO \rightarrow CH_3 + CH_3O$	$k_{rev} \cdot K_{eq}$	b
1311	$CH_3 + HCHO \rightarrow CH_2 + CH_3O$	$k_{rev} \cdot K_{eq}$	b
1312	$CH_4 + HCHO \rightarrow CH_2OH + CH_3$	$k_{rev} \cdot K_{eq}$	b
1313	$C_2H_4 + OH \rightarrow CH_2 + CH_2OH$	$k_{rev} \cdot K_{eq}$	b
1314	$CH_3 + HCHO \rightarrow CH_2 + CH_2OH$	$k_{rev} \cdot K_{eq}$	b
1315	$CH_2OH + CH_3 \rightarrow CH_2 + CH_3OH$	$k_{rev} \cdot K_{eq}$	b
1316	$CH_3 + CH_3O \rightarrow CH_2 + CH_3OH$	$k_{rev} \cdot K_{eq}$	b
1317	$CH_3 + CH_3OOH \rightarrow CH_3OO + CH_4$	$k_{rev} \cdot K_{eq}$	b
1318	$CH_3O + CH_3O \rightarrow CH_3 + CH_3OO$	$k_{rev} \cdot K_{eq}$	b
1319	$CH_3O + HCHO \rightarrow CH_2 + CH_3OO$	$k_{rev} \cdot K_{eq}$	b
1320	$C_2H_5 + O_2 \rightarrow CH_2 + CH_3OO$	$k_{rev} \cdot K_{eq}$	b
1321	$CO + HCHO \rightarrow HCO + HCO$	$k_{rev} \cdot K_{eq}$	b
1322	$CH_3OH + CO \rightarrow CH_3O + HCO$	$k_{rev} \cdot K_{eq}$	b
1323	$CH_3OH + CO \rightarrow CH_2OH + HCO$	$k_{rev} \cdot K_{eq}$	b
1324	$HCHO + HCHO \rightarrow CH_2OH + HCO$	$k_{rev} \cdot K_{eq}$	b
1325	$CH_3OH + HCHO \rightarrow CH_3O + CH_3O$	$k_{rev} \cdot K_{eq}$	b
1326	$CH_3OH + HCHO \rightarrow CH_2OH + CH_3O$	$k_{rev} \cdot K_{eq}$	b
1327	$CH_3OH + HCHO \rightarrow CH_2OH + CH_2OH$	$k_{rev} \cdot K_{eq}$	b
1328	$CH_3OOH + HCHO \rightarrow CH_3O + CH_3OO$	$k_{rev} \cdot K_{eq}$	b
1329	$CH_2OH + CH_3OOH \rightarrow CH_3OH + CH_3OO$	$k_{rev} \cdot K_{eq}$	b
1330	$CH_3O + CH_3OOH \rightarrow CH_3OH + CH_3OO$	$k_{rev} \cdot K_{eq}$	b
1331	$CH_3OOH + HCHO \rightarrow CH_2OH + CH_3OO$	$k_{rev} \cdot K_{eq}$	b
1332	$CH_3OH + HCOOH \rightarrow CH_2OH + CH_3OO$	$k_{rev} \cdot K_{eq}$	b
1333	$CH_3OOH + HCO \rightarrow CH_3OO + HCHO$	$k_{rev} \cdot K_{eq}$	b
1334	$C_2H_4 + H_2O \rightarrow C_2H_5 + OH$	$k_{rev} \cdot K_{eq}$	b
1335	$C_2H_4 + H_2O_2 \rightarrow C_2H_5 + HO_2$	$k_{rev} \cdot K_{eq}$	b
1336	$CH_3 + HCHO \rightarrow C_2H_4 + OH$	$k_{rev} \cdot K_{eq}$	b
1337	$CH_3CHO + H \rightarrow C_2H_4 + OH$	$k_{rev} \cdot K_{eq}$	b
1338	$CH_3 + HCO \rightarrow C_2H_3 + OH$	$k_{rev} \cdot K_{eq}$	b
1339	$CH_3CO + H \rightarrow C_2H_3 + OH$	$k_{rev} \cdot K_{eq}$	b
1340	$C_2H_2 + H_2O \rightarrow C_2H_3 + OH$	$k_{rev} \cdot K_{eq}$	b
1341	$CH_2CO + H_2 \rightarrow C_2H_3 + OH$	$k_{rev} \cdot K_{eq}$	b
1342	$CH_4 + CO \rightarrow C_2H_3 + OH$	$k_{rev} \cdot K_{eq}$	b
1343	$C_2H_4 + OH \rightarrow C_2H_3 + H_2O$	$k_{rev} \cdot K_{eq}$	b
1344	$C_2H_4 + HO_2 \rightarrow C_2H_3 + H_2O_2$	$k_{rev} \cdot K_{eq}$	b
1345	$CH_2CO + H \rightarrow C_2H_2 + OH$	$k_{rev} \cdot K_{eq}$	b

#	Reaction	Rate equation	Ref.
1346	$C_2H_2 + O \rightarrow C_2H + OH$	$k_{rev} \cdot K_{eq}$	b
1347	$CH_2 + CO \rightarrow C_2H + OH$	$k_{rev} \cdot K_{eq}$	b
1348	$C_2H_2 + O_2 \rightarrow C_2H + HO_2$	$k_{rev} \cdot K_{eq}$	b
1349	$HCCO + OH \rightarrow C_2H + HO_2$	$k_{rev} \cdot K_{eq}$	b
1350	$CH_3CHO + H \rightarrow C_2H_5 + O$	$k_{rev} \cdot K_{eq}$	b
1351	$CH_3 + HCHO \rightarrow C_2H_5 + O$	$k_{rev} \cdot K_{eq}$	b
1352	$C_2H_4 + OH \rightarrow C_2H_5 + O$	$k_{rev} \cdot K_{eq}$	b
1353	$CH_3 + HCO \rightarrow C_2H_4 + O$	$k_{rev} \cdot K_{eq}$	b
1354	$CH_2CO + H_2 \rightarrow C_2H_4 + O$	$k_{rev} \cdot K_{eq}$	b
1355	$C_2H_3 + HO_2 \rightarrow C_2H_4 + O_2$	$k_{rev} \cdot K_{eq}$	b
1356	$C_2H_2 + OH \rightarrow C_2H_3 + O$	$k_{rev} \cdot K_{eq}$	b
1357	$CH_3 + CO \rightarrow C_2H_3 + O$	$k_{rev} \cdot K_{eq}$	b
1358	$CH_2 + HCO \rightarrow C_2H_3 + O$	$k_{rev} \cdot K_{eq}$	b
1359	$HCHO + HCO \rightarrow C_2H_3 + O_2$	$k_{rev} \cdot K_{eq}$	b
1360	$CH_2 + CO \rightarrow C_2H_2 + O$	$k_{rev} \cdot K_{eq}$	b
1361	$H + HCCO \rightarrow C_2H_2 + O$	$k_{rev} \cdot K_{eq}$	b
1362	$HCO + HCO \rightarrow C_2H_2 + O_2$	$k_{rev} \cdot K_{eq}$	b
1363	$CH + CO \rightarrow C_2H + O$	$k_{rev} \cdot K_{eq}$	b
1364	$CO + HCO \rightarrow C_2H + O_2$	$k_{rev} \cdot K_{eq}$	b
1365	$CH + CO_2 \rightarrow C_2H + O_2$	$k_{rev} \cdot K_{eq}$	b
1366	$C_2H_5 + CH_3OOH \rightarrow C_2H_6 + CH_3OO$	$k_{rev} \cdot K_{eq}$	b
1367	$C_2H_6 + CO \rightarrow C_2H_5 + HCO$	$k_{rev} \cdot K_{eq}$	b
1368	$C_2H_6 + HCHO \rightarrow C_2H_5 + CH_3O$	$k_{rev} \cdot K_{eq}$	b
1369	$C_2H_4 + CH_3OH \rightarrow C_2H_5 + CH_2OH$	$k_{rev} \cdot K_{eq}$	b
1370	$C_2H_6 + HCHO \rightarrow C_2H_5 + CH_2OH$	$k_{rev} \cdot K_{eq}$	b
1371	$CH_3CH_2O + CH_3O \rightarrow C_2H_5 + CH_3OO$	$k_{rev} \cdot K_{eq}$	b
1372	$C_2H_5 + CO_2 \rightarrow C_2H_4 + COOH$	$k_{rev} \cdot K_{eq}$	b
1373	$C_2H_5 + HCHO \rightarrow C_2H_4 + CH_2OH$	$k_{rev} \cdot K_{eq}$	b
1374	$C_2H_4 + HCO \rightarrow C_2H_3 + HCHO$	$k_{rev} \cdot K_{eq}$	b
1375	$C_2H_4 + HCHO \rightarrow C_2H_3 + CH_3O$	$k_{rev} \cdot K_{eq}$	b
1376	$C_2H_4 + HCHO \rightarrow C_2H_3 + CH_2OH$	$k_{rev} \cdot K_{eq}$	b
1377	$C_2H_4 + CH_2OH \rightarrow C_2H_3 + CH_3OH$	$k_{rev} \cdot K_{eq}$	b
1378	$C_2H_4 + CH_3O \rightarrow C_2H_3 + CH_3OH$	$k_{rev} \cdot K_{eq}$	b
1379	$C_2H_3 + CO_2 \rightarrow C_2H_2 + COOH$	$k_{rev} \cdot K_{eq}$	b
1380	$C_2H_3 + HCHO \rightarrow C_2H_2 + CH_2OH$	$k_{rev} \cdot K_{eq}$	b
1381	$C_2H_2 + HCHO \rightarrow C_2H + CH_3O$	$k_{rev} \cdot K_{eq}$	b
1382	$C_2H_2 + HCHO \rightarrow C_2H + CH_2OH$	$k_{rev} \cdot K_{eq}$	b
1383	$C_2H_2 + CH_2OH \rightarrow C_2H + CH_3OH$	$k_{rev} \cdot K_{eq}$	b
1384	$C_2H_2 + CH_3O \rightarrow C_2H + CH_3OH$	$k_{rev} \cdot K_{eq}$	b
1385	$CH_3O + HCCO \rightarrow C_2H + CH_3OO$	$k_{rev} \cdot K_{eq}$	b

#	Reaction	Rate equation	Ref.
1386	$CH_2 + CO \rightarrow H + HCCO$	$k_{rev} \cdot K_{eq}$	b
1387	$CH_3 + CO \rightarrow CH_2CO + H$	$k_{rev} \cdot K_{eq}$	b
1388	$H_2 + HCCO \rightarrow CH_2CO + H$	$k_{rev} \cdot K_{eq}$	b
1389	$CH_3 + HCO \rightarrow CH_3CO + H$	$k_{rev} \cdot K_{eq}$	b
1390	$CH_2CO + H_2 \rightarrow CH_3CO + H$	$k_{rev} \cdot K_{eq}$	b
1391	$CH_2OH + CH_3 \rightarrow CH_3CH_2O + H$	$k_{rev} \cdot K_{eq}$	b
1392	$CH_3CH_2OH \rightarrow CH_3CH_2O + H$	$k_{rev} \cdot K_{eq}$	b
1393	$C_2H_5 + OH \rightarrow CH_3CH_2O + H$	$k_{rev} \cdot K_{eq}$	b
1394	$C_2H_4 + H_2O \rightarrow CH_3CH_2O + H$	$k_{rev} \cdot K_{eq}$	b
1395	$CH_3CHO + H_2 \rightarrow CH_3CH_2O + H$	$k_{rev} \cdot K_{eq}$	b
1396	$CH_4 + HCHO \rightarrow CH_3CH_2O + H$	$k_{rev} \cdot K_{eq}$	b
1397	$CH_3CH_2OH \rightarrow CH_3CHOH + H$	$k_{rev} \cdot K_{eq}$	b
1398	$CH_2OH + CH_3 \rightarrow CH_3CHOH + H$	$k_{rev} \cdot K_{eq}$	b
1399	$C_2H_5 + OH \rightarrow CH_3CHOH + H$	$k_{rev} \cdot K_{eq}$	b
1400	$C_2H_4 + H_2O \rightarrow CH_3CHOH + H$	$k_{rev} \cdot K_{eq}$	b
1401	$CH_3CHO + H_2 \rightarrow CH_3CHOH + H$	$k_{rev} \cdot K_{eq}$	b
1402	$CH_4 + HCHO \rightarrow CH_3CHOH + H$	$k_{rev} \cdot K_{eq}$	b
1403	$C_2H_5 + H_2O \rightarrow CH_3CH_2OH + H$	$k_{rev} \cdot K_{eq}$	b
1404	$CH_3CHOH + H_2 \rightarrow CH_3CH_2OH + H$	$k_{rev} \cdot K_{eq}$	b
1405	$CH_2CH_2OH + H_2 \rightarrow CH_3CH_2OH + H$	$k_{rev} \cdot K_{eq}$	b
1406	$CH_3CH_2O + H_2 \rightarrow CH_3CH_2OH + H$	$k_{rev} \cdot K_{eq}$	b
1407	$CH_2OH + CO \rightarrow CH_2CO + OH$	$k_{rev} \cdot K_{eq}$	b
1408	$H_2O + HCCO \rightarrow CH_2CO + OH$	$k_{rev} \cdot K_{eq}$	b
1409	$HCHO + HCO \rightarrow CH_2CO + OH$	$k_{rev} \cdot K_{eq}$	b
1410	$CH_3 + CO_2 \rightarrow CH_2CO + OH$	$k_{rev} \cdot K_{eq}$	b
1411	$CH_2CO + H_2O \rightarrow CH_3CO + OH$	$k_{rev} \cdot K_{eq}$	b
1412	$CH_3CO + H_2O \rightarrow CH_3CHO + OH$	$k_{rev} \cdot K_{eq}$	b
1413	$CH_3 + HCOOH \rightarrow CH_3CHO + OH$	$k_{rev} \cdot K_{eq}$	b
1414	$CH_3COOH + H \rightarrow CH_3CHO + OH$	$k_{rev} \cdot K_{eq}$	b
1415	$CH_2CH_2OH + H_2O \rightarrow CH_3CH_2OH + OH$	$k_{rev} \cdot K_{eq}$	b
1416	$CH_3CHOH + H_2O \rightarrow CH_3CH_2OH + OH$	$k_{rev} \cdot K_{eq}$	b
1417	$CH_3CH_2O + H_2O \rightarrow CH_3CH_2OH + OH$	$k_{rev} \cdot K_{eq}$	b
1418	$CH_3CHOH + H_2O_2 \rightarrow CH_3CH_2OH + HO_2$	$k_{rev} \cdot K_{eq}$	b
1419	$CH + CO_2 \rightarrow HCCO + O$	$k_{rev} \cdot K_{eq}$	b
1420	$CO + HCHO \rightarrow CH_2CO + O$	$k_{rev} \cdot K_{eq}$	b
1421	$HCO + HCO \rightarrow CH_2CO + O$	$k_{rev} \cdot K_{eq}$	b
1422	$CH_2 + CO_2 \rightarrow CH_2CO + O$	$k_{rev} \cdot K_{eq}$	b
1423	$CH_2CO + OH \rightarrow CH_3CO + O$	$k_{rev} \cdot K_{eq}$	b
1424	$CH_3 + CO_2 \rightarrow CH_3CO + O$	$k_{rev} \cdot K_{eq}$	b
1425	$CH_3CO + OH \rightarrow CH_3CHO + O$	$k_{rev} \cdot K_{eq}$	b

#	Reaction	Rate equation	Ref.
1426	$CH_3CO + HO_2 \rightarrow CH_3CHO + O_2$	$k_{rev} \cdot K_{eq}$	b
1427	$CH_3CHO + HO_2 \rightarrow CH_3CH_2O + O_2$	$k_{rev} \cdot K_{eq}$	b
1428	$CH_3 + HCOOH \rightarrow CH_3CHOH + O$	$k_{rev} \cdot K_{eq}$	b
1429	$CH_3CHO + OH \rightarrow CH_3CHOH + O$	$k_{rev} \cdot K_{eq}$	b
1430	$CH_3COOH + H \rightarrow CH_3CHOH + O$	$k_{rev} \cdot K_{eq}$	b
1431	$CH_3CHO + HO_2 \rightarrow CH_3CHOH + O_2$	$k_{rev} \cdot K_{eq}$	b
1432	$CH_2OH + HCHO \rightarrow CH_2CH_2OH + O$	$k_{rev} \cdot K_{eq}$	b
1433	$CH_3CHOH + OH \rightarrow CH_3CH_2OH + O$	$k_{rev} \cdot K_{eq}$	b
1434	$CH_2CH_2OH + OH \rightarrow CH_3CH_2OH + O$	$k_{rev} \cdot K_{eq}$	b
1435	$CH_3CH_2O + OH \rightarrow CH_3CH_2OH + O$	$k_{rev} \cdot K_{eq}$	b
1436	$CH_3CHOH + HO_2 \rightarrow CH_3CH_2OH + O_2$	$k_{rev} \cdot K_{eq}$	b
1437	$CH_2CH_2OH + HO_2 \rightarrow CH_3CH_2OH + O_2$	$k_{rev} \cdot K_{eq}$	b
1438	$CH_3CH_2O + HO_2 \rightarrow CH_3CH_2OH + O_2$	$k_{rev} \cdot K_{eq}$	b
1439	$C_2H_5 + CO \rightarrow CH_2CO + CH_3$	$k_{rev} \cdot K_{eq}$	b
1440	$CH_4 + HCCO \rightarrow CH_2CO + CH_3$	$k_{rev} \cdot K_{eq}$	b
1441	$C_2H_4 + CO \rightarrow CH_2 + CH_2CO$	$k_{rev} \cdot K_{eq}$	b
1442	$CH_3 + HCCO \rightarrow CH_2 + CH_2CO$	$k_{rev} \cdot K_{eq}$	b
1443	$CH_2CO + CH_4 \rightarrow CH_3 + CH_3CO$	$k_{rev} \cdot K_{eq}$	b
1444	$CH_2CO + CH_3 \rightarrow CH_2 + CH_3CO$	$k_{rev} \cdot K_{eq}$	b
1445	$CH_3CHOH + CH_4 \rightarrow CH_3 + CH_3CH_2OH$	$k_{rev} \cdot K_{eq}$	b
1446	$CH_2CH_2OH + CH_4 \rightarrow CH_3 + CH_3CH_2OH$	$k_{rev} \cdot K_{eq}$	b
1447	$CH_3CH_2O + CH_4 \rightarrow CH_3 + CH_3CH_2OH$	$k_{rev} \cdot K_{eq}$	b
1448	$CH_3CHO + CO \rightarrow CH_3CO + HCO$	$k_{rev} \cdot K_{eq}$	b
1449	$CH_3CHO + HCO \rightarrow CH_3CO + HCHO$	$k_{rev} \cdot K_{eq}$	b
1450	$CH_2CO + CH_3OH \rightarrow CH_3CO + CH_3O$	$k_{rev} \cdot K_{eq}$	b
1451	$CH_3CHO + HCHO \rightarrow CH_3CO + CH_3O$	$k_{rev} \cdot K_{eq}$	b
1452	$CH_2OH + CH_3CHO \rightarrow CH_3CO + CH_3OH$	$k_{rev} \cdot K_{eq}$	b
1453	$CH_3CO + CH_3OH \rightarrow CH_3CHO + CH_3O$	$k_{rev} \cdot K_{eq}$	b
1454	$CH_3CO + CH_3OOH \rightarrow CH_3CHO + CH_3OO$	$k_{rev} \cdot K_{eq}$	b
1455	$CH_2CO + CH_3CHO \rightarrow CH_3CO + CH_3CO$	$k_{rev} \cdot K_{eq}$	b
1456	$CO + OH \rightarrow COOH$	$k_{rev} \cdot K_{eq}$	b
1457	$CO_2 + H \rightarrow COOH$	$k_{rev} \cdot K_{eq}$	b
1458	$H + HCO \rightarrow HCHO$	$k_{rev} \cdot K_{eq}$	b
1459	$H + HCHO \rightarrow CH_2OH$	$k_{rev} \cdot K_{eq}$	b
1460	$CH_2 + H_2O \rightarrow CH_3OH$	$k_{rev} \cdot K_{eq}$	b
1461	$CH_2OH + H \rightarrow CH_3OH$	$k_{rev} \cdot K_{eq}$	b
1462	$CH_3O + OH \rightarrow CH_3OOH$	$k_{rev} \cdot K_{eq}$	b
1463	$CH_3 + COOH \rightarrow CH_3COOH$	$k_{rev} \cdot K_{eq}$	b
1464	$CH_3 + HCHO \rightarrow CH_3CHOH$	$k_{rev} \cdot K_{eq}$	b
1465	$C_2H_4 + OH \rightarrow CH_2CH_2OH$	$k_{rev} \cdot K_{eq}$	b

#	Reaction	Rate equation	Ref.
1466	$CO + O \rightarrow C + O_2$	$k_{rev} \cdot K_{eq}$	b
1467	$CO_2 + O_2 \rightarrow CO + O_3$	$k_{rev} \cdot K_{eq}$	b
1468	$CO + CO \rightarrow C + CO_2$	$k_{rev} \cdot K_{eq}$	b

Constants:

$$N_A = 6.02214076 \times 10^{23} mol^{-1}$$

$$k_B = 1.38064852 \times 10^{-23} J/K$$

$$R = 8.31446261815324 JK^{-1} mol^{-1}$$

$$n_M = \text{total number density of neutral species } (cm^{-3})$$

Notes:

a falloff expression, Lindemann-Hinshelwood expression with broadening factor:

$$k = \frac{k_0[M]k_\infty}{k_0[M]+k_\infty} F; \log F = \frac{\log F_c}{1 + \left[ \frac{\log(k_0[M]/k_\infty)}{N} \right]^2}; N = 0.75 - 1.27 \log F_c$$

b reaction rate expression calculated from equilibrium constant and reverse reaction rate:

$$K_{eq} = e^{\left( \frac{-\Delta G_r}{RT} \right)} \cdot \left( \frac{p}{R \cdot T} \right)^{\Delta v}; p = 1 bar; \Delta v = \sum \mu_P - \sum \mu_R$$

c estimated: equal to  $O^- + M \rightarrow e + O + M$  [158]

d estimated: equal to  $O + O \rightarrow O_2^+ + e$  [163]

e estimated: equal to  $e + e + A^+ \rightarrow e + A$  [150]

f estimated: equal to  $e + A^+ + M \rightarrow A + M$  [150]

Cross sections reference list

Table S2: Cross sections reference list

#	Process	Type	Ref.
1	$C \rightarrow C$	<i>effective</i>	[148]
2	$C \rightarrow C(1D)(1.264eV)$	<i>excitation</i>	[148]
3	$C \rightarrow C(1S)(2.684eV)$	<i>excitation</i>	[148]
4	$CH \rightarrow CH$	<i>effective</i>	[148]
5	$CH_2 \rightarrow CH_2$	<i>effective</i>	[148]
6	$CH_3 \rightarrow CH_3$	<i>effective</i>	[148]
7	$CH_4 \rightarrow CH_4$	<i>elastic</i>	[24]
8	$CH_4 \rightarrow CH_4(V24)(0.162eV)$	<i>excitation</i>	[24]
9	$CH_4 \rightarrow CH_4(V13)(0.361eV)$	<i>excitation</i>	[24]
10	$C_2H_2 \rightarrow C_2H_2$	<i>elastic</i>	[175]
11	$C_2H_2 \rightarrow C_2H_2(v5)(0.09eV)$	<i>excitation</i>	[175]
12	$C_2H_2 \rightarrow C_2H_2(V2)(0.255eV)$	<i>excitation</i>	[175]
13	$C_2H_2 \rightarrow C_2H_2(V31)(0.407eV)$	<i>excitation</i>	[175]
14	$C_2H_2 \rightarrow C_2H_2 * (1.911ev)$	<i>excitation</i>	[175]
15	$C_2H_2 \rightarrow C_2H_2 * (5.089eV)$	<i>excitation</i>	[175]
16	$C_2H_2 \rightarrow C_2H_2 * (7.902eV)$	<i>excitation</i>	[175]
17	$C_2H_4 \rightarrow C_2H_4$	<i>elastic</i>	[175]
18	$C_2H_4 \rightarrow C_2H_4(V1)(0.11eV)$	<i>excitation</i>	[175]
19	$C_2H_4 \rightarrow C_2H_4(V2)(0.36eV)$	<i>excitation</i>	[175]
20	$C_2H_4 \rightarrow C_2H_4(3.8eV)$	<i>excitation</i>	[175]
21	$C_2H_4 \rightarrow C_2H_4(5eV)$	<i>excitation</i>	[175]

#	Process	Type	Ref.
22	$C_2H_4 \rightarrow C_2H_4(7eV)$	<i>excitation</i>	[175]
23	$C_2H_6 \rightarrow C_2H_6$	<i>elastic</i>	[175]
24	$C_2H_6 \rightarrow C_2H_6(V24)(0.16eV)$	<i>excitation</i>	[175]
25	$C_2H_6 \rightarrow C_2H_6(v13)(0.371eV)$	<i>excitation</i>	[175]
26	$C_2H_6 \rightarrow C_2H_6 * (7.53eV)$	<i>excitation</i>	[175]
27	$C_2H_6 \rightarrow C_2H_6 * (10.12eV)$	<i>excitation</i>	[175]
28	$CO \rightarrow CO$	<i>elastic</i>	[24]
29	$CO \rightarrow CO(J = 0 - J = 1)(0.000479992eV)$	<i>rotational</i>	[46]
30	$CO \rightarrow CO(J = 1 - J = 2)(0.000959985eV)$	<i>rotational</i>	[46]
31	$CO \rightarrow CO(J = 2 - J = 3)(0.00143998eV)$	<i>rotational</i>	[46]
32	$CO \rightarrow CO(J = 3 - J = 4)(0.00191997eV)$	<i>rotational</i>	[46]
33	$CO \rightarrow CO(J = 4 - J = 5)(0.00239996eV)$	<i>rotational</i>	[46]
34	$CO \rightarrow CO(J = 5 - J = 6)(0.00287995eV)$	<i>rotational</i>	[46]
35	$CO \rightarrow CO(J = 6 - J = 7)(0.00335995eV)$	<i>rotational</i>	[46]
36	$CO \rightarrow CO(J = 7 - J = 8)(0.00383994eV)$	<i>rotational</i>	[46]
37	$CO \rightarrow CO(J = 8 - J = 9)(0.00431993eV)$	<i>rotational</i>	[46]
38	$CO \rightarrow CO(J = 9 - J = 10)(0.00479992eV)$	<i>rotational</i>	[46]
39	$CO \rightarrow CO(J = 10 - J = 11)(0.00527992eV)$	<i>rotational</i>	[46]
40	$CO \rightarrow CO(J = 11 - J = 12)(0.00575991eV)$	<i>rotational</i>	[46]
41	$CO \rightarrow CO(J = 12 - J = 13)(0.0062399eV)$	<i>rotational</i>	[46]
42	$CO \rightarrow CO(J = 13 - J = 14)(0.00671989eV)$	<i>rotational</i>	[46]
43	$CO \rightarrow CO(J = 14 - J = 15)(0.00719989eV)$	<i>rotational</i>	[46]
44	$CO \rightarrow CO(J = 15 - J = 16)(0.00767988eV)$	<i>rotational</i>	[46]

#	Process	Type	Ref.
45	$CO \rightarrow CO(J = 16 - J = 17)(0.00815987eV)$	<i>rotational</i>	[46]
46	$CO \rightarrow CO(v0 - v1)(0.266eV)$	<i>excitation</i>	[24]
47	$CO \rightarrow CO(v0 - v2)(0.54eV)$	<i>excitation</i>	[24]
48	$CO \rightarrow CO(v0 - v3)(0.81eV)$	<i>excitation</i>	[24]
49	$CO \rightarrow CO(v0 - v4)(1.07eV)$	<i>excitation</i>	[24]
50	$CO \rightarrow CO(v0 - v5)(1.33eV)$	<i>excitation</i>	[24]
51	$CO \rightarrow CO(v0 - v6)(1.59eV)$	<i>excitation</i>	[24]
52	$CO \rightarrow CO(v0 - v7)(1.84eV)$	<i>excitation</i>	[24]
53	$CO \rightarrow CO(v0 - v8)(2.09eV)$	<i>excitation</i>	[24]
54	$CO \rightarrow CO(v0 - v9)(2.33eV)$	<i>excitation</i>	[24]
55	$CO \rightarrow CO(v0 - v10)(2.58eV)$	<i>excitation</i>	[24]
56	$CO \rightarrow CO(a3P)(6.006eV)$	<i>excitation</i>	[24]
57	$CO \rightarrow CO(a3Su+)(6.8eV)$	<i>excitation</i>	[24]
58	$CO \rightarrow CO(A1P)(8.024eV)$	<i>excitation</i>	[24]
59	$CO \rightarrow CO(b3Su+)(10.399eV)$	<i>excitation</i>	[24]
60	$CO \rightarrow CO(B1Su+)(10.777eV)$	<i>excitation</i>	[24]
61	$CO \rightarrow CO(C1Su+)(11.396eV)$	<i>excitation</i>	[24]
62	$CO \rightarrow CO(E1P)(11.524eV)$	<i>excitation</i>	[24]
63	$CO_2 \rightarrow CO_2$	<i>effective</i>	[24]
64	$CO_2 \rightarrow CO_2(v010)(0.083eV)$	<i>excitation</i>	[24]
65	$CO_2 \rightarrow CO_2(v020)(0.167eV)$	<i>excitation</i>	[24]
66	$CO_2 \rightarrow CO_2(v100)(0.167eV)$	<i>excitation</i>	[24]
67	$CO_2 \rightarrow CO_2(v030 + 110)(0.252eV)$	<i>excitation</i>	[24]

#	Process	Type	Ref.
68	$CO_2 \rightarrow CO_2(v001)(0.291eV)$	<i>excitation</i>	[24]
69	$CO_2 \rightarrow CO_2(v040 + 120 + 011)(0.339eV)$	<i>excitation</i>	[24]
70	$CO_2 \rightarrow CO_2(Xv200)(0.339eV)$	<i>excitation</i>	[24]
71	$CO_2 \rightarrow CO_2(Xv050 + 210 + 130 + 021 + 101)(0.422eV)$	<i>excitation</i>	[24]
72	$CO_2 \rightarrow CO_2(Xv300)(0.5eV)$	<i>excitation</i>	[24]
73	$CO_2 \rightarrow CO_2(Xv060 + 220 + 140)(0.505eV)$	<i>excitation</i>	[24]
74	$CO_2 \rightarrow CO_2(Xv0n0 + n00)(2.5eV)$	<i>excitation</i>	[24]
75	$CO_2 \rightarrow CO_2(e1)(7eV)$	<i>excitation</i>	[24]
76	$CO_2 \rightarrow CO_2(e2)(10.5eV)$	<i>excitation</i>	[24]
77	$H \rightarrow H$	<i>elastic</i>	[24]
78	$H \rightarrow H(1p)(10.21eV)$	<i>excitation</i>	[24]
79	$H \rightarrow H(2s)(10.21eV)$	<i>excitation</i>	[24]
80	$H \rightarrow H(3)(12.11eV)$	<i>excitation</i>	[24]
81	$H \rightarrow H(4)(12.76eV)$	<i>excitation</i>	[24]
82	$H \rightarrow H(5)(13.11eV)$	<i>excitation</i>	[24]
83	$H_2 \rightarrow H_2$	<i>elastic</i>	[24]
84	$H_2 \rightarrow H_2(J = 0 - J = 2)(0.044eV)$	<i>rotational</i>	[46]
85	$H_2 \rightarrow H_2(J = 1 - J = 3)(0.073eV)$	<i>rotational</i>	[46]
86	$H_2 \rightarrow H_2(J = 2 - J = 4)(0.1eV)$	<i>rotational</i>	[46]
87	$H_2 \rightarrow H_2(J = 3 - J = 5)(0.12eV)$	<i>rotational</i>	[46]
88	$H_2 \rightarrow H_2(v0 - v1)(0.516eV)$	<i>excitation</i>	[24]
89	$H_2 \rightarrow H_2(v0 - v2)(1eV)$	<i>excitation</i>	[24]
90	$H_2 \rightarrow H_2(v0 - v3)(1.5eV)$	<i>excitation</i>	[24]

#	Process	Type	Ref.
91	$H_2 \rightarrow H_2(b3Su)(8.9eV)$	<i>excitation</i>	[24]
92	$H_2 \rightarrow H_2(B1Su)(11.4eV)$	<i>excitation</i>	[24]
93	$H_2 \rightarrow H_2(c3Pu)(11.75eV)$	<i>excitation</i>	[24]
94	$H_2 \rightarrow H_2(a3Sg)(11.8eV)$	<i>excitation</i>	[24]
95	$H_2 \rightarrow H_2(C1Pu)(12.4eV)$	<i>excitation</i>	[24]
96	$H_2 \rightarrow H_2(E1Sg, F1Sg)(12.4eV)$	<i>excitation</i>	[24]
97	$H_2 \rightarrow H_2(e3Su)(13.4eV)$	<i>excitation</i>	[24]
98	$H_2 \rightarrow H_2(B1Su)(13.8eV)$	<i>excitation</i>	[24]
99	$H_2 \rightarrow H_2(D1Pu)(14eV)$	<i>excitation</i>	[24]
100	$H_2 \rightarrow H_2(B1Su)(14.6eV)$	<i>excitation</i>	[24]
101	$H_2 \rightarrow H_2(D1Pu)(14.6eV)$	<i>excitation</i>	[24]
102	$H_2O \rightarrow H_2O$	<i>elastic</i>	[46]
103	$H_2O \rightarrow H_2O(R)(0.04eV)$	<i>excitation</i>	[46]
104	$H_2O \rightarrow H_2O(VA)(0.198eV)$	<i>excitation</i>	[46]
105	$H_2O \rightarrow H_2O(V1)(0.453eV)$	<i>excitation</i>	[46]
106	$O \rightarrow O$	<i>elastic</i>	[24]
107	$O \rightarrow O(1D)(1.96eV)$	<i>excitation</i>	[24]
108	$O \rightarrow O(1S)(4.18eV)$	<i>excitation</i>	[24]
109	$O \rightarrow O(4S0)(9.2eV)$	<i>excitation</i>	[24]
110	$O \rightarrow O(2D0)(12.5eV)$	<i>excitation</i>	[24]
111	$O \rightarrow O(2P0)(14.1eV)$	<i>excitation</i>	[24]
112	$O \rightarrow O(3P0)(15.7eV)$	<i>excitation</i>	[24]
113	$O_2 \rightarrow O_2$	<i>effective</i>	[24]

#	Process	Type	Ref.
114	$O_2 \rightarrow O_2(v0 - v1)(0.19eV)$	<i>excitation</i>	[24]
115	$O_2 \rightarrow O_2(v0 - v2)(0.38eV)$	<i>excitation</i>	[24]
116	$O_2 \rightarrow O_2(v0 - v3)(0.6eV)$	<i>excitation</i>	[24]
117	$O_2 \rightarrow O_2(v0 - v4)(0.8eV)$	<i>excitation</i>	[24]
118	$O_2 \rightarrow O_2(a1Dg)(0.977eV)$	<i>excitation</i>	[24]
119	$O_2 \rightarrow O_2(b1Sg+)(1.627eV)$	<i>excitation</i>	[24]
120	$O_2 \rightarrow O_2(A3Su+, C3Du, c1Su-)(4.5eV)$	<i>excitation</i>	[24]
121	$O_2 \rightarrow O_2(9.97eV)$	<i>excitation</i>	[24]
122	$O_2 \rightarrow O_2(14.7eV)$	<i>excitation</i>	[24]
123	$O_3 \rightarrow O_3$	<i>effective</i>	[148]

Table S3: Overview of estimated power density from various literature sources. The plasma volume is not specifically measured in these sources and therefore, we could only make a rough estimate of the power density. Despite some outliers above  $1500 \text{ W cm}^{-3}$ , our chosen power density values ( $500$ ,  $1000$  and  $1500 \text{ W cm}^{-3}$ ) provide good coverage of this literature data.

Plasma	Power (W)	Volume ( $\text{cm}^{-3}$ )	Power density ( $\text{W cm}^{-3}$ )	Ref.
GAP	500	0.37	1351	[176]
GAP	224	0.383	585	[177]
GAP	225 – 475	0.13	1731 – 3653	[178]
APGD	90 – 160	0.43 <sup>a</sup>	209 – 372	[179]
cAPGD	100	0.43 <sup>a</sup>	233	[179]
cAPGD	80 – 125 <sup>b</sup>	0.43 <sup>a</sup>	186 – 291	[180]
GAP	349 – 472	0.14 <sup>a</sup>	2415 – 3266	[181]
MW	900 – 1400	1.08 – 2.19 <sup>a</sup>	639 – 833	[182]
MW	550 – 700	0.71 <sup>a</sup>	772 – 982	[183]
GA	1300	0.68 <sup>a</sup>	1916	[184]
GA	1000	0.75 <sup>a</sup>	1326	[185]

<sup>a</sup> Estimated based on the reactor geometry

<sup>b</sup> Estimated from figures

## References

- (1) S. S. Prasad and J. H. W. T., 1980, **43**, 1, DOI: 10.1086/190665.
- (2) N. Harada and E. Herbst, 2008, **685**, 272–280, DOI: 10.1086/590468.
- (3) D. McElroy, C. Walsh, A. J. Markwick, M. A. Cordiner, K. Smith and T. J. Millar, *Astronomy and Astrophysics*, 2013, **550**, A36, DOI: 10.1051/0004-6361/201220465.
- (4) M. J. Rabinowitz, J. W. Sutherland, P. M. Patterson and R. B. Klemm, *The Journal of Physical Chemistry*, 1991, **95**, 674–681, DOI: 10.1021/j100155a033.
- (5) D. L. Baulch, C. T. Bowman, C. J. Cobos, R. A. Cox, T. Just, J. A. Kerr, M. J. Pilling, D. Stocker, J. Troe, W. Tsang, R. W. Walker and J. Warnatz, 2005, **34**, 757–1397, DOI: 10.1063/1.1748524.
- (6) K.-W. Lu, H. Matsui, C.-L. Huang, P. Raghunath, N.-S. Wang and M. C. Lin, 2010, **114**, 5493–5502, DOI: 10.1021/jp100535r.
- (7) J. K. Kim and W. T. Huntress, 1975, **62**, 2820–2825, DOI: 10.1063/1.430817.
- (8) M. J. McEwan, G. B. I. Scott, N. G. Adams, L. M. Babcock, R. Terzieva and E. Herbst, *The Astrophysical Journal*, 1999, **513**, 287–293, DOI: 10.1086/306861.
- (9) N. Adams and D. Smith, *Chemical Physics Letters*, 1977, **47**, 383–387, DOI: 10.1016/0009-2614(77)80043-2.
- (10) W. Braun, A. M. Bass, D. D. Davis, J. D. Simmons, G. Porter and M. J. Lighthill, *Proceedings of the Royal Society of London. A. Mathematical and Physical Sciences*, 1969, **312**, 417–434, DOI: 10.1098/rspa.1969.0168.
- (11) A. J. Dean and R. K. Hanson, 1992, **24**, 517–532, DOI: 10.1002/kin.550240602.
- (12) J. Oscar Martinez, N. B. Betts, S. M. Villano, N. Eyet, T. P. Snow and V. M. Bierbaum, 2008, **686**, 1486–1492, DOI: 10.1086/591548.
- (13) C. M. Leung, E. Herbst and W. F. Huebner, 1984, **56**, 231, DOI: 10.1086/190982.
- (14) K. Tabayashi and S. Bauer, 1979, **34**, 63–83, DOI: 10.1016/0010-2180(79)90079-8.
- (15) T. Bohland, S. Dobe, F. Temps and H. G. Wagner, 1985, **89**, 1110–1116, DOI: 10.1002/bbpc.19850891018.
- (16) P. Han, K. Su, Y. Liu, Y. Wang, X. Wang, Q. Zeng, L. Cheng and L. Zhang, 2011, **32**, 2745–2755, DOI: 10.1002/jcc.21854.
- (17) S. Bauerle, M. Klatt and H. G. G. Wagner, 1995, **99**, 870–879, DOI: 10.1002/bbpc.19950990612.
- (18) W. Braun, J. R. McNesby and A. M. Bass, 1967, **46**, 2071–2080, DOI: 10.1063/1.1841003.
- (19) H. Tahara, K. ichiro Minami, A. Murai, T. Yasui and T. Y. T. Yoshikawa, *Japanese Journal of Applied Physics*, 1995, **34**, 1972, DOI: 10.1143/jjap.34.1972.
- (20) D. Smith and N. Adams, 1978, **54**, 535–540, DOI: 10.1016/0009-2614(78)85279-8.
- (21) K Tachibana, M Nishida, H Harima and Y Urano, *Journal of Physics D: Applied Physics*, 1984, **17**, 1727–1742, DOI: 10.1088/0022-3727/17/8/026.
- (22) R. K. Janev and D. Reiter, 2002, **9**, 4071–4081, DOI: 10.1063/1.1500735.
- (23) D. Reiter and R. K. Janev, *Contributions to Plasma Physics*, 2010, **50**, 986–1013, DOI: 10.1002/ctpp.201000090.
- (24) Obtained from LXCAT (IST-Lisbon database), www.lxcat.net.
- (25) W. Tsang and R. F. Hampson, 1986, **15**, 1087–1279, DOI: 10.1063/1.555759.
- (26) V. D. Knyazev, A. Bencsura, S. I. Stolarov and I. R. Slagle, *The Journal of Physical Chemistry*, 1996, **100**, 11346–11354, DOI: 10.1021/jp9606568.
- (27) V. G. Anicich, 1993, **22**, 1469–1569, DOI: 10.1063/1.555940.
- (28) G. I. Mackay, H. I. Schiff and D. K. Bohme, 1981, **59**, 1771–1778, DOI: 10.1139/v81-265.
- (29) D. Smith, P. Spaniel and C. A. Mayhew, 1992, **117**, 457–473, DOI: 10.1016/0168-1176(92)80108-d.
- (30) J. Kim, L. Theard and W. Huntress, *International Journal of Mass Spectrometry and Ion Physics*, 1974, **15**, 223–244, DOI: 10.1016/0020-7381(74)85001-1.
- (31) V. G. Anicich, J. H. Futrell, W. T. Huntress and J. Kim, *International Journal of Mass Spectrometry and Ion Physics*, 1975, **18**, 63–64, DOI: 10.1016/0020-7381(75)87007-0.

- (32) M. Mandal, S. Ghosh and B. Maiti, *The Journal of Physical Chemistry A*, 2018, **122**, 3556–3562, DOI: 10.1021/acs.jpca.8b01386.
- (33) A. Bergeat and J.-C. Loison, *Physical Chemistry Chemical Physics*, 2001, **3**, 2038–2042, DOI: 10.1039/b100656h.
- (34) N. Galland, F. Caralp, Y. Hannachi, A. Bergeat and J.-C. Loison, *The Journal of Physical Chemistry A*, 2003, **107**, 5419–5426, DOI: 10.1021/jp027465r.
- (35) Y. Ge, M. S. Gordon, F. Battaglia and R. O. Fox, *The Journal of Physical Chemistry A*, 2010, **114**, 2384–2392, DOI: 10.1021/jp911673h.
- (36) S. I. Stoliarov, V. D. Knyazev and I. R. Slagle, *The Journal of Physical Chemistry A*, 2000, **104**, 9687–9697, DOI: 10.1021/jp992476e.
- (37) A. Fiaux, D. Smith and J. Futrell, *International Journal of Mass Spectrometry and Ion Physics*, 1974, **15**, 9–21, DOI: 10.1016/0020-7381(74)80082-3.
- (38) G. I. Mackay, K. Tanaka and D. K. Bohme, 1977, **24**, 125–136, DOI: 10.1016/0020-7381(77)80020-x.
- (39) J. K. Kim, V. G. Anicich and W. T. Huntress, *The Journal of Physical Chemistry*, 1977, **81**, 1798–1805, DOI: 10.1021/j100534a002.
- (40) T. Ibuki and Y. Takezaki, *Bulletin of the Chemical Society of Japan*, 1975, **48**, 769–773, DOI: 10.1246/bcsj.48.769.
- (41) A. Fahr and D. C. Tardy, *The Journal of Physical Chemistry A*, 2002, **106**, 11135–11140, DOI: 10.1021/jp021497x.
- (42) M. R. Dash and B. Rajakumar, *Physical Chemistry Chemical Physics*, 2015, **17**, 3142–3156, DOI: 10.1039/c4cp04677c.
- (43) R. K. Janev and D. Reiter, *Physics of Plasmas*, 2004, **11**, 780–829, DOI: 10.1063/1.1630794.
- (44) P. Stewart, C. Larson and D. Golden, *Combustion and Flame*, 1989, **75**, 25–31, DOI: 10.1016/0010-2180(89)90084-9.
- (45) A. M. Dean, *The Journal of Physical Chemistry*, 1985, **89**, 4600–4608, DOI: 10.1021/j100267a038.
- (46) C Verheyen, T Silva, V Guerra and A Bogaerts, *Plasma Sources Science and Technology*, 2020, **29**, 095009, DOI: 10.1088/1361-6595/aba1c8.
- (47) Y. Itikawa and N. Mason, *Journal of Physical and Chemical Reference Data*, 2005, **34**, 1–22, DOI: 10.1063/1.1799251.
- (48) Obtained from LXCAT (TRINITI database), www.lxcat.net.
- (49) D. Nandi, E. Krishnakumar, A. Rosa, W.-F. Schmidt and E. Illenberger, *Chemical Physics Letters*, 2003, **373**, 454–459, DOI: 10.1016/s0009-2614(03)00622-5.
- (50) R. Riahi, P. Teulet, Z. B. Lakhdar and A. Gleizes, *The European Physical Journal D*, 2006, **40**, 223–230, DOI: 10.1140/epjd/e2006-00159-2.
- (51) S. D. T. Axford and A. N. Hayhurst, *Proc. R. Soc. A: Math. Phys. Eng. Sci.*, 1996, **452**, 1007–1033, DOI: 10.1098/rspa.1996.0051.
- (52) M. Capitelli, C. M. Ferreira, B. F. Gordiets and A. I. Osipov, Springer Berlin Heidelberg, 2000, DOI: 10.1007/978-3-662-04158-1.
- (53) S. P. Karkach and V. I. Osherov, *The Journal of Chemical Physics*, 1999, **110**, 11918–11927, DOI: 10.1063/1.479131.
- (54) R. Atkinson, D. L. Baulch, R. A. Cox, J. N. Crowley, R. F. Hampson, R. G. Hynes, M. E. Jenkin, M. J. Rossi and J. Troe, *Atmospheric Chemistry and Physics*, 2004, **4**, 1461–1738, DOI: 10.5194/acp-4-1461-2004.
- (55) E. E. Ferguson, *Atomic Data and Nuclear Data Tables*, 1973, **12**, 159–178, DOI: 10.1016/0092-640x(73)90017-x.
- (56) D. Albritton, *Atomic Data and Nuclear Data Tables*, 1978, **22**, 1–89, DOI: 10.1016/0092-640x(78)90027-x.
- (57) W. V. Gaens and A Bogaerts, *Journal of Physics D: Applied Physics*, 2013, **46**, 275201, DOI: 10.1088/0022-3727/46/27/275201.
- (58) D. L. Baulch, C. J. Cobos, R. A. Cox, P. Frank, G. Hayman, T. Just, J. A. Kerr, T. Murrells, M. J. Pilling, J. Troe, R. W. Walker and J. Warnatz, *Journal of Physical and Chemical Reference Data*, 1994, **23**, 847–848, DOI: 10.1063/1.555953.

- (59) R. Atkinson, D. L. Baulch, R. A. Cox, R. F. Hampson, J. A. K. (Chairman) and J. Troe, *Journal of Physical and Chemical Reference Data*, 1989, **18**, 881–1097, DOI: 10.1063/1.555832.
- (60) T. Murakami, K. Niemi, T. Gans, D. O. Connell and W. G. Graham, *Plasma Sources Science and Technology*, 2012, **22**, 015003, DOI: 10.1088/0963-0252/22/1/015003.
- (61) A. B. Rakshit and P. Warneck, 1980, **76**, 1084, DOI: 10.1039/f29807601084.
- (62) N. Harada, E. Herbst and V. Wakelam, *The Astrophysical Journal*, 2010, **721**, 1570–1578, DOI: 10.1088/0004-637x/721/2/1570.
- (63) C. J. Howard and B. J. Finlayson-Pitts, *The Journal of Chemical Physics*, 1980, **72**, 3842–3843, DOI: 10.1063/1.439601.
- (64) A. W. Sleight, J. D. Bierlein and P. E. Bierstedt, *The Journal of Chemical Physics*, 1975, **62**, 2826–2827, DOI: 10.1063/1.430818.
- (65) R. P. A. Bettens, T. A. Hansen and M. A. Collins, *The Journal of Chemical Physics*, 1999, **111**, 6322–6332, DOI: 10.1063/1.479937.
- (66) P. Glarborg, J. A. Miller, B. Ruscic and S. J. Klippenstein, 2018, **67**, 31–68, DOI: 10.1016/j.jpecs.2018.01.002.
- (67) V. G. Anicich, W. T. Huntress and J. H. Futrell, 1976, **40**, 233–236, DOI: 10.1016/0009-2614(76)85066-x.
- (68) S. J. Klippenstein, Y. Georgievskii and B. J. McCall, 2009, **114**, 278–290, DOI: 10.1021/jp908500h.
- (69) O. Martinez, Z. Yang, N. J. Demarais, T. P. Snow and V. M. Bierbaum, 2010, **720**, 173–177, DOI: 10.1088/0004-637x/720/1/173.
- (70) P. Tosi, S. Iannotta, D. Bassi, H. Villinger, W. Dobler and W. Lindinger, 1984, **80**, 1905–1906, DOI: 10.1063/1.446951.
- (71) W. Federer, H. Villinger, F. Howorka, W. Lindinger, P. Tosi, D. Bassi and E. Ferguson, 1984, **52**, 2084–2086, DOI: 10.1103/physrevlett.52.2084.
- (72) G. B. Scott, D. A. Fairley, C. G. Freeman, M. J. McEwan, P. Spanel and D. Smith, 1997, **106**, 3982–3987, DOI: 10.1063/1.473116.
- (73) V. Lissianski, H. Yang, Z. Qin, M. Mueller, K. Shin and W. Gardiner, *Chemical Physics Letters*, 1995, **240**, 57–62, DOI: 10.1016/0009-2614(95)00496-q.
- (74) P. Glarborg, M. U. Alzueta, K. Dam-Johansen and J. A. Miller, 1998, **115**, 1–27, DOI: 10.1016/s0010-2180(97)00359-3.
- (75) P. Glarborg and P. Marshall, 2009, **475**, 40–43, DOI: 10.1016/j.cplett.2009.05.028.
- (76) J. Jones, K. Birkinshaw and N. Twiddy, 1981, **77**, 484–488, DOI: 10.1016/0009-2614(81)85191-3.
- (77) Z. Karpas, V. Anicich and W. Huntress, 1978, **59**, 84–86, DOI: 10.1016/0009-2614(78)85620-6.
- (78) J. H. W. T., V. G. Anicich, M. J. McEwan and Z. Karpas, 1980, **44**, 481, DOI: 10.1086/190701.
- (79) G. Bogdanchikov, A. Baklanov and D. Parker, 2004, **385**, 486–490, DOI: 10.1016/j.cplett.2004.01.015.
- (80) C. Dombrowsky, S. M. Hwang, M. Rohrig and H. G. Wagner, 1992, **96**, 194–198, DOI: 10.1002/bbpc.19920960215.
- (81) A. A. Viggiano, D. L. Albritton, F. C. Fehsenfeld, N. G. Adams, D. Smith and F. Howorka, 1980, **236**, 492, DOI: 10.1086/157766.
- (82) F. C. Fehsenfeld, 1976, **209**, 638, DOI: 10.1086/154761.
- (83) N. Copp, M. Hamdan, J. Jones, K. Birkinshaw and N. Twiddy, 1982, **88**, 508–511, DOI: 10.1016/0009-2614(82)83164-3.
- (84) N. K. Srinivasan, M.-C. Su, J. W. Sutherland and J. V. Michael, 2005, **109**, 1857–1863, DOI: 10.1021/jp040679j.
- (85) N. Cohen and K. R. Westberg, 1991, **20**, 1211–1311, DOI: 10.1063/1.555901.
- (86) N. Cohen and K. R. Westberg, 1983, **12**, 531–590, DOI: 10.1063/1.555692.
- (87) J. H. W. T., 1977, **33**, 495, DOI: 10.1086/190439.
- (88) J. T. Petty, J. A. Harrison and C. B. Moore, 1993, **97**, 11194–11198, DOI: 10.1021/j100145a013.
- (89) B. Wang, H. Hou and Y. Gu, 1999, **103**, 8021–8029, DOI: 10.1021/jp991203g.
- (90) S. P. Sander and R. T. Watson, 1980, **84**, 1664–1674, DOI: 10.1021/j100450a002.

- (91) N. Adams, D. Smith and D. Grief, 1978, **26**, 405–415, DOI: 10.1016/0020-7381(78)80059-x.
- (92) T. Tsuboi and K. Hashimoto, 1981, **42**, 61–76, DOI: 10.1016/0010-2180(81)90142-5.
- (93) H. J. Curran, 2006, **38**, 250–275, DOI: 10.1002/kin.20153.
- (94) K. Brudnik, A. A. Gola and J. T. Jodkowski, 2009, **15**, 1061–1066, DOI: 10.1007/s00894-009-0461-x.
- (95) J. T. Jodkowski, M.-T. Rayez, J.-C. Rayez, T. Berces and S. Dobe, 1999, **103**, 3750–3765, DOI: 10.1021/jp984367q.
- (96) W. Tsang, 1987, **16**, 471–508, DOI: 10.1063/1.555802.
- (97) Y. Hidaka, T. Oki, H. Kawano and T. Higashihara, 1989, **93**, 7134–7139, DOI: 10.1021/j100357a022.
- (98) A. D. Sen, V. G. Anicich and S. R. Federman, 1992, **391**, 141, DOI: 10.1086/171331.
- (99) G. I. Mackay, A. C. Hopkinson and D. K. Bohme, 1978, **100**, 7460–7464, DOI: 10.1021/ja00492a003.
- (100) H. S. Lee, M. Drucker and N. G. Adams, 1992, **117**, 101–114, DOI: 10.1016/0168-1176(92)80088-i.
- (101) R. A. Yetter, H. Rabitz, F. L. Dryer, R. G. Maki and R. B. Klemm, 1989, **91**, 4088–4097, DOI: 10.1063/1.456838.
- (102) A. Galano, J. R. Alvarez-Idaboy, M. E. Ruiz-Santoyo and A. Vivier-Bunge, 2002, **106**, 9520–9528, DOI: 10.1021/jp020297i.
- (103) E. Assaf, C. Schoemaecker, L. Vereecken and C. Fittschen, 2018, **20**, 10660–10670, DOI: 10.1039/c7cp05770a.
- (104) S. H. Mousavipour and Z. Homayoon, 2011, **115**, 3291–3300, DOI: 10.1021/jp112081r.
- (105) M. Altarawneh, A. H. Al-Muhtaseb, B. Z. Dlugogorski, E. M. Kennedy and J. C. Mackie, 2011, **32**, 1725–1733, DOI: 10.1002/jcc.21756.
- (106) H.-G. Yu and J. S. Francisco, 2009, **113**, 3844–3849, DOI: 10.1021/jp809730j.
- (107) H. M. T. Nguyen, H. T. Nguyen, T.-N. Nguyen, H. V. Hoang and L. Vereecken, 2014, **118**, 8861–8871, DOI: 10.1021/jp506175k.
- (108) Z. Zhao, J. Song, B. Su, X. Wang and Z. Li, 2018, **122**, 5078–5088, DOI: 10.1021/acs.jpca.7b09988.
- (109) V. D. Knyazev, 2017, **685**, 165–170, DOI: 10.1016/j.cplett.2017.07.040.
- (110) A. M. Mebel, E. W. G. Diau, M. C. Lin and K. Morokuma, 1996, **118**, 9759–9771, DOI: 10.1021/ja961476e.
- (111) S. A. Carl, H. M. T. Nguyen, R. M. I. Elsamra, M. T. Nguyen and J. Peeters, 2005, **122**, 114307, DOI: 10.1063/1.1861887.
- (112) D. K. Bohme and G. I. Mackay, 1981, **103**, 2173–2175, DOI: 10.1021/ja00399a006.
- (113) Y. Hidaka, T. Nishimori, K. Sato, Y. Henmi, R. Okuda, K. Inami and T. Higashihara, 1999, **117**, 755–776, DOI: 10.1016/s0010-2180(98)00128-x.
- (114) J. Gimenez-Lopez, C. T. Rasmussen, H. Hashemi, M. U. Alzueta, Y. Gao, P. Marshall, C. F. Goldsmith and P. Glarborg, 2016, **48**, 724–738, DOI: 10.1002/kin.21028.
- (115) A. Raksit, 1986, **69**, 45–65, DOI: 10.1016/0168-1176(86)87041-0.
- (116) B. K. Decker, N. G. Adams and L. M. Babcock, 2000, **195-196**, 185–201, DOI: 10.1016/s1387-3806(99)00146-3.
- (117) G. B. I. Scott, D. B. Milligan, D. A. Fairley, C. G. Freeman and M. J. McEwan, 2000, **112**, 4959–4965, DOI: 10.1063/1.481050.
- (118) P.-C. Nam, P. Raghunath, L. K. Huynh, S. Xu and M. C. Lin, 2016, **188**, 1095–1114, DOI: 10.1080/00102202.2016.1151878.
- (119) Y. Hidaka, K. Kimura and H. Kawano, 1994, **99**, 18–28, DOI: 10.1016/0010-2180(94)90079-5.
- (120) L. K. Huynh and A. Violi, 2007, **73**, 94–101, DOI: 10.1021/jo701824n.
- (121) K. Ohmori, A. Miyoshi, H. Matsui and N. Washida, 1990, **94**, 3253–3255, DOI: 10.1021/j100371a006.
- (122) J. Warnatz, in Springer New York, 1984, pp. 197–360, DOI: 10.1007/978-1-4684-0186-8\_5.
- (123) R. Sivaramakrishnan, J. V. Michael and S. J. Klippenstein, 2009, **114**, 755–764, DOI: 10.1021/jp906918z.
- (124) Z. F. Xu, K. Xu and M. C. Lin, 2011, **115**, 3509–3522, DOI: 10.1021/jp110580r.
- (125) W.-K. Aders and H. G. Wagner, 1973, **77**, 332–335, DOI: <https://doi.org/10.1002/bbpc.19730770509>.

- (126) R. Sivaramakrishnan, M.-C. Su, J. V. Michael, S. J. Klippenstein, L. B. Harding and B. Ruscic, 2010, **114**, 9425–9439, DOI: 10.1021/jp104759d.
- (127) S.-Z. Xiong, Q. Yao, Z.-R. Li and X.-Y. Li, 2014, **161**, 885–897, DOI: 10.1016/j.combustflame.2013.10.013.
- (128) M. Cameron, V. Sivakumaran, T. J. Dillon and J. N. Crowley, 2002, **4**, 3628–3638, DOI: 10.1039/b202586h.
- (129) N. M. Marinov, 1999, **31**, 183–220, DOI: 10.1002/(sici)1097-4601(1999)31:3<183::aid-kin3>3.0.co;2-x.
- (130) C. Olm, T. Varga, E. Valko, S. Hartl, C. Hasse and T. Turanyi, 2016, **48**, 423–441, DOI: 10.1002/kin.20998.
- (131) D. Skouteris, N. Balucani, C. Ceccarelli, F. Vazart, C. Puzzarini, V. Barone, C. Codella and B. Lefloch, 2018, **854**, 135, DOI: 10.3847/1538-4357/aaa41e.
- (132) G. da Silva, J. W. Bozzelli, L. Liang and J. T. Farrell, 2009, **113**, 8923–8933, DOI: 10.1021/jp903210a.
- (133) A. S. Semenikhin, E. G. Shubina, A. S. Savchenkova, I. V. Chechet, S. G. Matveev, A. A. Konnov and A. M. Mebel, 2018, **50**, 273–284, DOI: 10.1002/kin.21156.
- (134) P. Frank, K. A. Bhaskaran and T. Just, 1986, **90**, 2226–2231, DOI: 10.1021/j100401a046.
- (135) E. Hassinen, K. Kalliorinne and J. Koskikallio, 1990, **22**, 741–745, DOI: 10.1002/kin.550220709.
- (136) G. Hoehlein and G. R. Freeman, 1970, **92**, 6118–6125, DOI: 10.1021/ja00724a004.
- (137) X. Zhang, L. Ye, Y. Li, Y. Zhang, C. Cao, J. Yang, Z. Zhou, Z. Huang and F. Qi, 2018, **191**, 431–441, DOI: 10.1016/j.combustflame.2018.01.027.
- (138) D. M. Golden, G. P. Smith, A. B. McEwen, C.-L. Yu, B. Eiteneer, M. Frenklach, G. L. Vaghjiani, A. R. Ravishankara and F. P. Tully, 1998, **102**, 8598–8606, DOI: 10.1021/jp982110m.
- (139) T. J. Held and F. L. Dryer, 1998, **30**, 805–830, DOI: 10.1002/(sici)1097-4601(1998)30:11<805::aid-kin4>3.0.co;2-z.
- (140) C. Dombrowsky, A. Hoffmann, M. Klatt and H. G. Wagner, *Berichte der Bunsengesellschaft fur physikalische Chemie*, 1991, **95**, 1685–1687, DOI: 10.1002/bbpc.19910951217.
- (141) P. Frank, K. Bhaskaran and T. Just, 1988, **21**, 885–893, DOI: 10.1016/s0082-0784(88)80320-5.
- (142) K. Yasunaga, S. Kubo, H. Hoshikawa, T. Kamesawa and Y. Hidaka, 2007, **40**, 73–102, DOI: 10.1002/kin.20294.
- (143) C. Cavallotti, M. Pelucchi and A. Frassoldati, *Proceedings of the Combustion Institute*, 2019, **37**, 539–546, DOI: 10.1016/j.proci.2018.06.137.
- (144) E. E. Dames, 2014, **46**, 176–188, DOI: 10.1002/kin.20844.
- (145) Z. F. Xu, K. Xu and M. C. Lin, 2009, **10**, 972–982, DOI: 10.1002/cphc.200800719.
- (146) B. Ganguli, M. A. Biondi, R. Johnsen and J. L. Dulaney, *Physical Review A*, 1988, **37**, 2543–2547, DOI: 10.1103/physreva.37.2543.
- (147) W. D. Geppert, R. Thomas, A. Ehlerding, J. Semaniak, F. Osterdahl, M. af Ugglas, N. Djuric, A. Paal and M. Larsson, *Faraday Discuss.*, 2004, **127**, 425–437, DOI: 10.1039/b314005a.
- (148) Obtained from LXCAT (Morgan database), www.lxcat.net.
- (149) Obtained from LXCAT (Itikawa database), www.lxcat.net.
- (150) I. A. Kossyi, A. Y. Kostinsky, A. A. Matveyev and V. P. Silakov, *Plasma Sources Science and Technology*, 1992, **1**, 207–220, DOI: 10.1088/0963-0252/1/3/011.
- (151) C. PARK, in *24th Thermophysics Conference*, DOI: 10.2514/6.1989-1740.
- (152) S. G. Belostotsky, D. J. Economou, D. V. Lopaev and T. V. Rakhimova, *Plasma Sources Science and Technology*, 2005, **14**, 532–542, DOI: 10.1088/0963-0252/14/3/016.
- (153) A. Cenian, A. Chernukho and V. Borodin, *Contributions to Plasma Physics*, 1995, **35**, 273–296, DOI: 10.1002/ctpp.2150350309.
- (154) L. E. Khvorostovskaya and V. A. Yankovsky, *Contributions to Plasma Physics*, 1991, **31**, 71–88, DOI: 10.1002/ctpp.2150310109.
- (155) W. Wang, R. Snoeckx, X. Zhang, M. S. Cha and A. Bogaerts, *The Journal of Physical Chemistry C*, 2018, **122**, 8704–8723, DOI: 10.1021/acs.jpcc.7b10619.

- (156) H. Hokazono, M. Obara, K. Midorikawa and H. Tashiro, *Journal of Applied Physics*, 1991, **69**, 6850–6868, DOI: 10.1063/1.347675.
- (157) C. Lifshitz, R. L. C. Wu, J. C. Haartz and T. O. Tiernan, *The Journal of Chemical Physics*, 1977, **67**, 2381, DOI: 10.1063/1.435078.
- (158) D. S. Stafford and M. J. Kushner, *Journal of Applied Physics*, 2004, **96**, 2451–2465, DOI: 10.1063/1.1768615.
- (159) J. T. Gudmundsson and E. G. Thorsteinsson, *Plasma Sources Science and Technology*, 2007, **16**, 399–412, DOI: 10.1088/0963-0252/16/2/025.
- (160) T. G. Beuthe and J.-S. Chang, *Japanese Journal of Applied Physics*, 1997, **36**, 4997–5002, DOI: 10.1143/jjap.36.4997.
- (161) L. Polak and D. Slovetsky, *International Journal for Radiation Physics and Chemistry*, 1976, **8**, 257–282, DOI: 10.1016/0020-7055(76)90070-x.
- (162) Obtained from LXCAT (Biagi database), www.lxcat.net.
- (163) C. Park, J. T. Howe, R. L. Jaffe and G. V. Candler, *Journal of Thermophysics and Heat Transfer*, 1994, **8**, 9–23, DOI: 10.2514/3.496.
- (164) A. J. Dean, D. F. Davidson and R. K. Hanson, *The Journal of Physical Chemistry*, 1991, **95**, 183–191, DOI: 10.1021/j100154a037.
- (165) S. J. Petuchowski, E. Dwek, J. A. J. E. and I. N. J. A., *The Astrophysical Journal*, 1989, **342**, 406, DOI: 10.1086/167601.
- (166) L. M. Arin and P. Warneck, *The Journal of Physical Chemistry*, 1972, **76**, 1514–1516, DOI: 10.1021/j100655a002.
- (167) M. McFarland, D. L. Albritton, F. C. Fehsenfeld, E. E. Ferguson and A. L. Schmeltekopf, *The Journal of Chemical Physics*, 1973, **59**, 6629–6635, DOI: 10.1063/1.1680043.
- (168) F. C. Fehsenfeld and E. E. Ferguson, *The Journal of Chemical Physics*, 1972, **56**, 3066–3070, DOI: 10.1063/1.1677642.
- (169) D. Husain and A. N. Young, *Journal of the Chemical Society, Faraday Transactions 2*, 1975, **71**, 525, DOI: 10.1039/f29757100525.
- (170) D. W. Fahey, F. C. Fehsenfeld and E. E. Ferguson, *Geophysical Research Letters*, 1981, **8**, 1115–1117, DOI: 10.1029/gl008i010p01115.
- (171) M. Burmeister and P. Roth, *AIAA Journal*, 1990, **28**, 402–405, DOI: 10.2514/3.10406.
- (172) I. Mendez, F. J. Gordillo-Vazquez, V. J. Herrero and I. Tanarro, *The Journal of Physical Chemistry A*, 2006, **110**, 6060–6066, DOI: 10.1021/jp057182+.
- (173) D. X. Liu, P Bruggeman, F Iza, M. Z. Rong and M. G. Kong, *Plasma Sources Science and Technology*, 2010, **19**, 025018, DOI: 10.1088/0963-0252/19/2/025018.
- (174) B. Gordiets, C. M. Ferreira, M. J. Pinheiro and A. Ricard, *Plasma Sources Science and Technology*, 1998, **7**, 363–378, DOI: 10.1088/0963-0252/7/3/015.
- (175) Obtained from LXCAT (Hayashi database), www.lxcat.net.
- (176) E. Cleiren, S. Heijkers, M. Ramakers and A. Bogaerts, *ChemSusChem*, 2017, **10**, 4025–4036, DOI: 10.1002/cssc.201701274.
- (177) S. Heijkers, M. Aghaei and A. Bogaerts, *The Journal of Physical Chemistry C*, 2020, **124**, 7016–7030, DOI: 10.1021/acs.jpcc.0c00082.
- (178) M. Ramakers, G. Trenchev, S. Heijkers, W. Wang and A. Bogaerts, *ChemSusChem*, 2017, **10**, 2642–2652, DOI: 10.1002/cssc.201700589.
- (179) G. Trenchev, A. Nikiforov, W. Wang, S. Kolev and A. Bogaerts, *Chemical Engineering Journal*, 2019, **362**, 830–841, DOI: 10.1016/j.cej.2019.01.091.
- (180) B. Wanten, S. Maerivoet, C. Vantomme, J. Slaets, G. Trenchev and A. Bogaerts, *Journal of CO<sub>2</sub> Utilization*, 2022, **56**, 101869, DOI: 10.1016/j.jcou.2021.101869.
- (181) J. Slaets, M. Aghaei, S. Ceulemans, S. Van Alphen and A. Bogaerts, *Green Chemistry*, 2020, **22**, 1366–1377, DOI: 10.1039/C9GC03743H.
- (182) K. Green, M. Borras, P. Woskov, G. Flores, K. Hadidi and P. Thomas, *IEEE Transactions on Plasma Science*, 2001, **29**, 399–406, DOI: 10.1109/27.922753.
- (183) S. Y. Moon and W. Choe, *Physics of Plasmas*, 2006, **13**, DOI: 10.1063/1.2357722.

- (184) J.-L. Liu, H.-W. Park, W.-J. Chung, W.-S. Ahn and D.-W. Park, *Chemical Engineering Journal*, 2016, **285**, 243–251, DOI: 10.1016/j.cej.2015.09.100.
- (185) D. K. Dinh, G. Trenchev, D. H. Lee and A. Bogaerts, *Journal of CO<sub>2</sub> Utilization*, 2020, **42**, 101352, DOI: 10.1016/j.jcou.2020.101352.